ETHYLENEDIAMINETETRAACETIC ACID (EDTA) MODIFIED RICE HUSK AS AN ADSORBENT FOR DYES AND HEAVY METALS REMOVAL

By

LEE WENG NAM

A dissertation submitted to the Department of Science,
Faculty of Engineering and Science,
Universiti Tunku Abdul Rahman,
in partial fulfillment of the requirements for the degree of
Master of Science
April 2014

ABSTRACT

ETHYLENEDIAMINETETRAACETIC ACID (EDTA) MODIFIED RICE HUSK AS AN ADSORBENT FOR DYES AND HEAVY METALS REMOVAL

Lee Weng Nam

The potential of various chemically modified rice husk to remove Methylene Blue (MB) and Reactive Orange 16 (RO16) from aqueous solution was investigated. It was found that ethylenediamine tetraacetic acid modified rice husk (ERH) has the highest adsorption capacity for both MB and RO16. ERH was produced by treating natural rice husk (NRH) with 0.5 g of ethylenediamine tetraacetic acid (EDTA) in 300 mL of 1 mol/dm^3 NaOH. Fourier Transform Infrared Spectroscopy (FTIR) was used to analyse the surface functional groups of ERH. Surface morphology analysis by atomic force microscopy (AFM) and scanning electron microscopy (SEM) showed that the surface topography of ERH was higher and smoother than NRH.

The effect of pH, contact time, influence of initial dye concentration, amount of adsorbent used, agitation rate and effect of particle size on the adsorption of MB and RO16 in single and binary systems were investigated under batch experiments. Equilibrium data were fitted into Brunauer-Emmet-Teller (BET), Freundlich and Langmuir model equations. It was found that the

equilibrium fitted well in Freundlich isotherm with higher regression coefficient value, R^2. The maximum adsorption capacities of MB and RO16 in binary system were 49.5 mg/g and 17.2 mg/g, respectively. Adsorption kinetic was studied by fitting the experimental data with pseudo-first and pseudo-second order kinetic models. Results showed that pseudo-second order kinetic model provided a better description of MB and RO16 adsorption in single and binary dye solutions as compared to pseudo-first order kinetic model.

The adsorption behavior of MB and RO16 onto column packed with ERH was investigated under continuous flow mode with three different parameters; the effect of influent concentration, the effect of bed depth and the effect of flow rate. Results obtained showed that the breakthrough time is longer for MB at both lower influent concentration and flow rate. An unusual rapid breakthrough was observed for RO16 in single and binary dye solutions. This implied that the adsorption of RO16 is a slow process and an effective adsorption only takes place after a sufficient lapse of time. Bed depth service time (BDST) model, Adams-Bohart model and Clark model were employed in this study to describe the adsorption behavior of dyes under continuous flow conditions. The breakthrough curves predicted by Clark model agreed well with the experimental breakthrough curves at various flow rates.

The optimum adsorption conditions for the uptake of MB and RO16 in both single and binary dye solutions by ERH were studied using Plackett-Burman coupled with response surface methodology (RSM). From Plackett-Burman, the

significant variables in affecting the uptake of single MB were determined to be pH and adsorbent dosage. As for single RO16, binary RO16 and binary MB, pH and contact time were found to be significant in affecting the percentage uptake. The combined effects of interaction between the significant variables were determined using ANOVA analysis.

In heavy metal analysis, the potential of ERH in removing heavy metal ions was investigated. The adsorption of both Cu(II) and Cd(II) ions were found to be pH dependent. Greater uptake was observed at higher pH. Experimental data showed a better fitting in Langmuir isotherm as compared to Freundlich isotherm. The maximum adsorption capacities of 7.9 mg/g and 12.9 mg/g were obtained for Cu(II) and Cd(II) ions, respectively. With the presence of chelators, the uptake of both metal ions by ERH decreased.

ERH therefore appeared to be a potential and efficient adsorbent for the removal of dyes such as MB and RO16 in textile wastewater as well as heavy metal ions in electroplating wastewater.

ACKNOWLEDGEMENTS

I, Lee Weng Nam, wish to express sincere gratitude and appreciation to my supervisor, Assistant Professor Dr. Ong Siew Teng for her guidance insight, availability, patience and support throughout my research and preparation of this thesis.

Appreciation expressed to Mr. Khoo Eng Cheong for his precious opinion throughout my study. Also, special thanks to Ms. Siew Kim from Department of Chemical Engineering, Universiti Tunku Abdul Rahman (UTAR) for lending her guidance in using ICP. Thanks to UTAR laboratory for all the facilities and support provided.

I would like to thank the financial support from the International Foundation of Science, Stockholm, Sweden and the Organisation for the Prohibition of Chemical Weapons, The Hague, The Netherlands via grant no. W/4368-1.

Finally, and most of all, I would like to thank my parents and my wife, Kimberley for their eternal support, love, and encouragement. I would be lost without you.

APPROVAL SHEET

This dissertation/thesis entitle "**ETHYLENETRAEDIAMINETETRAACETIC ACID (EDTA) MODIFIED RICE HUSK AS AN ADSORBENT FOR DYES AND HEAVY METALS REMOVAL"** was prepared by LEE WENG NAM and submitted as partial fulfillment of the requirements for the degree of Master of Science at Universiti Tunku Abdul Rahman.

Approved by:

_____
(Asst. Prof. Dr. Ong Siew Teng)
Date: …………………..
Supervisor
Department of Chemical Science
Faculty of Science
Universiti Tunku Abdul Rahman

FACULTY OF ENGINEERING AND SCIENCE

UNIVERSITI TUNKU ABDUL RAHMAN

Date: _____

SUBMISSION OF ~~FINAL YEAR PROJECT~~ /DISSERTATION/~~THESIS~~

It is hereby certified that Lee Weng Nam (ID No: 08UEM08114) has completed this ~~final year project~~/ dissertation/ ~~thesis~~* entitled "ETHYLENEDIAMINETETRAACETIC ACID (EDTA) MODIFIED RICE HUSK AS AN ADSORBENT FOR DYES AND HEAVY METALS REMOVAL" under the supervision of Asst. Prof. Dr. Ong Siew Teng from the Department of Chemical Science, Faculty of Science.

I understand that University will upload softcopy of my ~~final year project~~ / dissertation/ ~~thesis~~* in pdf format into UTAR Institutional Repository, which may be made accessible to UTAR community and public.

Yours truly,

_____
(Lee Weng Nam)

*Delete whichever not applicable

DECLARATION

I _____ hereby declare that the dissertation is based on my original work except for quotations and citations which have been duly acknowledged. I also declare that it has not been previously or concurrently submitted for any other degree at UTAR or other institutions.

_____
(LEE WENG NAM)

Date _____

TABLE OF CONTENTS

Page

LIST OF TABLES

LIST OF FIGURES

LIST OF ABBREVIATIONS

A	Clark equation constant
AB40	Acid Blue 40
AC	Activated carbon
ADIM	American Dye Manufactures Institute
AFM	Atomic force microscope
AG25	Acid Green 25
ANOVA	Analysis of variance
AO12	Acid Orange 12
AR18	Acid Red 18
AR73	Acid Red 73
B	BET constant
b	Constant related to the energy of the adsorbent
BASS	Borassus aethiopum seed shells
BB3	Basic Blue 3
BET	Brunauer-Emmet-Teller
BF	Basic Fuchsin
BDST	Bed depth service time
BOD	Biological oxygen demand
BPH	H_3PO_4 treated bagasse pith
BPK	KOH treated bagasse pith
CCD	Central composite design
CCRD	Central composite rotatable design

CMK	Tubular structured ordered mesoporous carbon
CNS	Cashew nut shell
COD	Chemical oxygen demand
CONS	Cocos nucifera shells
CR	Congo Red
CTAB	Cetyltrimethylammonium bromide
CV	Crystal Violet
C.V	Coefficient of variance
C_e	Equilibrium concentration
C_o	Initial concentration
C_i	Initial concentration
C_t	Concentration at time t
C_{eq}	Saturation of solute
DCB	Degreased coffee beans
DOE	Department of environment
DP	Durian Peel
DSAC	Durian shell activated carbon
DY-12	Direct Yellow 12
EDA	Ethylenediamine
EDARH	Ethylenediamine modified rice husk
EDTA	Ethylenediamine tetraacetic acid
ERH	Ethylenediamine tetraacetic acid modified rice husk
F	Influent linear velocity

FTIR	Fourier-transform infrared spectrophotometry
GAC	Granular activated carbon
GLP	Guava leaf powder
ΔG^o	Gibbs free energy
HNRH	Nitric acid modified rice husk
H	Bed height
h	Initial adsorption rate
ΔH^o	Enthalpy change
IAST	Ideal adsorbed solution theory
ICPAES	Inductively couple plasma atomic emission spectroscopy
JS	Jain and Snoeyink
K	Mass transfer coefficient
k_1	Rate constant of pseudo-first order kinetics
k_2	Rate constant of pseudo-second order kinetics
K_a	Langmuir constant
K_{BA}	Mass transfer coefficient
K_d	Distribution coefficient
K_p	Intraparticle diffusion coefficient
K_f	Freundlich constant for adsorption capacity
LiP	Lignin Peroxidise Enzyme
MB	Methylene Blue
MG	Malachite Green
MO	Methyl Orange
MRH	HNO_3 modified rice husk

MSWI	Municipal solid waste incinerator
MTZ	Mass transfer zone
N_e	Dye adsorbed at equilibrium
$N*$	Maximum adsorption capacity
N_o	Adsorption capacity
n	Freundlich constant for intensity
NaRH	NaOH modified rice husk
NTARH	Nitrilotriacetic acid modified rice husk
NWQS	National water quality standards
NRH	Natural rice husk
OFAT	One-factor-at-a-time
PAC	Powdered activated carbon
QRH	Quartenized rice husk
q_e	Dyes adsorbed at equilibrium
q_{BA}	Dye solution untaken by adsorbent
q_t	Dyes adsorbed at time t
R	Gas constant
R^2	Correlation coefficient
RB5	Reactive Black 5
RO16	Reactive Orange 16
RSM	Response surface methodology
RSAC	Rattan sawdust activated carbon
SA	Salicylic acid

SAR	Sulphoricin oleic acid
SB	Sugarcane bagasse
SBC	Phosphoric acid modified sugarcane bagasse
SEM	Scanning electron microscope
SMBS	Surfactant modified barley straw
SSRE	Sum of squares of relative error
SWP	Silkworm pupa
ΔS^o	Entropy change
T	Absolute temperature
t	Time
TARH	Tartaric acid modified rice husk
TCU	True color unit
TEM	Transmission electron micrograph
UV-Vis	Ultraviolet-visible
v	Linear flow rate of solution
WQI	Water quality index
Z	Bed depth of column

CHAPTER 1

INTRODUCTION

1.1 Colorants

In the early stage of mankind, colorants are used for painting and dyeing of surroundings, cloths as well as skins. All colorants applied were from natural sources until the middle of 19th century. There are two types of colorants, namely organic and inorganic. Organic colorants are usually applied as textile dyes. These dyes are aromatic compounds originated from plants, for instance, indigo from wood. Inorganic colorant such as Ultramarine is a natural blue colorant derived from a semiprecious mineral of the sodalite group found in Afghanistan. It was used as a colorant for illumination and later paintings. Lead has also been known and used as colorant since ancient times due to the ease with which it can be isolated in the Free State. Lead was converted into lead carbonate which is an essential component of artists' palettes.

1.2 Pigments and Dyes

Colorants can also be classified into either pigments or dyes. Pigments are colored, white or fluorescent particulate organic and inorganic solid. It is generally insoluble or partially soluble in the medium in which they are incorporated with. In 19th century, during the Industrial Revolution, scientists were driven by the demand for new permanent colors and new minerals have been utilized for the invention of variety of colors. For instance, in 1802, Thenard discovered Cobalt Blue. It was used for ceramics due to its moderate tinting strength, fast drying and water color characteristics. In 1846, Cadmium Yellows were discovered and it has great permanence and high opacity. Titanium White was the most opaque white and non-hazardous pigment in 20th century. Nowadays, pigments are mostly applied in the manufacture of paint, printing inks, coloration application for popular textiles such as polyester and nylon.

The main difference between pigments and dyes is that dyes are water soluble. Dyes can be obtained from natural sources and also can be synthesized in the laboratory. Synthetic dye was first manufactured in 1856 by W.H. Perkin, an English chemist who attempting to synthesize quinine but a bluish compound was obtained with excellent dyeing properties instead. This compound is known as Aniline Purple. The invention was patented and a production line was set up at his age of 18. The concept of research was followed by others resulted in the formation of new dyes. In the early of 20th century, synthetic dyes have been used as a substitute for natural dyes.

Generally, aromatic compounds that absorb light with wavelength in the visible range (350 nm $-$700 nm) are colored. Dyes are colored aromatic compounds containing chromophores and auxochromes. Chromophore is the part of the compound that responsible for colors and it consists of conjugated double bonds whereas auxochrome is acts as an electron-donating or electron-withdrawing group that alters the overall energy of the conjugated system. Some examples of chromophores include -C=O, -C=N, -C=C, -N=N and -NO$_2$, whereas -NH$_3$, -COOH, SO$_3$H and -OH are the common examples of auxochromes in dye molecules.

1.2.1 Classification of dyes

Based on the chemical structure of dyes or chromophores, dyes can be classified into anionic, cationic and nonionic dyes. Anionic dyes can be grouped into, acid, direct and reactive dyes. Acid dyes consist of acidic groups in its structure such as sulphonate and carboxyl which are negatively charged and will bind to cationic NH$_4^+$ ion of fabrics like wool, polyamide and silk. An example of acid dyes, Acid Red 266 is shown in Figure 1.1.

Figure 1.1

3
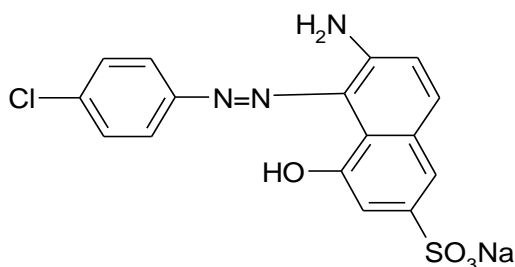
For direct dyes, its molecule is relatively large and has high affinity for cellulose fibre. The interaction between direct dyes molecule and fibre is mainly due to Van der Waals forces. Figure 1.2 shows the chemical structure of Direct Blue 86.
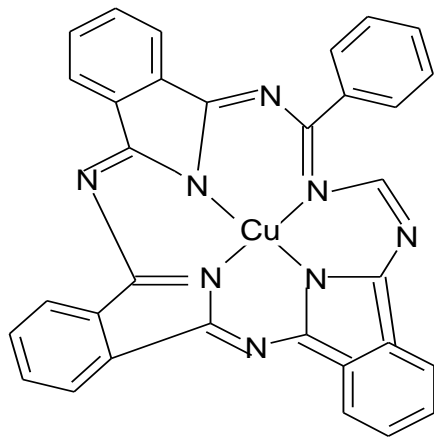
Figure 1.2

Reactive dyes tend to form covalent bonds with hydroxyl, amine and sulfide groups in fibre like cotton and wool due to the presence of reactive groups in its structure. Reactive group is a heterocyclic aromatic ring substituted with either fluoride or chloride. Vinyl sulphone is one of the examples of reactive group which can be found in Reactive Orange 7 as shown in Figure 1.3.
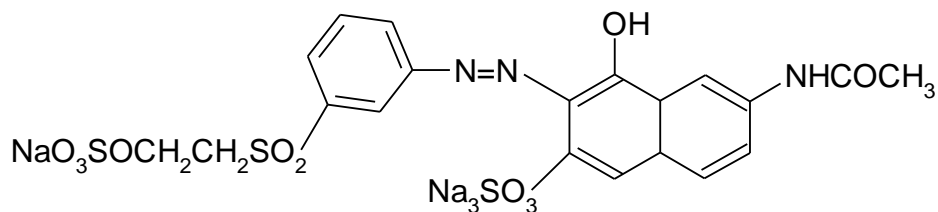
Figure 1.3

Basic dyes are categorised as cationic dyes which are readily soluble in water and commonly used for dyeing acrylic fibre or acid-group fibre. The cationic functional groups on basic dyes are $-NR_3^+$ and $=NR_2^+$ which would be attracted to the negatively charged sulphonate, SO_3^- and carboxyl, COO^- groups With the aid of acetic acid in the dye bath, the uptake of dyes onto the fibre can be improved. Basic dyes were used extensively in dyeing leather due to their great tinctorial strength and brightness which are not easily faded by light and are able to combine with leather without the use of a mordant. Mordant is a chemical that used to combine dyes and fibre. Dichromates is a commonly used mordant. An example of basic dye, Basic Green is shown in Figure 1.4.
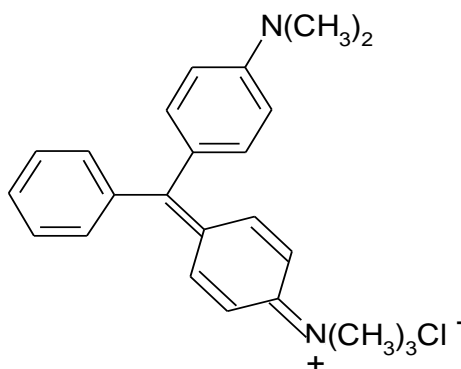
Figure 1.4

Disperse dyes are the only water insoluble dyes that used for dyeing acetate rayon and polyester since it is difficult for dye molecules to penetrate these hydrophobic synthetic fibres. Hence, an alternative dyeing method can be used, that is, immerse the fabrics in an aqueous dispersion of insoluble dyes in which the dyes transfer into the fibres with the aid of sulphoricin oleic acid (SAR) as dispersing agent. Figure 1.5 showed the chemical structure of Disperse Yellow.
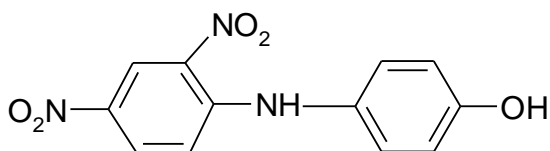
Figure 1.5

1.3 Methylene Blue

Methylene Blue (CAS No. 61-73-4) is categorised as basic dye due to the presence of cationic functional group of $=NR_2^+$ with molecular formula $C_{16}H_{18}N_3SCl$. It is a dark green crystal with bronze luster or crystalline powder, soluble in water and is odourless. Methylene Blue is mostly applied to cotton and wool. This is because it has a positively charged amino group that attached to a larger aromatic structures giving them water solubility and affinity for negatively charged fibre.

Acute exposure to Methylene Blue orally or by intravenous injection may cause hypertension, dizziness and tissue necrosis in humans (Yasin et al., 2007). Methylene Blue may induce anemia in individuals with G-6-PD enzyme deficiency. The chemical structure of Methylene Blue is shown in Figure 1.6.
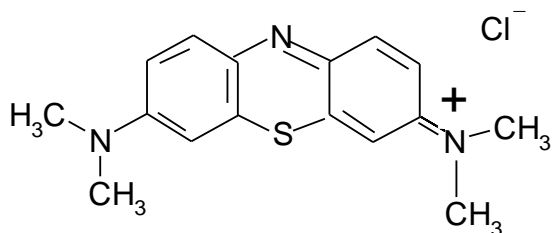
Figure 1.6

1.4 Reactive Orange 16

Reactive Orange 16 (CAS No. 12225-83-1) is an orange to dark red powder with molecular formula $C_{20}H_{17}N_3Na_2O_{11}S_3$. It can be considered as an azo dye since it has one double-bonded nitrogen unit linking aromatic units in its structure. Reactive Orange 16 is widely used for the colouration of cellulosic fibres, wool and nylon.

Reactive Orange 16 is a water-soluble dye and are capable of generating a carcinogenic metabolites (Netpradit et al., 2003). It may cause contact dermatitis, allergic conjunctivitis, allergic rhinitis and occupational asthma. It might combines with human protein at body temperature which leads to respiratory sensitisation. The chemical structure of Reactive Orange 16 is illustrated in Figure 1.7.
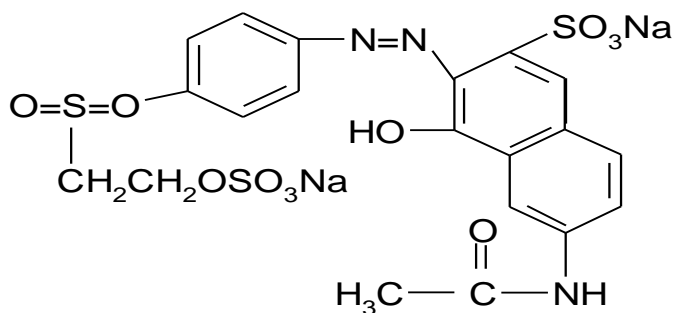
Figure 1.7

1.5   Heavy Metals

Many of the elements in periodic table can be considered as heavy metal such as lead, mercury, cadmium, copper, chromium, zinc and iron. The term 'heavy metal' is referring to both metals and semi-metals that are toxic to human and environment. Some metals are known to be important to human life. For instance, zinc acts as cofactor for carbonic anhydrase; iron is an important constituent of haemoglobin; copper and chromium are essential in human diet. These heavy metals might engender pernicious effects if taken in large quantity.

The hazardous effects of heavy metals are on regulatory concern as gallon of water containing toxic heavy metals are discharged from various industries. The classic example of heavy metal contamination is the Minimata Bay disaster. In 1950s, industrial effluent was continuously disposed into Japan's Minimata Bay and mercury was accumulated to high concentration in local fish. The greatest impact of this disaster was on the new generation where many were born with severe neurological deficits.

1.5.1   Copper

Copper (Cu) is an element with proton number 29. It is a metal with high thermal and electrical conductivity and good corrosion resistance. It is used as a thermal and electrical conductor, a building material, a constituent of various

metal alloys and electroplating industries (Igwe and Abia, 2007). Copper ions are often imparting blue or green colours to its compounds and so it is also used as pigments. At low concentration, Cu^{2+} ions function as fungicides, wood preservatives, important trace element to plants and animals. However, in sufficient amount, Cu^{2+} ions can be poisonous and accumulated in living cells which engender various diseases and disorders (Wan Ngah and Hanafiah, 2007). Toxicity can occur by eating food cooked with copper cookware. Cirrhosis of the liver in children has been linked to boiling milk in copper cookware. Cu^{2+} ions are usually known to deposit in brain, skin, liver and myocardium (Davis et al., 2000).

1.5.2   Cadmium

Cadmium (Cd) is a metal with atomic number of 48. This metal is chemically similar to zinc and mercury. Similar to Zinc, it prefers +2 oxidation states in its compounds and shows low melting point as compared to other transition metals. Cadmium is not considered as transition metal since it does not contains partially filled d orbitals in its common oxidation states. The metal has been used as pigments and for coating process to improve corrosion protection on steel. It is also used to stabilise plastic. However, the use of cadmium is actually decreasing in its applications due to cadmium's toxicity in certain forms and concentration. Cadmium is a potential environmental hazard and it is a non-essential element to living organisms. Diseases such as hypertension and anemia

are affiliated with high concentration of cadmium accumulated in body (Kumar, 2006).

1.6 Rice Husk

Paddy consists of 72% of rice, 8% of bran and 22% of husk (Muthadhi et al., 2007). In Malaysia, rice husk can be readily obtained in huge amount since more than 350,000 metric tons of rice husk are produced annually as a result of paddy cultivation (Annual Report of Bernas Sdn Bhd, 2008). Most of the rice husk from milling is burnt or dumped as waste and this will result in disposal problem. In order to overcome the disposal nuisance caused by rice husk, researchers have made use of it to produce variety of products such as panel board and adsorbent for the removal of pollutants.

Rice husk in its natural state contains high proportion of cellulose (32.34%) and hemicellulose (21.34%) (Wan Ngah and Hanfiah, 2008). These made rice husk possess high mechanical strength and thus making it a good adsorbent for treating various types of pollutant (Ong et al., 2010; Wan Ngah and Hanafiah, 2008). When immersed in water, rice husk will become partially negatively charged which produce columbic interaction with cationic species in water (McKay et al., 1987; Laszlo, 1994; Kumar, 2006).

In order to intensify the adsorption capacities of rice husk in treating dyes and heavy metals, various modification methods have been studied (Wong et al.,

2003; Mane et al., 2007; Gong et al., 2008; Lakshmi et al., 2009; Ong et al., 2009a). In order to reduce the content of hemicelluloses, lignin and increase the porosity, a pretreatment of natural rice husk has to be done.

1.7   Ethylenediaminetetraacetic Acid

Ethylenediaminetetraacetic acid (EDTA) is a polybasic acid with carboxylic acid group and amine group. It can be synthesised from ethylenediamine, ethanal (formaldehydes) and sodium cyanide. Structure of EDTA is shown in Figure 1.8.
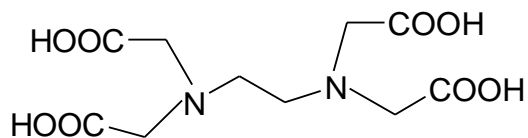
Figure 1.8

EDTA acts as a hexadentate ligand that is capable to bind to a central metal atom or ion at six points. Chelation is a process whereby a polydentate ligand binds to a metal ion, forming a ring. The complex that formed from this process is known as chelate whereas the polydentate ligand is referred as chelating agent. Molecules that chelate tend to be thermodynamically stable and this chelating molecule tends to displace modentates ligand in coordination complexes in solution. For instance, as shown in the equation below, EDTA chelates Fe^{3+} ion by displacing water ligands from its coordination complex.

$$Fe(H_2O)_6^{3+} + EDTA \leftrightarrow [Fe(EDTA)^- + 6H_2O]$$ (1.1)
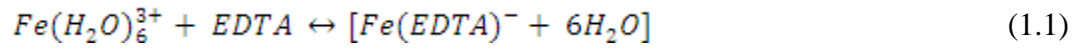
There are several chemical formulas for the same basic product called EDTA which are designed for the removal of metals. Food grade EDTA such as calcium salts of EDTA is commonly used as sequestrants in many foods and beverages. EDTA used in food products (Chelation Therapy) is recommended by American Heart Association for removing toxic metals from the body. Whereas, industrial grade EDTA is used in batteries. In the field of pharmaceutical, EDTA is used to remove unwanted metals such arsenic, cadmium, lead, and mercury from the body's organs and cardiovascular system.

1.8   Statistical and Mathematical Analysis

Response Surface Methodology (RSM) is a statistical analysis techniques used to optimise processes. RSM is usually applied to a particular situation where there are several input variables that potentially affect the performance measure of a process. The performance measure is called the response. Both input variable and response are subject to the control of the scientist. RSM consists of experimental strategy that used to explorer space of the independent variables, optimisation method for determining the values of the variables, and empirical statistical modeling for the development of a fitting relationship between yield and the variables.

Most of the applications of RSM are divided into 3 phases. In phase 1, some ideas are generated in concern of which variables are important in response surface study. The screening of variables is to reduce the list of possible variables and so the subsequent experiments will become more efficient.

During phase 2, the experimenters need to ascertain whether the settings of the independent variables will generate a response at its optimum level. A set of alteration has to be made to the variables in order to shift the process towards the optimum condition.

In phase 3, the process is now considered to be near the optimum condition. At this stage also, a second-order model should be used to determine whether the generated model will approximate the true response function within a small region around the optimum condition. Once the approximating model has been obtained, it will be analysed and the optimum condition for the process can be determined.

1.9   Industrial Wastewater

1.9.1 Textile Wastewater

The ever-growing population and rapid industrialisation in many developing countries have given rise to the destruction of water quality. Due to industrial activities, a variety of pollutants or chemicals was discharged and contaminates natural water resources and reservoir.

One of the main classes of pollutants is synthetic dyes. Synthetic dyes are applied in various fields such as textile, agricultural research, photoelectrochemical cells and hair colouring (Slampova et al., 2001; Forgacs et al., 2004). There are nearly 40000 dyes and pigments listed which consists of 7000 different chemical structures (Demirbas, 2009). According to Mane et al (2007), there are over 7×10^5 tons of dyes being produced annually. Some researches reveal that about 12 % of synthetic dyes from textile industries are lost into the wastewater stream (Hema et al., 2007).

Dyes can be considered as dangerous organic compounds to the environment. Dyes have a complex molecular structure making them resistant to biodegradation (Forgacs et al., 2004). The release of dyes into streams affects the transmission of light into stream and reduces the process of photosynthesis. The toxicity of commercial dyes was tested using algae and it was found that the most toxic dyes for algae are basic dyes (Zee van der, 2000). For fish mortality tests,

the most acute toxic dyes for fish are both basic and acid dyes (Zee van der, 2000). Therefore, the discharge of dyes in open waters raises the risk of bioaccumulation that might affect human being through food chain.

The chronic effect of reactive dyes had been studied for several decades. Reactive dyes are categorized under azo dyes which are not directly mutagenic or carcinogenic in its purified form. However, the breaking of azo bonds (reduction) would result in the formation of aromatic amines or free amino groups which are known carcinogen. In mammals, the reduction of azo dyes could occur in the intestinal tract due to the anaerobic bacterial activity. The carcinogenicity of aromatic amines is due to the production of acyloxy amines through N-hydroxylation, N-acetylation and O-acylation. Acyloxy amines are capable of changing into nitremium and carbonium ions that are believed to be the ultimate genotoxic intermediate that interacts with DNA (Ioannides and Lewis, 2004).

1.9.2 Electroplating Wastewater

Electroplating involve the plating of a metal layer onto a surface of other metal using electrolytic processes. All the chemical wastes from electroplating process are discharged into the wastewater stream via dumping of process baths or due to spillage. The overall composition of wastewater stream is extremely variable but they are usually high in heavy metals content. These metals may include cadmium, chrome, lead, copper, zinc, and nickel.

Heavy metals are non-biodegradable and therefore it is difficult to be removed from the environment. The toxic effects of heavy metals are mainly due to the ability of metals and their 'free radicals' to disrupt the function of essential biological molecules such as enzymes and DNA. The replacement of certain essential metals in our body such as zinc by a similar metal, cadmium, would result in toxicity. This is because cadmium can alter the structure of certain enzymes which in turn gives rise to toxic consequences.

1.10 Environmental Quality (Sewage and Industrial Regulation)

As Malaysia is fast becoming an industrial country, many of the rivers are polluted by the discharge of toxic effluents such as dyes from textile industry and heavy metals electroplating industry. Therefore, the Department of Environment (DOE) employed Water Quality Index (WQI) to assess the river water quality. The WQI function as the basis for the environmental assessment of water systems in relation to pollution load categorisation under the National Water Quality Standards (NWQS). NWQS has prescribed effluents standards for various quality parameters. For color effluents, maximum contaminant level is 15 measured in True Color Unit (TCU) (Interim National Water Quality Standard for Malaysia, 2004).

With the amendment to Environmental Quality Act 1979, fifth schedule, the acceptable limit for discharge of color effluents for standard A is 100 measured in American Dye Manufactures Institute (ADIM) unit. The discharge of

16

heavy metals such as copper and cadmium ions for standard A are limited to 0.2 mg/L and 0.01 mg/L, respectively. Standard A is referring to the discharge of industrial effluent into any inland waters within the catchment areas such as the state of Johor, Pahang and Selangor. As for standard B, the limit for discharge of color effluents into any other inland waters which are not specified as catchment areas is 200 ADIM. The permitted level for the discharge of copper and cadmium ions for standard B are fixed at 1.0 mg/L and 0.02 mg/L, respectively. In seventh schedule, the discharged of effluent from textile industry for standard A and B are 80 mg/L and 250 mg/L, respectively (Environmental Quality (Industrial Effluent) Regulation 2009).

1.11 Existing Approaches of Dyes and Heavy Metals Removal

Because of the potential toxicity of dyes and heavy metals to the environment, efforts have been carried out in order to overcome the aesthetic problems caused by both pollutants. Various methods were employed for the removal of dyes and heavy metals including oxidation, coagulation or flocculation, biological treatments, membrane filtration and adsorption. Every method have its own limitation and there are several factors that need to be considered in determining the economic feasibility of each removal method like types of pollutant, wastewater composition, operation cost, chemical cost and handling cost of generated waste products.

1.11.1 Chemical Oxidation

Chemical oxidation, a process that makes use of oxidants to reduce Chemical Oxygen Demand (COD) and Biological Oxygen Demand (BOD) levels, and to remove organic and inorganic pollutants such as dyes and heavy metals. Chemical oxidation is an appropriate process for the treatment of effluents containing refractory, toxic or non-biodegradable materials. However, this process has high capital and operating costs as compared to biological process.

Hydrogen peroxide, H_2O_2 is the common oxidant used in combination with UV light for the removal of dyes. It involves the generation of hydroxyl free radicals through UV photolysis.

$$H_2O_2 + light\ energy\ (hv) \rightarrow 2OH\cdot \tag{1.2}$$

The hydroxyl free radicals would oxidise the organic pollutants by heterolytic fission to form organic radicals which then lead to an abstraction of hydrogen atoms or addition to double bonds.

In addition, metal semiconductors can also be used to destroy environmental pollutants by means of light-induced redox reactions.

Ozone is also used as an oxidant in paper and textile industries for the oxidation of contaminants. This process is reviewed as an effective technique based on the following factors:

i. Ozone reacts readily with unsaturated organics in wastewater;

ii. The forming ability of wastewaters is reduced following ozone treatment.

iii. Partial oxidation of aromatic compounds using ozone often renders the wastewater more susceptible to conventional biological degradation.

The main benefit of ozone is it able to oxidise contaminants with the formation of no by-product. Since ozone has a noticeable odour, it can be perceived at very low concentration and it is safe to work with ozone. However, the ozone molecule is unstable and has short half-life. Hence, it will easily decompose into its original form of oxygen.

$$2O_3 \rightarrow 3O_2 \tag{1.3}$$

Oxidising agents such as permanganate (MnO_4^-), chlorine (Cl_2) and oxygen (O_2) are commonly applied for the elimination of heavy metals. For instance, the soluble Fe^{2+} and Mn^{2+} ions can be removed by precipitation as $Fe(OH)_3$ and MnO_2 via oxidation.

When oxygen acts as an oxidising agent, both Fe^{2+} and Mn^{2+} ions can be precipitated as follow:

$$2Fe^{2+} + \frac{1}{2}O_2 + 5H_2O \rightarrow 2Fe(OH)_3 + 4H^+ \tag{1.4}$$

$$Mn^{2+} + \frac{1}{2}O_2 + H_2O \rightarrow MnO_2 + 2H^+ \tag{1.5}$$
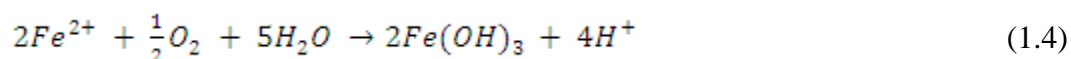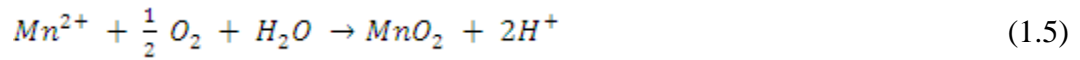
When chlorine acts as an oxidising agent, both ions can be precipitated as follow:

$$Fe^{2+} + \frac{1}{2}Cl_2 + 3H_2O \rightarrow 2Fe(OH)_3 + Cl^- + 4H^+ \tag{1.6}$$

$$Mn^{2+} + Cl_2 + 2H_2O \rightarrow MnO_2 + 2Cl^- + 4H^+ \tag{1.7}$$
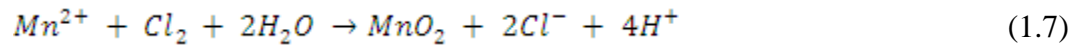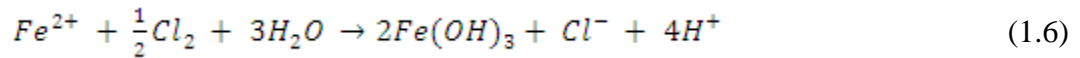
When permanganate ion acts as an oxidising agent, the precipitation of Fe^{2+} and Mn^{2+} ions are as follow:

$$3Fe^{2+} + MnO_4^- + 7H_2O \rightarrow 3Fe(OH)_3 + MnO_2 + 5H^+ \tag{1.8}$$

$$3Mn^{2+} + MnO_4^- + 2H_2O \rightarrow 5MnO_2 + 4H^+ \tag{1.9}$$
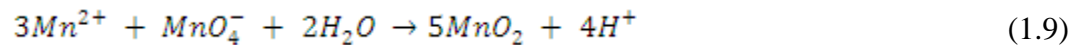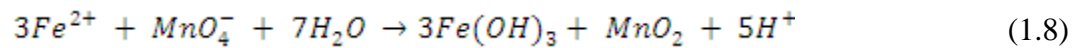
1.11.2 Coagulation / Flocculation

Chemical coagulation has been used for decades to destabilise suspension and to precipitate the soluble metal species and inorganic species from aqueous solutions. The removal of these heavy metals is then achieved through filtration or sedimentation. The destabilisation process is known as coagulation whereas the agglomeration of particles to form bigger flocs is known as flocculation. There are two main types of chemical coagulants, primary coagulant and coagulant aid. Primary coagulants such as alum, ferric sulfate and polymer are always used in the coagulation / flocculation process whereas lime and bentonite are added as coagulant aids to reduce flocculation time.

Alum, also known as aluminum sulfate is used to neutralize the negatively charged particles in the water and allows them to clump together forming floc. The trivalent ions are found to be more effective than divalent ions as a coagulant. There are four mechanisms which are thought to occur during coagulation process and these include: (i) ionic layer compression, (ii) adsorption and charge neutralization, (iii) entrapment in a flocculent mass and (iv) intraparticle bridging. These processes, however, tends to produce large volume of sludge with high water content that can be slow to filter and dewater.

1.11.3 Biological Treatment

The utilisation of microorganisms for the removal of dyes provides noticeable benefits. This method is economical and the end products produced are non-toxic (Forgacs et al., 2004). It is a commonly used method in dye wastewater treatment (Bromley-Challenor et al., 2000; Barragan et al., 2007).

Enzymes secreted by bacteria under aerobic conditions are used to breakdown the dye compounds. However, some dyes are unlikely to be decomposed by activated sludge in an aerobic condition.

The anaerobic pretreatment for dyes wastewater can be a substitute for aerobic treatment as expensive aeration is excluded and problem with bulking sludge are prevented (Gupta and Suhas, 2009). However, there is a drawback

when using anaerobic treatment, where BOD removal is insufficient and dyes and are not mineralized.

The combined effect of aerobic and anaerobic conditions is recommended to provide promising results. Such system can lead to complete mineralization due to the synergistic action of different organisms (Stolz, 2001). The reduction of azo linkage in dye molecules can be obtained under reducing conditions in anaerobic bioreactors (anaerobic decolourization) and the resulting aromatic amines can be solidified under aerobic post-treatment (Forgacs et al., 2004).

Microorganism has also been used for the removal of heavy metals. Metal ions can be actively bound by living microorganisms by means of the following mechanisms: intracellular accumulation, extracellular precipitation, and chemical transformation catalysed by these microorganisms such oxidation, reduction, methylation and demethylation (Kulbat et al., 2003).

1.11.4 Membrane Filtration

The principle of membrane filtration is physical separation. The extent to which dissolved organic and inorganic pollutants are removed is determined by the pore size of the membrane. Micro filtration, ultra filtration, nano filtration and reverse osmosis are the latest membrane technology used in wastewater treatment. Both micro and ultra filtration are pressure-dependent processes which dissolved

solids from water to lesser extent as compared to nano filtration and reverse osmosis.

Micro filtration, by employing $0.1 – 10$ μm pore size membrane, is mainly used to remove bacteria. This filtration method can be used to remove particles with a diameter greater than 0.1 mm. Although viruses are smaller than the pore size of micro filtration, there is only small part of the viral contamination is caught up in the process. This is because viruses can attach themselves to bacterial biofilm that formed on the surface of the membrane due to the accumulation of bacteria.

The pores of ultra filtration membrane can remove particles with diameter $0.001 - 0.1$ μm. Therefore, it is mainly used for the removal of viruses. As for nano filtration, it is a pressure related process that applied in drinking water purification process such as discolouring and pollutant removal. In reversed osmosis, the water is passing through a membrane with high pressure and leaving impurities behind.

Effort has been done for the last 20 years on the utilisation of membrane filtration for the removal of pollutants. For instance, low cost $ZnAl_2O_4$-TiO_2 ultra filtration membrane deposited on support made of Moroccan clay was utilised for the elimination of Pb^{2+}, Cr^{3+}, Cd^{2+} and Acid Orange (Saffaj et al., 2004). The ionic interactions between charged species and surface material of the membrane govern the elimination of heavy metals and dye molecules.

23

However, there are some drawbacks in these techniques like high energy consumption and short membrane life due to the clogging problems by dye molecules.

1.11.5 Adsorption

Adsorption involves separation of a substance from gas or liquid phase to a solid surface. The adsorbing phase is known as the adsorbent and the substance adsorbed at the surface of adsorbent is called adsorbate. There are two types of adsorption, namely physisorption and chemisorption. Physisorption is mainly due to the formation of van der Waals forces and electrostatic forces between adsorbate molecules and the surface of the adsorbent. Chemisorption is an irreversible process of the molecules in a surface of adsorbent forming valence bonds with the adsorbate molecules that come into contact with them. Since valence bonds are formed between adsorbate molecules and adsorbent, the adsorbate molecules will occupy certain adsorption sites on the surface and only monolayer of adsorbed molecules is formed. Changes in the electronic state of the molecules can be detected as valence bond is involved.

Adsorption process is widely used for purification of wastewaters by using solids such as activated carbon and synthetic resins as an adsorbent. Activated carbon is a versatile adsorbent due to its superficial chemical groups which can be modified through physical-chemical treatment. For example HNO_3, NH_3 and H_2

gas were used as a reagent in modifying activated carbon (Faria et al., 2004). It is notable that adsorption using activated carbon is an effective method for the removal of different types dye (Al-Degs et al., 2001), metal ions (Gabaldon et al., 2000) and phenols (Dabrowski et al., 2005).

1.12 Significance of Study

Colour is considered as the first pollutant to be identified in wastewater and it is mostly caused by the effluents discharged from dyeing industries such as paper, rubber, cosmetics, textile and plastics. Majority of dyes are visually detected even at the concentration of less than 1 mg/L. In addition, some dyes or their metabolites are either toxic or mutagenic and carcinogenic (Pavan et al., 2007). Thus, the discharge of dyes into water has severe environmental impact and therefore the adsorption of dyes from wastewater has becomes a challenging and perplexing problem.

Other than dyes, the disposal of heavy metals into wastewater has always been a major environmental issue. Since most of the heavy metals are non-degradable and are toxic to aquatic and human life (Agiri et al., 2009), their concentrations have to be reduced to an acceptable level before being discharged into water stream.

In order to overcome this problem, various physicochemical and biological techniques have been studied extensively. Nevertheless, adsorption of

dyes and heavy metals onto activated carbon has been considered as the most efficient method for the removal of various dyes. However, due to the high generation cost of activated carbon (Tsai et al., 2007), many low-cost adsorbents prepared from native agricultural by-products had been investigated as an alternative adsorbent, such as peanut hull, tea dust leaves, paddy straw, wood products, coir pith, baggage pith, degrease coffee bean, maize cob, dehydrated wheat bran and sawdust (Kadirvelu et al., 2003; Ozer et al., 2003; Kaikake et al., 2007; Igwe et al., 2007; Lim et al., 2008).

A wide variety of modifications on these agricultural by-products were introduced in order to enhance their adsorption capacities such as ethylenediamine modified rice husks for the removal of dyes and modified coconut pollen grains for the uptake of heavy metals (Ong et al., 2007; Agiri et al., 2007). Most of the studies indicated that the modified adsorbents are capable of binding either the positively charged or negatively charged species but not both. Nevertheless, a mixture of different dyes is usually found in the industrial effluents. Therefore, it is necessary to have adsorbents that are able to remove different types of dye in either single or binary dye solution.

Typical ways of studying an experiment by retaining other variables involved at a fixed level without describing the combined effect of all variables (Ravikumar et al., 2006). RSM which is an efficient experimental strategy to determine optimal conditions for a multivariable system (Alam et al., 2009) was used to overcome this limitation. The application of RSM in textile industries

might result in improvement of decolourisation process by reducing process variability and time (Tavares et al., 2009). This application has been studied on the optimization of medium composition, fermentation and food process (Weuster-Botz, 2000; Chang et al., 2002; Taveres et al., 2005; Singh et al., 2008).

In this study, RSM was used to optimise the percentage uptake of dyes which is influenced by several independent variables such as pH, initial dye concentration, adsorbent dosage, temperature and contact time. The optimisation is aimed to reduce the cost of adsorption and time.

1.13 Objectives of Study

The objectives of this study are as follow:-

o   To prepare a single low-cost and efficient adsorbent for the removal of basic and reactive dyes as well as heavy metals.

o   To identify the optimal conditions for removal of both dyes under batch and continuous flow conditions.

o   To identify significant variables that affects the uptake of dyes using Plackett Burman.

o   To optimise the conditions for adsorption of dyes using Response Surface Methodology (RSM).

o   Characterisation of the adsorbent using Atomic Force Microscope (AFM), Scanning Electron Microscope (SEM) and Fourier-Transform Infrared Spectroscopy (FTIR).

CHAPTER 2

LITERATURE REVIEWS

2.1 Adsorbent

2.1.1 Activated carbon

Activated carbon is one of the commonly used adsorbents for the removal of dyes owing to its high porosity. Activated carbon can be prepared from different carbonaceous sources such as coconut shell, petroleum coke, sawdust, lignin and rice hulls.

2.1.1.1 Batch study

The use of CMK-5, a tubular structured mesoporous carbon, was studied by Hao et al. (2010) for the removal of industrial dyes, Fuchsin Basic, Acid Red 57 and Reactive Blue 19. It was found that CMK-5 showed high adsorption rate with maximum adsorption capacities of 733, 1131 and 1403 mg/g for Reactive Blue 19, Acid Red 57 and Fuchsin Basic, respectively. CMK-5 can be regenerated using ethanol extraction. The regenerated CMK-5 can reach to 55% of the original adsorption capacity whereas for thermal annealing, 77% of the original adsorption capacity can be achieved. Redlich-Peterson, Freundlich and Langmuir models were used to define the adsorption behavior of these dyes. Based on the

R^2 values obtained, it revealed that the experimental data for both Reactive Blue 19 and Fuchsin Basic were fitted well in Langmuir isotherm whereas for Acid Red 57, the experimental data was well-presented by Redlich-Peterson model.

Amin (2009) studied the utilisation of pomegranate peel for the adsorption of Direct Blue-106. The adsorption of Direct Blue-106 onto pomegranate peel activated carbon was highly dependent on pH, concentration of dye, temperature and contact time. Maximum removal of Direct Blue-106 was observed at pH 12 and equilibrium was achieved at 120 minutes. The experimental data was well presented by Langmuir, Freundlich and Temkin isotherm models as compared to Dubinin-RadushKevich and Harkins-Jura isotherms. From the kinetic study, results indicated that the kinetic data followed pseudo-second order model with intra-particle diffusion as one of the rate-determining steps. The negative value of enthalpy change (ΔH^o) indicated that the adsorption process is an exothermic reaction while the negative entropy change (ΔS^o) suggested the decrease in randomness at the solid-liquid interface during adsorption.

In the study of adsorption of Methylene Blue onto activated carbon prepared from durian shell (DSAC), Chandra et al. (2007) reported that the equilibrium data fitted well in Langmuir isotherm as compared to Freundlich isotherm. The maximum adsorption capacities of DSAC for three different isothermal temperatures are 21.85 mg/g, 21.93 mg/g and 25.27 mg/g at 303.15 K, 313.15 K and 323.15 K, respectively. Three kinetics models were used to evaluate the adsorption kinetics of Methylene Blue, namely pseudo-first order, pseudo-

second order and Langmuir surface kinetics. They found out that the kinetics data were well described by both Langmuir surface kinetics and pseudo-first order models. For pore characteristic, DSAC showed a higher capacity than Filtrasorb 400 activated carbon under nitrogen adsorption isotherm and the pore nature DSAC is a combination of both microporous and mesoporous.

Hema et al. (2007) carried out a comparative study on the adsorption kinetics and thermodynamics of dyes onto acid activated carbon. The adsorption of Congo Red, Rhodamine B and Malachite Green was studied under batch experiments and the equilibrium data agreed well with both Langmuir and Freundlich isotherms. The adsorption of dyes was pH, initial dye concentration and temperature dependent. The positive values for both ΔH^o and ΔS^o indicated that the adsorption of dyes was an endothermic reaction and the degree of disorder increased at the solid-solution interface of the activated carbon. ΔG^o showed a negative value which indicated that the adsorption of Rhodamine B, Congo Red and Malachite Green was a spontaneous process.

The utilisation of activated carbon prepared from bagasse pith (BP) for the removal of Rhodamine B was studied by Gad et al. (2009). Two activating agents, H_3PO_4 and KOH, were used for the preparation of two different activated carbons, namely BPH and BPK, respectively. Results obtained showed that the adsorption capacity of BPH was 198.6 mg/g which is higher than that of BPK by approximately 10 folds. In kinetic study, the experimental data followed pseudo-second order model and the adsorption process was found to be controlled by film

diffusion at the beginning whereas intra-particle diffusion appeared to be more important at the latter stage. The effect of temperature revealed that the adsorption of Rhodamine B is an endothermic process with enthalpy change, $\Delta H^{\circ} = 4.151$ kJ/mol. Adsorption isotherm was analysed using Langmuir, Freundlich, Temkin, Harkins-Jura and Halsey isotherm models. The equilibrium data was well presented by Langmuir isotherm model with high R^2 value (0.997). Desorption of 2.7, 5.4 and 7.8% of adsorbed Rhodamine B was obtained by using water medium, HCl and NaOH, respectively.

Noroozi et al. (2008) investigated the adsorption of Basic Blue 41 and Basic Red 18 onto granular activated carbon (GAC) as well as silkworm pupa (SWP) in single and binary dye solutions. From the nitrogen adsorption analysis, it showed that the pore size of GAC was ranging from 4 to 800 Å whereas for SWP, no significant porosity was found. Langmuir, Freundlich and Myers isotherms were used to model the single dye adsorption and the equilibrium data for both dyes on GAC were best described by Myers isotherm. Adsorption of Basic Red 18 onto SWP showed no correlation with all three isotherm models. However, for Basic Blue 41, the data was well presented in Freundlich isotherm. For binary system, the adsorption data were analysed using extended Langmuir isotherm, Jain and Snoeyink (JS) extended Langmuir isotherm and Ideal Adsorbed Solution Theory (IAST). The evaluation was done by calculating the sum of squares of relative error (SSRE). The adsorption of both dyes on GAC was well described by IAST judging by the low SSRE values. IAST does not predict

the adsorption of dyes on SWP because this model can only be applied to physisorption.

In a study carried out by Khaled et al. (2009), orange peel was converted into activated carbon to enable the uptake of Direct Yellow 12 (DY-12) from aqueous solution. The adsorption of DY-12 onto the activated carbon was dependent on the operating variables such as adsorbent mass, pH, initial dye concentration and contact time. The optimal pH for the uptake of DY-12 was 1.5. For the effect of contact time, results showed that 75% removal was achieved in the first 10 minutes and equilibrium was reached after 120 minutes. Langmuir, Freundlich, Koble-Corrigan, Redlich-Peterson, Tempkin and Dubinin-Radushkevich isotherms were used to investigate the equilibrium data. The data obtained fitted well in all isotherm models except Redlich-Peterson model. The maximum adsorption capacity of the activated carbon was determined to be 75.76 mg/g at room temperature. Kinetic studies showed a good agreement between the experimental data with the second-order kinetic model. The correlation coefficients obtained from this model were equal to unity under all concentrations used.

Ai et al. (2010) carried out a research on the adsorption of Methyl Orange (MO) and Basic Fuchsin (BF) onto activated carbon (AC)/ferrospinel composite. This adsorbent was prepared by a low temperature refluxing method in the presence of AC suspension. Under batch experiments, the adsorption of both dyes was independent of pH value. The adsorption capacities of MO and BF were

increased at the first 5 minutes followed by a slower rate and achieved equilibrium after 30 minutes. Three different isotherm models were used to analyse the adsorption behaviour, namely Langmuir, Freundlich and Dubinin-Radushkevich models. The equilibrium data were well described by Langmuir isotherm judging by the high correlation coefficients for MO (0.9926) and BF (0.9920). Results indicated that the monolayer adsorption capacities of the composite were 95.8 mg/g and 101.0 mg/g for MO and BF, respectively. The kinetic data obtained were best fitted in pseudo-second order kinetic model.

Activated carbon prepared from peach stones by using H_3PO_4 activation was carried out by Attia et al. (2006) for the adsorption of Methylene Blue. Different concentrations of acid were used for the activation process and results revealed that a carbon obtained by 70% H_3PO_4 activation exhibited the best properties. Nitrogen adsorption at 77 K was used to characterise the porosity of the activated carbon and results indicated that this adsorbent is having a surface area of 1400 m^2/g and pore volume up to 0.83 mL/g. Under equilibrium conditions, an adsorption capacity of 400 mg/g was attained for Methylene Blue.

A comparative study between the removal efficiency of 30% KOH treated activated carbon (30%-ACKOH) and activated carbon (AC) for Methylene Blue (MB) was done by Yasin et al. (2007). The effect of pH, contact time and adsorbent dosage in the removal of MB was examined and it showed that the percentage removal increases with an increase in contact time, pH and adsorbent dosage. The experimental results for both 30%-ACKOH and AC were well

presented by Langmuir isotherm model. The adsorption capacity of 30%-ACKOH and AC are 45.8 mg/g and 17.8 mg/g, respectively.

The utilisation of bamboo-based activated carbon for the removal of Methylene Blue was studied by Hameed et al. (2007). Potassium hydroxide (KOH) and carbon dioxide were used to activate bamboo at 850^oC for 2 hours. The BET surface area, total pore volume and average pore diameter for the activated carbon was found to be 1896 m^2/g, 1.109cm^3/g and 2.34 nm, respectively. Two isotherm models were employed in this study, namely Langmuir and Freundlich isotherms. The adsorption behaviour was well described by Langmuir isotherm with maximum adsorption capacity of 454.2 mg/g. The kinetics data was found to be followed the pseudo second-order model.

Fairus et al. (2007) studied the adsorption of Methylene Blue (MB) from aqueous solutions using activated carbon prepared from palm oil fibre. The adsorption behaviour of MB onto activated carbon was evaluated under batch parameters such as contact time, initial concentration, pH and adsorbent dose. It revealed that the percentage removal of MB increased with an increase in adsorbent dose but decreased with increasing initial dye concentration. MB was effectively being removed at all pH ranging from pH 3 to 9. Equilibrium was attained after 90 minutes and the data fitted well in both Langmuir and Freundlich isotherms. The maximum adsorption capacity was found to be 26.65 mg/g.

The removal of Reactive Orange (RO) using activated carbon prepared from sugarcane bagasse pith was studied by Amin. (2008). Two methods were used for the activation of sugarcane bagasse pith, namely chemical and physical activations. For chemical method, two types of activated carbon were prepared, AC1 by 28%, H_3PO_4 activation and AC2 by 50% $ZnCl_2$ followed by pyrolysis at 600^oC. For physical method, bagasse pith was treated at 600^oC in the absence of air and labelled as AC3. Under batch condition, it was found that the adsorption of RO was highly dependent on contact time, adsorbent dosage and initial dye concentration. The equilibrium data was well described by both Freundlich and Langmuir isotherm models. It was reported that the maximum adsorption capacities of AC1, AC2 and AC3 were 3.48, 2.83 and 1.80 mg/g, respectively. As for kinetics data, it was well described by pseudo second-order model. The adsorption process was governed by both external mass transfer and intraparticle diffusion.

2.1.1.2 Column study

Al-Degs et al. (2009) studied the adsorption characteristics of reactive dyes in fixed bed column of activated carbon. From the mass transfer zone (MTZ) characteristics of Reactive Yellow and Reactive Black, it showed that a better column adsorption was achieved at diluted influent concentration and with longer bed depth. The maximum adsorption capacity of Reactive Yellow was 0.74 kg/kg which was 2.5 fold higher than that of Reactive Black. Results showed that a service time of 36.5 hours was needed for the adsorption of Reactive Yellow to

achieve 90 % column exhaustion at a bed depth of 0.09 m, influent dye concentration of 0.19 kg/m^3, flow rate at 5.0 X 10^{-6} m^3/min, pH 5 and particle diameter ranging from 600-700 µm.

The removal of Acid Blue 92 and Basic Red 29 was investigated by Sivakumar et al. (2009) under packed bed column prepared from *Euphorbia antiquorum L* activated carbon. The adsorption of both dyes increased with increasing influent concentration and bed depth but decreased when higher flow rate was employed. Two mathematical models, namely Thomas and Yoon-Nelson models were used to evaluate the performance of column and results obtained revealed that the maximum adsorption capacity of Acid Blue 92 and Basic Red 29 were 275.5 mg/g and 140.8 mg/g, respectively. In addition, the adsorption behaviour of dyes fitted well in Yoon-Nelson model with correlation coefficient higher than that of Thomas model.

The summary for some of the reported works on the adsorption capacities of dyes by activated carbon was shown in Table 2.1.

Table 2.1: Adsorption capacities of dyes by activated carbon

Adsorbent	Dye	Adsorption capacity	References
Tubular structured ordered mesoporous carbon (CMK 5)	Reactive Blue 19 Reactive Red 57 Fuchsin Basic	733.00 mg/g 1131.00 mg/g 1403.00 mg/g	Hao et al. (2010)
Activated carbon/ Ferrospinel composite	Methyl Orange Fuchsin Basic	95.80 mg/g 101.00 mg/g	Ai et al. (2010)
Activated carbon prepared from bagasse pith (BPH)	Rhodamine B	198.60 mg/g	Gad et al. (2009)
Activated carbon prepared from orange peel	Direct Yellow 12	75.76 mg/g	Khaled et al. (2009)
Euphorbia antiquorum L activated carbon	Acid Blue 92 Basic Red 29	275.50 mg/g 140.80 mg/g	Sivakumar et al. (2009)
Activated carbon	Reactive Yellow Reactive Black	0.74 kg/kg 0.30 kg/kg	Al-Degs et al. (2008)
Activated carbon prepared from peach stone	Methylene Blue	400 mg/g	Attia et al. (2008)
Activated carbon prepared from sugarcane bagasse	Reactive Orange	3.48 mg/g	Amin. (2008)
Activated carbon prepared from durian shell (DSAC)	Methylene Blue	25.27 mg/g	Chandra et al. (2007)
30% KOH activated carbon	Methylene Blue	45.8 mg/g	Yasin et al. (2007)
Bamboo based activated carbon	Methylene Blue	454.2 mg/g	Hameed et al. (2007)
Activated carbon prepared from palm oil fibre	Methylene Blue	26.65 mg/g	Fairus et al. (2007)

2.1.2 Agricultural Wastes

Although activated carbon is an adsorbent with high adsorption capacity, this feature, however, do not make it as an attractive and economical adsorbent due to its high generation and regeneration cost (Tsai et al., 2007). As such, much of the effort has been devoted to prepare low cost adsorbents from native agricultural wastes as an alternative adsorbent.

2.1.2.1 Batch study

The potential of durian peel (DP) as an adsorbent was investigated by Hameed et al. (2008). DP was used for the adsorption of Acid Green 25 (AG25) under batch conditions with various initial dye concentrations, pH and temperature. The removal efficiency of AG25 decreased with an increase in temperature and pH. However, the adsorption capacity increased from 27.31 to 56.57 mg/g with increasing initial dye concentration. This is because the initial concentration provides the necessary driving force to overcome the resistance of the mass transfer of dye between the aqueous and solid phase. The interaction between dye and the DP adsorbent also increased with increasing initial dye concentration. Results from both Langmuir and Freundlich isotherms proved that the equilibrium data was in agreement with Langmuir model with maximum adsorption capacity of 63.29 mg/g. Kinetic studies indicated that the adsorption of AG25 followed pseudo second-order equation at 30°C.

Oliveira et al. (2008) studied the utilisation of untreated coffee husk as an adsorbent for the adsorption of Methylene Blue (MB) under various batch conditions such as temperature, contact time, adsorbent dosage and pH. The adsorption data was well described by Langmuir model. Maximum adsorption capacity of untreated coffee husk was found to be 90.09, 111.11 and 72.99 mg/g at temperature of $30^{o}C$, $40^{o}C$ and $50^{o}C$, respectively. The thermodynamic parameters were also evaluated in this study and showed that the adsorption of MB was a spontaneous and endothermic process. The adsorption process followed pseudo second-order equation. Variation of pH value from 3 to 11 demonstrated no convincing effect on the removal of MB.

Ponnusami et al. (2008) utilised guava leaf powder (GLP) as low cost adsorbent for the treatment of aqueous solution containing Methylene Blue (MB). The potential of GLP for the removal of MB was found to be excellent under both batch and continuous flow studies. The adsorption behaviour of MB onto GLP was tested under the effect of pH, adsorbent dosage, temperature, initial concentration and particle size. The experimental data revealed that it fitted well in Langmuir isotherm with high maximum adsorption capacity, 295 mg/g. From the kinetic studies, the adsorption of MB onto GLP was well described by pseudo second-order model and both external and intraparticle diffusion play important role in the adsorption process.

Yellow passion fruit peel was utilised as an adsorbent for the adsorption of Methylene Blue (MB) by Pavan et al. (2008). In this study, the adsorption of MB was evaluated under the effect of pH and contact time. The removal efficiency of MB was pH dependent with optimum pH values ranging from 7-10. The percentage uptake of MB was also affected by contact time and a duration of 50 hours was required to attain equilibrium. From the Langmuir isotherm, the maximum adsorption capacity of yellow passion fruit peel was 0.0068 mmol/g.

Uddin et al. (2009) studied the potentiality of tea waste for the adsorption of Methylene Blue from aqueous solution. The removal of Methylene Blue was affected by pH, contact time, dye concentration and adsorbent dosage. Results showed that the adsorption equilibrium was attained after 5 hours. By varying the pH value from 3 to 10, it was found that the percentage removal of Methylene Blue increased with increasing pH from 3 to 5. This is closely related to the pH_{pzc} of tea waste which is 4.3 ± 0.2. Therefore, at pH higher than pH_{pzc}, the surface of tea waste is negatively charged and hence favoured the adsorption of Methylene Blue. Kinetic studies indicated that the data followed pseudo-second order model. For adsorption isotherm, the equilibrium data was well presented using Langmuir isotherm model with maximum adsorption capacity of 85.16 mg/g. Desorption of Methylene Blue was carried out as a function of pH and the results obtained indicated that the adsorption process followed ion-exchange mechanism and it was reversible.

The removal of Congo Red (CR) from aqueous solution using Cashew nut shell (CNS) was studied by Kumar et al. (2010). The adsorption of CR has been found to be dependent of initial dye concentration and adsorbent dosage. Maximum removal of CR was observed at pH 3 and below. This is because low pH leads to an increase in H^+ ions and the surface of CNS will acquire positively charge by adsorbing H^+ ions. Hence, this favours the adsorption of the anionic dye molecules. The specific surface area and pore structure of CNS was calculated by using BET equation. Results showed that the BET surface area, pore volume, average pore diameter and bulk density of CNS were 395 m^2/g, 0.4732 cm^3/g, 5.89 nm and 0.415g/cm^3, respectively. The thermodynamic studies indicated that the adsorption process is spontaneous and exothermic in nature. At all the studied initial dye concentrations, straight lines were obtained with high correlation coefficients (>0.998) for the plot of t/q_t versus t. This suggested that the experimental data were well presented by pseudo-second order kinetic model.

2.1.2.2 Column study

Low cost sugarcane bagasse ash was used by Kanawade et al. (2010) as adsorbent for the removal of Acid Orange-II from aqueous solution. The effect of bed depth and flow rate on the breakthrough curves was investigated. Two mathematical models, namely Thomas and Yoon-Nelson models were used to test for the suitability of surgacane bagasse as an adsorbent. Results showed that the predicted breakthrough curves from both models agreed well with the

experimental curves. They also found that the percentage removal of Acid Orange-II increased with increasing bed depth and decreasing flow rate.

The removal of Congo red by using rice husk from aqueous solution was studied by Han et al. (2008). The effects of initial pH, flow rate, influent concentration of Congo Red were studied. Yoon-Nelson, Thomas and Adam-Bohart models were employed to predict the breakthrough curves using non-linear regression and to determine the characteristic parameters of the column useful for process design. Bed depth service time (BDST) analysis model was used to describe the effect of bed depth on the breakthrough curves. The result fitted well in Thomas model. As for Adams-Bohart model, it was well presented only for an initial part of the dynamic behavior of the rice husk column. The experimental data were agreeable with the BDST model in predicting the breakthrough curve.

Column studies were conducted by Han et al. (2007) by using rice husk as for the uptake of MB. Important variables such as initial pH value, existed salt, flow rate, influent concentration of MB and bed depth were studied. The data obtained from different variables were fitted into the Thomas mathematical model, in order to obtain the predicted breakthrough curves and the process design of the column. As for different bed-depth, the BDST model was applied to predict the breakthrough curves. Both of the models were found suitable for describing the adsorption process of rice husk in column study. Results suggested that the optimised conditions for rice husk to remove MB from solution are with flow rate

of 8.2 mL/min and the influent concentration of 50 mg/L. According to the Thomas model, the equilibrium adsorption of the biomass is 4.41 mg/g.

The summary of the adsorption capacities of dye by some agricultural wastes is shown in Table 2.2.

Table 2.2: Adsorption capacities of dyes by agricultural waste

Adsorbent	Dye	Adsorption capacity	References
Tea wastes	Methylene Blue	85.16 mg/g	Uddin et al. (2009)
Jackfruit peel	Methylene Blue	285.71 mg/g	Hameed (2008c)
Durian peel (DP)	Acid Green 25 (AG25)	56.57 mg/g	Hameed et al. (2008)
Coffee husk	Methylene Blue	111.11 mg/g	Oliveira et al. (2008)
Guava leaf powder (GLP)	Methylene Blue	295.00 mg/g	Ponnusami et al. (2008)
Yellow passion fruit peel	Methylene Blue	0.0068 mmol/g	Pavan et al. (2008)
Papaya seeds	Methylene Blue	555.56 mg/g	Hameed (2008b)
Banana stalk	Methylene Blue	243.90 mg/g	Hameed et al. (2008)
Castor seed shell	Methylene Blue	158.00 mg/g	Oladoja et al. (2008)
Rice husk	Methylene Blue	40.58 mg/g	Vadivelan and Kumar. (2005)
Peanut hull	Basic Blue 3 Basic Red 22 Basic Yellow 21	63.00 mg/g 48.00 mg/g 56.00 mg/g	Matthews. (2003)

2.1.3   Chemically modified agricultural wastes

Most of the studies indicated that agricultural by-products showed high adsorption capacity for the removal of dyes, however, the removal efficiency is

restricted to a specific pollutant and therefore, the adsorbent had been modified using various chemicals in order to enhance its efficiency in binding most of the desired pollutants (Wong et al., 2003; Ong et al., 2009a).

2.1.3.1 Batch study

The potential of ethylenediamine (EDA) rice hull as an adsorbent for the uptake of both reactive and basic dyes was explored by Ong et al. (2007). The adsorption behaviour of Reactive Orange 16 (RO16) and Basic Blue 3 onto EDA rice hull was evaluated and results indicated that the removal of both dyes either in single or binary dye solutions was highly depended on pH, particle size, initial dye concentration, agitation rate and adsorbent dosage. Experimental data showed a better correlation to pseudo second-order kinetic model as compared to pseudo first-order. Both Langmuir and Freundlich isotherms provided a good description for the equilibrium data and the adsorption capacity for both BB3 and RO16 was found to be 14.68 and 60.24 mg/g, respectively. The authors suggested that there is a synergistic effect on the adsorption of both dyes in binary solutions.

Surface modification of coir pith was performed by Namasivayam et al. (2006) using hexadecyltrimethylammonium bromide. The feasibility of this modified coir pith for the adsorption of Acid Brilliant Blue and Procion Orange was tested using Langmuir and Freundlich isotherms. The equilibrium data fitted well in both models with maximum adsorption capacity of 159 and 89 mg/g for Acid Brilliant Blue and Procion Orange, respectively. The adsorption kinetics of

both dyes onto modified coir pith obeyed pseudo second-order model. They suggested that the mechanism for the adsorption process involved chemisorption and ion exchange. The same modified coir pith was also used for the removal of Direct Red 12B and Rhodamine B in a study carried out by Sureshkumar et al. (2008). The maximum adsorption capacity for Direct Red 12B and Rhodamine B was 76.3 mg/g and 14.9 mg/g, respectively.

In a study by Saad et al. (2010), batch experiments were conducted using phosphoric acid modified sugarcane bagasse (SBC) as the low cost adsorbent for the removal of Methyl Red (MR). The adsorption performance of SBC was tested under the effect of initial dye concentration, contact time, pH and adsorbent dosage in comparison with natural sugarcane bagasse (SB) as well as powedered activated carbon (PAC). Results indicated that the adsorption efficiency of the three adsorbents can be arranged in the following order PAC > SBC > SB. The equilibrium time for SBC was attained at 180 minutes and pH values from 2 to 6 were the optimum pH for the removal of MR by SBC. In this study, it was proven that when adsorbent dosage increases, the percentage removal of MR also increased. The experimental data showed that it followed pseudo-second order kinetic model and Langmuir isotherm. The maximum adsorption capacity of SB, SBC and PAC were found to be 5.66, 10.98 and 48.42 mg/g, respectively.

Gong et al. (2005) utilised oxalic acid modified rice straw as an adsorbent for the removal of Basic Blue 9 and Basic Green 4. Results obtained revealed that the removal of both Basic Blue 9 and Basic Green 4 was kept above 97% with

initial dye concentration ranging from 50 to 250 mg/L and with 2 g/L of adsorbent being used. The effect of ion strength in the removal Basic Blue 9 and Basic Green 4 was examined with the addition of sodium chloride. Results showed that the removal of dye decreased with increasing amount of sodium chloride. This is due to the competition between dye molecules and Na^+ ions for the adsorption site.

Janos et al. (2009) explored the adsorption of both Methylene Blue (MB) and Egacid Orange onto chemically modified wood shavings. Better adsorption ability for MB was observed for both Na_2CO_3 and Na_2HPO_4 treated wood shavings whereas HCl treated wood shavings showed a good adsorption capacity for Egacid Orange. The equilibrium data obtained fitted well into Langmuir-Freundlich isotherm with maximum adsorption capacities ranging from 0.060 to 0.165 mmol/g and 0.045 to 0.513 mmol/g for MB and Egacid Orange, respectively. Adsorption of both dyes onto modified wood shavings was found to be pH dependent. A higher pH favoured the adsorption of Egacid Orange whereas the opposite trend is better in the removal of MB.

2.1.3.2 Surface characterisation

Surface characterisation of ethylenediamine (EDA) modified rice hull was carried out by Ong et al. (2010) by scanning electron microscopy (SEM) and atomic force microscope (AFM). The results revealed that there is only a minimal change between natural and modified rice hull. Both adsorbent appeared to be

non-porous materials. From the AFM analysis, it showed that the grain size in NRH was ranging from 0.718 to 2.364 μm which is larger compared to MRH ranging from 1.370-2.085 μm. The average surface roughness also increased by 160.6 nm after the introduction of amine groups. From the Fourier-Transform Infrared Spectroscopy (FTIR) analysis, the presence of amide functional group on surface of MRH was proven by the N-H bands together with the unusual low value for C=O stretch.

In a study carried out by Oei et al. (2009), the surfactant modified barley straw (SMBS) was used as an adsorbent for the adsorption of Acid Blue 40 (AB40) and Reactive Black 5 (RB5). The impregnation of a surfactant cetylpyridinium chloride (CPC) enhanced the positive charge on the surface of barley straw which leads to a strong attraction forces between the negatively charged dyes and the modified barley straw. From Langmuir isotherm, it showed that the maximum adsorption capacity of AB40 and RB5 were 1.02×10^{-4} mol/g and 2.54×10^{-5} mol/g, respectively. Nitrogen adsorption isotherm proved that SMBS was a non-porous structure with pore size distribution ranging from 15 to 60 Å. FTIR spectrum of SMBS revealed that there was a very intense peak in the region 1742-1620 cm^{-1} which indicates the presence of carbonyl groups. The peak close to 2400 cm^{-1} indicating the presence of C-C group and this peak was not observed in the spectrum of raw barley straw. The presence of C-C group might due to the introduction of the surfactant.

Table 2.3 summarised some of the adsorption capacities of dyes by chemically modified agricultural wastes.

2.1.4 Industrial Waste Materials

Other than agricultural waste, waste from industrial processes may also be used as an alternative adsorbent in removing pollutants since large amount of wastes would lead to disposal problem.

2.1.4.1 Batch study

Lignin is one of the by-products in pulp industry which can be used to remove dyes from textile wastewater. The potential of lignin for the removal of Brilliant Red HE-3B reactive dye was investigated by Suteu et al. (2010) under batch condition. Results showed that the optimum pH for the removal of reactive dye is 1.5. For the effect of contact time, maximum adsorption of dye was observed at 1.5 hours. The equilibrium adsorption data were fitted into Langmuir, Freundlich, Dubinin-Radushkevich and Tempkin isotherm models. The data were well presented by Langmuir isotherm with correlation coefficient of 0.9982. The maximum adsorption capacity of Brilliant Red HE-3B was found to be 10.173 mg/g at $20^{\circ}C$. As for thermodynamic parameters, values obtained for ΔG° were negative whereas for both ΔH° and ΔS° were positive. These values indicated that adsorption of reactive dye is a spontaneous, endothermic and entropy-driven process. Kinetic studies showed a good agreement of experimental data with

pseudo-second order model, indicating the chemisorption of reactive dye onto lignin.

Table 2.3: Adsorption capacities of dyes by chemically modified agricultural wastes

Adsorbent	Dye	Adsorption capacity	References
Phosphoric acid modified sugarcane bagasse (SBC)	Methyl Red	10.98 mg/g	Saad et al. (2010)
Surfactant modified barley straw (SMBS)	Acid Blue 40	1.02×10^{-4} mol/g	Oei et al. (2009)
	Reactive Black 5	2.54×10^{-5} mol/g	
Na_2CO_3 modified wood shavings	MB	0.06 mmol/g	Janos et al. (2009)
	Egacid Orange	0.165 mmol/g	
HCl wood shavings	MB	0.045 mmol/g	
	Egacid Orange	0.513 mmol/g	
Ethylenediamine modified rice hulls	Basic Blue 3	14.68 mg/g	Ong et al. (2007)
	Reactive Orange 16	60.24 mg/g	
Hexadecyltrimethylammonium bromide modified coir pith	Acid Brilliant Blue	159.00 mg/g	Namasivayam et al. (2006)
	Procion Orange	89.00 mg/g	
	Rhodamine B	14.90 mg/g	Sureshkumar et al. (2008)
	Direct Red 12B	76.30 mg/g	

Atar et al. (2009) studied the removal of Basic Blue 41 and Acid Blue 225 by using boron waste as a low cost adsorbent. Batch experiments were carried out

with different operating variables such as initial dye concentration, contact time, solution pH and adsorbent dosage. Results indicated that the optimum pH for the removal of Basic Blue 41 and Acid Blue 225 were pH 9 and 1, respectively. The zeta potential measurements in boron waste containing solutions against pH have shown that boron waste exhibits a negative charge at pH > 4.1 and positive charge at pH < 4.1. Hence, at higher pH, the adsorption of Basic Blue 41 was higher due to the presence of $-NH_3^+$ groups in its structure whereas for Acid Blue 225, the percent removal was higher at lower pH due to the presence of SO_3^- groups. The percentage removal of both dyes increased with increasing contact time and adsorbent dosage. SEM showed that there was a difference in the surface morphology before and after adsorption. Boron waste consists of tiny particles of various sizes, however, after adsorption, the intraparticle spaces between particles disappeared. This is due to the formation of a monolayer of adsorbate over the adsorbent surface after the adsorption process.

Bottom ash generated from municipal solid waste incinerator (MSWI) was converted into low cost adsorbent by Gupta et al. (2005) for the removal of Alizarin Yellow, Fast Green and Methyl Violet from wastewater. Under batch conditions, it has been found that Alizarin Yellow, Fast Green and Methyl Violet were adsorbed by 87.5%, 97% and 73%, respectively. The optimum contact time for these dyes was found to be 4 hours. As for the effect of pH, maximum adsorption was observed at pH 5.5, 5.0 and 8.0 for Alizarin Yellow, Fast Green and Methyl Violet, respectively. Results indicated that the equilibrium data fitted well in both Freundlich and Langmuir isotherm models. Thermodynamic

parameters such as free energy (ΔG^{o}), enthalpy change (ΔH^{o}) and entropy (ΔS^{o}) were evaluated. The negative values of enthalpy change for Alizarin Yellow and Fast Green are due to the exothermic nature of adsorption whereas the positive values of enthalpy for Methyl Violet indicate endothermic adsorption.

2.1.5   Other Adsorbents

2.1.5.1 Batch study

Humic acid immobilized polyacrylamide bentonite composites with amine functionality (HA-Am-PAA-B) was used as an adsorbent by Anirudhan et al. (2009) for the removal of Malachite Green (MG), Methylene Blue (MB) and Crystal Violet (CV). The adsorption equilibrium was attained within 1 hour and maximum dye removal was observed at pH 5 to 8. Three well-known kinetic models were employed to describe the kinetic data, namely pseudo-first order, pseudo-second order and Elovich kinetic models. By comparing the R^{2} value, it was found that the kinetic data was well described by pseudo-second order model. As for adsorption isotherm, Langmuir isotherm showed a better fit for the equilibrium data. The maximum adsorption capacity for MG, MB and CV were found to be 656.5 µmol/g, 648.4 µmol/g and 510.4 µmol/g, respectively. Regeneration of spent adsorbent was carried out using 0.1 M HNO_3 and results showed that the adsorbent can be reused for four cycles.

Adsorption of Congo Red onto $Ni(OH)_2$ and NiO nanosheets was investigated by Cheng et al. (2010). The nanosheets were synthesised by a simple chemical precipitation method using nickel chloride as precursors and urea as precipitating agent. Both $Ni(OH)_2$ and NiO nanosheets were characterised by X-Ray diffraction, SEM and nitrogen adsorption-desorption isotherms. Results showed that the pore structure of $Ni(OH)_2$ and NiO nanosheets are composed of at least three levels of hierarchical porous organization. The equilibrium data was well presented by Langmuir isotherm and it was reported that the maximum adsorption capacity for both $Ni(OH)_2$ and NiO was found to be 82.9 mg/g and 151.7 mg/g, respectively. Pseudo-second order and intraparticle diffusion models showed a better description for the adsorption kinetics.

Cheung et al. (2009) investigated the potentiality of nanochitosan as an adsorbent for the removal of Acid Orange 10 (AO10), Acid Orange 12 (AO12), Acid Red 18 (AR18) and Acid Red 73 (AR73). The nanochitosan was prepared in a suspension form by adding drop-wise of tripolyphosphate solution into a chitosan solution. Based on the results obtained from the analysis of equilibrium data using Langmuir, Freundlich and Redlich-Peterson isotherms, the data for AO10, AO12 and AR18 were well fitted in Langmuir isotherm whereas for AR73, it was well described by Redlich-Peterson isotherm. The maximum adsorption capacity of AO10, AO12, AR18 and AR73 were determined to be 1.77, 4.33, 1.37 and 2.13 mmol/g, respectively. From the results obtained, it showed that smaller dye molecule sizes have superior adsorption capacity due to

deeper penetration of dye molecules into the internal pore structure of nanochitosan.

The decolourization of dye wastewaters using tourmaline (non-metallic mineral) was investigated by Guan et al. (2009). Experimental data showed that tourmaline has selectivity on Acid Blue Black and the maximum adsorption of 1000 g of tourmaline was 18 g of dye. Results also indicated that tourmaline decolourization is a combined action of chemical and physical adsorption.

Asuha et al. (2010) investigated the adsorption of Methyl Orange using mesoporous TiO_2 prepared by hydrothermal method. In this method, cetyltrimethylammonium bromide (CTAB) was used as a structure-directing agent. Results from transmission electron micrograph (TEM) and nitrogen adsorption –desorption study showed that mesoporous TiO_2 has an average pore size of 5.2 nm and surface area of 161.2 m^2/g. The maximum adsorption capacity for Methyl Orange was 454.5 mg/g.

The summary of adsorption capacities of dyes by industrial wastes and other adsorbents was shown in Table 2.4.

Table 2.4: Adsorption capacities of dyes by industrial wastes and other adsorbents

Adsorbent	Dye	Adsorption capacity	References
Lignin	Brilliant Red HE-3B	10.17 mg/g	Suteu et al. (2010)
Mesoporous TiO$_2$	Methyl Orange3	454.50 mg/g	Asuha et al. (2010)
Ni(OH)$_2$ nanosheet	Congo Red	82.90 mg/g	Cheng et al. (2010)
NiO nanosheet	Congo Red	151.70 mg/g	
Humic acid immobilized polyacrylamide bentonite composite	Malachite Green	656.50 µmol/g	Anirudhan et al. (2009)
	Methylene Blue	648.40 µmol/g	
	Crystal Violet	510.40 µmol/g	
Nanochitosan	Acid Orange 10	1.77 mmol/g	Cheung et al. (2009)
	Acid Orange 12	4.33 mmol/g	
	Acid Red 18	1.37 mmol/g	
	Acid Red 73	2.13 mmol/g	
Tourmaline	Acid Blue Black	18.00 g/1000g	Guan et al. (2009)

2.2   Response Surface Methodology

RSM is a collection of mathematical and statistical techniques for empirical model building. The objective of RSM is to optimise the output variable (response) of an experiment which is influenced by various input variables.

The optimum conditions for the preparation of activated carbon from rattan sawdust (RSAC) were investigated by Ahmad et al. (2009) using RSM. The effect of activation temperature, activation time and chemical impregnation ratio

on the activated carbon yield as well as the percentage removal of Disperse Orange 30 were evaluated based on a three-variable central composite design. Through the analysis, it was found that the activation temperature and chemical impregnation ratio have significant effects on activated carbon yield. The R^2 values of the response parameters indicated a good fit of the quadratic model with experimental data. From the SEM image, the RSAC prepared under optimum condition was found to have well developed pores in its surface. Results showed that the BET surface area of RSAC was 1037.18 m^2/g and various functional groups have been identified from the FTIR spectrum such as quinone and aromatic ring. The maximum adsorption capacity of RSAC was found to be 133 mg/g based on Langmuir isotherm.

The decolourisation of Acid Red 151 using a fungal isolate *Aspergillus fumigates Fresenius* has been studied by Sharma et al. (2009). Central composite design (CCD) matrix and RSM were applied in designing 20 experiments with different variables such as temperature, pH and initial dye concentration. The interactive effects between variables were tested and results obtained showed a high regression coefficient between all the variables ($R^2 = 0.9934$). This indicated that the designed model was feasible with negligible variations. The optimum conditions for the degradation of Acid Red 151 are at pH 5.5, temperature of 30°C and 150 mg/L of initial dye concentration.

The removal of Methylene Blue (MB) using lignin peroxidise enzyme (LiP) produced from white-rot-fungus *Phanerochaete chrysosporium* was

investigated by Alam et al. (2009). Optimisation of experimental conditions was carried out using one-factor-at-a-time (OFAT) and RSM. For OFAT, it indicated that the optimum condition for the removal of MB was at pH 5.0 with H_2O_2 concentration of 4.0 mM, initial dye concentration of 20 mg/L and LiP activity 0.487 U/mL. Whilst for RSM, the initial dye concentration and activity of LiP enzyme were optimised at 15 mg/L and 0.687 U/mL, respectively. Statistical data showed that percentage removal of MB was 65% and 90% in static mode and agitated mode, respectively.

Tavares et al. (2009) applied the statistical experimental design (Three-level Box-Behnken factorial design) together with RSM to optimise the dye decolourisation of Reactive Red 239, Reactive Yellow 15 and Reactive Blue 114 using commercial laccase. From the analysis of variance (ANOVA), the suggested models presented high correlation coefficients (R^2), 0.99363, 0.99983 and 0.99804 for the degradation of Reactive Yellow 15, Reactive Red 239 and Reactive Blue 114, respectively which indicate the accuracy of the quadratic polynomial models was good. pH was found to be the only significant factor that affects the degradation of three dyes whilst temperature and enzyme concentration presented low or no effect on dye degradation. The optimum pH value for the percentage removal of 90% and above was found to be 6.6 for Reactive Yellow 15, 5.5 to 7.0 for Reactive Blue 114 and 7.0 to 7.5 for Reactive Red 239.

Guven et al. (2008) explored the electrochemical treatment of deproteinated whey wastewater produced from cheese manufacture. From

preliminary studies, the suitable electrode used for electrochemical treatment was found to be iron owing to its high removal efficiency of chemical oxygen demand (COD) and turbidity. The treatment conditions were optimised using RSM. A series of experimental conditions were generated by CCD and the effects of independent variable as well as the interactive effect between variables were studied. The optimum condition for the effective removal of COD were as follows, 11.29 V applied voltage, 100% waste concentration (40 g/L lactose) and 19.87 g/L electrolyte concentration (NaCl).

Pinheiro et al. (2008) employed the CCD in designing a series of experimental runs with different independent variables for the extraction of high-ester pectin from passion fruit peel with citric acid. Citric acid concentration and extraction time were the two variables that being investigated in this study. RSM was used to optimise the experimental conditions for better extraction. From the analysis of variance (ANOVA), the regression was found to be significant, lack of fit showed the opposite and the pure error was low. Moreover, the correlation coefficient was high (0.99) which indicates that the data fitted well in the quadratic model. RSM analysis showed that the optimum conditions for the extraction were 0.086% w/v citric acid and 60 minutes of extraction time.

Biobleaching of paper pulp in an expanded bed bioreactor with immobilised alkali stable xylanase from *Aspergillus fischeri* was studied by Senthikumar et al. (2008). In order to optimise the condition for biobleaching the paper pulp in a continuous mode, RSM and central composite rotatable design

(CCRD) were employed. The combined effect of independent variables in this study was investigated such as temperature, flow rate and concentration of the pulp. Response of the variables was measured by assessing the kappa number of the pulp. Kappa number is defined as the amount of 0.1N potassium permanganate solution consumed by 1.0 g of dry pulp. Reduction in kappa number, from 66 to 20 was observed which proved that the alkali stable xylanase was effective in the biobleaching of paper pulp. The authors reported that the optimum condition for the biobleaching process were at 60^oC, 5% w/v pulp concentration and flow rate of 2 ml/min.

2.3 Removal of Heavy metals

Metal ions produced and released during industrial activities may pose a serious threat to the environment and these metal ions can be harmful to aquatic life and human health (Agiri et al., 2009). Hence a number of studies had been done in order to remove heavy metal using adsorption method.

2.3.1   Activated Carbon

2.3.1.1 Batch study

The adsorption isotherm of Pb (II), Cu (II), Cr (II) and Co (II) ions onto activated carbon was studied by Abbas et al. (2012). Six adsorption isotherm models were used to examine the equilibrium data, namely Radk-Prausnitz, Sips

and Temkin, Redlich-Peterson, Freundlich and Langmuir isotherms. The equilibrium data indicated best fit to Radk-Prausnitz, Langmuir, Redlich-Peterson and Sips isotherm models with correlation coefficient (R^2) value ranging from 0.999 to 0.978. As for Freundlich and Temkin isotherms, the R^2 values are 0.971 and 0.937, respectively. The data obtained was best fitted with pseudo-second order model ($R^2 = 0.999$) as compared with pseudo-first order model.

Adie et al. (2012) carried out a study to compare the adsorption of Pb (II) and Cd (II) ions using activated carbon from Borassus aethiopum seed shells (BASS) and Cocos nucifera shells (CONS). Pseudo-first order and pseudo-second order models were employed to describe the kinetic data. Results showed that the data was well described by pseudo-second order model. From statistical analysis, pseudo-second order model was found to be statistically significant (for both metal ions using activated BASS and CONS) based higher correlation coefficients (0.998 to 0.996) and lower values of total error (1.4 X 10^{-3} to 1.0 X 10^{-2}), root mean square error (0.01 to 0.06) and Chi squared (3.2 X 10^{-4} to 3.9 X 10^{-2}). The equilibrium data were well represented by both Langmuir and Freundlich isotherm models. The maximum adsorption capacity for Pb (II) ion was found to be 12.19 mg/g and 24.39 mg/g for activated BASS and CONS, respectively. As for Cd (II) ion, the maximum adsorption capacity was 10.20 mg/g and 25.80 mg/g, for activated BASS and CONS, respectively.

A study of the removal of Pb (II) ion from industrial wastewater by activated carbon prepared from Periwinkle shells was conducted by Badmus et al.

(2007). The mechanisms of the rate of adsorption were analysed using both Elovich equation and pseudo-second order equation. Experimental data showed that the correlation coefficient (R^2) for pseudo-second order equation and Elovich equation are 0.9274 and 0.903, respectively. A higher R^2 obtained through the pseudo-second order equation indicates that the kinetic data is well explained by this model. On the basic of the excellent fit of the pseudo-second order equation, it was concluded that the main adsorption mechanism was probably a chemisorption.

Sudha et al. (2007) explored the removal of copper ion onto acid activated Pandanus carbon by varying the contact time as well as initial metal ion concentration. Results showed that the percentage uptake of copper ion decreased with an increase in initial metal ion concentration, but in fact, the actual amount of metal ions adsorbed per unit mass of carbon increased with increase in metal ion concentration. For all studied concentrations, equilibrium was achieved within the first 40 minutes.

2.3.2   Agricultural Wastes

2.3.2.1 Batch study

The removal of lead, copper and zinc ions using sawdust was investigated by Lim et al. (2007). It was found that the adsorption of metal ions on sawdust increased with increasing adsorbent dosage and pH. The equilibrium data was

evaluated by using Langmuir and Freundlich isotherm models and results indicated that the data fitted well in both models. The maximum adsorption capacity for lead, copper and zinc ions were 26 milligrams per gram, 22.5 milligrams per gram and 19.75 milligrams per gram, respectively. In the presence of other cations such as magnesium and calcium ions, the adsorption of lead, copper, and zinc was depressed. Kinetic studies showed that the adsorption process followed pseudo-second order model. The intraparticle diffusion studies showed that surface adsorption and pore diffusion were both involved during the process.

Kaikake et al. (2007) studied the adsorption of Cd (II) ion using degreased coffee beans (DCB). The reaction mechanism was found to be an ion exchange reaction between Cd (II) ions and DCB. Langmuir isotherm was applied and the data obtained showed that Langmuir model was well fitted with an adsorption equilibrium constant of 55.2 millimole per cubic decimetre and an adsorption capacity of 5.98×10^{-2} millimole per gram. Desorption study showed that about 90% of Cd (II) ion was desorbed from DCB by using aqueous solution of hydrochloric acid or nitric acid at more than 0.01 mol/dm^3. Surface characterisation was done by using SEM and specific surface area analyzer. Results showed that the cell wall of DCB has porous structure with surface area1.2 square metre per gram.

The uptake of lead ions by okra waste was studied by Hashem (2007). With a temperature of 318 K, pH values ranging from 4 to 6 and adsorbent dosage

of 6 to 8 g, a removal of 99% of lead ions from the aqueous solution could be achieved. Both Langmuir and Freundlich isotherm were employed on the experimental data and results showed that adsorption of lead ions onto okra wastes was a favorable adsorption process with the formation of a monomolecular type.

The adsorption of lead, chromium and copper by peanut hull was studied by Li et al. (2008). The experiments were carried out under batch conditions. Results showed that the adsorption of these metal ions was pH dependent. The adsorption behavior was investigated using two isotherm models, namely Freundlich and Langmuir isotherms. The equilibrium data was well presented by both models. For the adsorbent amount of 2 grams per litre and initial metal ion concentration of 10 milligrams per litre, the maximum adsorption capacities for lead, chromium and copper were 4.59 mg/g, 3.34 mg/g and 2.96 mg/g, respectively. The experimental data fitted well in pseudo-second order kinetic model with high correlation coefficient (R^2) values.

2.3.3   Chemically Modified Agricultural Waste

2.3.3.1 Batch study

Wong et al. (2003) reported that tartaric acid modified rice husk (TARH) showed high binding capacity for both Cu (II) and Pb (II) ions under batch conditions. The removal of Cu (II) and Pb (II) ions was highly depended on pH,

initial dye concentration, agitation rate and particle size. From the effect of temperature, it revealed that the adsorption of Cu (II) and Pb (II) ions was an exothermic reaction and the values of ΔH^o and ΔS^o were calculated from the Van't Hoff plots. The experimental data complied with the Langmuir isotherm with maximum adsorption capacity of 29 mg/g and 108 mg/g for Cu (II) and Pb (II), respectively. A better correlation was obtained by fitting the adsorption data in pseudo second-order kinetic model and this suggested that the rate determining step is chemical adsorption rather than diffusion.

The potentiality of natural rice husk (RH) and HNO_3 modified rice husk (MRH) as an adsorbent for the removal of copper and cadmium ions was studied by Ong et al. (2007). Results showed the adsorption capacity of RH improved after the modification with HNO_3. The experimental data was well described by both Langmuir and Freundlich equations. The value of dimensionless separation factor of Langmuir isotherm obtained was smaller than 1. This indicates that the removal of copper and cadmium by MRH was a favourable process. For kinetic adsorption data, it obeyed the pseudo second-order model which indicates chemisorption is the rate-determining step.

Igwe et al. (2007) studied the adsorption of cobalt, iron and copper ions by using ethylenediamine tetra acetic acid (EDTA) modified and unmodified maize cob. The effect of contact time was being studied and the results showed that modification with EDTA enhanced the adsorption due to chelates formation. Based on the correlation coefficient (R^2) values, the adsorption data fitted well in

pseudo second-order equation. Elovich equation was applied to the adsorption process and the R^2 values obtained are close to unity indicating best fit of the adsorption data to the equation.

The used of chemically modified for the removal of Cu (II), Ni (II) and Zn (II) ions was assessed by Shukla et al. (2005). The jute fibre was modified using two different chemicals, namely Reactive Orange 13 and hydrogen peroxide. Adsorption isotherm indicated that the experimental data fitted well to Langmuir model for both modified jute fibre. The Reactive Orange 13 modified jute fibre showed maximum adsorption capacity values of 8.4, 5.26 and 5.95 mg/g for Cu (II), Ni (II) and Zn (II) ions, respectively. Meanwhile, the corresponding values for hydrogen peroxide oxidized jute fibre were 7.73, 5.57 and 8.02 mg/g. Both modified jute fibre gave higher adsorption capacity as compared to unmodified jute fibre.

2.3.3.2 Column study

Chun et al. (2009) studied the fixed-bed adsorption with virgin and polyethyleneimine-impregnated palm shell activated carbon as a media for the removal of single Ni^{2+} or Cu^{2+} ions from aqueous solution. The studies were conducted in a vertical down flow Perspex column. Both Ni^{2+} and Cu^{2+} solutions had an influent concentration of 1mmol/L and pH value of 5. The adsorption data were fitted with the linear regression method for three well established mathematical models, which are the BDST, Thomas model, and Yoon-Nelson

model. For the adsorption of Cu^{2+}, the experimental data agreed well with the theoretical curves modeled by BDST, Thomas and Yoon-Nelson models. The good agreements between experimental data and predicted data shows the applicability of all three models in predicting the fixed-bed Cu^{2+} adsorption behavior of virgin and polyethyleneimine-impregnated activated carbon.

The summary of the adsorption capacities of heavy metals by some natural and chemically modified agricultural wastes is shown in the Table 2.5.

Table 2.5: Adsorption capacities of heavy metals by natural and chemically modified agricultural wastes

Adsorbent	Heavy metals	Adsorption capacity	References
Peanut husk	Pb (II)	4.59 mg/g	Li et al. (2008)
	Cr (II)	3.34 mg/g	
	Cu (II)	2.96 mg/g	
Degreased coffee bean (DCB)	Cd (II)	0.06 mmol/g	Kaikake et al. (2007)
Sawdust	Pb (II)	26.00 mg/g	Lim et al. (2007)
	Cu (II)	22.50 mg/g	
	Zn (II)	19.75 mg/g	
Sodium hydroxide modified sawdust	Cd (II)	73.62 mg/g	Memon et al. (2007)
Hydrochloric acid modified sawdust	Cu (II)	3.60 mg/g	Argun et al. (2007)
	Ni (II)	3.37 mg/g	
	Cr (VI)	1.74 mg/g	
Sulfuric acid modified peanut husk	Pb (II)	29.14 mg/g	Li et al. (2007)
	Cr (III)	7.67 mg/g	
	Cu (II)	10.15 mg/g	
Sulfuric acid wheat bran	Cd (II)	101.00 mg/g	Ozer and Pirincci. (2006)
Ethylenediamine modified sugarcane bagasse	Cd (II)	189.00 mg/g	Junior et al. (2006)
	Cu (II)	139.00 mg/g	
	Pb (II)	164.00 mg/g	
Tartaric acid modified rice husk	Cu (II)	29.00 mg/g	Wong et al. (2003)
	Pb (II)	108.00 mg/g	

CHAPTER 3

MATERIALS AND METHODOLOGY

3.1 Adsorbent

3.1.1   Natural Rice Husk

The rice husk was assembled from rice mill. It was washed with water and rinsed with distilled water before sun dried. The dried rice husk was ground to the size of 1 mm using a grinder and labelled as natural rice husk (NRH).

3.1.2   Modified Rice Husk

3.1.2.1 Quartenized Rice Husk (QRH)

Five grams of NRH was left in 6.25 millilitre of 5 mol/dm^3 sodium hydroxide (NaOH) solution for 30 minutes subsequently added 5 millilitre of 4 mol/dm^3 N-(3-chloro-2-hydroxypropyl)trimethylammonium   chloride.   The mixture was then heated in the oven at 70°C for 4 hours. After heating, it was washed with distilled water and immersed in HCl solution for 30 minutes. The resulting mixture was washed to neutral and then dried in the oven and labeled as QRH.

3.1.2.2 Nitric acid Modified Rice Husk (HNRH)

Five grams of NRH was weighed and soaked in 150 mL of 0.5 mol/dm^3 nitric acid (HNO_3) solution for 2 hours. Then, the mixture was filtered and rinsed with distilled water until neutral. It was dried in the oven at 50°C and labeled as HNRH.

3.1.2.3 NaOH Modified Rice Husk (NaRH)

NRH was mixed with 0.5 mol/dm^3 sodium hydroxide (NaOH) and boiled for 2 hours. The mixture was then filtered and rinsed with distilled water until the pH was neutral. It was dried in the oven at 50°C and labeled as NaRH.

3.1.2.4 Nitrilotriacetic Acid Modified Rice Husk (NTARH)

Five grams of NRH was weighed and soaked in 35 mL of 1.2 mol/dm^3 nitrilotriacetic acid (NTA). The mixture was subjected to heat treatment at 140°C in the oven for 2 hours. The heated product was rinsed with distilled water until the filtrate reach neutral pH and labeled as NTARH after drying in the oven at 50°C.

3.1.2.5 Ethylenediamine Modified Rice Husk (EDARH)

Natural rice husk was treated with ethylenediamine (EDA) in a ratio of 0.02 mole of EDA to 1 g of rice husk in a water bath at 80°C. The resulting mixture was rinsed with distilled water and dried in the oven. The rice husk was labeled as EDARH.

3.1.2.6 Ethylenediamine Tetraacetic Acid Modified Rice Husk (ERH)

Eight grams of grinded NRH was mixed with 0.5 g of ethylenediamine tetraacetic acid (EDTA) and the mixture was left in 300 mL of 1.0 mol/dm^3 NaOH for 3 hours at 70°C. The treated rice husk was filtered and washed with excess of distilled water. Then, it was dried in the oven and labeled as ERH.

3.1.3 Other Chemical Modifications of Surface Functional Groups

3.1.3.1 Esterification of Carboxyl Groups

In order to esterify the carboxyl groups on the surface of ERH, 60 mL of ethanol was added to 2 g of ERH with 10 drops of concentrated H_2SO_4 and heated under reflux for 2 hours. The product was labeled as esterified ERH.

3.1.3.2 Acetylation of Amine Groups

Acetylation of amine groups on the surface of ERH was carried out by adding 10 mL of acetic anhydride and 60 mL of ethanoic acid to 2 g of ERH. The mixture was heated to $50^{o}C$ for 2 hours. The end product was labeled as acetylated ERH.

3.2 Adsorbates

3.2.1 Preparation of Standard Dye Solutions

In the study of dye adsorption, synthetic dye of Methylene Blue (MB) and Reactive Orange 16 (RO16) were used. All dyes used were from Sigma-Aldrich Pte. Ltd. (United State of America). A stock solution of 1000 mg/L was prepared and diluted when necessary. For binary dye solutions, both dyes were mixed homogeneously according to the desired concentration.

3.2.2 Preparation of Standard Heavy Metal Ion Solutions

For the adsorption of heavy metal, synthetic heavy metal solutions of copper(II) sulfate ($CuSO_4$) and cadmium(II) chloride ($CdCl_2$) were used without further purification. A 500 mg/L stock solution of both $CuSO_4$ and $CdCl_2$ was obtained by dissolving the exact quantity of the two metals ions in deionized

water. The experimental solutions were prepared by diluting the stock solution into desired concentrations.

3.3 Instrumental Analysis

The instruments involved in this study include UV-Vis Spectrophotometry, Inductively Couple Plasma Atomic Emission Spectroscopy (ICP-AES), Fourier Transform Infrared Spectroscopy (FTIR), Scanning Electron Microscopy (SEM) and Atomic Force Microscopy (AFM).

3.3.1   UV-Vis Spectroscopy

The concentration of dye solutions before and after adsorption was determined using double-beam UV-Vis spectrometer (Perkin Elmer Lambda 35). Dye solution was placed in a cuvette with internal diameter of 1.0 cm and it is made of high quality quartz glass. The scanning range was fixed from 400 nm to 800 nm and the absorbance value was measured at respective maximum wavelength of MB (664 nm) and RO16 (494 nm).

3.3.2   Inductively Couple Plasma Atomic Emission Spectroscopy (ICP-AES)

In the heavy metal analysis, ICP-AES (SPS1700HVR, wavelength range: 160-800 nm) was used to produce excited metal atoms which emit electromagnetic radiation at their respective wavelengths. The emitted radiation is

indicative of the concentration of the metal ions presence within the analysed sample. In this study, the sample of heavy metal solutions before and after adsorption was placed in a 15 mL centrifuge tube and tested using ICP-AES with the function of auto-sampling.

3.3.3 Fourier-Transform Infrared Spectroscopy (FTIR)

FTIR (Perkin Elmer 1725X) was used to investigate the functional groups presence on rice husk before and after chemical modification. The wave number was ranging from 400-4000 cm^{-1}. KBr powder was mixed with the adsorbent in the ratio of 10 portions of KBr to 1 portion of adsorbent. The mixed sample was pressed using a pellet compressor followed by instrumental analysis.

3.3.4 Scanning Electron Microscopy (SEM)

SEM was used to study the surface morphology of NRH and ERH. Before the analysis was carried out, the adsorbents were first pelletized using a pellet compressor.

3.3.5 Atomic Force Microscopy (AFM)

The surface morphology and topography of NRH and ERH were also studied by using AFM (Quensant Q-Scope 250). It is a stylus-type instrument that scanned in raster fashion.

3.4 Batch Experiments on Dyes

Batch studies were conducted using 0.1 g of adsorbent in 20 mL of 25 mg/L dye solution and were shaken for 4 hours at 150 rpm. The supernatant was analysed for its dye concentration using double beam UV-vis spectrophotometer with the maximum absorption wavelength of 664 nm and 494 nm for MB and RO16, respectively. All experiments were conducted in duplicates and the results shown are the means. Controls with no adsorbent were simultaneously carried out to ensure that adsorption was due to adsorbent and not the wall of the centrifuge tube.

3.4.1 Comparative Study on Various Chemically Modified Rice Husk

The percent removal of MB and RO16 by both NRH and various chemically modified rice husk in single dye solutions was being compared and analysed using double beam UV- Vis spectrophotometer with the condition of 0.1 g of adsorbent shaken for 4 hours at 150 rpm in 20 mL of 25 mg/L single dye solutions.

3.4.2 Effect of pH

For the effect of pH, the removal of dyes in both single and binary systems was studied by equilibrating adsorption-mixture at different initial pH (pH 2 to pH 10). The desired pH was adjusted by using hydrochloric acid (HCl) and sodium hydroxide (NaOH) in trace amount. 20 mL of 25 mg/L dye solution was shaken with 0.1 g of adsorbent at 150 rpm for 4 hours.

3.4.3 Effect of Initial Dye Concentrations and Contact Time

In the study of contact time and initial dye concentrations, 0.1 g of adsorbent was added to a series of dye solutions with different initial concentrations in the range of 15 - 25 milligrams per litre. The adsorption-mixture was then shaken at 150 rpm at a predetermined time intervals of 5, 10, 15, 30, 60, 120, 180, 240, 300, 360 and 420 minutes.

3.4.4 Effect of Agitation Rate

The agitation speed was manipulated from 50 rpm to 200 rpm in order to study the effect of agitation rate. For each experiment, 20 mL of single and binary dye solutions with the concentration of 25 mg/L were shaken with 0.1 g of adsorbent at a predetermined time intervals of 5, 10, 15, 30, 60, 180 and 240 minutes.

3.4.5　Effect of Adsorbent Dosage

A quantity of adsorbent ranged from 0.05 g to 0.2 g was agitated in 20 millilitres of 25 milligrams per litre dye solution for 4 hours at 150 revolutions per minutes in both single and binary dye solutions.

3.4.6　Effect of Particle Size

To study the effect of particle size, the adsorbent was sieved into four different size ranges, 150-300 micron, 300-600 micron, 600-800 micron and >800 micron. A dye solution of 20 mL with the concentration of 25 mg/L was used and shaken for 4 hours at 150 rpm for both single and binary dye solutions.

3.4.7　Effect of Temperature

To study the effect of temperature, 20 millilitres of 25 milligrams per litre dye solution with 0.1 g adsorbent was prepared for single and binary dye solutions. It was then shaken at 150 rpm for 4 hours at different initial temperature ranging from 30 ^{o}C to 70 ^{o}C.

3.4.8   Adsorption Isotherm

Three isotherm models were employed to study the adsorption isotherm, namely Langmuir, Freundlich and Brunauer, Emmet and Teller (BET) model. In this study, 20 mL of single and binary dye solutions with different concentrations, 5 mg/L to 150 mg/L were prepared. The adsorbent dosage used was 0.1 g and then the mixture was shaken at 150 rpm for 4 hours.

3.5 Column Study on Dyes

Continuous flow studies were conducted using a glass column of 1.0 cm internal diameter. Cotton wool was placed at the bottom of the column. The packed column was covered with a layer of sand to avoid the flotation problem. Distilled water was run through the column prior to the dye solutions to achieve hydraulic equilibrium. The dye solution was fed and the eluant was collected at 10 mL fractions. A peristaltic pump was used to control the flow rate of eluant. The eluant was analysed for its dye concentration using UV- Vis Spectrophotometer.

3.5.1   Effect of Influent Concentrations

The effect of different influent concentrations of dyes solution on the breakthrough curve was studied using 5, 10 and 15 mg/L for both MB and RO16. The column was packed to a bed height of 7.0 cm using 1.0 g of ERH. The flow rate used was 10 mL/min.

3.5.2 Effect of Bed Depth

As for the effect of bed depth, the column was packed with 0.5 grams, 0.75 grams and 1.0 grams of ERH, which corresponds to a height of 2.5 cm, 4.5 cm and 7.0 cm, respectively. The flow rate used was 10 mL/min and the influent concentration of dyes was fixed to 10 mg/L.

3.5.3 Effect of Flow Rate

To study the effect of flow rate, the experiments were performed by varying the flow rate from 5 to 15 mL/min. The bed depth and influent concentration were fixed at 7 cm height and 10 mg/L, respectively.

3.6 Optimisation using Statistical Experimental Methodology

3.6.1 Plackett Burman Design

Plackett Burman Design was used to identify the variable(s) that has a significant effect on the removal of dyes. Six variables (pH, contact time, adsorbent dosage, initial dye concentration, agitation rate and temperature) were used in this study and screened in 12 experimental designs. The designs as well as the uptake of both MB and RO16 were evaluated. All experimental designs were carried out in duplicate and the mean value of the percentage uptake was taken as

response. Experimental design and statistical analysis of data were done by using Design Expert Version 7.1.3.

3.6.2   Response Surface Methodology

A factorial central composite design (CCD) model for significant variables with replicates was used in this study. The significant variables for MB and RO16 in both single and binary dye solutions were coded at 5 levels, $-\alpha$, -1, 0, $+1$ and $+\alpha$. All experiments were conducted in duplicate and the mean value of percentage uptake was used as response. Cubic equation used for the optimisation of percentage uptake of dye is shown as follows:

$$Y = \beta_o + \sum_{i=1}^{2} \beta_i X_i + \sum_{i=1}^{2} \beta_{ii} X_i^2 + \sum_{i=1}^{2} \beta_{iii} X_i^3 + \sum_{i=1}^{1} \sum_{j=i+1}^{2} \beta_{ij} X_i X_j$$
$$+ \sum_{i=1}^{1} \sum_{j=i+1}^{2} \beta_{ijj} X_i X_j^2 + \sum_{i=1}^{1} \sum_{j=i+1}^{2} \beta_{iij} X_i^2 X_j$$

(3.1)

where, β_o, β_i, β_{ii}, β_{iii}, β_{ij}, β_{ijj} and β_{ijj} are the constant coefficients, and X_i, and X_j are the independent variables. All the experimental design and statistical analysis of the data were done by using Design Expert Version 7.1.3.

3.7 Batch Experiments on Heavy Metal Ion

The potential of ERH in the removal of Cu(II) and Cd(II) ions was investigated under batch experiments by shaking 0.1 g of adsorbent in 20 mL of

25 mg/L metal solutions on an orbital shaker for 4 hours at 150 rpm. All experiments were conducted in duplicate and the results shown are the mean. Control with no adsorbent was simultaneously carried out to ensure that adsorption was due to adsorbent and not the wall of the centrifuge tube.

3.7.1 Effect of pH

For the effect of pH on the removal of heavy metals, the pH of the heavy metal solutions was manipulated to a range of 2-9 by adding hydrochloric acid (HCl) or sodium hydroxide (NaOH) in a trace amount. The mixture consisting of 0.1 g of adsorbent in 20 mL of 25 mg/L metal solution and was shaken at 150 rpm for 4 hours.

3.7.2 Effect of Initial Metal Ion Concentrations and Contact Time

In the study of the effect of initial metal ion concentration and contact time, the experiments were performed by varying the metal ion concentrations ranging from 20 – 30 mg/L of Cd (II) and Cu (II) ions. The adsorption-mixture was then shaken at 150 rpm at a predetermined time intervals of 5, 10, 15, 30, 60, 120, 180, 240, 300, 360 and 420 minutes.

3.7.3   Adsorption Isotherm

Adsorption isotherms were studied by employing both Langmuir and Freundlich models. The metal ion concentrations was being varied from 15 mg/L to 50 mg/L with 0.1 g adsorbent and shaken at 150 rpm for 4 hours.

3.7.4   Chelating Effect

A commonly found chelator in the environment, salicylic acid (SA) was being investigated to determine its influence on Cu (II) and Cd (II) ions removal by ERH. This chelator was added into the metal ion solutions in different Cu (II)/Cd (II): chelator ratios, namely 1:0.5, 1:1, 1:2 and 1:5 moles. In this experiment, 20 mL of each of these mixtures was shaken with 0.1 g of ERH at 150 rpm for 4 hours.

CHAPTER 4

RESULTS AND DISCUSSIONS

4.1 Preliminary Test on Different Chemically Modified Rice Husk

In order to enhance the adsorption capability of rice husk towards both Methylene Blue (MB) and Reactive Orange 16 (RO16), five different chemical reagents were used to modify rice husk, namely N-(3-chloro-2-hydroxypropyl)trimethylammonium chloride, nitric acid, sodium hydroxide, nitrilotriacetic acid (NTA), ethylenediamine (EDA) and ethylenediamine tetraacetic acid (EDTA). The percentage uptake of dye was calculated using the following equation:

$$\%Uptake = \frac{C_i - C_t}{C_i} \times 100\%$$

(4.1)

where C_i = the initial dye concentration.

C_t = the dye concentration at time t.

The percentage uptake of dyes by different modified rice husks were shown in Table 4.1. Results obtained revealed that most of the modified rice husks were able to remove either MB or RO16 but not both. Only EDA and EDTA modified rice husks were able to remove both dyes. EDTA modified rice husk was selected as an adsorbent throughout this study because it showed a higher percentage uptake for both dyes as compared to EDA modified rice husk.

Table 4.1: Percentage uptake of dyes by different chemically modified rice husks

Adsorbent	% uptake of dyes	
	MB	RO16
Natural rice husk	90.29	0.86
Quartenized rice husk	7.10	97.54
HNO_3 modified rice husk	97.36	0.60
NaOH modified rice husk	98.98	8.29
NTA modified rice husk	93.95	0.00
EDA modified rice husk	94.72	10.10
EDTA modified rice husk	99.25	14.19

4.2 Adsorption Mechanism

Ethylenediamine tetraacetic acid (EDTA) was used to modify natural rice husk (NRH). The structure of EDTA is shown below:

Figure 4.1

Rice husk in its natural state that composed of high proportion of cellulose (32.34 %), hemicellulose (21.34 %) and lignin (21.44 %) contains large number of hydroxyl groups (Marshall et al., 1993; Wong et al., 2003; Wan Ngah et al., 2007). The presence of hydroxyl group played an important role in the EDTA modification process. EDTA was heated to form anhydride by removing water molecule from two carboxyl groups. The anhydride formed will react with the hydroxyl group of rice husk forming ester (Gusmão et al., 2013). The proposed mechanism for the modification process is as follow:

$$\text{EDTA} + 2\,\text{NaOH} \xrightarrow{\text{Heat}} \text{EDTA dianhydride (disodium)} + 3\,H_2O$$

$$\text{EDTA dianhydride (disodium)} + HO-\text{(rice husk)} \longrightarrow \text{EDTA modified rice husk ester} \tag{4.2}$$

where $HO-$⟨ represent the surface of natural rice husk.

The EDTA modified rice husk (ERH) contains two positively-charge quaternary amine groups and four negatively-charged carboxyl groups when immersed in water. The positively-charged amine groups attract the negatively-charged sulphonate groups present in RO16 dye molecule whereas the negatively-

charged carboxyl groups are likely to be responsible for the adsorption of positively-charged MB molecule. The adsorption of both MB and RO16 dye molecule is proposed as below:

$$\text{Na}^+ {}^-\text{OOC} \quad \text{Na}^+ {}^-\text{OOC} \quad N^+ H \quad N^+ H \quad \text{COO}^- \text{Na}^+ \quad C \quad O \quad O \quad + \quad 3\,\text{MB}^+ \quad + \quad 2\,\text{RO16}^-$$

$$\downarrow$$

$$\text{MB}^+ {}^-\text{OOC} \quad \text{MB}^+ {}^-\text{OOC} \quad \text{RO16}^- \quad N^+ H \quad N^+ H \quad \text{RO16}^- \quad \text{COO}^- \text{MB}^+ \quad C \quad O \quad O \quad + \quad 3\,\text{Na}^+$$
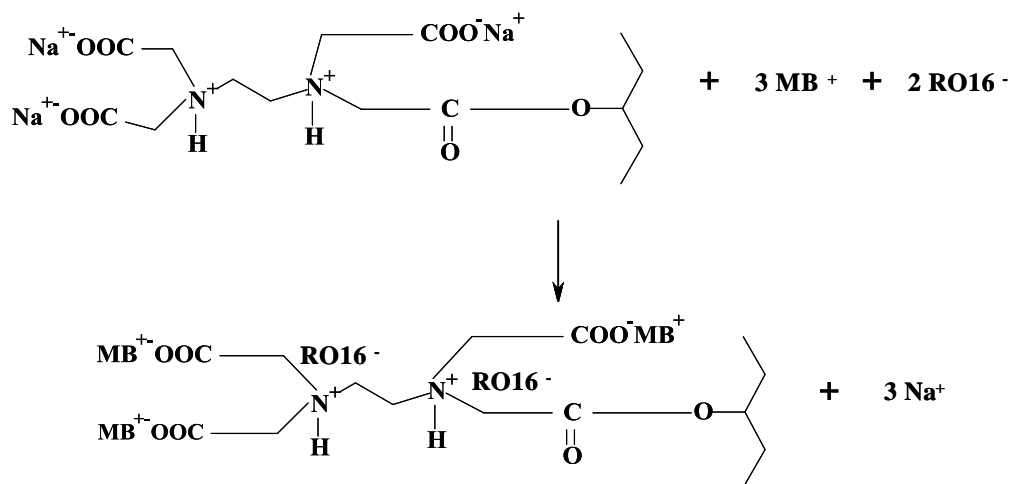
(4.3)

The percent removal of RO16 was enhanced in binary system (from 8.35 % to 39.48 %) and this could be related to the surface charge of ERH upon the adsorption of MB molecules. The reaction is postulated as follow:

$MB^{+-}OOC$ —— $RO16^-$

$MB^{+-}OOC$

COO^-MB^+

$RO16^-$

N^+ — C — O

H H O

$+$ $4\ RO16^-$

↓

$RO16^-\ MB^{+-}OOC$ —— $RO16^-$

$RO16^-\ MB^{+-}OOC$

$COO^-MB^+\ RO16^-$

$RO16^-$

N^+ — C — O

H H O
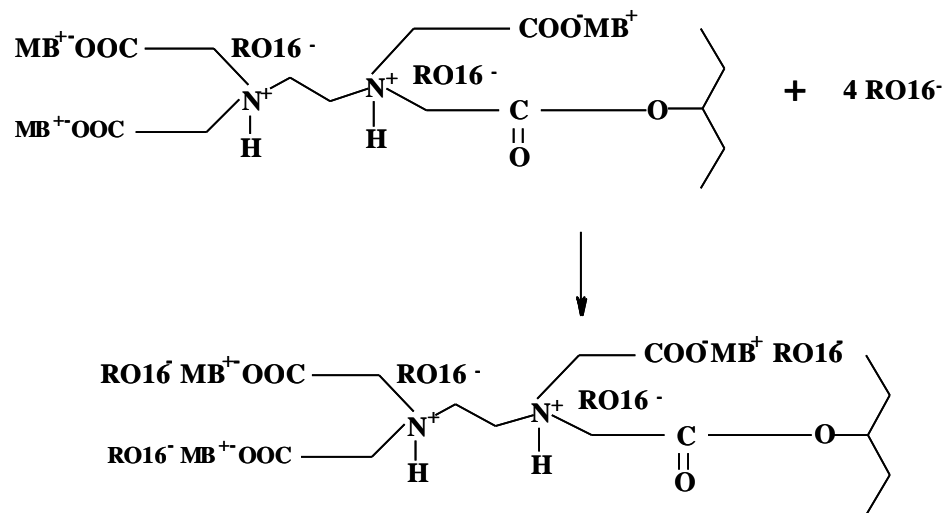
(4.4)

The adsorbed MB molecules increase positive charges on the surface of ERH and hence enhance the adsorption of RO16 by 4 times.

4.3 Chemical Modification of Surface Functional Groups

4.3.1 Esterification of Carboxyl Groups

Esterification of ERH with ethanol is shown by the equation below:

$$RH - COOH\ +\ CH_3CH_2OH\ \rightarrow\ RH - COOCH_2CH_3\ +\ H_2O \qquad (4.5)$$

where RH- COOH represent the surface carboxyl group of ERH.

The percentage uptake of MB by esterified ERH was depressed from 99.25 % to 96.63 %. This is due to the reduction in the number carboxyl groups on the surface of ERH. Therefore, it showed that the carboxyl groups are the main binding site for MB.

As for RO16, the percentage uptake was increased from 14.19 % to 16.00 %. This is due to the surface of esterified ERH becomes less negative (less carboxyl groups) and hence less electrostatic repulsion between RO16 and ERH.

4.3.2   Acetylation of Amine Groups

The main principle of this method is to combine the amine groups of ERH with acetyl groups, hence rendering the surface of ERH less polar and more hydrophobic. Blocking of amine groups caused a reduction of 11.6 % of the adsorption of RO16. Hence, the amino group plays an important role in the adsorption of RO16.

$$RH - N: + CH_3CO - O - OC - CH_3 \rightarrow RH - N - CO - CH_3 + CH_3COO^- \qquad (4.6)$$

where $RH - N:$ represent the amine group of ERH that with a lone pair of electrons.

The percentage uptake of MB by acetylated ERH was decreased from 99.25 % to 98.88 %. This can be attributed to the steric hindrance between the bulky acetyl groups (CH_3-CO) and MB molecules.

The effect of chemical modification on surface functional groups of ERH on the percentage uptake of both MB and RO16 was shown in the chart below.
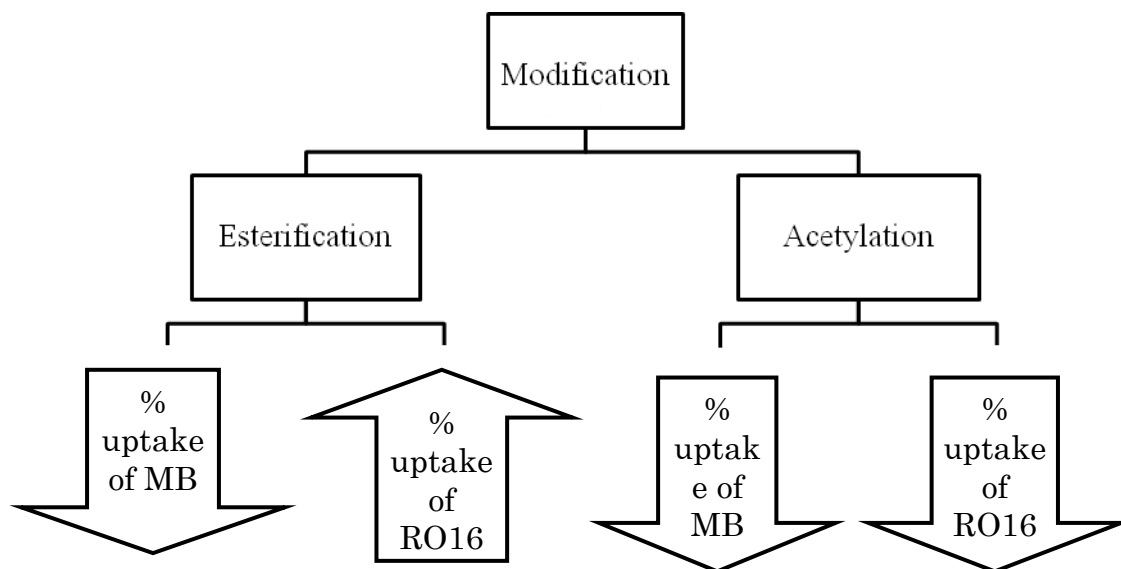
Figure 4.2: Effects of chemical modification on the surface functional group of ERH

4.4 Instrumental Analysis

4.4.1   Fourier Transform Infrared Spectroscopy (FTIR)

Figure 4.3 shows the FTIR spectra of both NRH and ERH. From the FTIR analysis, no significant difference was observed in the functional groups of NRH and ERH. Absorption peaks at 3413 cm^{-1} and 3432 cm^{-1} for both NRH and ERH, respectively are due to the O-H stretching vibrations. The wide O-H peak observed in both NRH and ERH are due to the vibrational mode that being complicated by hydrogen bonding (Ong et al., 2010). The modification of NRH by EDTA will yield carboxyl groups and quaternary amine groups on the surface of NRH. Therefore, ERH spectrum showed a peak at 1637 cm^{-1} which indicates the presence of C=O stretch or conjugated C=C. The same peak was observed in

the spectrum of NRH. This might due to the presence of lignin in rice husk which consists of both carbonyl group and C=C stretch. No N-H stretch was observed in the spectrum of ERH near region 3310-3500 cm^{-1} as the amine groups present are in quaternary structure. Another broad peak was observed in the spectrum of NRH at 1096 cm^{-1} which could be indicative of C-O anti-symmetrical stretching. This C-O stretching was absence from the spectrum of ERH because the OH groups of NRH were being substituted by EDTA during the modification process. The peaks at 467 cm^{-1} to 800 cm^{-1} in the spectrum of NRH are attributed to the Si-H groups indicating the presence of silica. From the ERH spectrum, these peaks were not observed. This is due the modification process that might reduce the percentage of silica in ERH. The peak identification of the FTIR spectra is shown in Tables 4.2 and 4.3.

Table 4.2: Peak identification of FTIR spectrum of NRH

Functional Group	Wavenumber (cm^{-1})
O-H stretch	3413
C=O stretch	1637
C-O anti-symmetrical stretch	1096
Si-H	467-800

Table 4.3: Peak identification of FTIR spectrum of ERH

Functional Group	Wavenumber (cm^{-1})
O-H stretch	3432
C=O stretch	1637
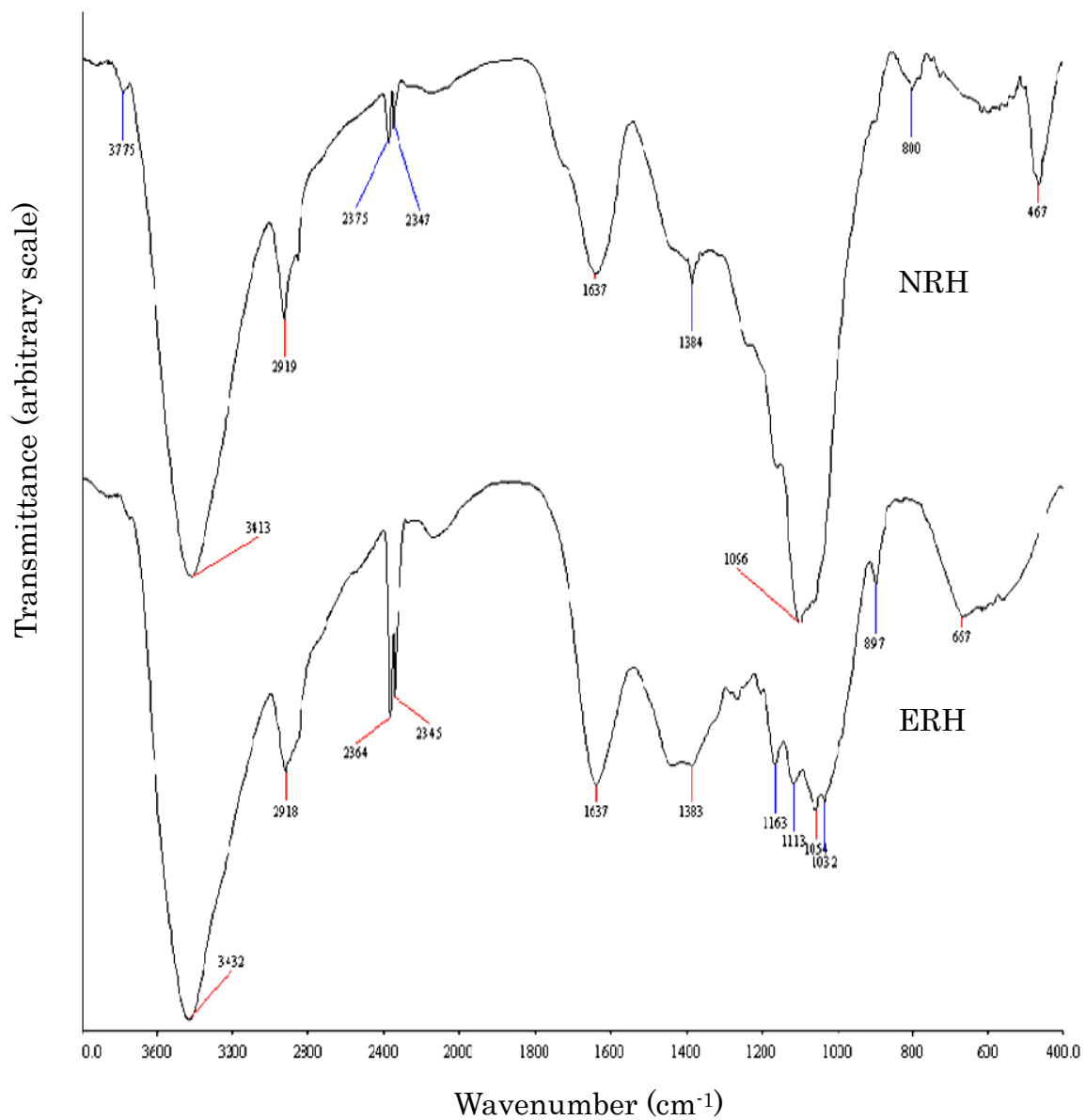
Figure 4.3: Infrared spectra of NRH and ERH

4.4.2   Scanning Electron Microscopy (SEM)

The SEM micrographs of NRH and ERH were shown in Figures 4.4 and 4.5, respectively. It was noticed that the surface texture of ERH appeared to be smoother as compared to NRH which showed a rough and heterogeneous surface. This is due to the introduction of both amine and carboxyl groups on the surface of rice husk using EDTA. It was also found that both NRH and ERH are in a compact structure with no cavities and pores.

Similar observation was obtained in a study carried out by Rahmadini et al. (2011) in which the rice husk was modified with Liquid Epoxidized Natural Rubber (LENR). The SEM micrograph of the LENR modified rice husk was smoother than the raw rice husk. This is due to the dispersion of LENR on the surface of rice husk and indicates that LENR was able to penetrate into the roughness and fibrillation of rice husk fibres.
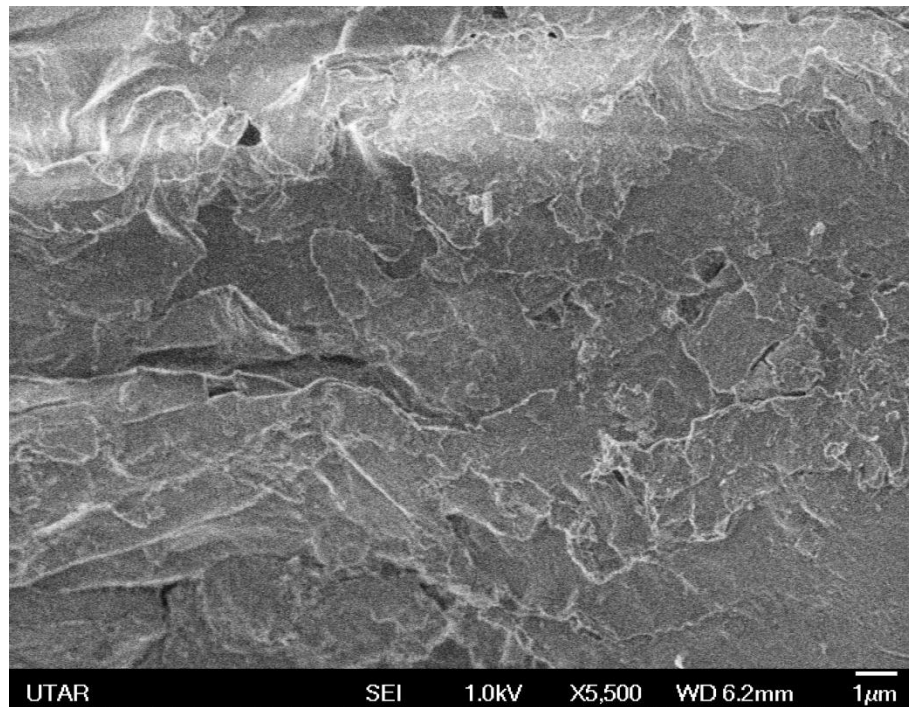
Figure 4.4: SEM micrograph of NRH
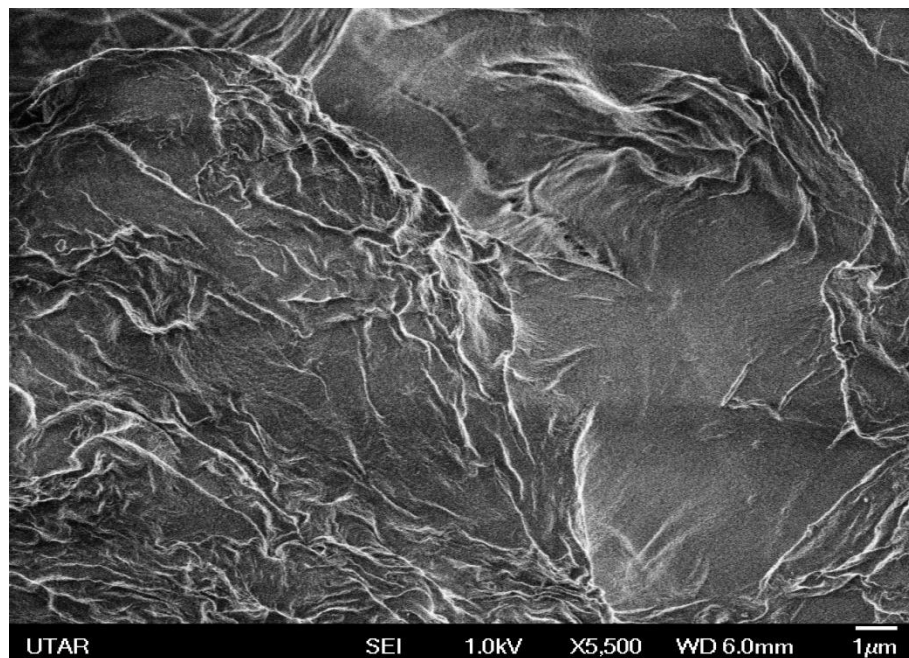
Figure 4.5: SEM micrograph of ERH

4.4.3   Atomic Force Microscopy (AFM)

The surface topography of NRH and ERH were studied using contact mode by AFM on a 20 X 20 μm^2 area as shown in Figures 4.6 and 4.7, respectively. Colour mapping was used to display the data where light colour indicates high topography whereas darker colour shows lower topography. With the addition of carboxyl and amine groups, surface of rice husk becomes more intense. Hence a higher topography (lighter colour) was observed for ERH.

Ong et al. (2009) reported that by taking AFM measurements, the ethylenediamine modified rice husk showed a higher surface topography (light colour) as compared to natural rice husk. This may be attributed to the introduction of amine groups on the surface of rice husk and making it more intense.
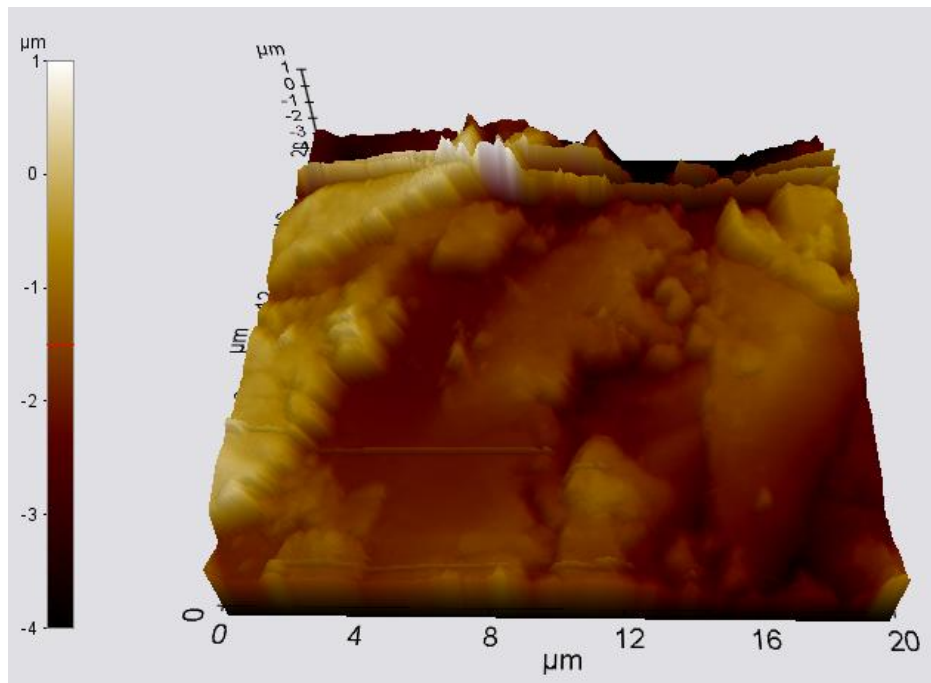
Figure 4.6: AFM topography picture of NRH
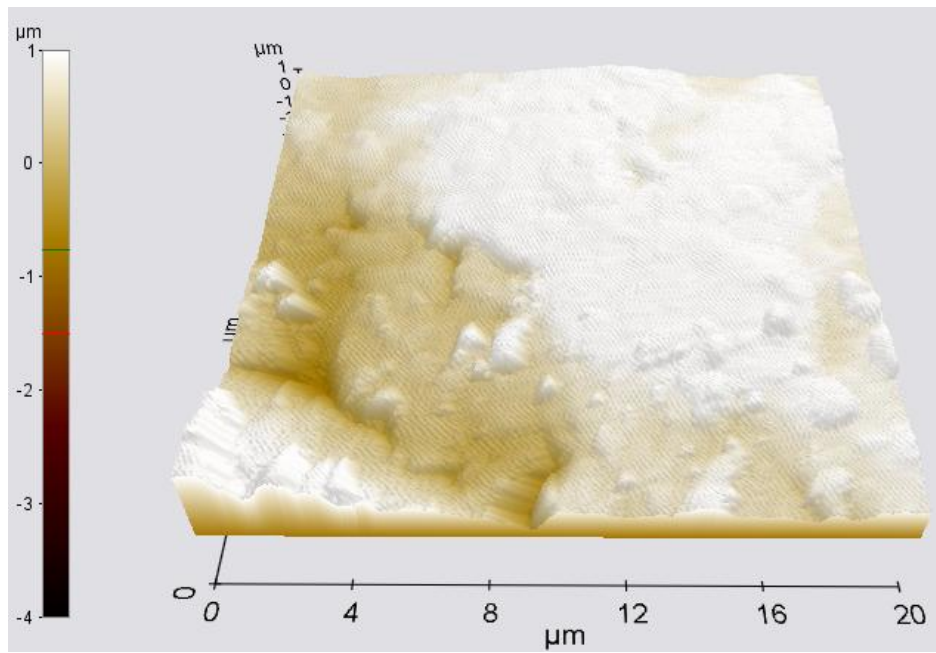
Figure 4.7: AFM topography picture of ERH

4.5 Batch Experiments on Dyes

4.5.1　Comparative Study on Uptake of Dyes by NRH and ERH

A comparative study of adsorption of MB and RO16 in both single and binary dye solutions was carried out by using NRH and ERH as adsorbents as shown in Figure 4.8. The results showed that MB was adsorbed by NRH with 90.3 % and 90.8 % in single and binary dye solutions, respectively. Rice husk in its natural state consists of high proportion of cellulose and the cellulosic surface that would become negatively charged when immersed in water (Kumar, 2006). Therefore, when the molecule of MB dissociates into a positively charged species, an electrostatic interaction formed between the surface of NRH and MB dye molecule. However, the percentage uptake of RO16 by NRH was relatively low and this may due to the repulsion between the anionic dyes and the negatively-charged surface groups of NRH (Ong et al., 2007).

After modification, ERH showed its adsorption capability for different charged dyes, in either single or binary dye solutions. The high affinity of ERH for both MB and RO16 is probably due to the presence of carboxyl and amine groups introduced from the EDTA modification. The negatively charged carboxyl group is likely to be responsible for the adsorption of positively-charged MB whereas the negatively charged RO16 is attracted to the positively-charged amine group. There were studies reported that chemical modification of rice husk is
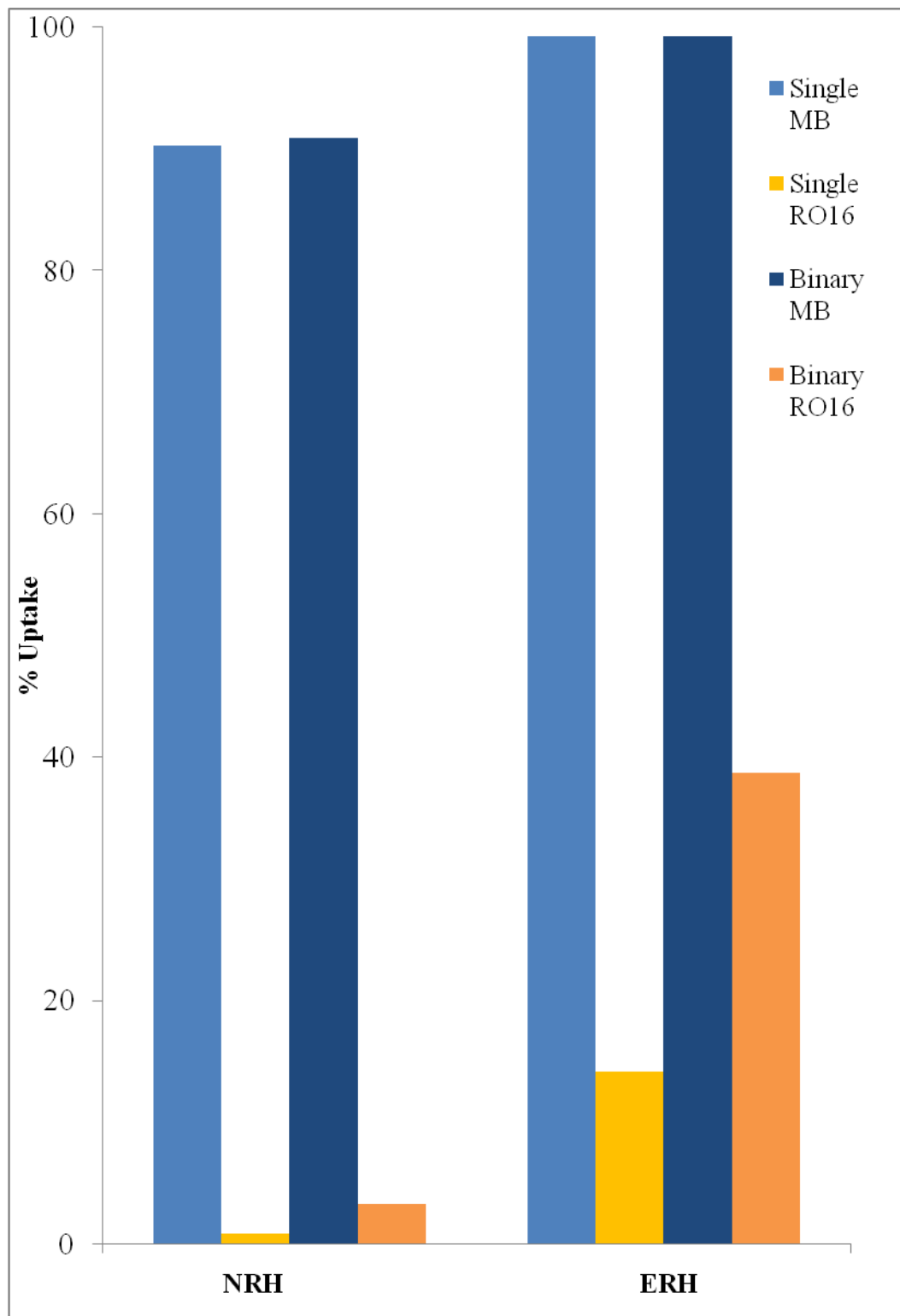
Figure 4.8: Comparative study on the uptake of dyes by NRH and ERH

capable of enhancing adsorption capacities for metal ions and other pollutants such as dyes (Daifullah et al., 2004; Chuah et al., 2005; Hsu et al., 2007). In a study conducted by Igwe and Abia, (2007), EDTA was used to modify maize husk and results showed that the modified maize husk has higher adsorption capacity for Co (II), Fe (II) and Cu (II) ions as compared to unmodified maize husk due to the chelating ability of EDTA.

4.5.2 Effect of pH

The pH value is an essential process-controlling variable in the adsorption study since it determines the surface charge of the adsorbent. Figure 4.9 showed that the percentage uptake of RO16 decreased from 84.2 % to 10.1 % with the increase in pH from 2 to 10. As the pH of the system increases, this lead to the removal of proton from carboxyl groups and the presence of excess OH^-, results in the repulsion between the anionic dye and negatively charged sites. Similar behaviour was observed in binary RO16. Amin (2009) investigated the uptake of Direct Blue-106 using activated carbon prepared from pomegranate peel at different pH values. Results showed that the percentage uptake of Direct Blue-106 decreased with increasing pH. This is due to the carbon surface acquires positive charge by adsorbing H^+ ions at low pH and hence, high electrostatic forces exist between the positively charged carbon surface and Direct Blue-106.
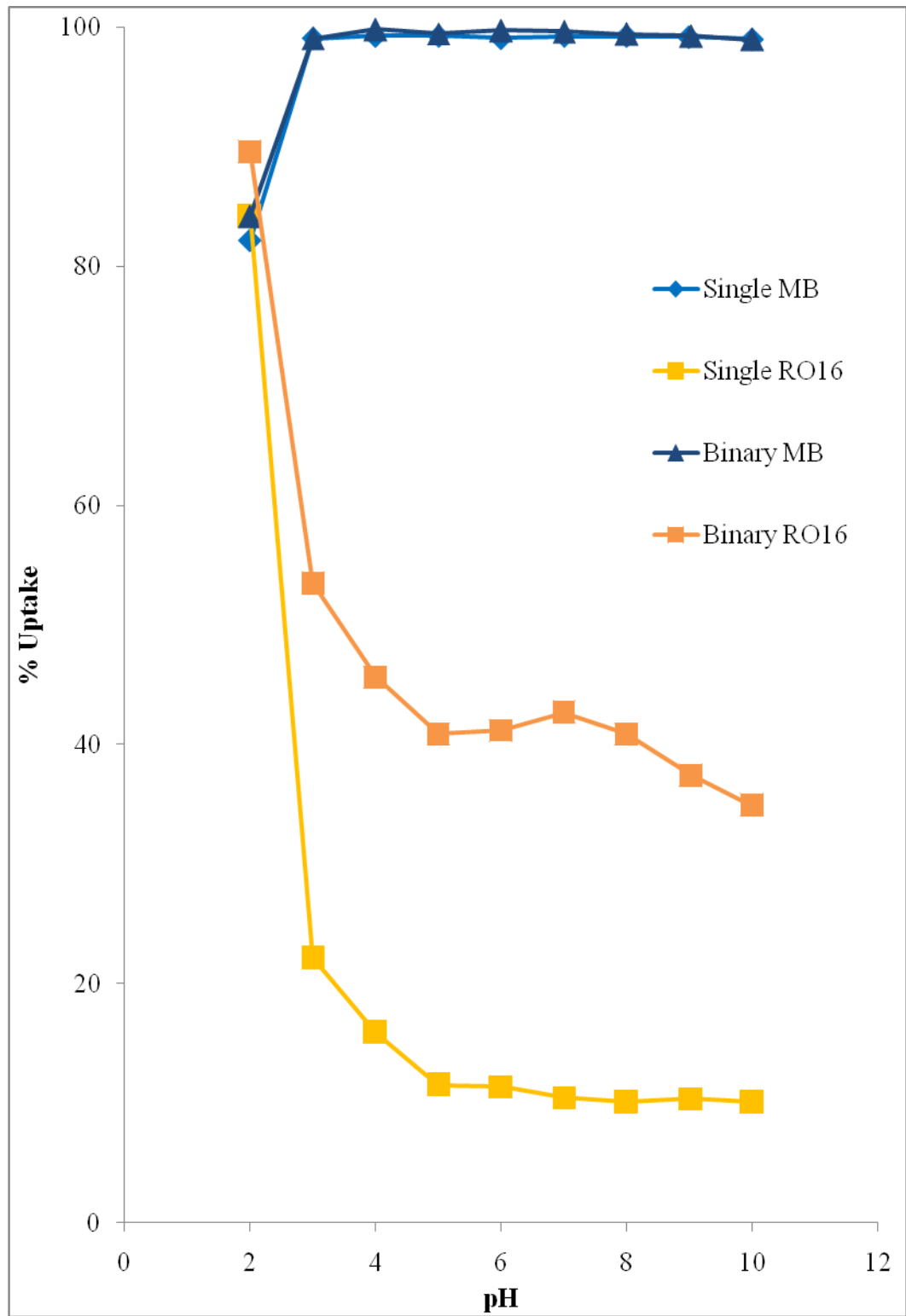
Figure 4.9: Effect of pH on the adsorption of MB and RO16 in single and binary dye solutions

The reverse pattern was shown for the uptake of MB in which the percent removal was more favourable at high pH as shown in Figure 4.9. This is due to the surface of the adsorbent was surrounded by hydrogen ions (H^+) at low pH, which prevented the MB dye molecules from approaching the binding sites. With increasing pH, the carboxyl groups are predominantly deprotonated, resulting in adsorption sites that were available for binding with MB. In a study conducted by Saad et al. (2010), the uptake of Methyl Red was favoured at high pH due to the increasing negatively charged adsorbent sites.

4.5.3   Effect of Initial Dye Concentration and Contact Time

The rate of adsorption of single MB by ERH as a function of initial concentration is shown in Figure 4.10. Similar plots were also obtained for single RO16, binary MB and binary RO16 as shown in Figures 4.11, 4.12 and 4.13, respectively. The uptake rate was fast at the first 60 min followed by a slower uptake. The fast uptake at first is due to the quick adsorption dye molecules to the surface of the adsorbent followed by slower adsorption due to intraparticle diffusion (Amin, 2008). The quick adsorption rate at the initial stage may also be due to the higher number of adsorption sites and therefore there is an increase in driving force of concentration gradient between adsorbate in solution and adsorbate in the adsorbent (Ju et at., 2008; Kavitha and Namasivayam, 2007). With increasing initial concentration of dye solutions, the percentage uptake of MB and RO16 in both single and binary dye solutions decreased. This indicates the saturation of the binding site on the adsorbent as the number of dye molecules
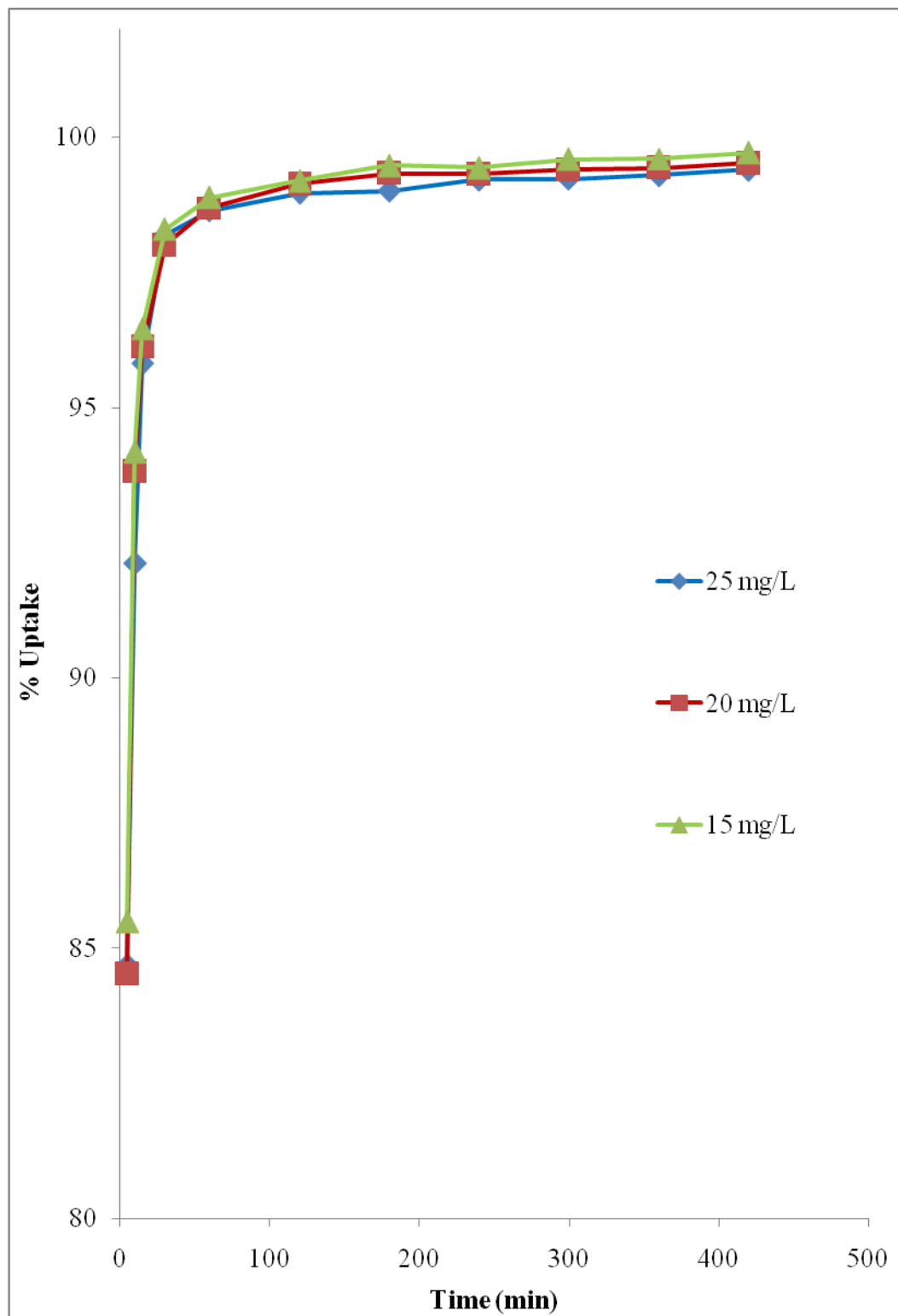
Figure 4.10: Effect of initial concentration and contact time on the adsorption of MB in single dye solutions
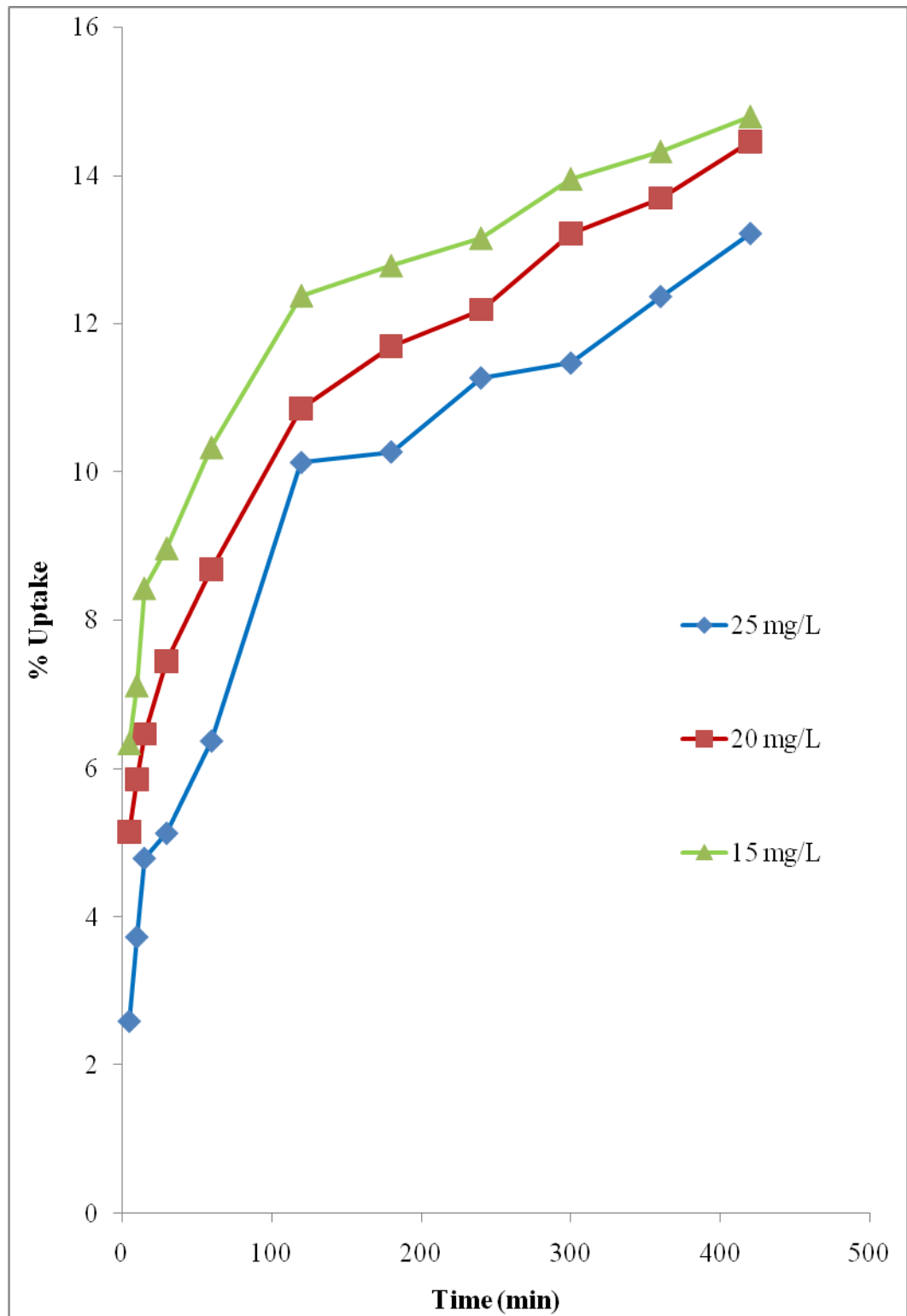
Figure 4.11: Effect of initial concentration and contact time on the adsorption RO16 in single dye solutions
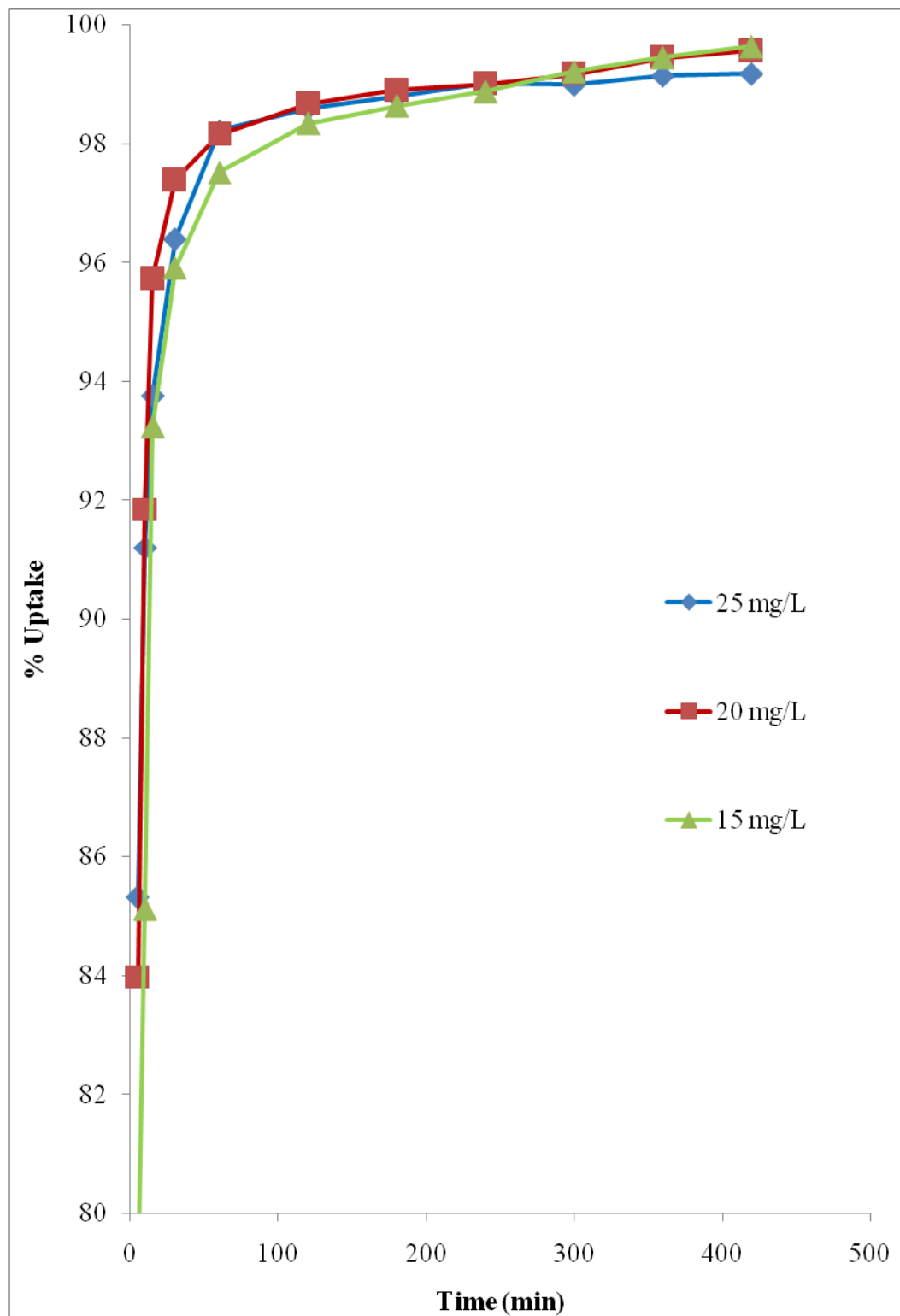
Figure 4.12: Effect of initial concentration and contact time on the adsorption of MB in binary dye solutions
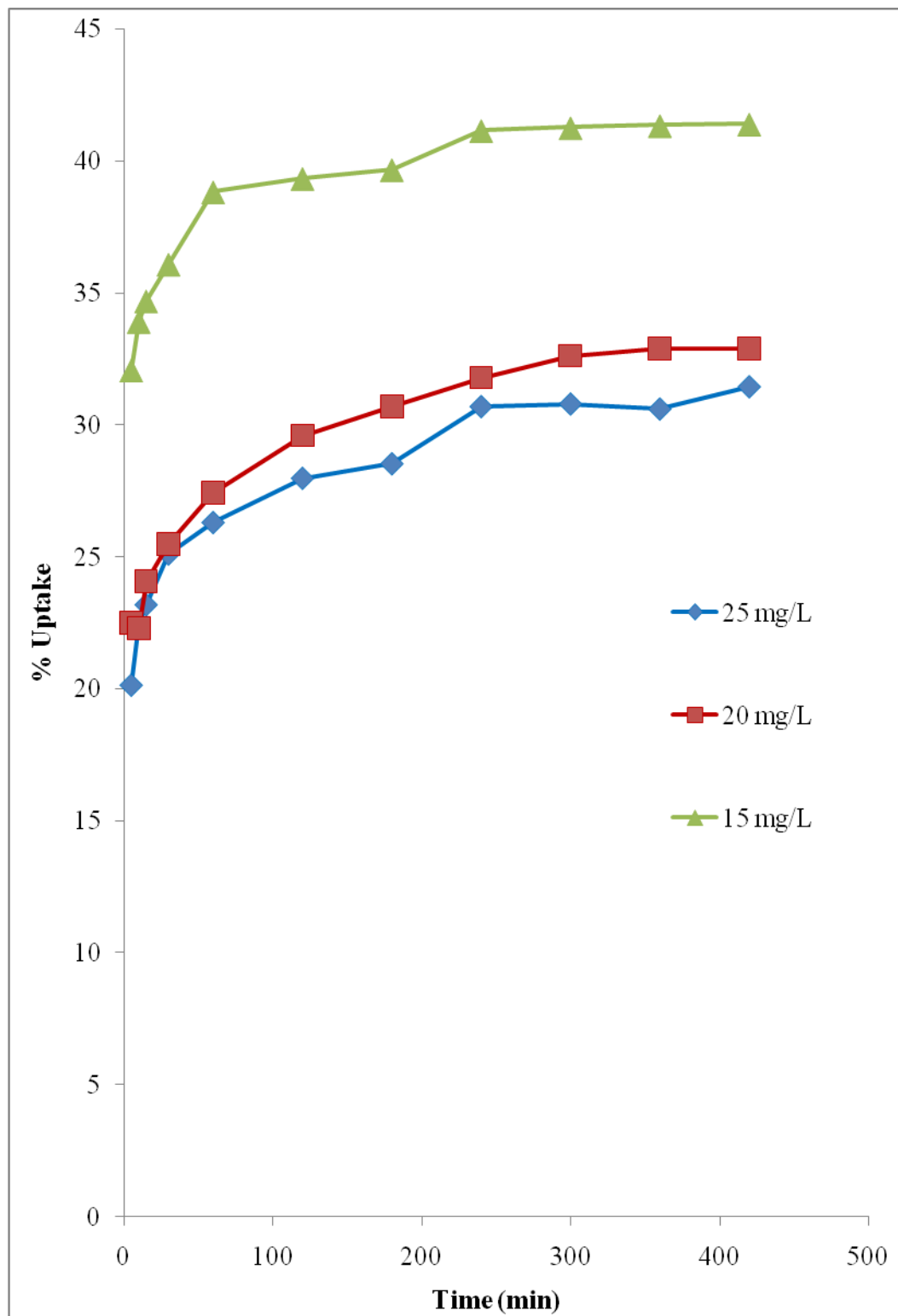
Figure 4.13: Effect of initial concentration and contact time on the adsorption of RO16 in binary dye solutions

per unit volume increased. Amin (2008) reported that when the concentration of dye increases, there is a reduction in dye adsorption due to the lack of available binding sites.

4.5.4 Adsorption Kinetics

In order to explore the potential rate-determining steps involved in the adsorption of MB and RO16 onto ERH, both pseudo-first and pseudo-second kinetics models have been used to fit experimental data at various dye concentrations. The pseudo-first order (Lagergren, 1898) and pseudo-second equations (Ho and McKay, 1999) are expressed as in equations (4.7) and (4.8), respectively.

$$\log(q_e - q_t) = \log qe - \frac{k_1 t}{2.303} \qquad (4.7)$$

and

$$t / q_t = 1/h + t / q_e \qquad (4.8)$$

where q_e = the amount of dyes adsorbed at equilibrium (mg/g), q_t = the amount of dyes adsorbed at time t (mg/g), k_1 = the rate constant of pseudo-first order adsorption (1/min), $h = (k_2 q_e^2)$ = the initial adsorption rate (mg/g min) and k_2 = the rate constant of pseudo-second order kinetics (g/ mg min).

The various adsorption capacities and correlation coefficients based on pseudo-first and pseudo-second order kinetics were summarised in Table 4.4. From all the systems studied, good correlation coefficients are obtained ($R^2 \approx 1$) by fitting the experimental data to pseudo-second order kinetics rather than that of pseudo-first order kinetic model. Besides, the equilibrium adsorption capacities calculated from based on pseudo-second order kinetic model agreed well with

Table 4.4: Adsorption capacities and correlation coefficients based on pseudo first and pseudo-second kinetics

Dye	Initial Concentration	Pseudo-first order		Pseudo-second order		Experimental adsorption capacities (mg/g)
		Adsorption capacities (mg/g)	R^2	Adsorption capacities (mg/g)	R^2	
Single MB	15	7.153	0.327	2.994	1.000	2.991
	20	16.226	0.321	3.986	1.000	3.980
	25	25.305	0.338	4.975	1.000	4.969
Binary MB	15	7.309	0.439	2.994	1.000	2.988
	20	16.259	0377	3.986	1.000	3.982
	25	25.345	0.444	4.967	1.000	4.958
Single RO16	15	9.899	0.851	0.327	0.993	0.307
	20	9.756	0.910	0.567	0.989	0.558
	25	9.774	0.877	0.684	0.986	0.658
Binary RO16	15	9.337	0.744	0.901	0.999	0.889
	20	9.367	0.849	1.039	0.998	1.013
	25	8.543	0.820	1.832	0.999	1.829

those obtained experimentally. Therefore, the adsorption behaviour is well presented by pseudo-second order model which is based on the assumption that the rate limiting step may be chemisorption involving valency forces through sharing or exchange of electron between adsorbent and adsorbate (Ho and McKay, 1999).

According to Ho and McKay (2000), the values of q_e, k_2 and h against C_o in the corresponding linear plots of the pseudo-second order equation can be regressed to obtain expressions for these values in terms of initial concentration (Table 4.5). These parameters can be expressed as a function of C_o for MB and RO16 on ERH as follows:

$$q_e = \frac{C_o}{A_q C_o + B_q} \tag{4.9}$$

$$k_2 = \frac{C_o}{A_k C_o + B_k} \tag{4.10}$$

$$h = \frac{C_o}{A_h C_o + B_h} \tag{4.11}$$

where A_q, B_q, A_k, B_k, A_h, B_h are constant for the respective equations. The theoretical model derived for MB and RO16 at concentrations of 15-25 mg/L was applied to the uptake of both dyes and the result was compared to the experimental values in Figures 4.14 to 4.17. It is quite apparent that the theoretical curve agreed well with the experimental data for MB in both single and binary solutions. The q_t values for RO16 in single dye solution are lower than expected due to the slow adsorption process. However, a higher than expected q_t values
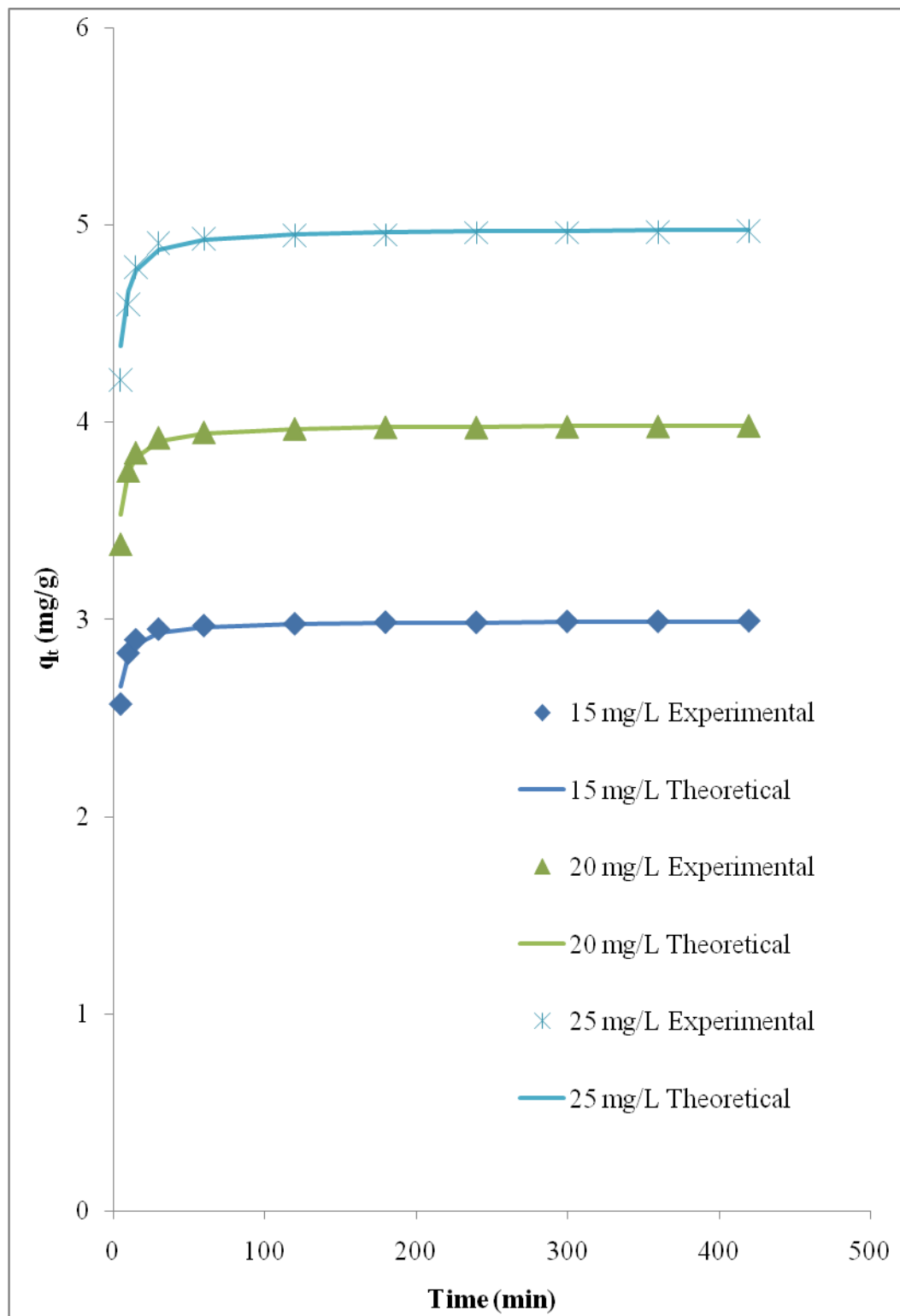
Figure 4.14: Comparison between the measured and pseudo-second order modelled time profiles for MB in single dye solutions
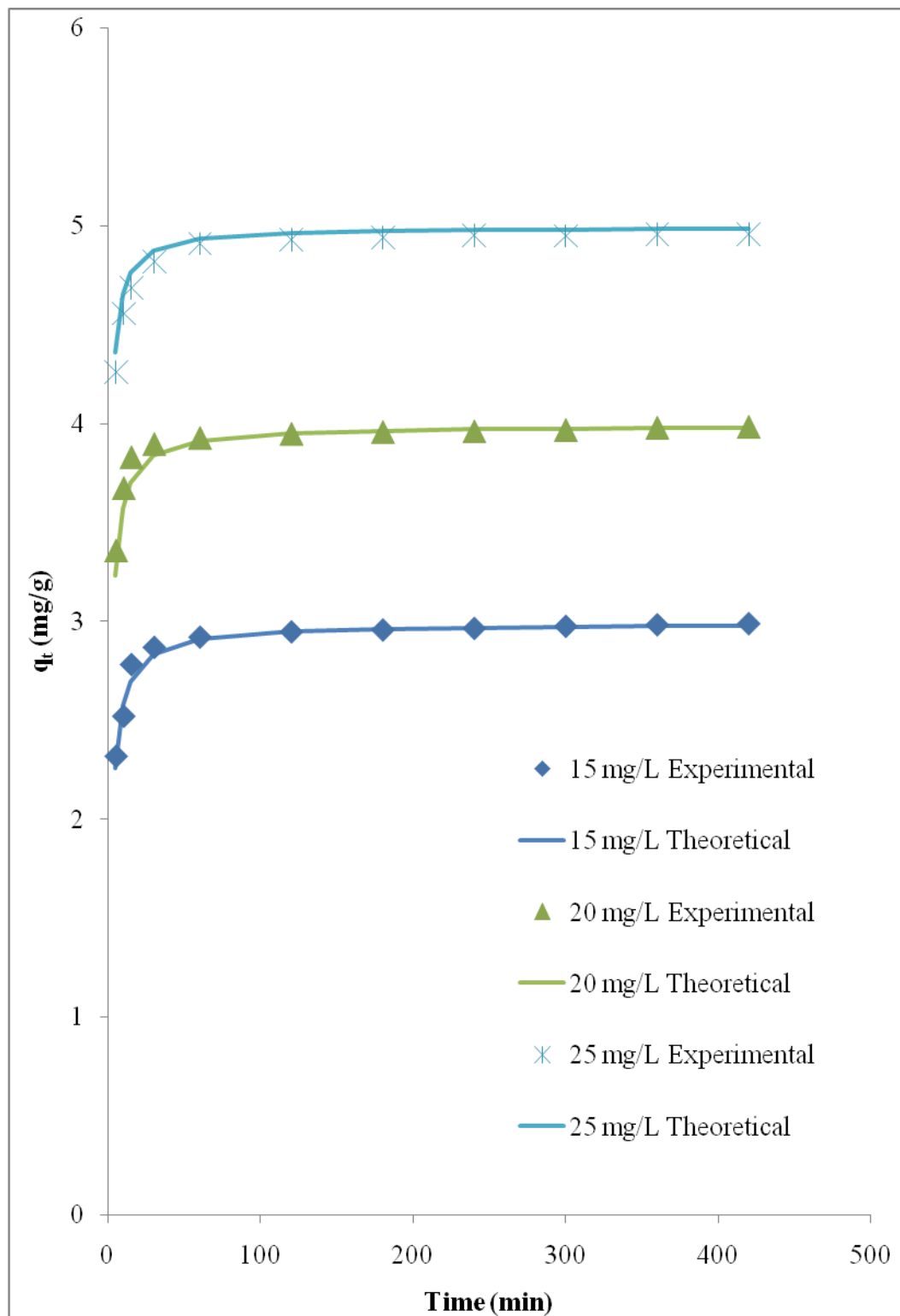
Figure 4.15: Comparison between the measured and pseudo-second order modelled time profiles for MB in binary dye solutions
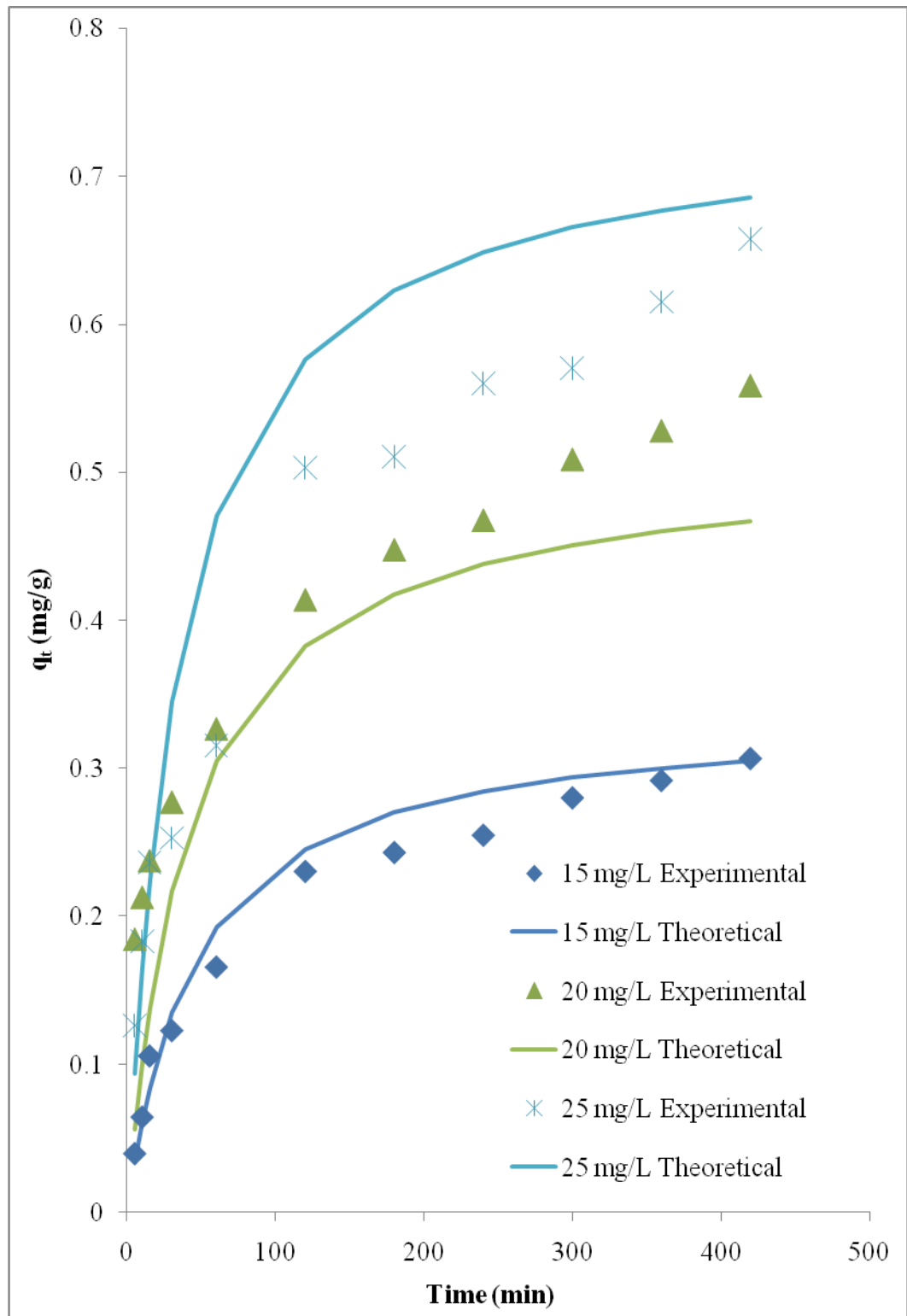
Figure 4.16: Comparison between the measured and pseudo-second order modelled time profiles for RO16 in single dye solutions
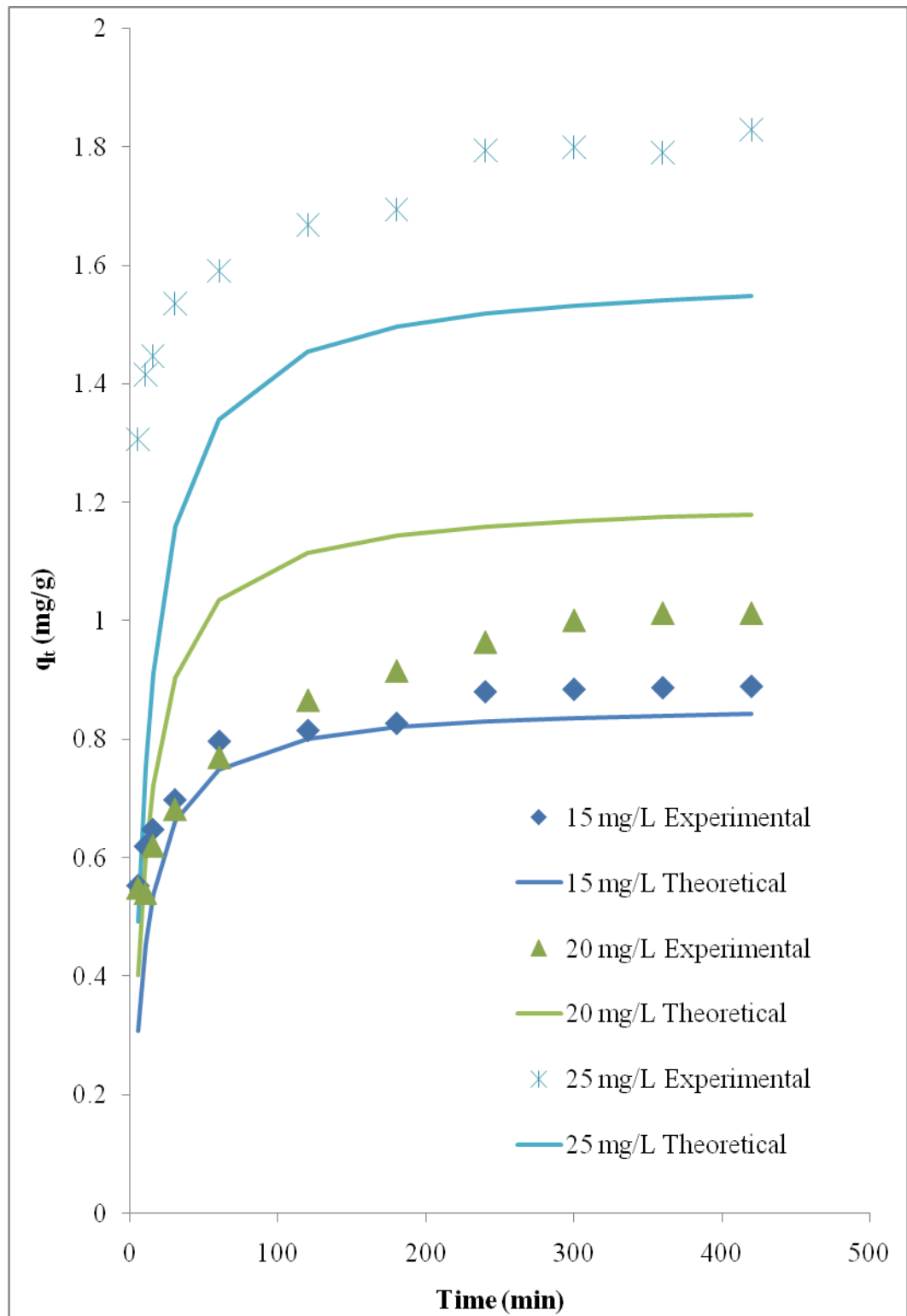
Figure 4.17: Comparison between the measured and pseudo-second order modelled time profiles for RO16 in binary dye solutions

were obtained for RO16 in binary dye solution. This is due to the synergistic effect between the adsorbed dye molecules.

Table 4.5: Empirical parameters for predicted q_e, k and h from C_o

Dyes	A_q (g/mg)	B_q (g/L)	A_k (mg min/g)	B_k (mg^2min/g L)	A_h (gmin/mg)	B_h (gmin/L)
Single MB	0.000	5.014	5.596	-56.727	0.031	2.636
Binary MB	0.000	5.027	2.423	39.498	-0.448	14.822
Single RO16	-1.066	60.333	55.685	-655.980	-84.524	3277.900
Binary RO16	-0.168	19.930	25.400	-257.650	1.813	129.920

4.5.5   Effect of Agitation Rate

The variation of dyes uptake with agitation rate ranging from 50 rpm to 200 rpm in both single and binary dye solutions is shown in Figures 4.18 and 4.19. Results obtained revealed that the uptake of MB in both single and binary dye solutions increased rapidly in the first 15 minutes and slowly achieved equilibrium at about 30 minutes. As the agitation rate increase, the film boundary layer surrounding the adsorbent particles decrease, hence increasing the external film mass transfer coefficient and thus the percentage uptake. According to Shiau et al. (2004), an increase in agitation rate would increase the adsorption efficiency due to the reduction in film resistance. The transfer rate of a solute to a particle is affected by liquid film thickness surrounding the particle and the film thickness is dependent upon agitation rate.
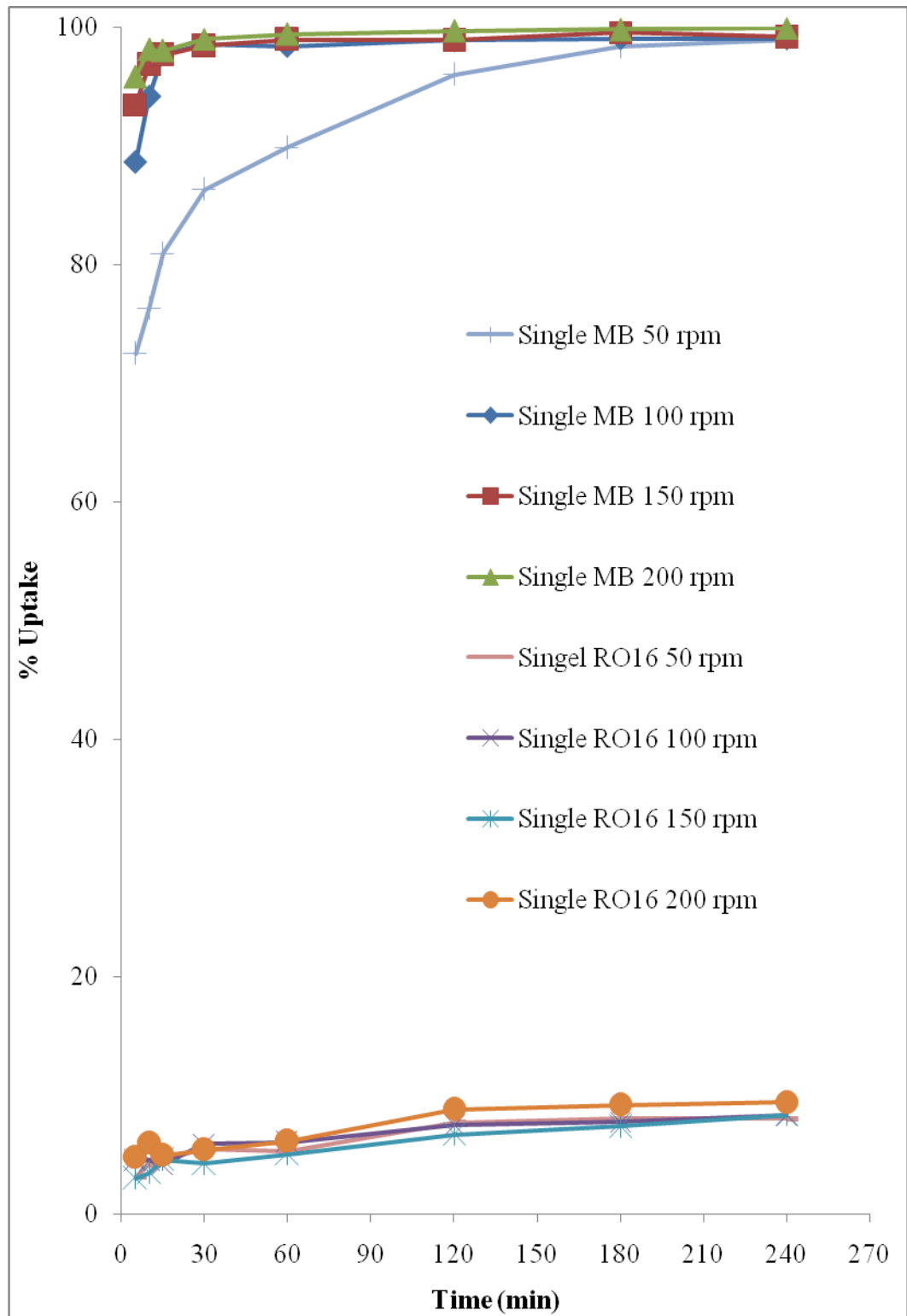
Figure 4.18: Effect of agitation rate on the adsorption of MB and RO16 in single dye solutions
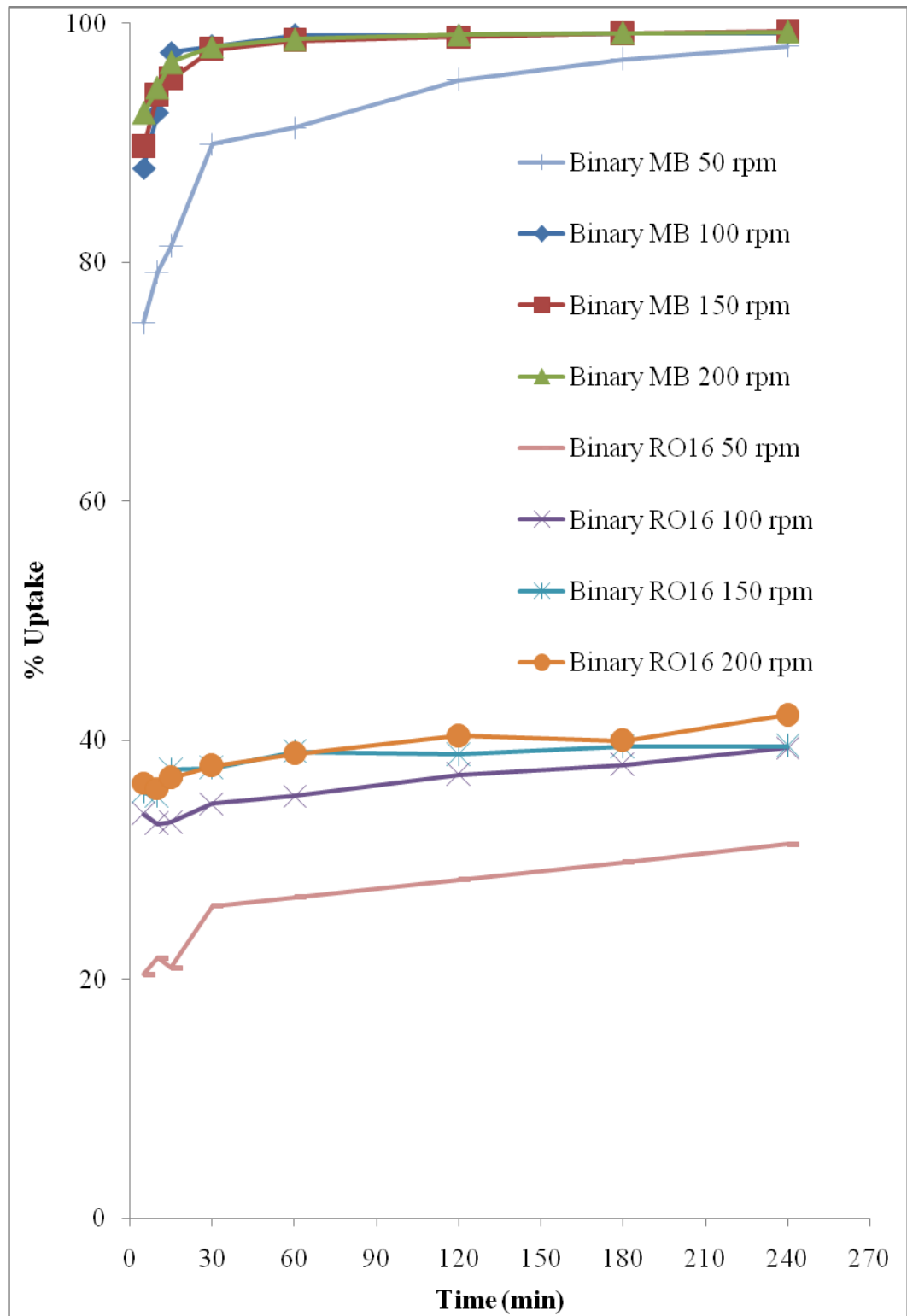
Figure 4.19: Effect of agitation rate on the adsorption of MB and RO16 in binary dye solutions

As for single and binary RO16, the uptake was found to be independent of agitation rate. This might due to the quick uptake of the dye. The minimal effect of agitation rate on the dye adsorption by adsorbent indicated that the external mass is not the sole rate-limiting factor in a well agitated system. Similar trend was reported by Ong et al. (2007) for the adsorption of Basic Blue 3 (BB3) onto ethylenediamine modified rice husk (MRH).

4.5.6 Intraparticle Diffusion

In order to study the mechanism of adsorption process, the intraparticle diffusion model (Weber and Moris, 1963) was employed and the equation is shown as below:

$$K_p = \frac{q_t}{\sqrt{t}} \tag{4.12}$$

where K_p is an intraparticle diffusion coefficient (mg/g min$^{0.5}$) which can be obtained from the slope of the plot q_t versus $\sqrt{t}$ presented in Figures 4.20 to 4.23. q_t is the amount of MB or RO16 adsorbed by ERH at time t. According to Weber and Moris (1963), the plot of q_t versus $\sqrt{t}$ should yield a straight line that passing through the origin if intraparticle diffusion is the only rate-determining step. However, if a multi-linear plot was obtained, then two or more steps involved and are influencing the adsorption process.

From the trend observed in Figures 4.20 to 4.23, there are three separate portions that can be seen. Initial curve portion is attributed to boundary layer effect while the linear portion is due to the intrapaticle diffusion (Arivoli et al., 2007). The final portion can be attributed to the final stage in which the intraparticle diffusion starts to slow down due to the low adsorbate concentration. Similar case was observed in a study conducted by Lakshmi et al. (2009) where rice husk ash was used as adsorbent for the uptake of Indigo Carmine dye from aqueous solution.

Deviation of plot from the origin indicates that the intraparticle diffusion is not the only rate-determining step. The intercept of the plots indicate the extent of the boundary layer effect, the higher the value of intercept, the greater the contribution of the surface adsorption in the rate-determining step. Table 4.6 shows the intraparticle diffusion coefficients and the value of intercept for all systems which were calculated from linear portion of the plots. The value of K_p increased with increasing dye concentrations, indicating the driving force of dye molecules from solution onto ERH and then into the particle increased. Besides, with increasing dye concentrations, the value of intercept increased. This also suggests that the rate of transfer of dye molecules from the bulk solution to the hydrodynamic boundary layer is faster at higher dye concentrations.
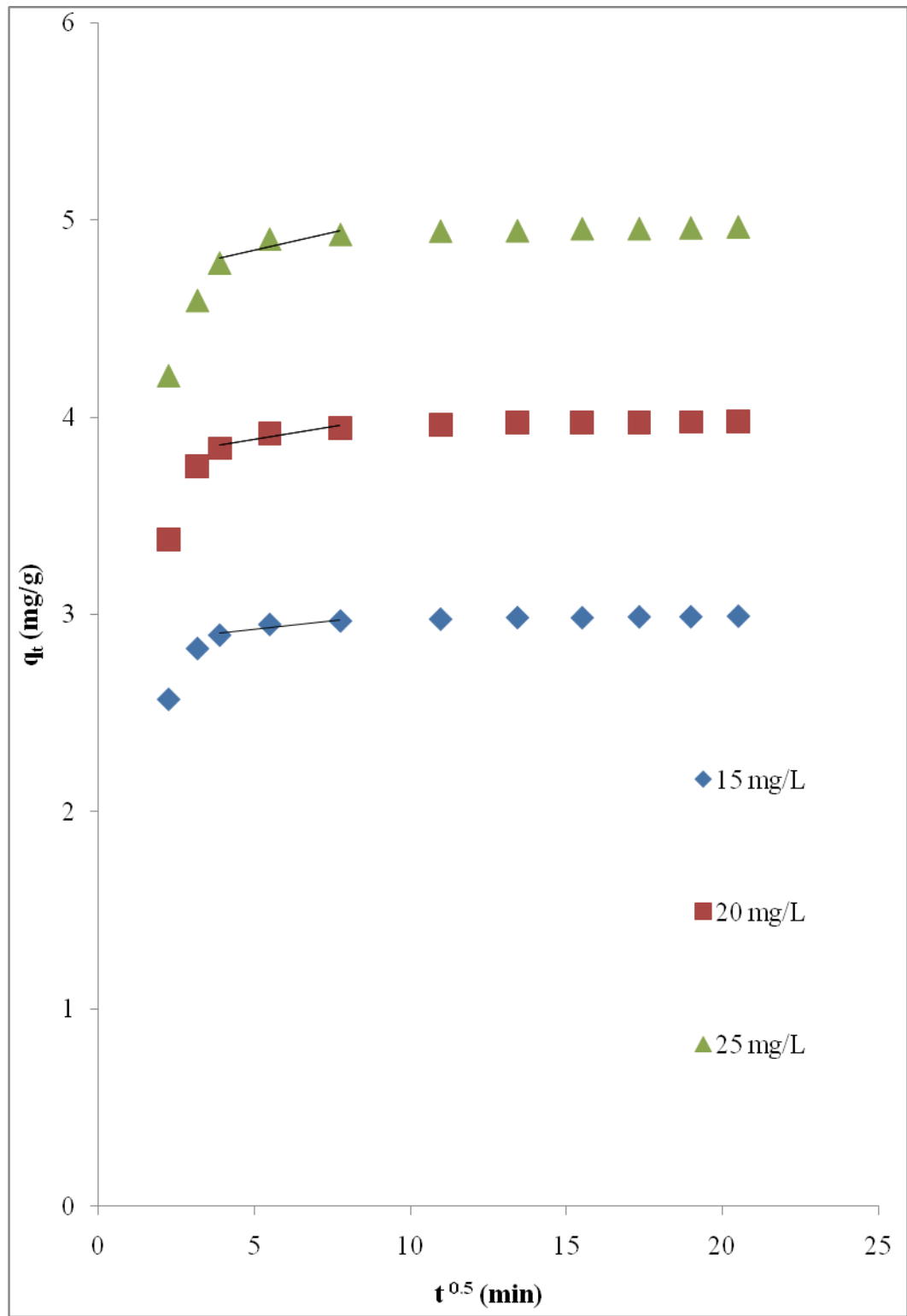
Figure 4.20: Intraparticle diffusion MB in single dye solutions in ERH
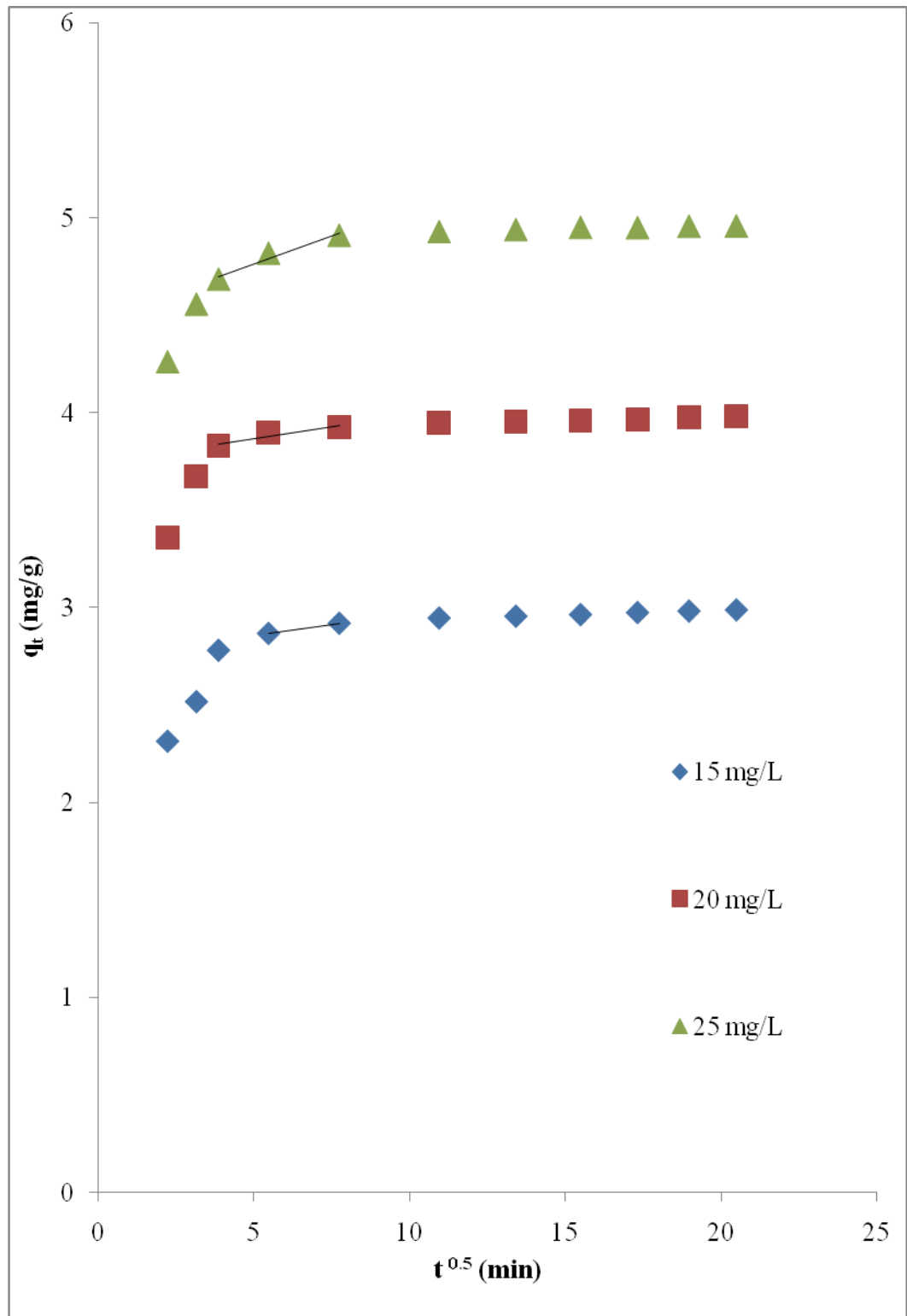
Figure 4.21: Intraparticle diffusion MB in binary dye solutions in ERH
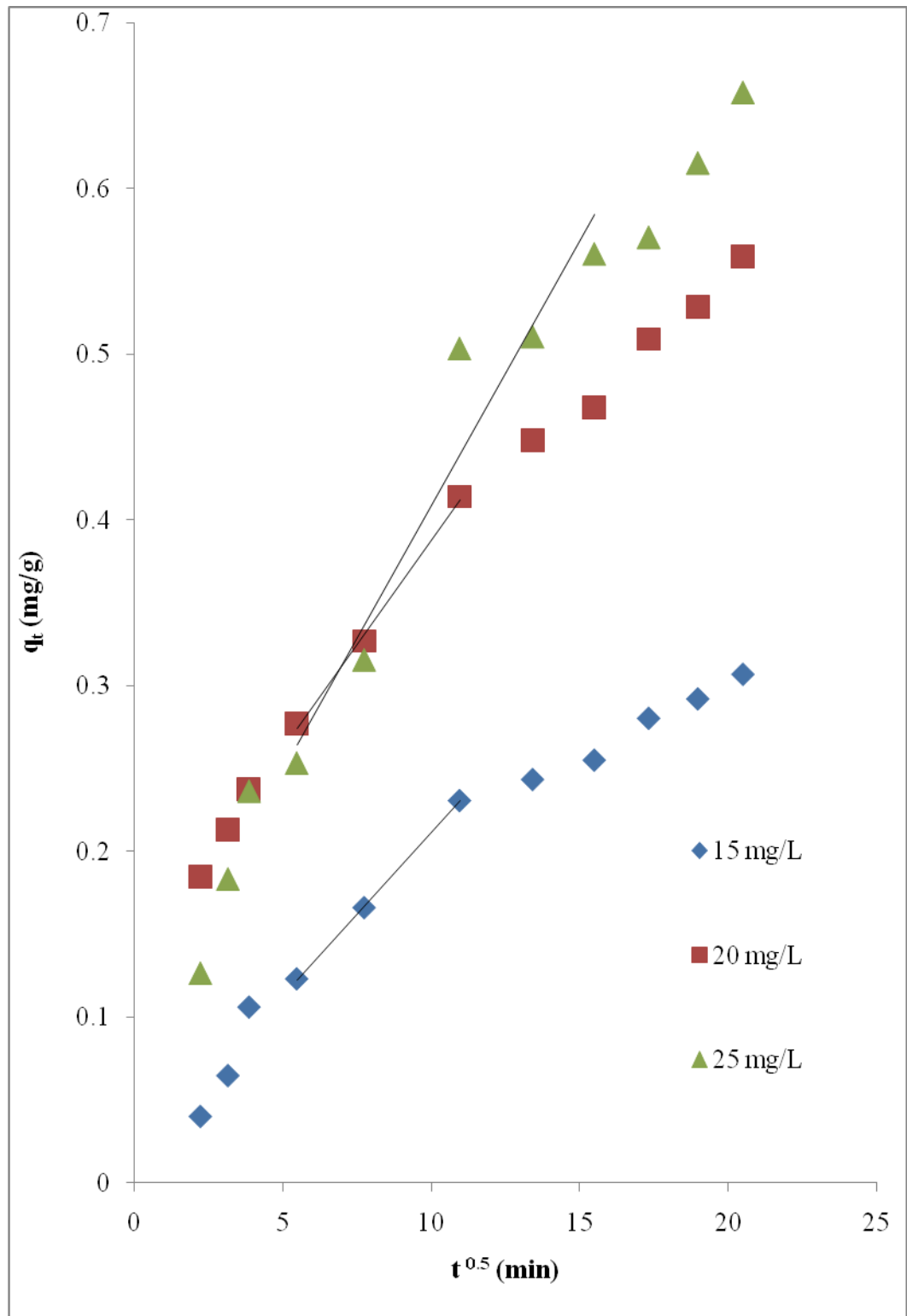
Figure 4.22: Intraparticle diffusion RO16 in single dye solutions in ERH
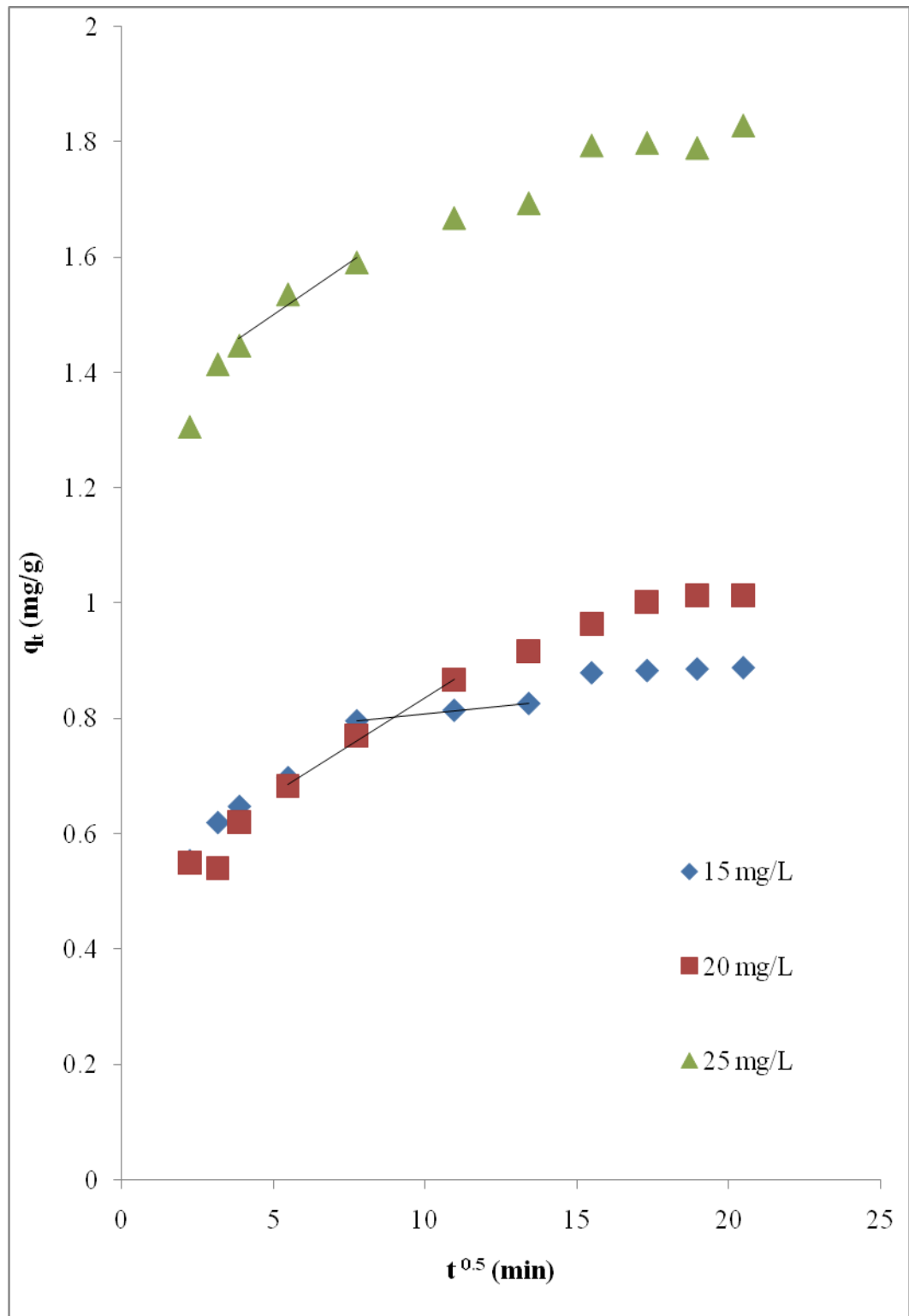
Figure 4.23: Intraparticle diffusion RO16 in binary dye solutions in ERH

Table 4.6: Intraparticle diffusion rate constants and regression coefficients for the adsorption of MB and RO16 in both single and binary dye solutions

Dye solutions	Initial dye concentration (mg/L)	K_p (mg/g min$^{0.5}$)	Intercept (mg/g)
Single MB	15	0.017	2.836
	20	0.025	3.756
	25	0.035	4.669
Binary MB	15	0.022	2.742
	20	0.024	3.745
	25	0.057	4.479
Single RO16	15	0.019	0.014
	20	0.025	0.089
	25	0.032	0.136
Binary RO16	15	0.005	0.503
	20	0.033	0.754
	25	0.036	1.318

4.5.7   Effect of Adsorbent Dosage

The effect of adsorbent dosage on adsorption of MB and RO16 in both single and binary dye solutions is shown in Table 4.7. For RO16, it followed the usual trend of increasing uptake as the adsorbent dosage increased. The percentage uptake of single and binary RO16 was increased by 16.19 % and 8.88 %, respectively. This can be attributed to an increase in active sites for adsorption. The percentage uptake of MB in single and binary dye solutions was increased from 97.96 % to 99.25 % and 97.99 % to 99.30 %, respectively with an increase in adsorbent dosage ranging from 0.05 g to 0.20 g. Saturation occurred at 0.20 g adsorbent whereby further increase in adsorbent dosage had slight effect on the

adsorption. This can be explained in terms of depletion of dye in solution and accumulation of dye molecules on the surface of ERH giving rise to hindering the rest of dye to diffuse inside the ERH matrix. This study is useful for establishing the optimal dosage of ERH needed in the uptake of dyes.

Similar behaviour was observed and reported by Amin (2008) where the adsorption of Reactive Orange onto activated carbon prepared from sugarcane bagasse increased with increasing dosage of adsorbent and this is due to the increase in availability of surface active sites for adsorption of dye molecules.

Table 4.7: Effect of adsorbent dosage

Dye Dosage	% Uptake (Single MB)	% Uptake (Single RO16)	% Uptake (Binary MB)	% Uptake (Binary RO16)
0.05 g	97.96	5.98	97.99	23.35
0.10 g	98.89	12.30	99.05	25.94
0.15 g	98.96	17.19	98.69	28.50
0.20 g	99.25	22.17	99.30	32.23

4.5.8   Effect of Particle Size

The experimental results obtained for the adsorption of RO16 in both single and binary dye solutions onto ERH by four different size ranges are presented in Figures 4.24 and 4.25. Results revealed that the dye uptake increased with decreasing particle size. In the case of MB, Figures 4.26 and 4.27 showed that the uptake was lying close to each other and this may due to the high affinity of ERH towards MB dye molecules. Results obtained suggest that surface area of the adsorbent plays an important role in the adsorption of dye molecules. Furthermore, smaller particle sizes move faster in dye solution and thus results in higher rate of adsorption.

Comparable results were observed in the uptake of Astrazon Yellow 7GL by wheat bran when the particle size reduced to 354 μm, the amount of dye adsorbed increased from 5.20 to 6.30 mg/g (Sulak et al., 2007). Satish et al. (2010) reported that the percentage uptake of Methylene Blue on teak tree bark powder increased with decreasing particle size. This is owing to the increase in available binding sites for the binding of dye molecules. For smaller particles, the diffusion resistance to mass transfer is low and hence, more internal surface of the particle can be utilised for adsorption.
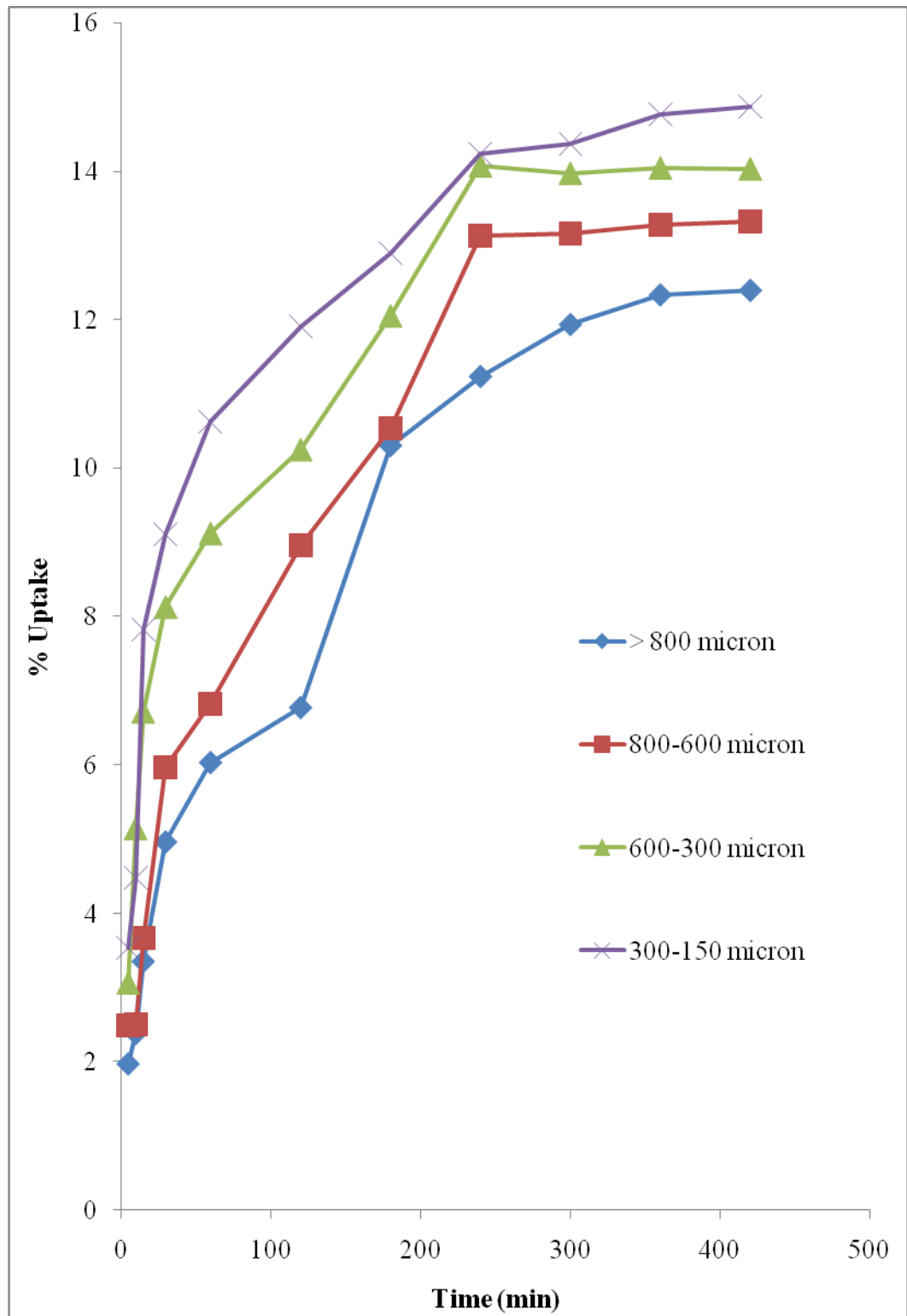
Figure 4.24: Effect of particle size for the adsorption of RO16 in single dye solutions
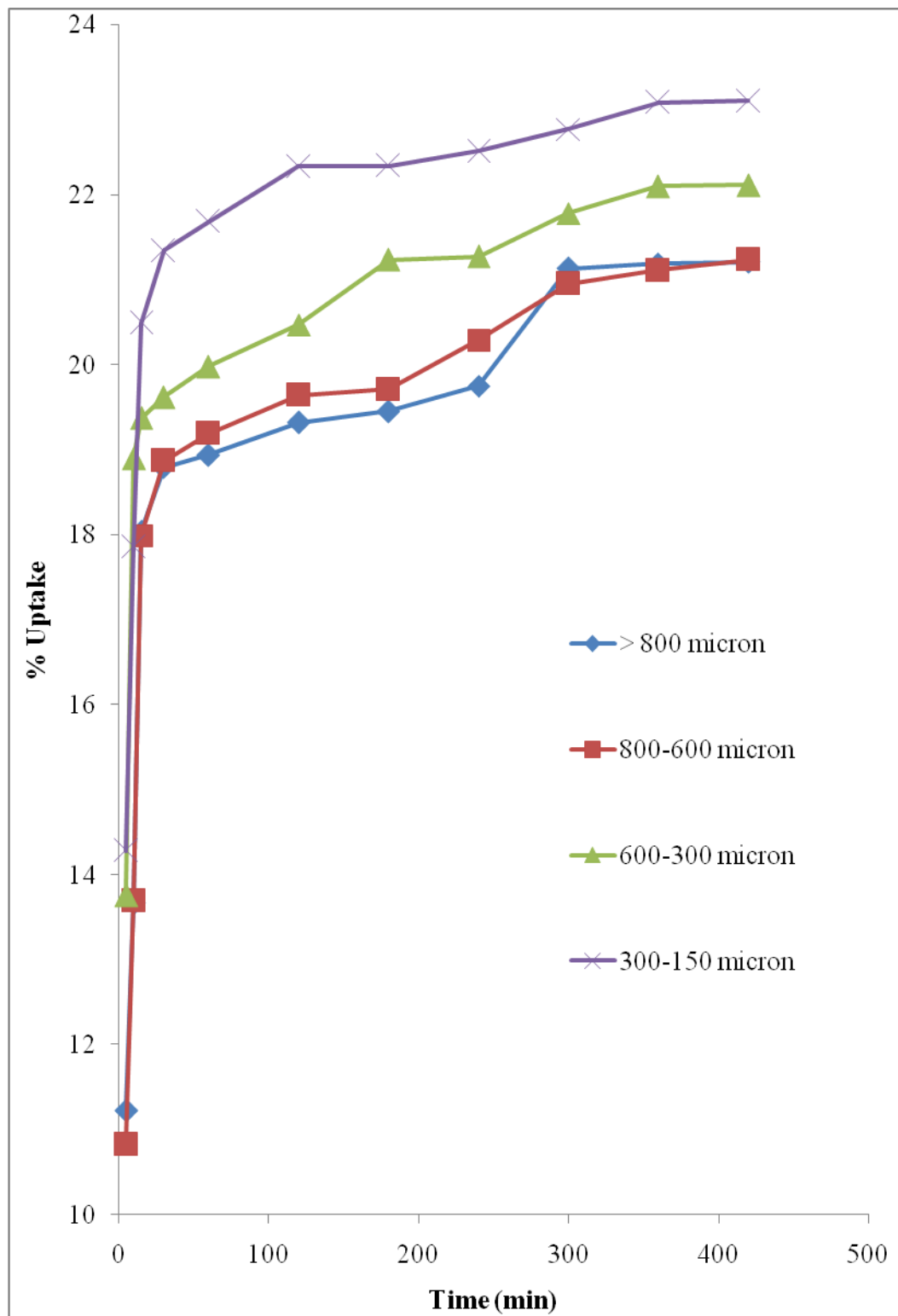
Figure 4.25: Effect of particle size for the adsorption of RO16 in binary dye solutions
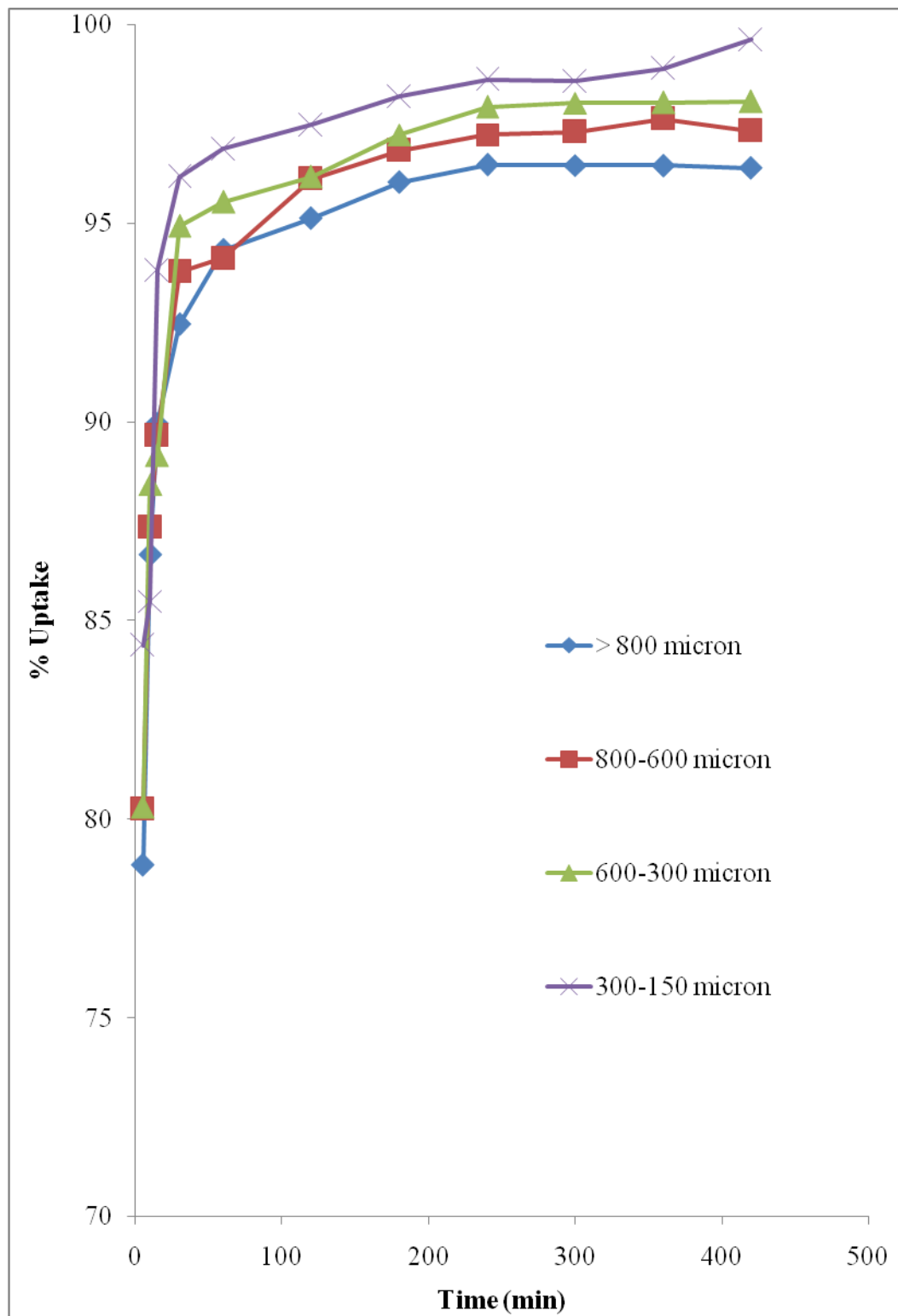
Figure 4.26: Effect of particle size for the adsorption of MB in single dye solutions
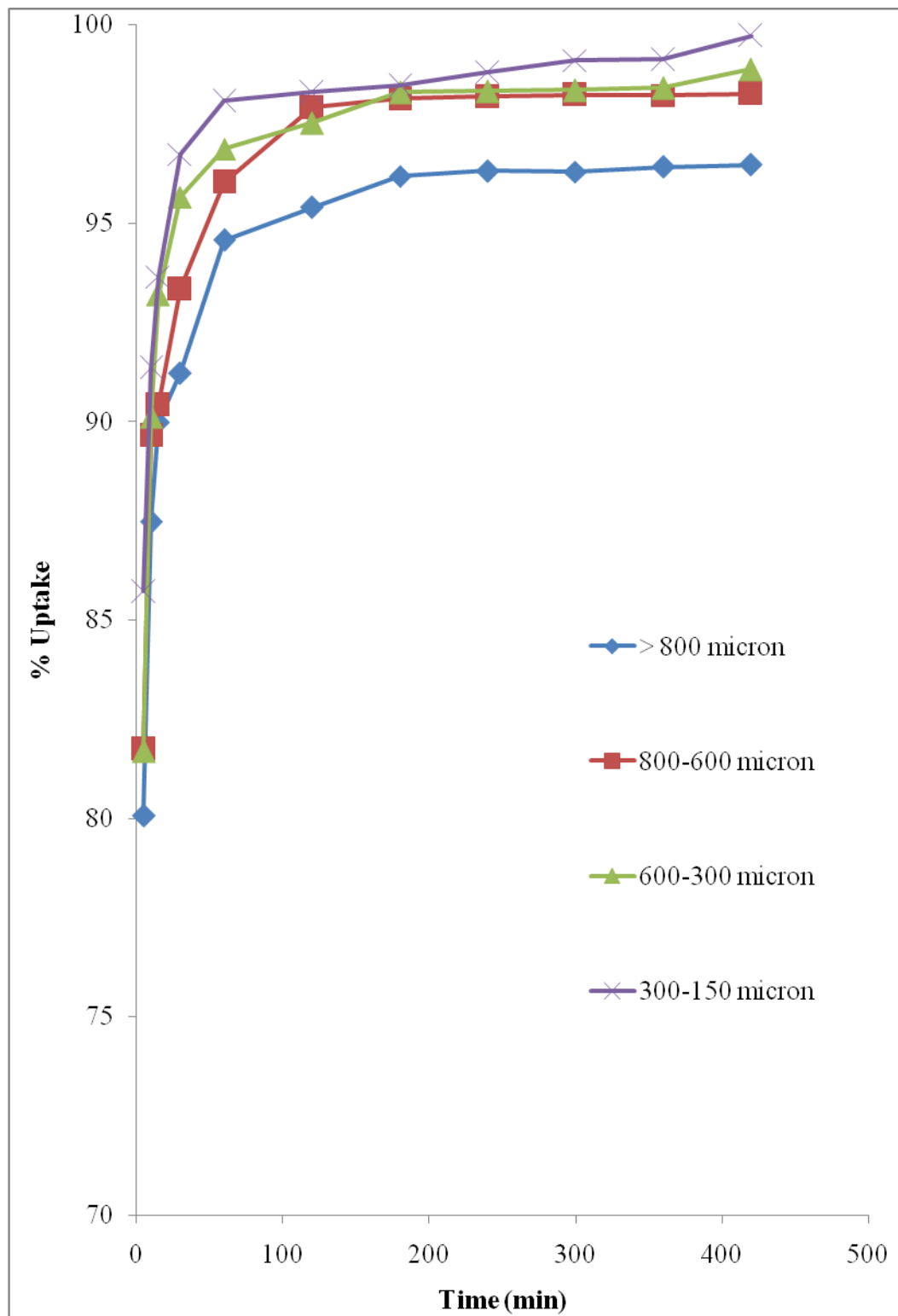
Figure 4.27: Effect of particle size for the adsorption of MB in binary dye solutions

4.5.9   Effect of Temperature

Figure 4.28 shows the effect of temperature in the adsorption of MB and RO16. A rise in temperature decreases the percentage uptake of MB from 99.3 % to 95.8 %, indicating that the adsorption process was exothermic. This is most probably due to the increasing of total energy of the adsorbate molecules at higher temperature and consequently their escaping tendency was also increased. Similar observations were reported in the adsorption of Cu and Pb ions (Wong et al., 2003) and Methylene Blue (Hamdaoui and Chiha 2007). On the other hand, adsorption of RO16 on ERH was more favourable at higher temperature. This is because at higher temperature, it gives rise to an increment in the mobility of the solute and the enlargement of the pore sizes of the adsorbent would favour the adsorption of dyes. Guo et al., (2003) suggested that adsorption of Malachite Green increased with temperature is due to the increase of intraparticle diffusion rate of the adsorbate into the internal layer of the adsorbent as diffusion is an endothermic process.

The dependence of dye adsorption on temperature can be further confirmed by the van't Hoff plots (Figure 4.29) based on the equation below:

$$\log K_d = \frac{\Delta S^o}{2.303\,R} - \frac{\Delta H^o}{2.303\,RT} \qquad\qquad (4.13)$$

where K_d = distribution coefficient defined as N_e/C_e (l/g), N_e = the amount of dye adsorbed at equilibrium (mg/g), C_e = equilibrium concentration (mg/l), T = absolute temperature (K), R = gas constant (8.3145 J/mol K), ΔS^o = entropy change (J/mol K), ΔH^o = enthalpy change (J/mol).

The values of ΔS^o and ΔH^o have presented in Table 4.8. It was found that, the negative value of enthalpy in the adsorption of MB indicates the exothermic nature of adsorption whereas the positive value of enthalpy indicates that the adsorption of RO16 is an endothermic reaction. The positive value of entropy change (ΔS^o_{total}) indicating an increase in disorder and randomness at the solid-solution interface of dye molecule with adsorbent (Arivoli et al., 2007) which can be attributed to the structural changes during the adsorption of MB and RO16.

Table 4.8: Thermodynamic parameters for the adsorption of MB and RO16 in both single and binary dye solutions

Dye solutions	ΔH^o, the enthalpy change (kJ/mol)	ΔS^o is the entropy change (J/mol)
Single MB	- 16.83 kJ/mol	30.32 J/mol
Binary MB	- 35.06 kJ/mol	87.40 J/mol
Single RO16	14.95 kJ/mol	15.76 J/mol
Binary RO16	11.25 kJ/mol	13.94 J/mol
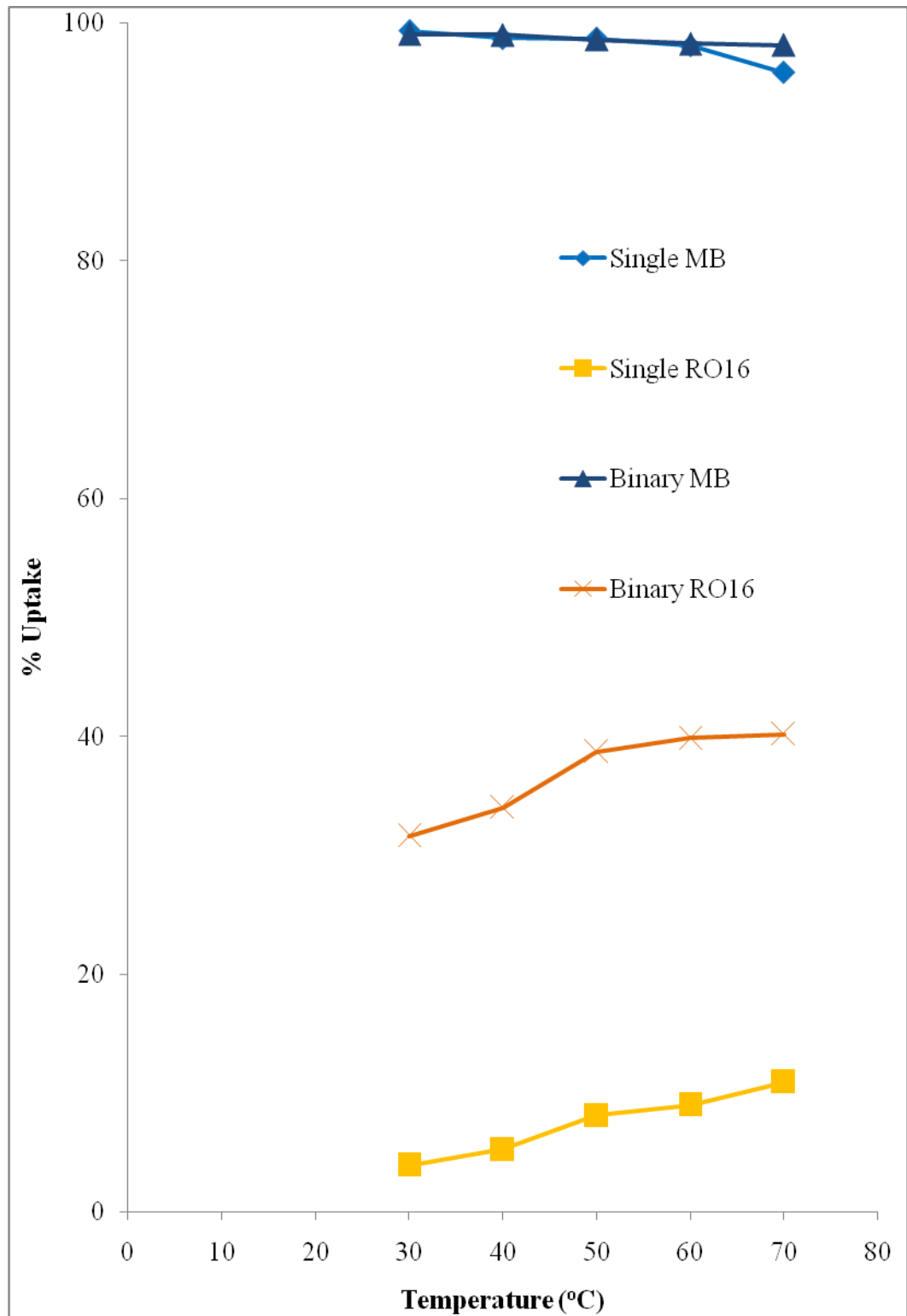
Figure 4.28: Effect of temperature for the adsorption of MB and RO16 in both single and binary dye solutions
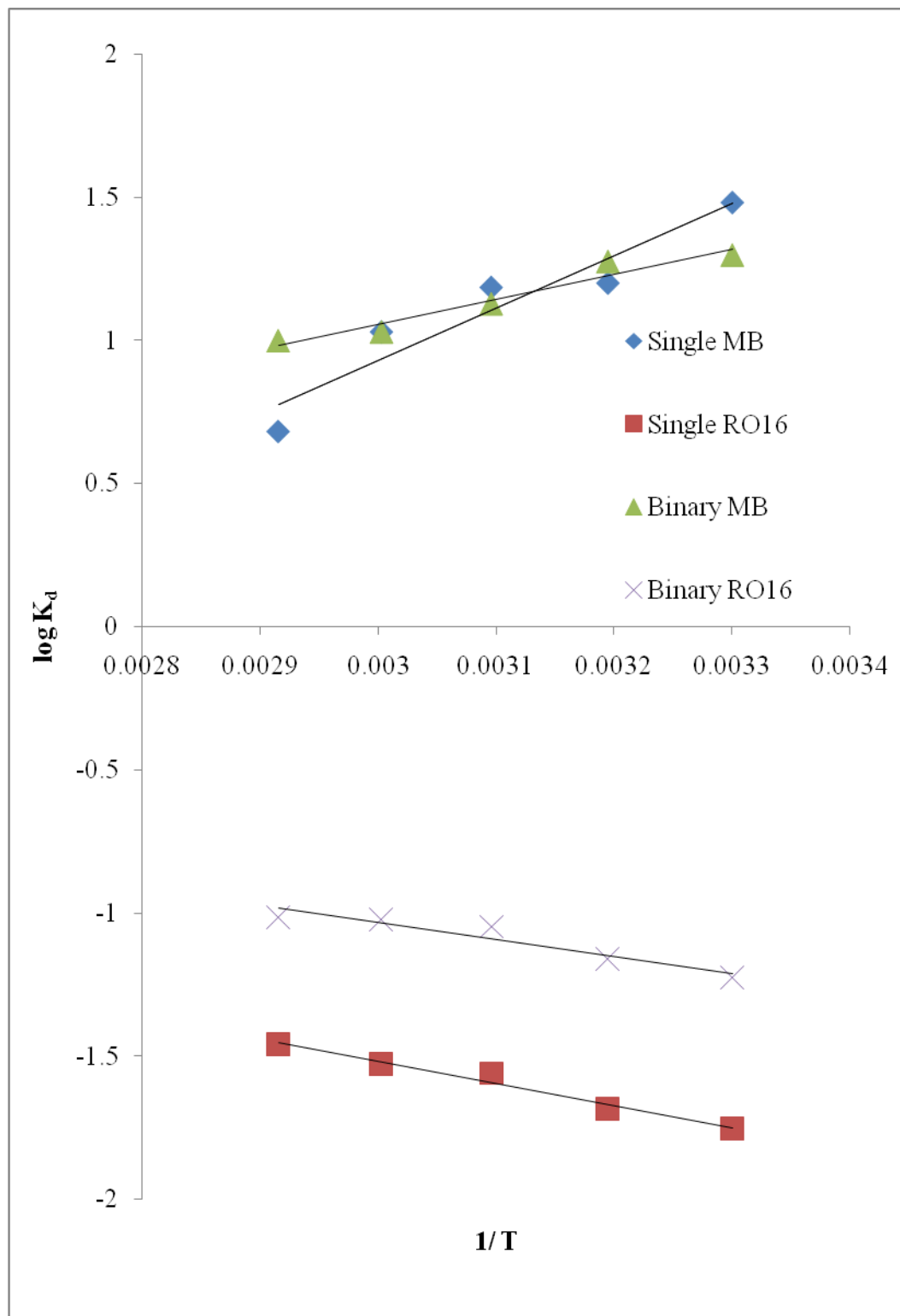
Figure 4.29: Van't Hoff plot for the adsorption of MB and RO16 in both single and binary dye solutions

4.5.10 Adsorption Isotherm

The adsorption of dyes by ERH is a function of the equilibrium dye concentration in solution at constant pH and temperature. Various models have been used to describe the adsorption behaviour between the two phases in the adsorption system. These include Langmuir, Freundlich and Brunauer- Emmet- Teller (BET) isotherm models. The linearised Langmuir model is written as:

$$\frac{C_e}{N_e} = \frac{1}{N*b} + \frac{C_e}{N*} \tag{4.14}$$

whereas the linear form of Freundlich can be represented as:

$$\log N_e = \frac{\log C_e}{n} + \log K_f \tag{4.15}$$

where C_e = equilibrium concentration of the dye solution (mg/L), N_e = amount of dye adsorbed at equilibrium (mg/g), $N*$ = maximum adsorption capacity (mg/g), b = constant related to the energy of the adsorbent (L/mg), n = Freundlich constant for intensity and K_f = Freundlich constant for adsorption capacity.

The Langmuir isotherm assumes the following:

   i.   The surface of the adsorbent is uniform, that is, all the adsorption sites are equal.

  ii.   Adsorbed molecules do not interact.

 iii.   All adsorption occurs through the same mechanism.

iv.   At the maximum adsorption, only a monolayer is formed: molecules of adsorbate do not deposit on other molecules but on the free surface of the adsorbent.

BET is actually the modified Langmuir isotherm model where it has the same assumptions as Langmuir. In BET model, however, it allows multilayer adsorption. The linearised form of BET shown as follow:-

$$C_e/ (C_{eq} - C_e)(N_e) = 1/ B_{N*} + \{(B - 1)/ B_{N*}\}\{(C_e) / C_{eq}\} \qquad (4.16)$$

$$\frac{C_e}{(C_{eq} - C_e)(N_e)} = \frac{1}{B_{N*}} + \left(\frac{B-1}{B_{N*}}\right) + \left(\frac{C_e}{C_{eq}}\right) \qquad (4.17)$$

where B is the BET constant expressive of the energy of interaction with surface, and C_{eq} is the saturation of solute (mg/L).

The linear plots of C_e/N_e versus C_e, log N_e versus log C_e and $C_e/(C_{eq} - C_e)(N_e)$ versus C_e/C_{eq} are shown in Figures 4.30 to 4.35. The coefficients for the linearised forms of three isotherm models were tabulated in Table 4.9. The applicability of the isotherm models used can be compared by judging the regression coefficient (R^2) values. Freundlich model appeared to provide reasonable fittings (with high R^2 values) for the adsorption data of MB and RO16 onto ERH, regardless of whether the dye was present in singly or in combination. This implies that the adsorption of dyes is in multilayer form and the surface of ERH is heterogeneous.
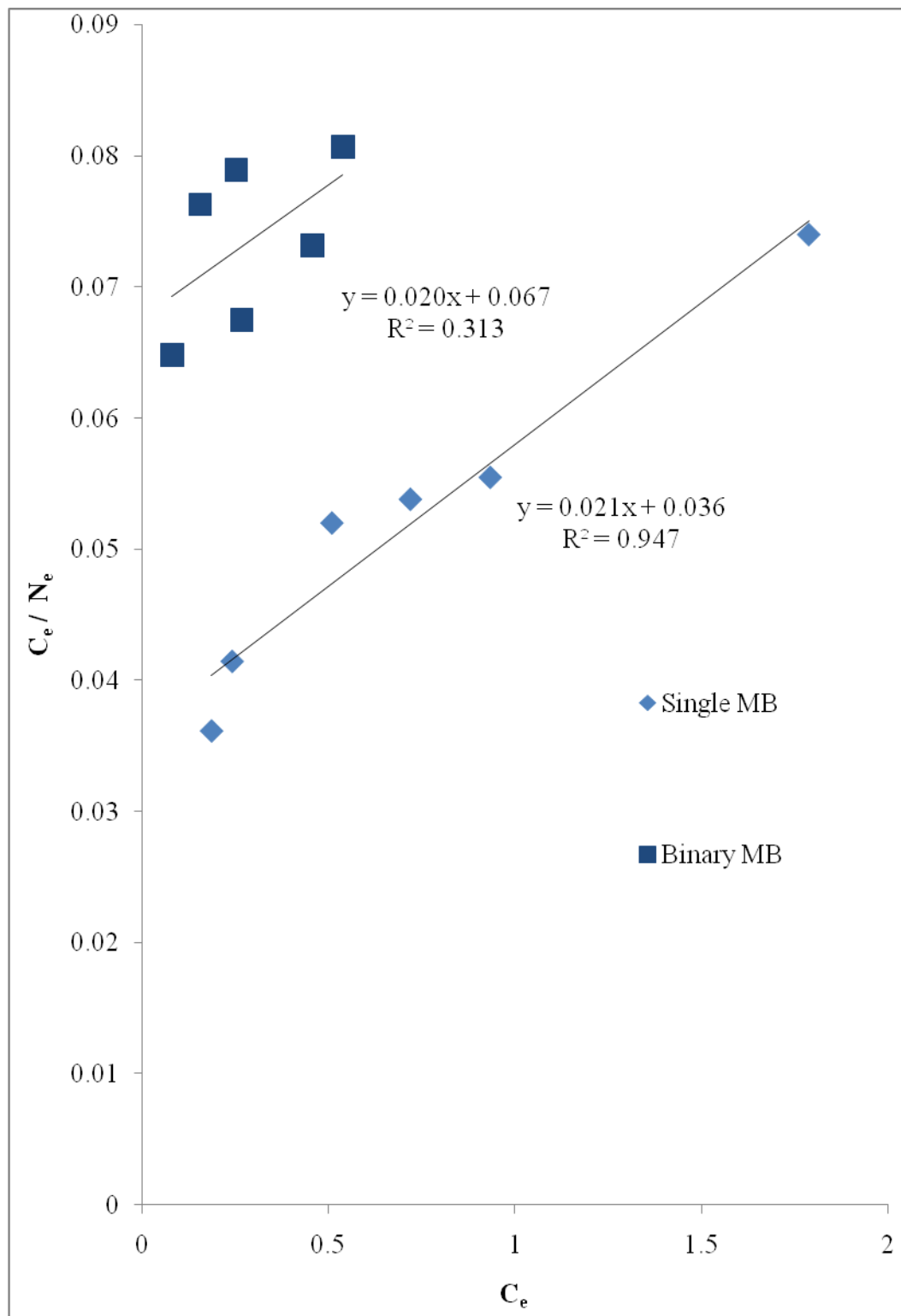
Figure 4.30: Langmuir isotherm for the adsorption of MB in both single and binary dye solutions
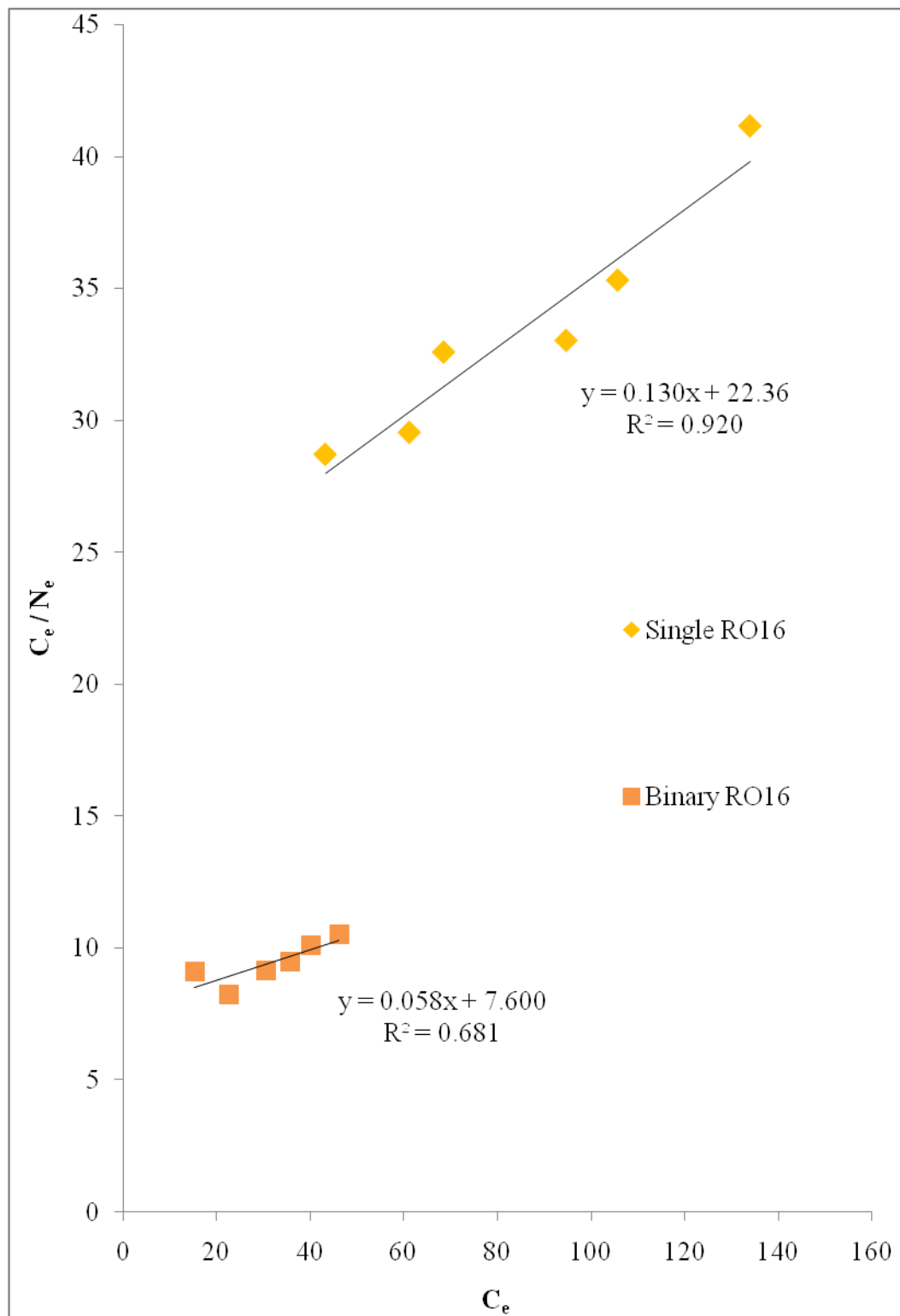
Figure 4.31: Langmuir isotherm for the adsorption of RO16 in both single and binary dye solutions
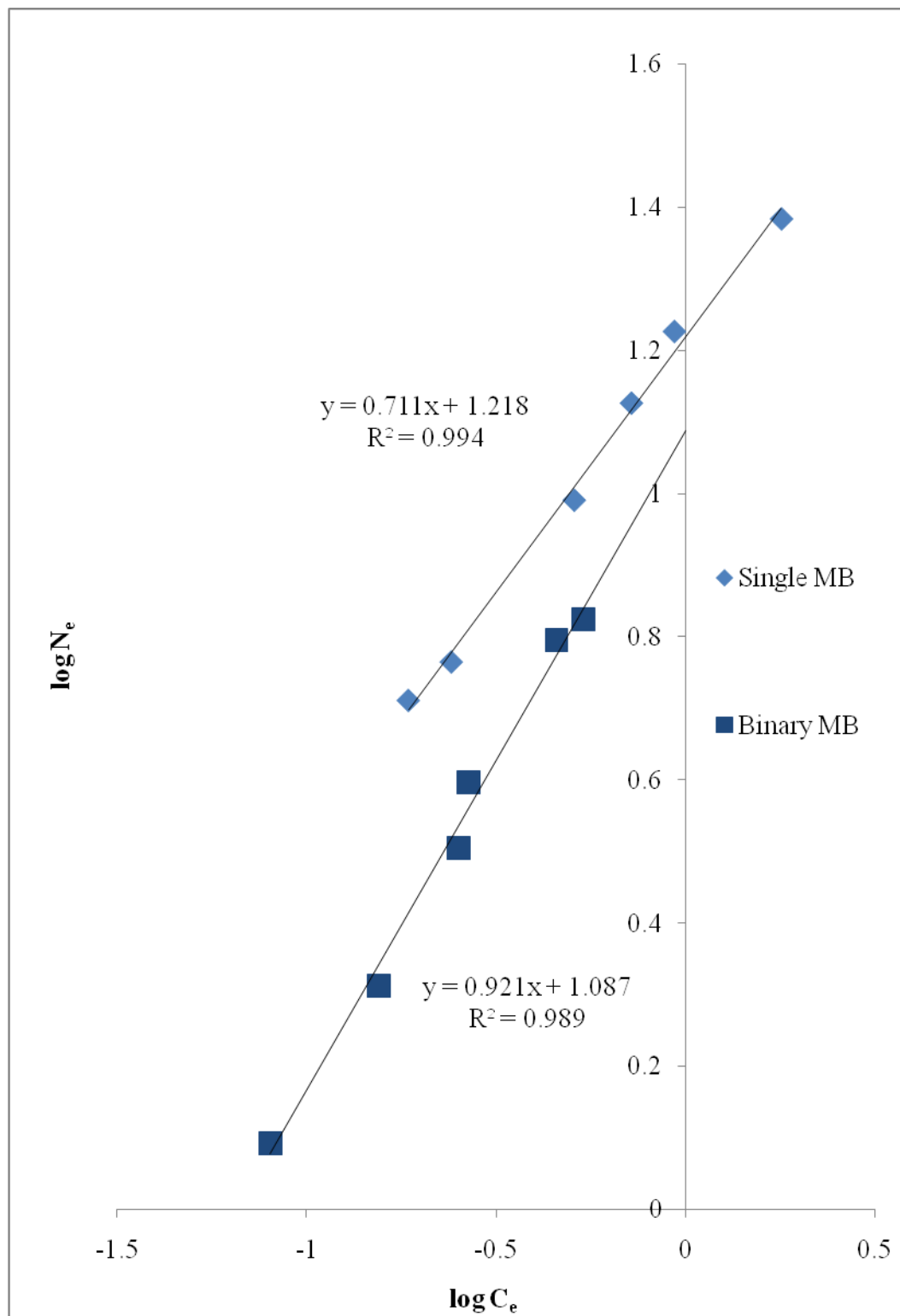
Figure 4.32: Freundlich isotherm for the adsorption of MB in both single and binary dye solutions
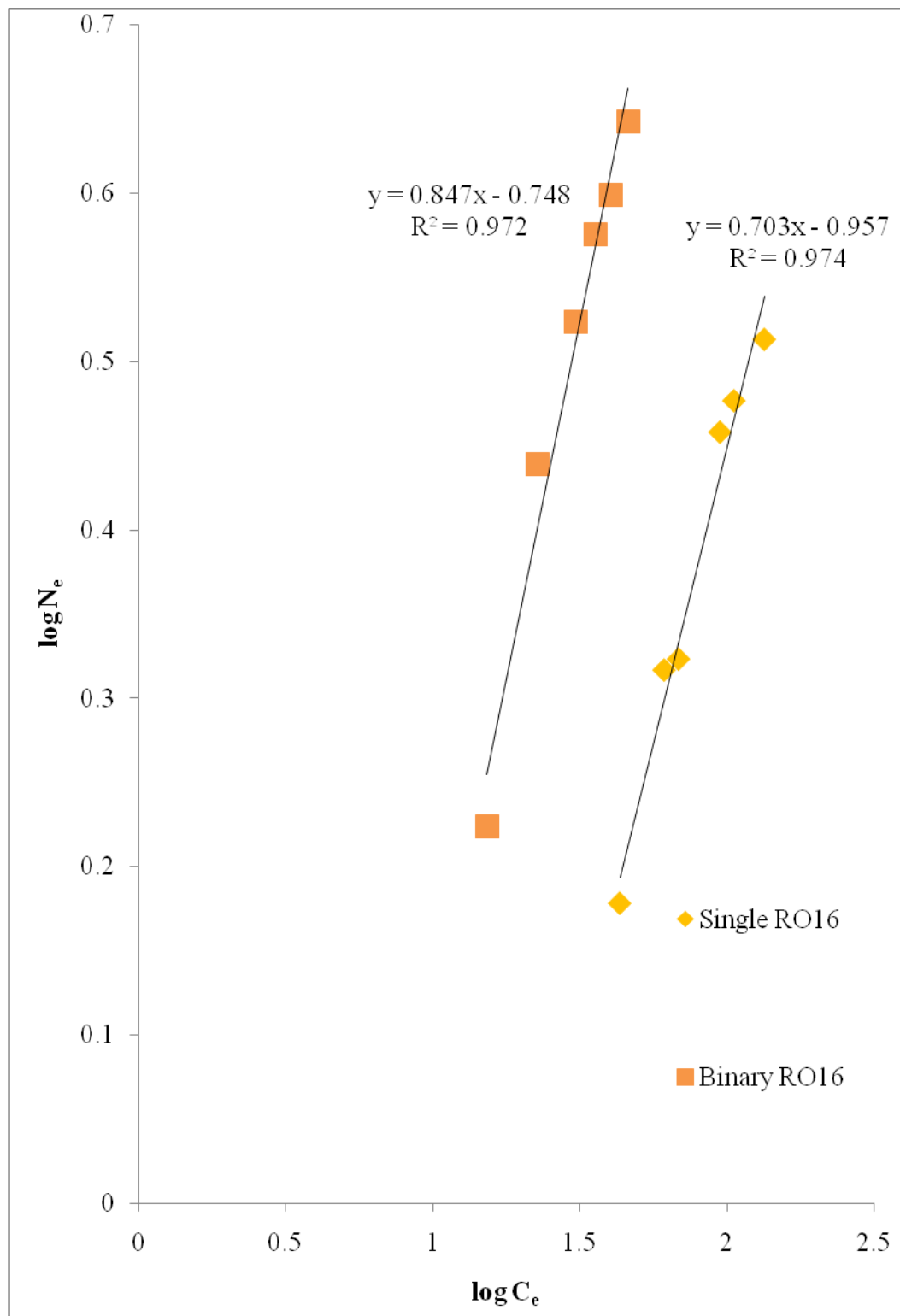
Figure 4.33: Freundlich isotherm for the adsorption of RO16 in both single and binary dye solutions
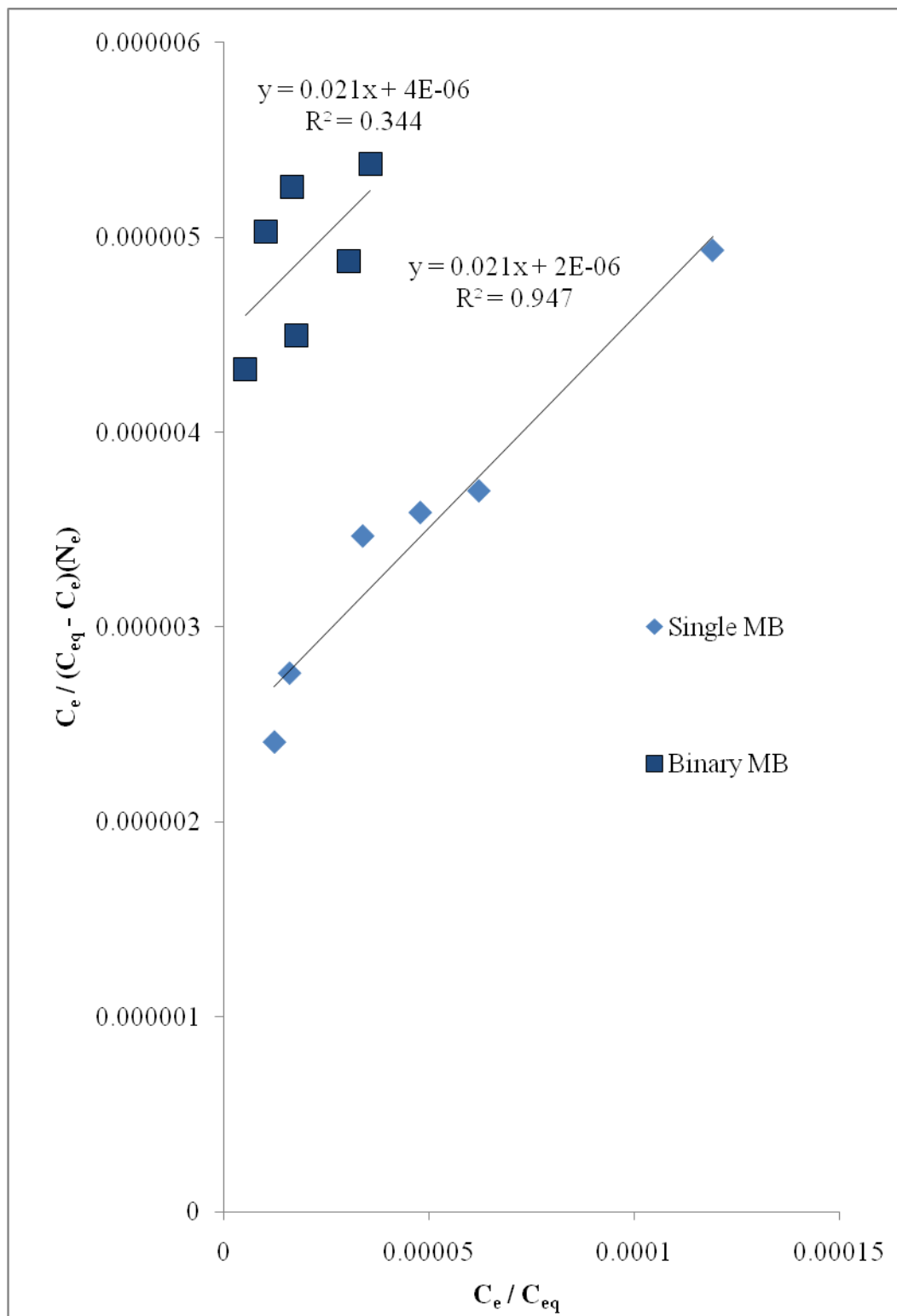
Figure 4.34: BET isotherm for the adsorption of MB in both single and binary dye solutions
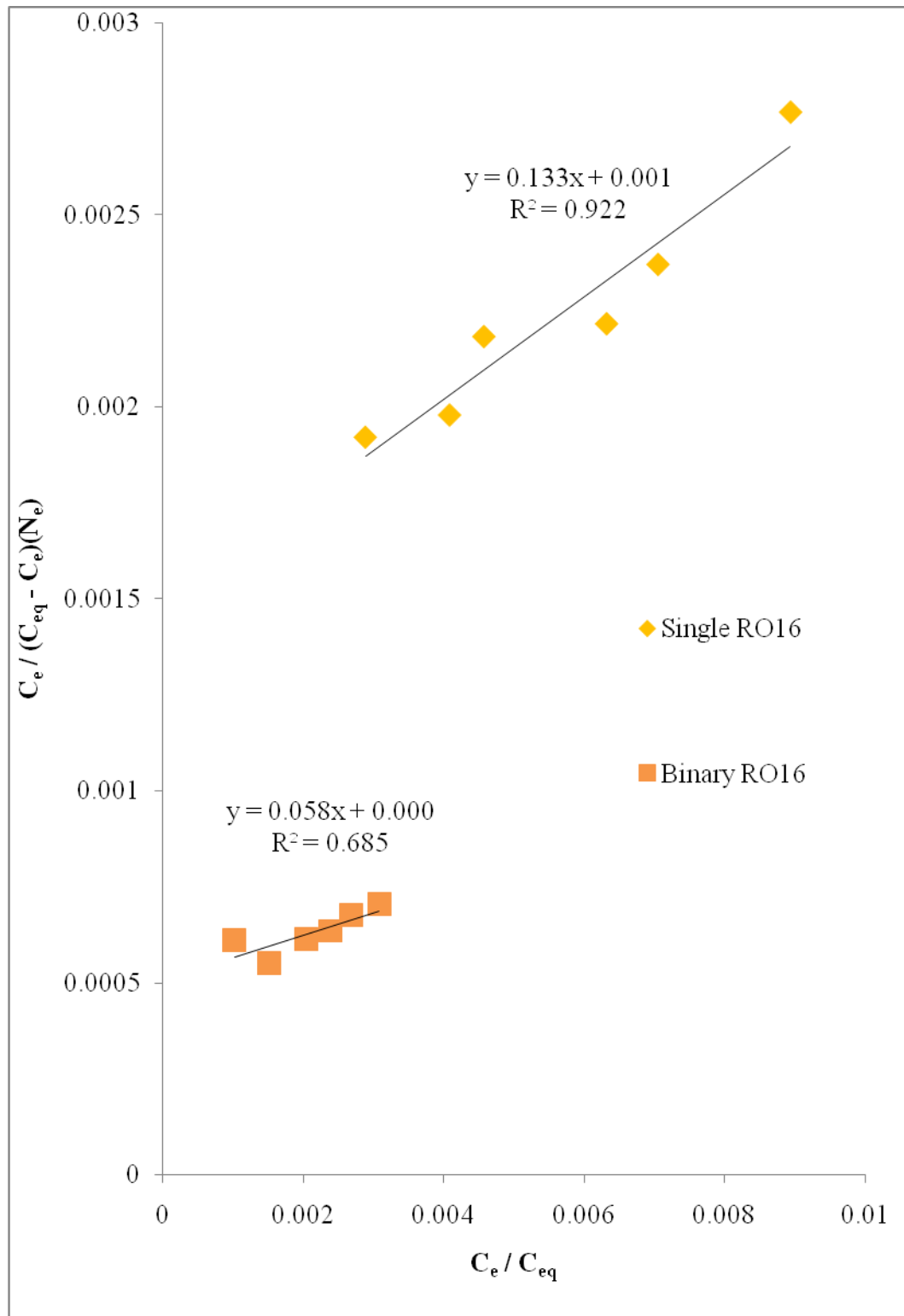
Figure 4.35: BET isotherm for the adsorption of RO16 in both single and binary dye solutions

The low values of R^2 for both Langmuir and BET models indicate that the ERH contains non-homogeneous surface and no interaction between the adsorbed dye molecules. Similar results were reported in the adsorption of Reactive Orange onto carbon of sugarcane bagasse pith by Amin (2008), where Freundlich isotherm model had higher regression coefficient value (0.992) as compared to Langmuir isotherm (0.980).

Although Langmuir model fails to provide a good fitting, this model allows the calculation of maximum adsorption capacity of ERH which could be used for the comparison of the adsorption efficiency of materials. The maximum adsorption capacities for MB and RO16 in binary dye solution were 49.5 mg/g and 17.2 mg/g, respectively. This corresponds to an enhancement of 3.2 mg/g for MB and 9.5 mg/g for RO16 as compared to single dye solution. The enhancement observed is most likely due to the synergistic effect that occurred between the dye molecules in binary system. Table 4.10 showed the maximum adsorption capacity of basic and reactive dyes onto various adsorbents.

Table 4.9: Langmuir, Freundlich and BET constants for the adsorption of MB and RO16 in both single and binary dye solutions

Dyes	Langmuir			Freundlich			BET	
	N^* (mg/g)	b (l/mg)	R^2	K_f	N	R^2	B	R^2
Single MB	46.296	0.589	0.947	82.737	1.406	0.995	-0.0660	0.947
Binary MB	49.505	0.313	0.571	11.625	1.172	0.989	0.0003	0.642
Single RO16	7.675	0.006	0.920	0.110	1.422	0.975	0.9310	0.209
Binary RO16	17.241	0.008	0.681	0.178	1.180	0.972	-0.0140	0.598

Table 4.10: Comparison of maximum adsorption capacity of both basic and reactive dyes onto various adsorbents

Dyes	Adsorbent	Maximum adsorption capacity (mg/g)	Reference
Single MB	ERH	46.3	This work
	Activated carbon prepared from coconut shell	17.8	Yasin et al. (2007)
Binary MB	ERH	49.5	This work
Single RO16	ERH	7.7	This work
	Activated carbon prepared from sugarcane bagasse pith	3.8	Amin (2008)
Binary RO16	ERH	17.2	This work

The essential characteristic of Langmuir isotherm can be expressed in terms of R_L, which predicts whether an adsorption system is favourable or unfavourable (El-Ashtoukhy et al., 2007).

R_L is defined as follow:

$$R_L = \frac{1}{1 + K_a C_o} \tag{4.18}$$

where C_o is the initial concentration of dye solution and K_a is the Langmuir constant. When R_L value is in between 0 and 1 then it is favourable, > 1 is unfavourable, $= 1$ is linear and $= 0$ is irreversible. As shown in Table 4.11, the R_L values for the adsorption of MB and RO16 in single and binary dye solutions are in between 0 and 1. This indicates that the adsorption of both dyes is a favourable process.

Table 4.11: The values of R_L for MB and RO16 dye solutions

Dye solutions	Initial concentration, C_o (mg/L)	R_L
Single MB	25	0.064
	30	0.054
	50	0.033
	70	0.024
	90	0.019
	150	0.011
Binary MB	5	0.364
	10	0.222
	15	0.160
	24	0.106
	30	0.086
	35	0.076
Single RO16	50	0.775
	70	0.772
	80	0.683
	100	0.633
	120	0.589
	150	0.535
Binary RO16	10	0.929
	15	0.898
	25	0.840
	30	0.814
	35	0.789
	40	0.767

4.6 Column Study on Dyes

4.6.1 Effect of Influent Concentrations

The uptake of MB and RO16 from both single and binary dye solutions was studied at different influent concentrations ranging from 5 mg/L to 15 mg/L while other variables were kept constant. The breakthrough curves of MB in

single dye solution were shown in Figure 4.36. A steeper 'S' shape curve was obtained at higher influent concentration with lower breakthrough volume. The breakthrough was observed at 870, 480 and 430 mL of dye solutions for influent concentration of 5, 10 and 15 mg/L, respectively. The data showed that the breakthrough time for single MB increased with decreasing influent concentration. This is because at a lower influent concentration, a weaker driving force would be anticipated due to the lower mass-transfer from the bulk solution to the particle surface. As such, a longer time is needed for the binding sites to become saturated. Similar trend was observed for binary MB as shown in Figure 4.37, where the breakthrough time decreased with increasing influent concentration. Sivakumar et al. (2009) also reported that on increasing the initial dye concentration of Acid Blue 92 and Basic Red 29, the breakthrough curves become steeper and the breakthrough volume decreases.

In the case of RO16, a rapid initial breakthrough was observed followed by an effective adsorption (Figures 4.38 and 4.39). This phenomenon indicates that the adsorption of RO16 was a slow process. Sufficient lapse of time was needed before RO16 can be adsorbed onto the column. This result was similar to the previously reported work by Lee et al. (2008). From Figure 4.38, it revealed that at 3000 mL of eluant volume, the C_t / C_o for 5 mg/L of RO16 is the lowest (0.54) followed by 10 mg/L of RO16 (0.78) and 15 mg/L of RO16 (0.82). This indicates that the adsorption of single RO16 is higher at lower influent concentration.
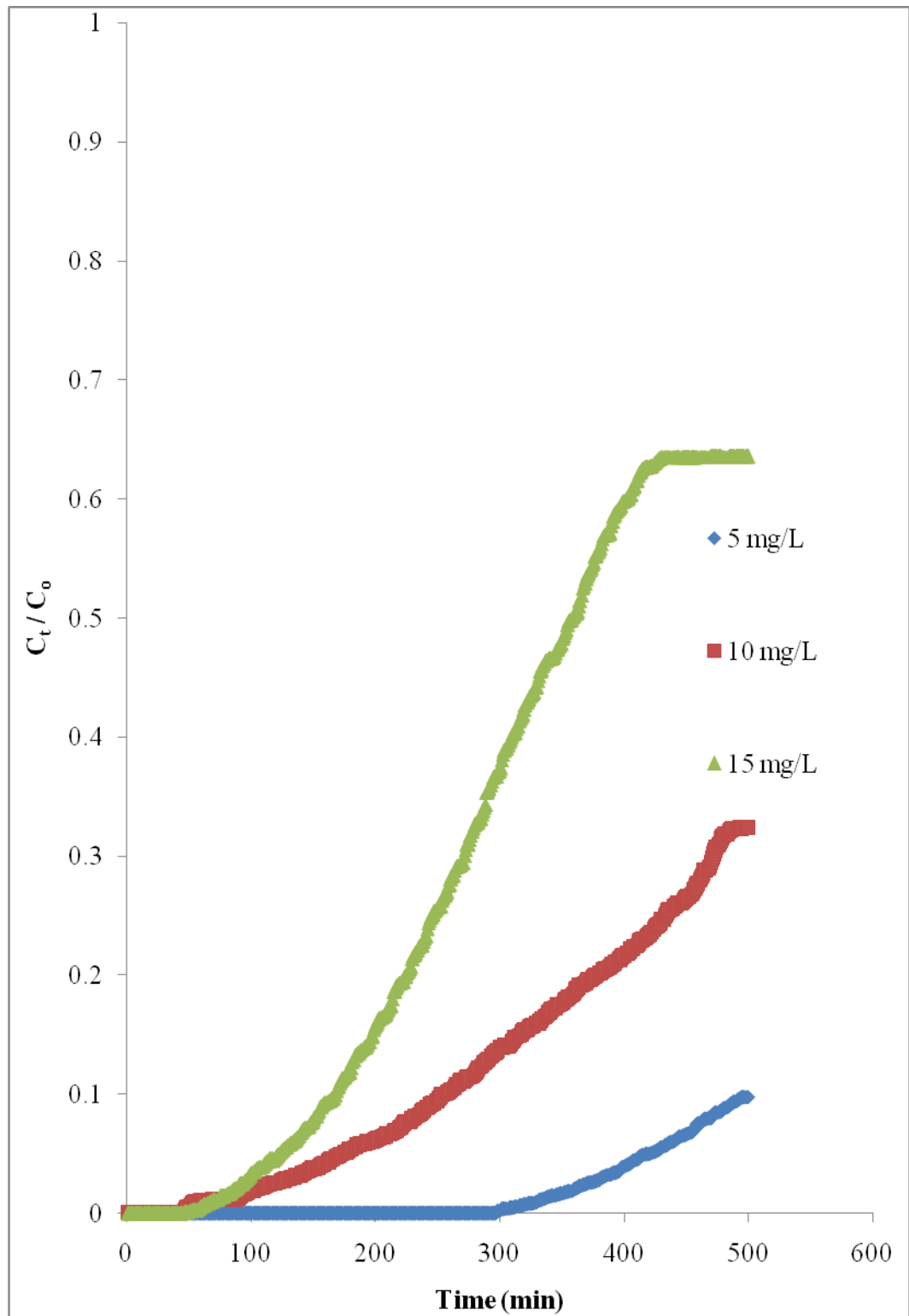
Figure 4.36: Effect of influent concentration on the breakthrough curve of MB in single dye solutions
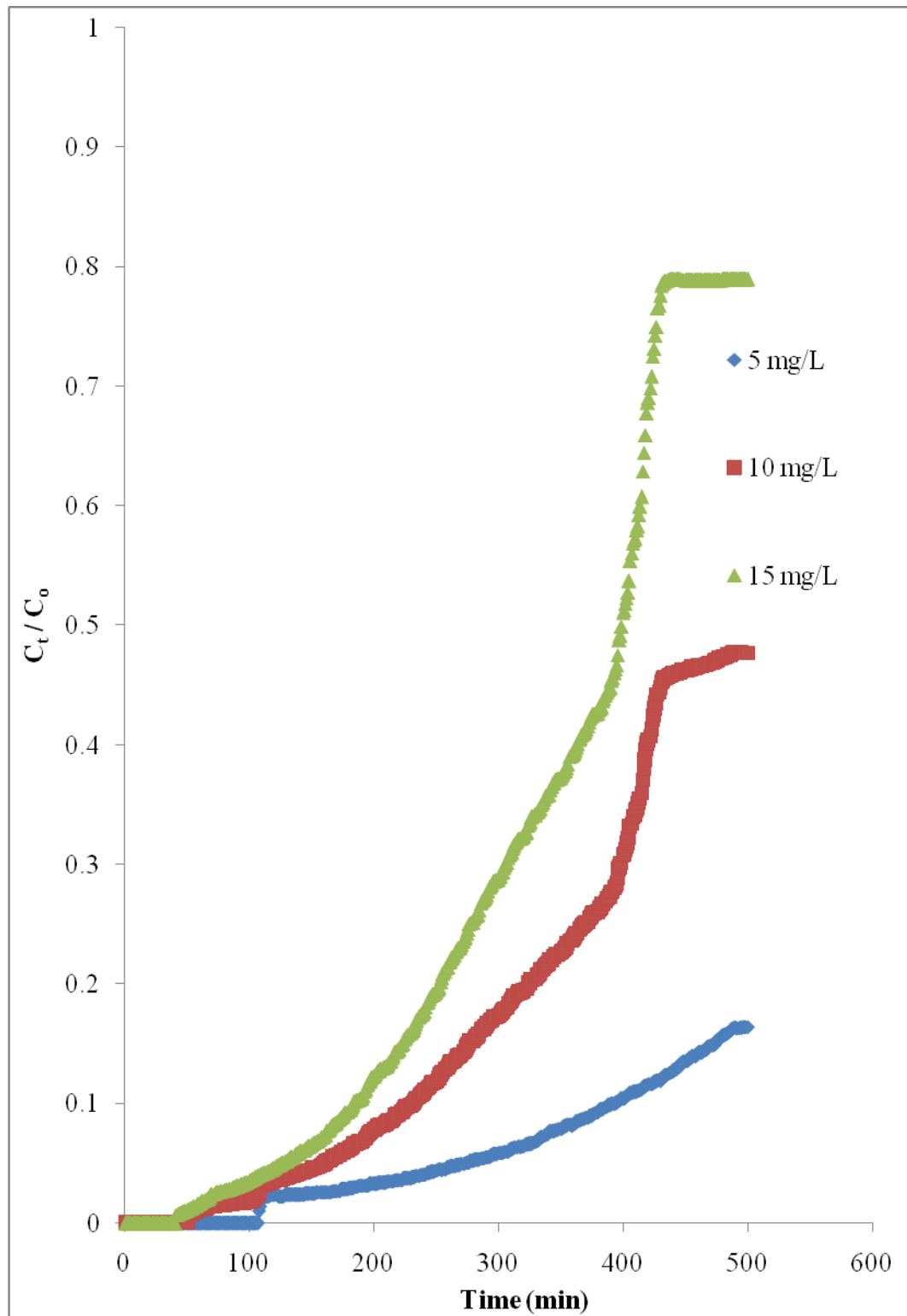
Figure 4.37: Effect of influent concentration on the breakthrough curve of MB in binary dye solutions
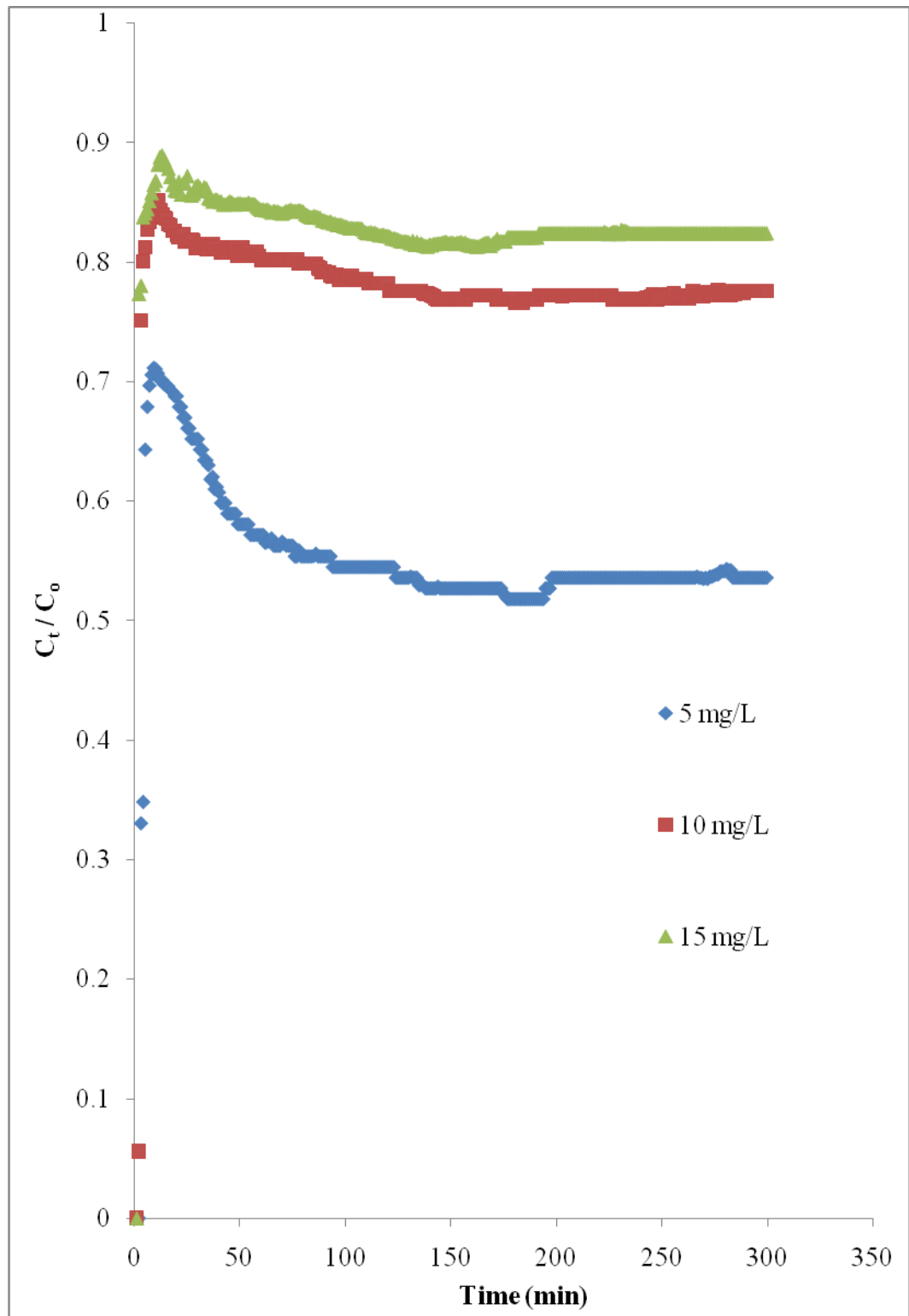
Figure 4.38: Effect of influent concentration on the breakthrough curve of RO16 in single dye solutions
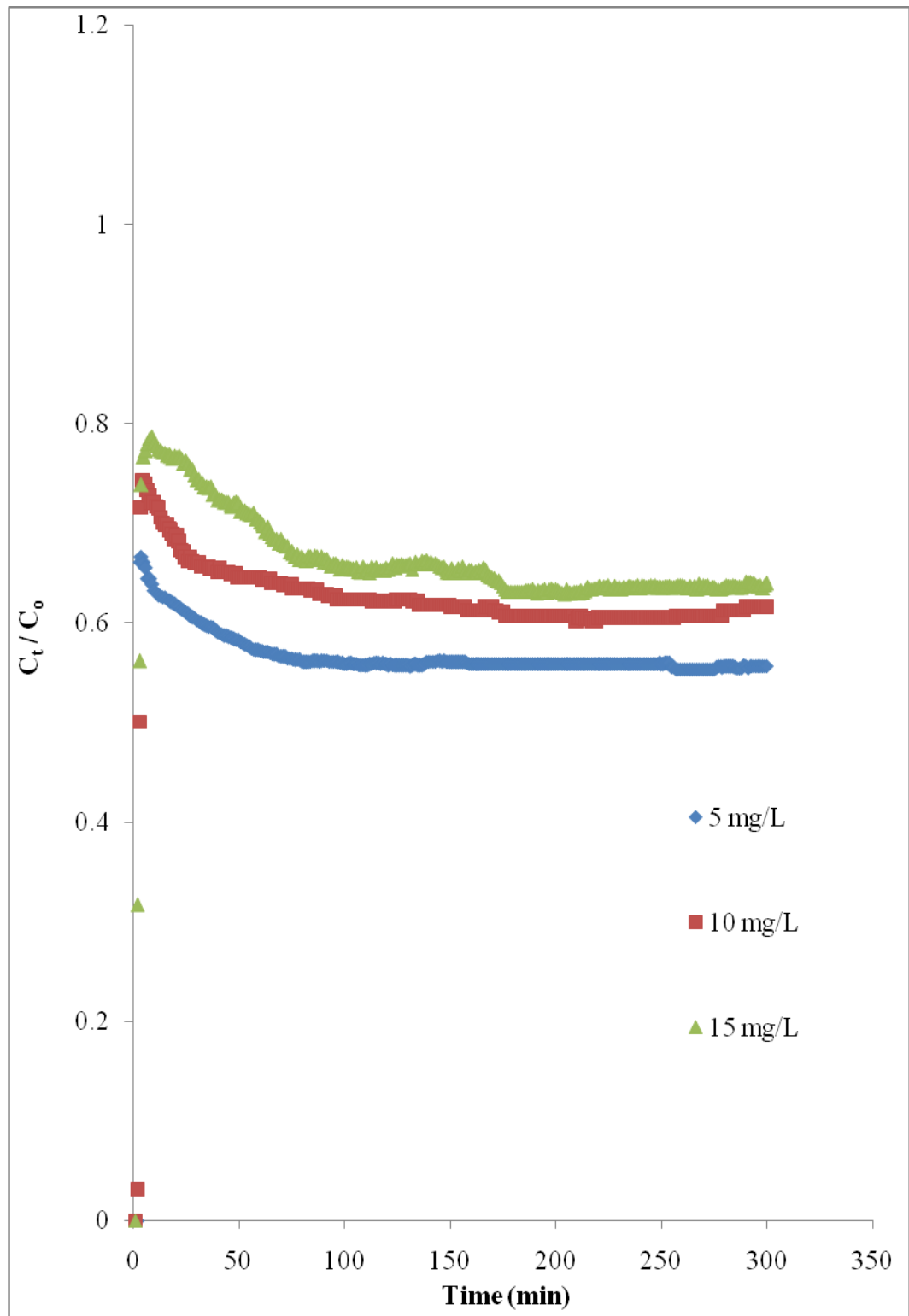
Figure 4.39: Effect of influent concentration on the breakthrough curve of RO16 in binary dye solutions

4.6.2 Adams-Bohart Model

Adams-Bohart model is a model used to determine the mass transfer co-efficient of an adsorption process in a continuous mode condition. The linearized Adams-Bohart equation (Bohart and Adams, 1920) is as follow:

$$ln\frac{C_t}{C_o} = K_{AB}.C_o.t - K_{BA}.q_{BA}.\frac{H}{v}$$ (4.19)

where,

C_t = Eluant concentration at time t (mg/L)

C_o = Influent concentration (mg/L)

K_{BA} = Mass transfer coefficient (L/min.mg)

q_{BA} = Amount of dye solution untaken by adsorbent (mg/L)

v = Linear flow rate of solution (mL/min)

H = Bed height (m)

t = Time (min)

From the Adams-Bohart modeling, the mass transfer coefficient K_{AB} is a diffusion rate constant that relates to mass transfer area, mass transfer rate and concentration gradient of a driving force. This constant value can be determined from the slope of the Adams-Bohart plot (Figures 4.40 and 4.41), which can be used to quantify the mass transfer between a fluid and a solid. As recorded in Table 4.12, the mass transfer coefficient decreases with increasing influent
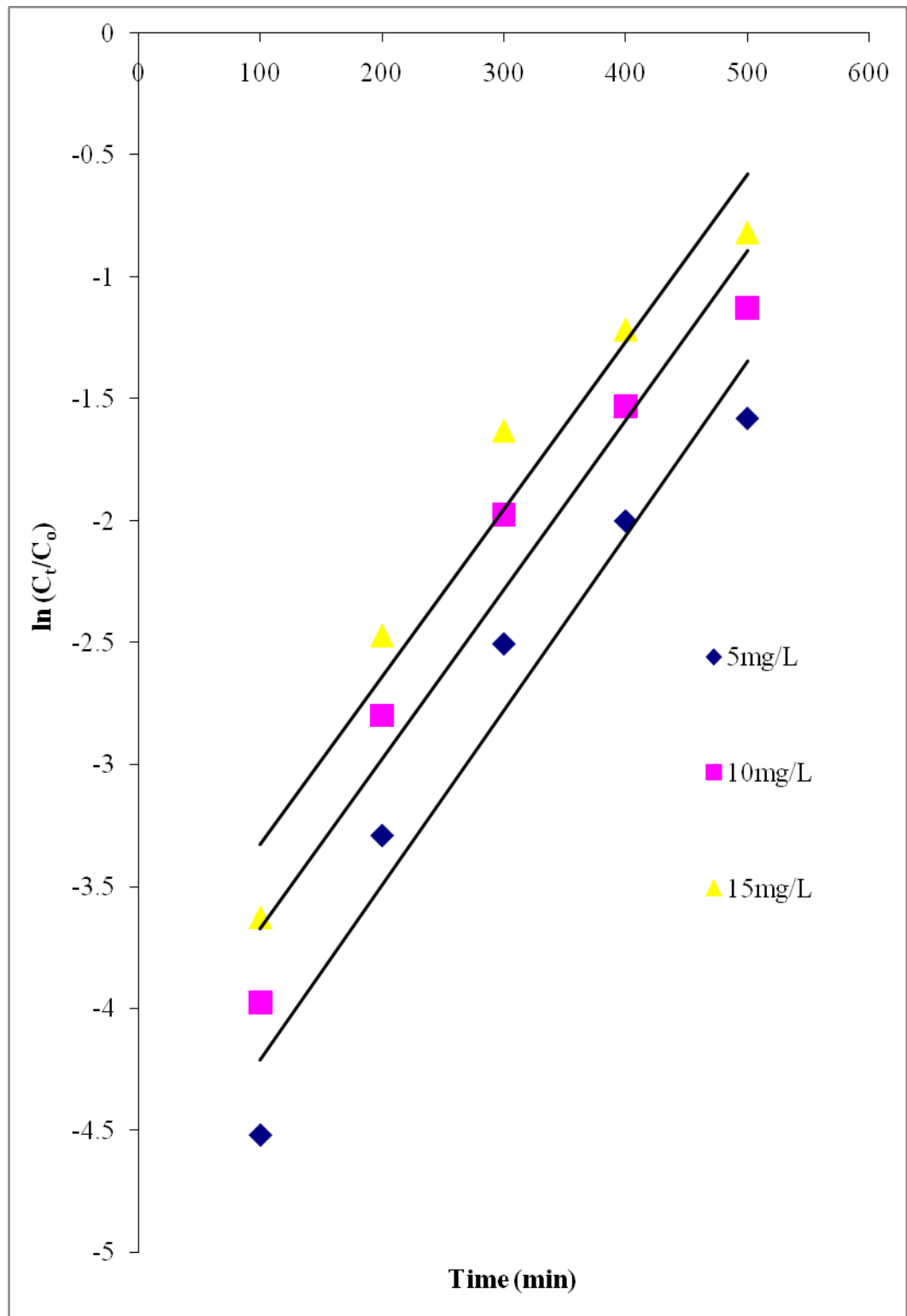
Figure 4.40: Adams-Bohart plot for single MB at different influent concentrations
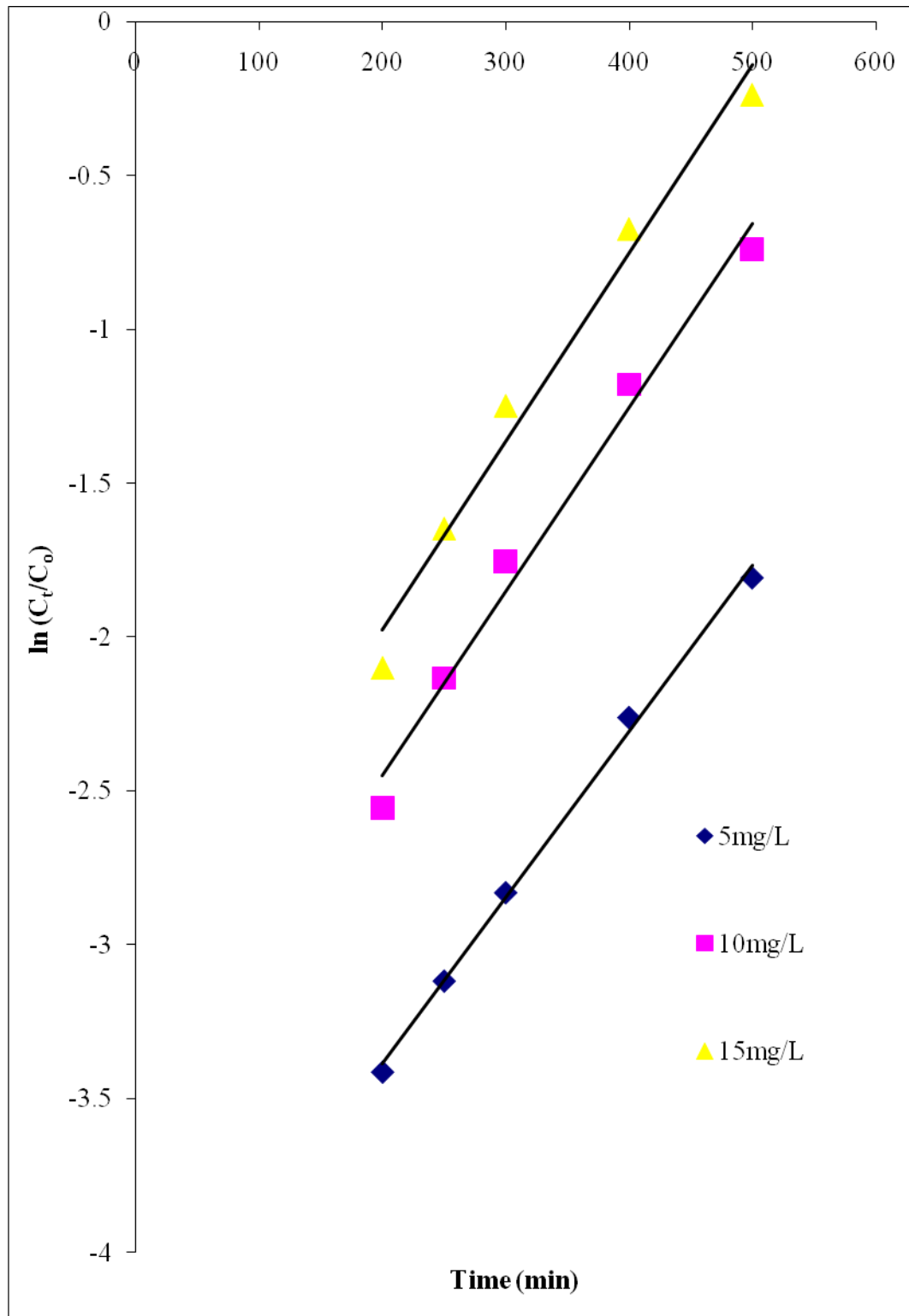
Figure 4.41: Adams-Bohart plot for binary MB at different influent concentrations

concentration of MB in single and binary dye solutions. This indicates that the

mass transfer of the dye molecules from the bulk solution to the surface of ERH is

more favorable at lower concentration (Kannan et al., 2007). As for the R^2 value,

it shows that the experimental data fitted reasonably well in Adams-Bohart model.

For the application of Adams-Bohart model, the breakthrough curves of

adsorption data must be in typical 'S' shape. Since the breakthrough curves of

RO16, in both single and binary dye solutions, did not follow the typical 'S'

shape, thus the model could not applied into it.

Table 4.12: Adams-Bohart constant

Dyes	Influent concentration (mg/L)	Bed depth (cm)	Flow rate (mL/min)	Mass transfer coefficient (k)	R^2
Single MB	5.0	7.0	10.0	0.00140	0.950
	10.0	7.0	10.0	0.00070	0.945
	15.0	7.0	10.0	0.00040	0.943
	10.0	2.5	10.0	0.00038	0.815
	10.0	4.5	10.0	0.00040	0.815
	10.0	7.0	10.0	0.00071	0.944
	10.0	7.0	5.0	0.00196	0.878
	10.0	7.0	10.0	0.00043	0.998
	10.0	7.0	15.0	0.00028	0.863
Binary MB	5.0	7.0	10.0	0.00108	0.997
	10.0	7.0	10.0	0.00060	0.984
	15.0	7.0	10.0	0.00041	0.979
	10.0	2.5	10.0	0.00038	0.815
	10.0	4.5	10.0	0.00040	0.815
	10.0	7.0	10.0	0.00080	0.939
	10.0	7.0	5.0	0.00192	0.861
	10.0	7.0	10.0	0.00055	0.959
	10.0	7.0	15.0	0.00028	0.852

4.6.3 Effect of bed depth

The effect of bed depth in the uptake of single MB dye solution shows that higher bed depth causes longer breakthrough time (Figure 4.42). It was found that at 50 % breakthrough curve, the breakthrough time ($t_{0.5}$) increased from 192 minutes to 201 and to 335 minutes for bed depth of 2.5 cm, 4.5 cm and 7.0 cm, respectively. This is attributed to the increase in available binding sites for adsorption which lead to an increase in the adsorption capacity. Results showed that by varying the bed depth from 4.5 cm to 7.0 cm, it has little effect on the breakthrough curves of MB. This is due to the rapid adsorption of MB by ERH. At lower bed depth, the mass transfer rate between MB molecules and ERH is also lower, based on the mass transfer coefficient value calculated from the slope of the Adams-Bohart plot as shown in Table 4.12. The breakthrough curve data fitted well in Adams-Bohart model (R^2 =0.944) when the column height was fixed at 7 cm. Similar findings were obtained for MB in binary dye solution (Figure 4.43). As shown in Table 4.12, it can be seen that the mass transfer coefficient value was also increased with increasing bed depth, indicating higher mass transfer rate of MB molecules onto ERH.

Similar results were obtained in the study carried out by Sivakumar et al. (2009) where a column of *Euphorbia antiquorum L* activated carbon was
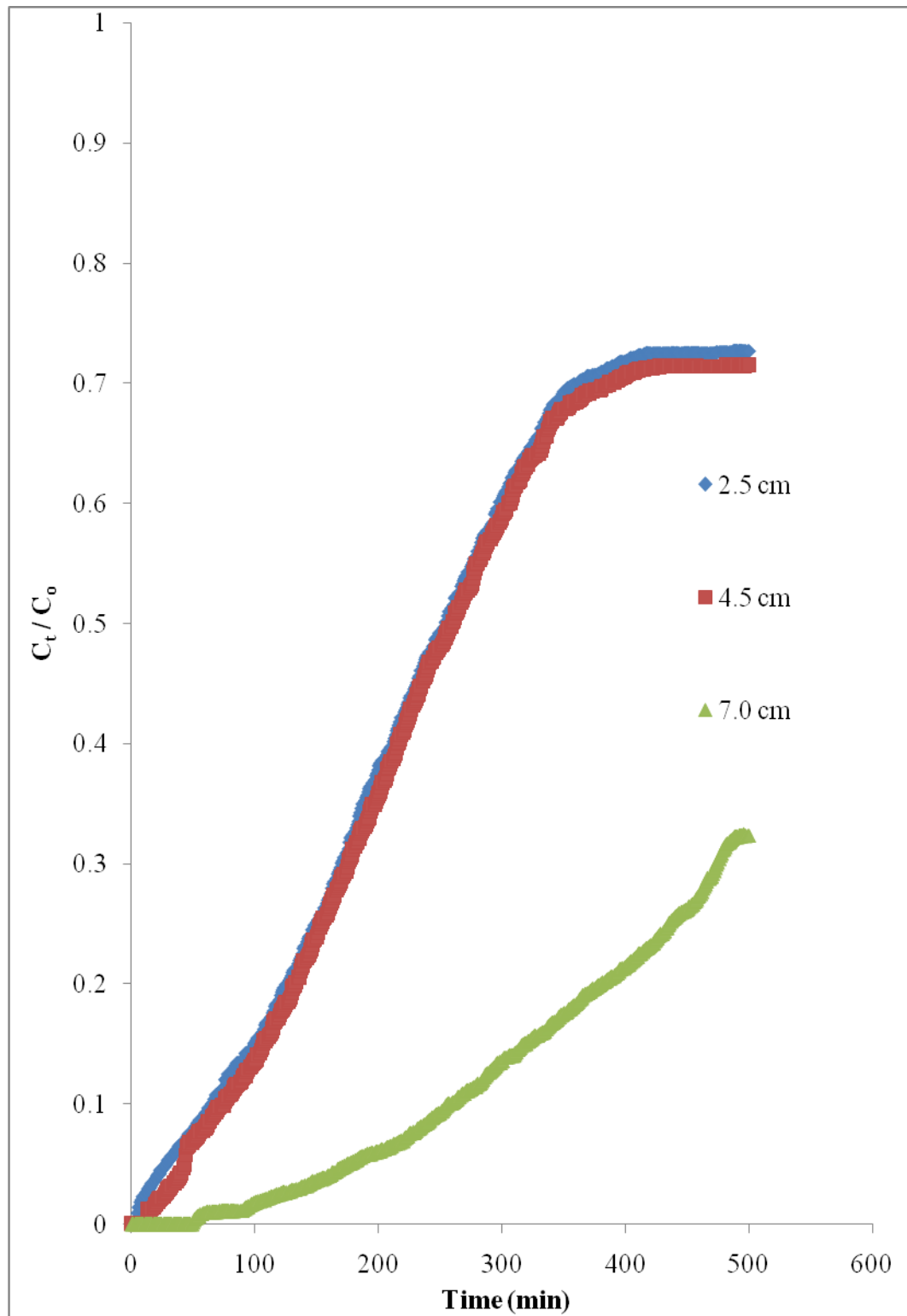
Figure 4.42: Effect of bed depth on the breakthrough curve of MB in single dye solutions
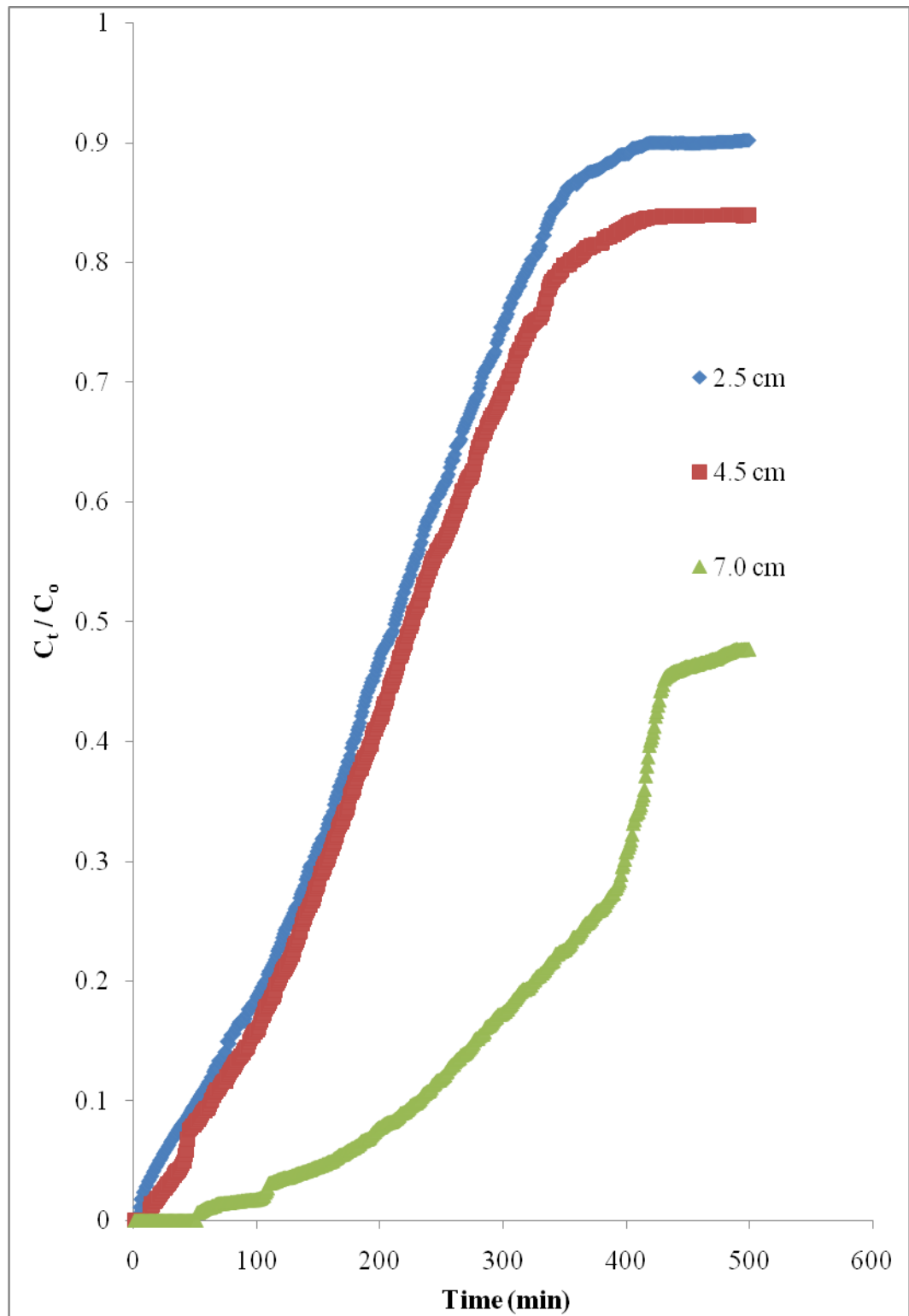
Figure 4.43: Effect of bed depth on the breakthrough curve of MB in binary dye solutions

used for the uptake of Acid Blue 92 and Basic Red 29. They reported that the breakthrough time of dye solution increases with an increase in bed depth due to the availability of more adsorption sites.

The breakthrough curves for RO16 showed a rapid breakthrough at the first few minutes before an effective adsorption could take place as shown in Figures 4.44 and 4.45. The rapid breakthrough might be due to the insufficient time for RO16 molecules to adsorb onto ERH. The adsorption data for single RO16 showed that at 3000 mL of eluant volume, the values of C_t / C_o decreased from 0.94 to 0.66 as the column height increased from 2.5 cm to 7.0 cm. This suggests that with the introduction of more adsorption sites, a better adsorption can be achieved. Besides, the adsorption of RO16 in binary dye solutions was enhanced as compared to single dye solutions and this could be related to the surface charge of the ERH upon adsorption of MB molecules.

Ong, (2006) reported a similar trend of adsorption of RO16 where ethylenediamine modified rice husk was used as an adsorbent in a column studies. Results showed that the breakthrough for RO16 was very rapid, followed by complete adsorption at high bed depth, low influent concentration and flow rate.
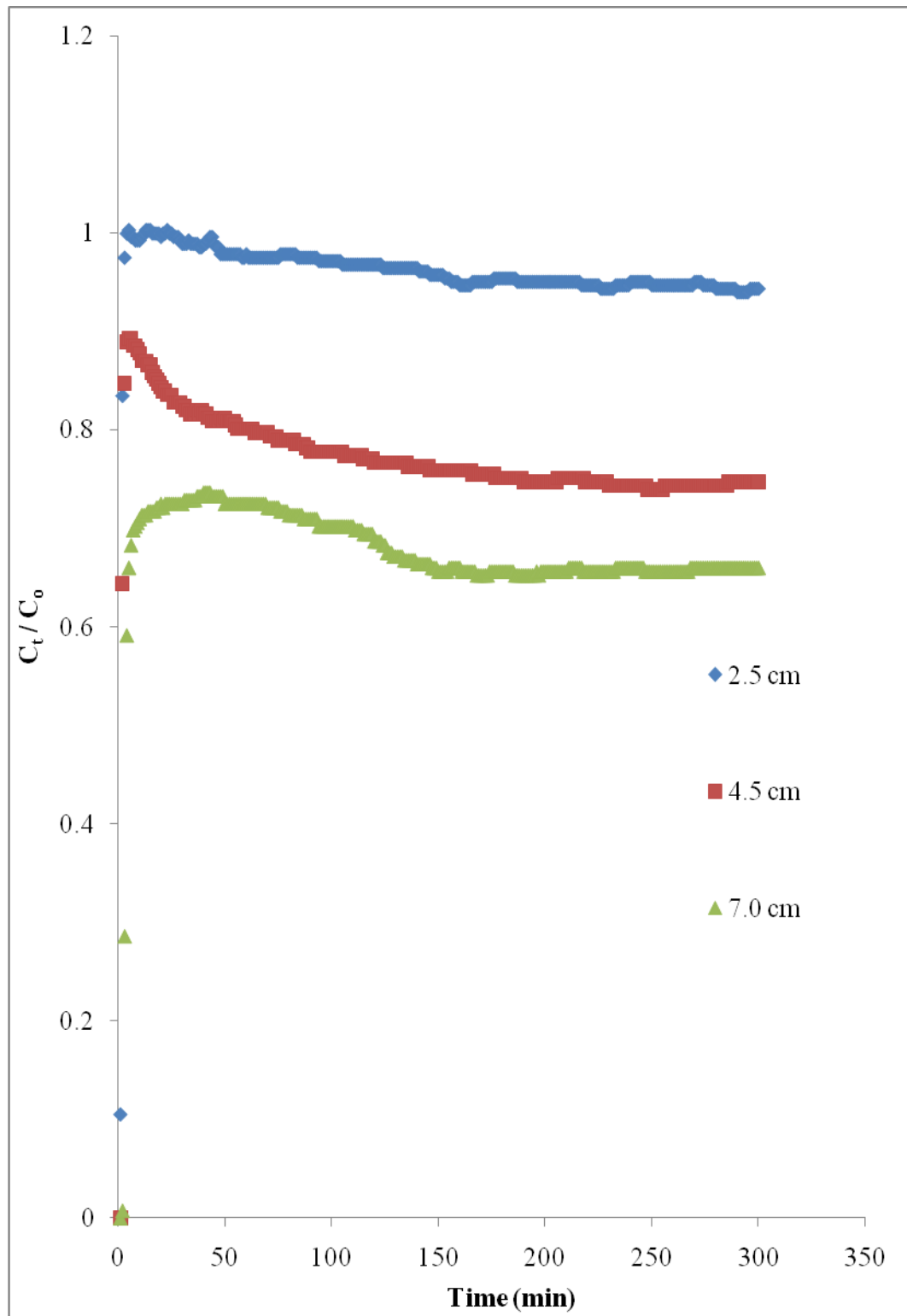
Figure 4.44: Effect of bed depth on the breakthrough curve of RO16 in single dye solutions
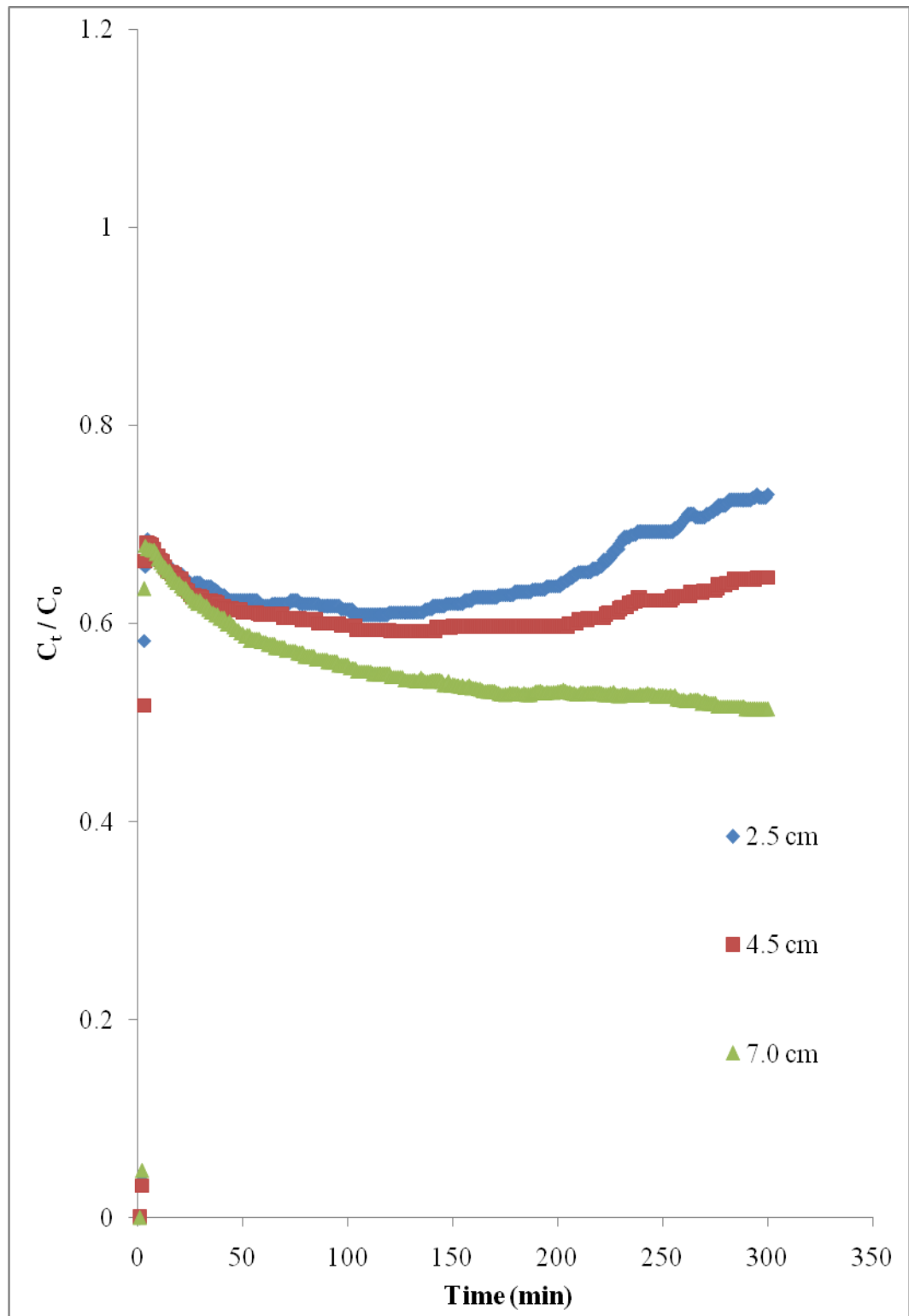
Figure 4.45: Effect of bed depth on the breakthrough curve of RO16 in binary dye solutions

4.6.4 Bed Depth Service Time (BDST) Model

The BDST model (Bohart and Adams, 1920) is commonly used to measure the capacity of a specific bed depth at different breakthrough times. BDST model assumed that both intraparticle mass transfer resistance and external film resistance are negligible. These assumptions enable the model to provide useful modelling equations for the changes in the system parameters (Ko et al., 2000). The equation of BDST model is as follows:

$$t = \frac{N_0}{C_0 F} Z - \frac{1}{K_a C_0} ln \left(\frac{C_0}{C_t} - 1 \right) \tag{4.20}$$

where,

C_t = Eluant concentration at time t (mg/L)

C_o = Influent concentration (mg/L)

F = Influent linear velocity (cm/min)

N_o = Adsorption capacity (mg/g)

K_a = Rate constant (L/mg.min)

t = Time (min)

Z = Bed depth of column (cm)

The linear curve of BDST model at 50% breakthrough for single and binary MB was shown in Figures 4.46 and 4.47, respectively. According to BDST model (equation 4.20), a straight line that passing through the origin should be obtained. However, results showed a straight line which does not pass through the
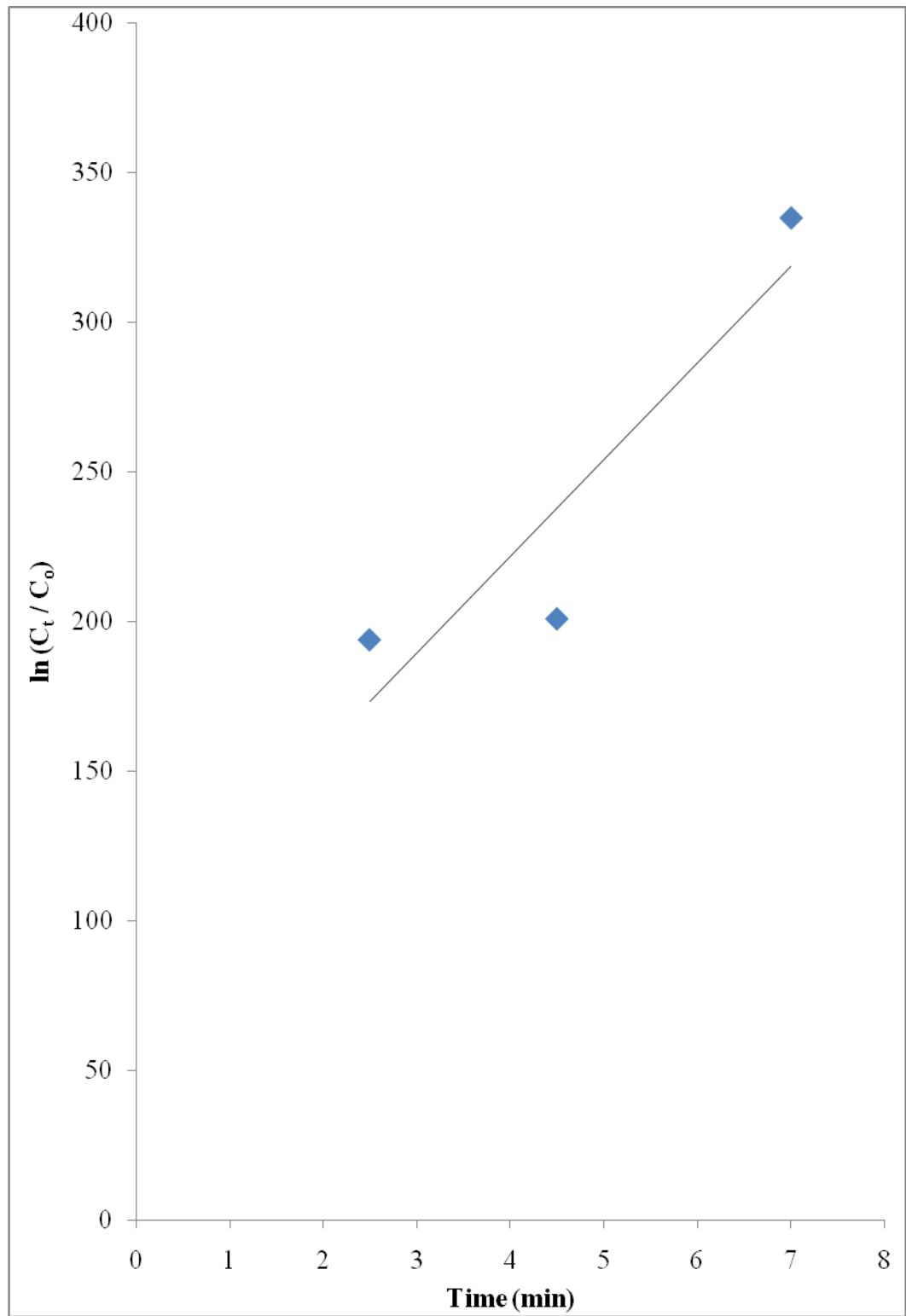
Figure 4.46: BDST plot for single MB
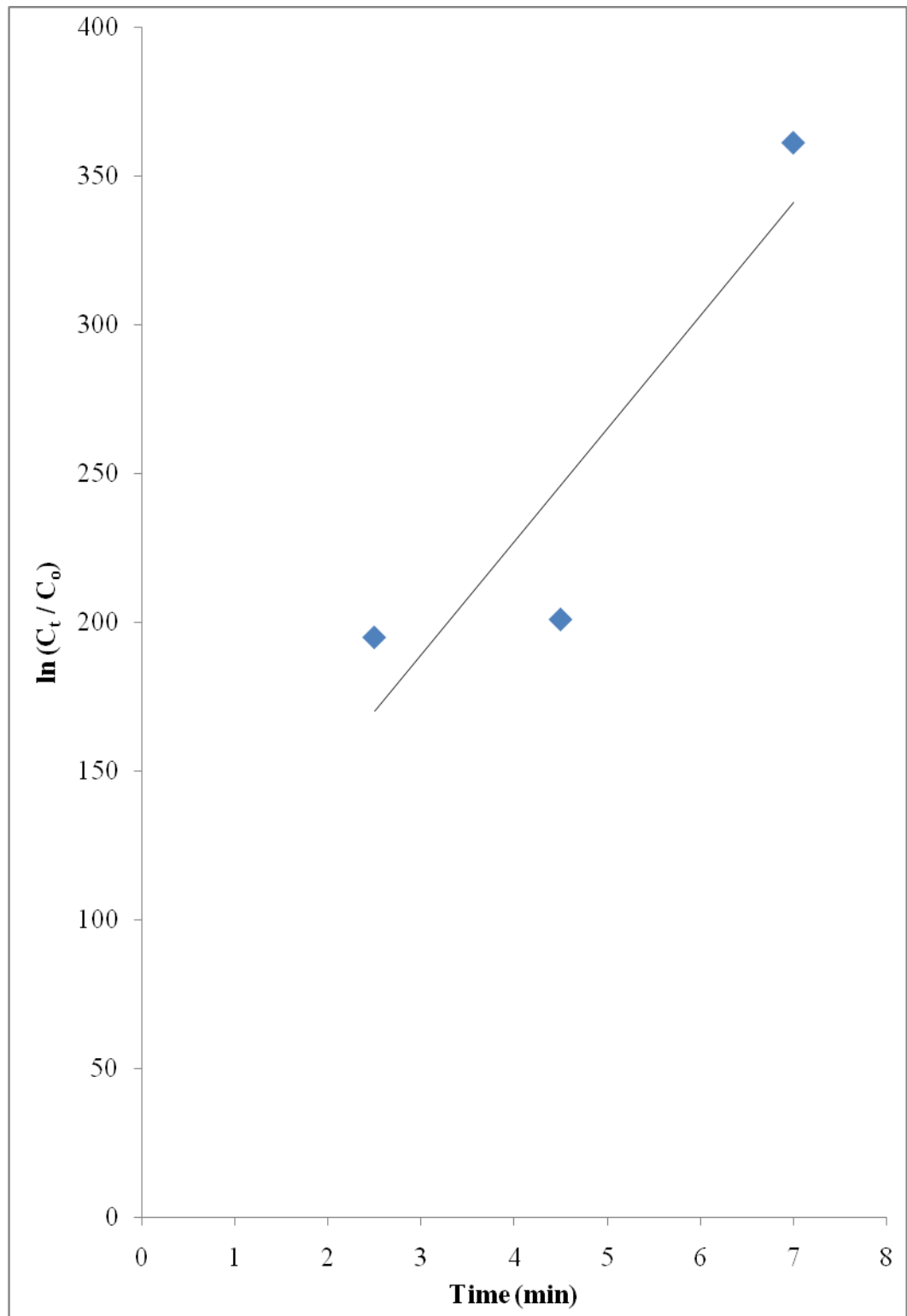
Figure 4.47: BDST plot for binary MB

origin with low R^2 value was obtained for both single and binary MB. This indicates that the adsorption of MB onto the column in single and binary dye solutions may consist of more than one rate controlling step (Wong et al., 2003) Similar trend was observed in the adsorption of Basic Blue 3 on ethylenediamine modified rice hulls (Lee et al., 2008).

The experimental data of RO16 was not tested on BDST model as the breakthrough curves did not exhibit the typical 'S' shape.

4.6.5   Effect of Flow Rate

Figures 4.48 and 4.49 showed the breakthrough curves of MB in single and binary dye solutions at different flow rates from 5 mL/min to 15 mL/min. The typical 'S' shape curves were obtained for MB in single dye solution. Results showed that the breakthrough time appeared to be shorter, from 2980 mL decreased to 450 mL as the flow rate increased from 5 to 15 mL/min. This is attributed to the decrease in contact time between ERH and dye molecules and hence the dye molecules leave the column before efficient adsorption could take place. This phenomenon is in agreement with the observed trend whereby the mass transfer coefficient decreases with increasing flow rate as shown in Table 4.12.
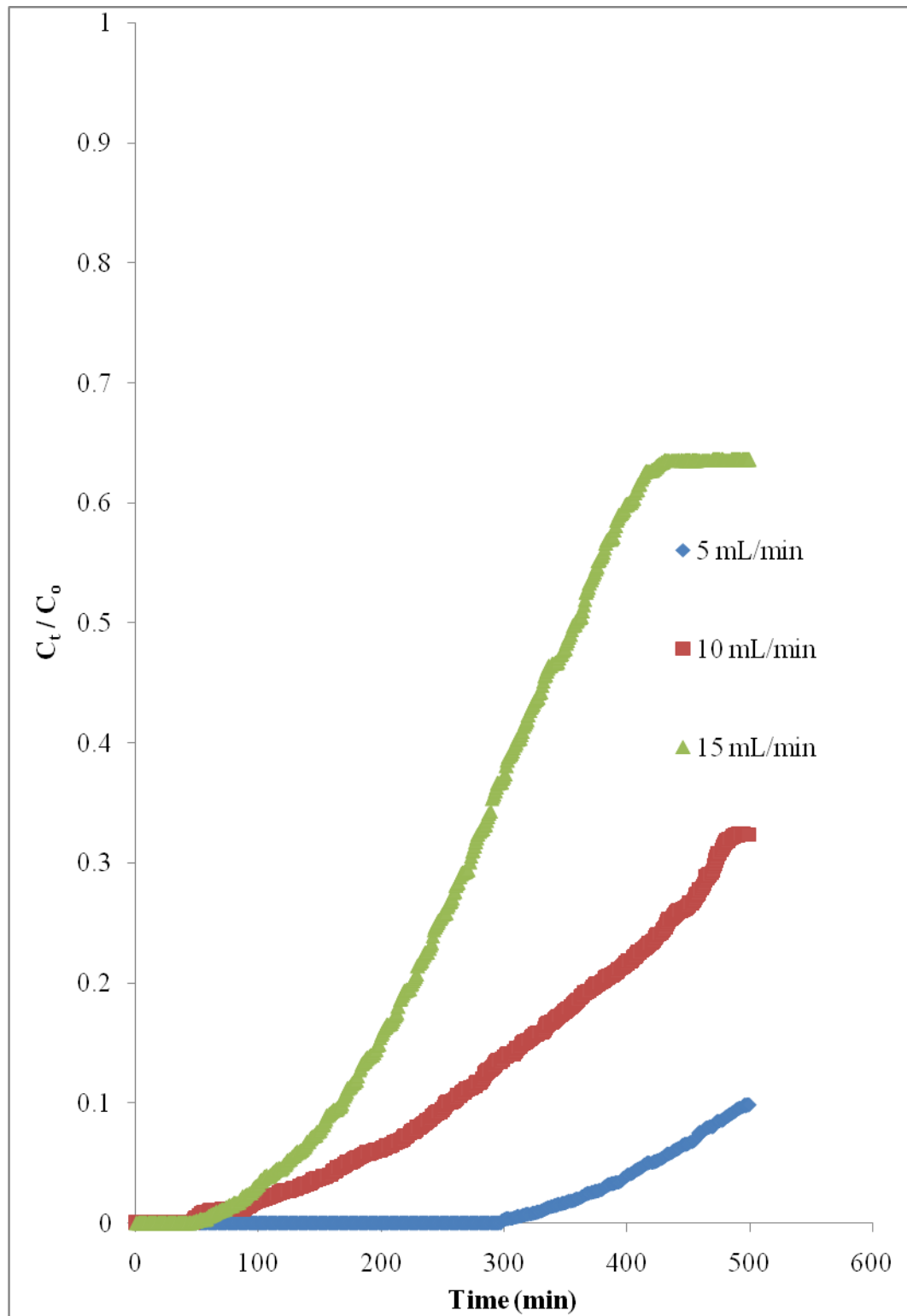
Figure 4.48: Effect of flow rate on the breakthrough curve of MB in single dye solutions
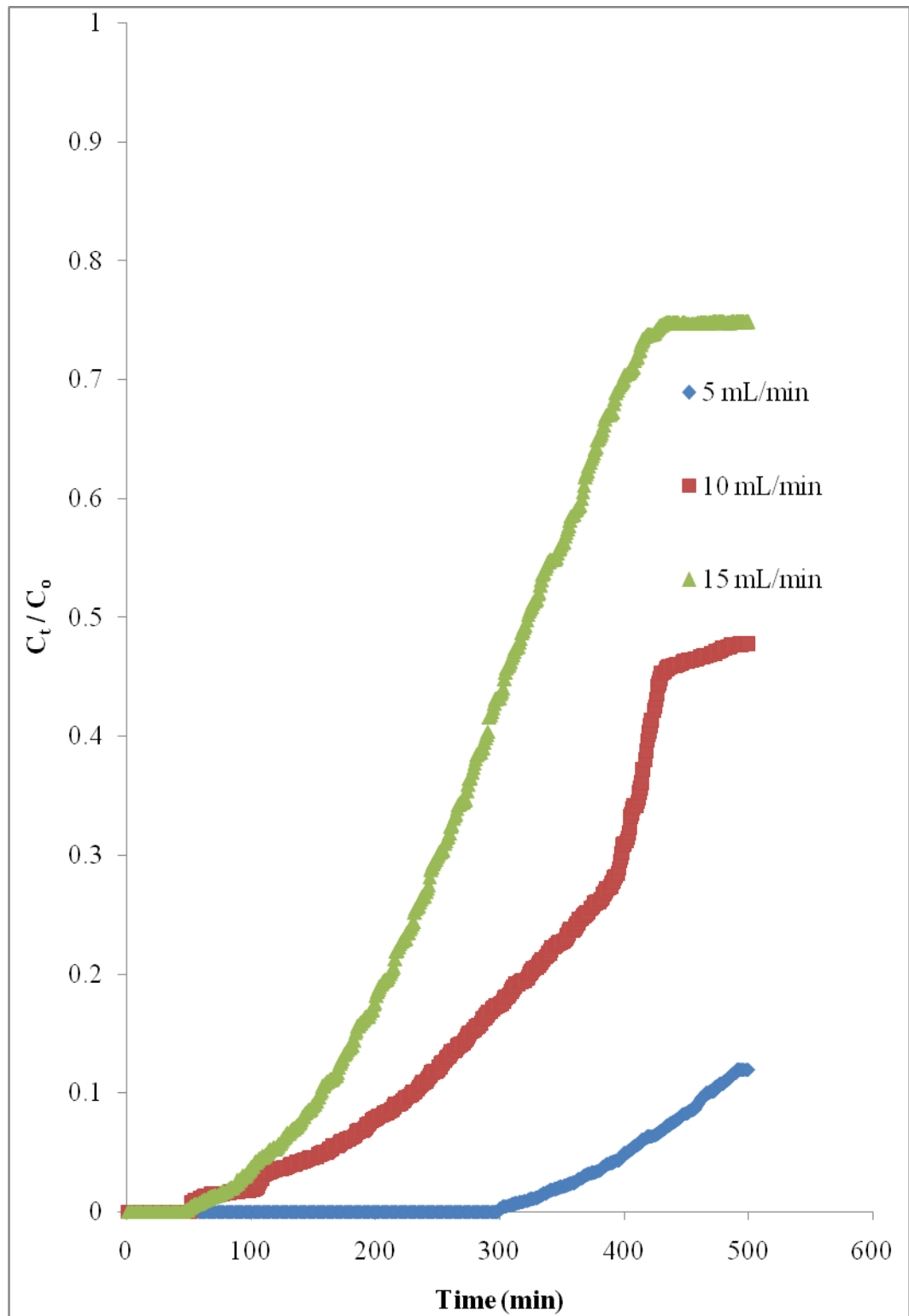
Figure 4.49: Effect of flow rate on the breakthrough curve of MB in binary dye solutions

According to Bhatnagar et al. (2006), comparable trend was observed on the breakthrough time of the adsorption of dyes and phenol onto carbonaceous adsorbent. It showed that when flow rate is reduced, the contact time increased and hence the volume of influent solution being treated was increased. This can be explained by the kinetics controlling process. The lower the flow rate, the longer the contact time and hence greater interaction between adsorbent and adsorbate.

The effect of flow rate for the adsorption of RO16 onto ERH in both single and binary dye solutions was shown in Figures 4.50 and 4.51. The breakthrough for RO16 was very rapid before adsorption could take place. The adsorption of RO16 reached equilibrium at 3000 mL of eluant volume. This indicates the adsorption of RO16 onto ERH was a slow process. From the figures, it was found that the values of C_t / C_o increased with increasing flow rate, indicating less adsorption occurred at higher flow rate. This is because the dye molecules have less time to penetrate and diffuse into the centre of adsorbent and consequently left the column before being adsorbed (Tan et al., 2008).
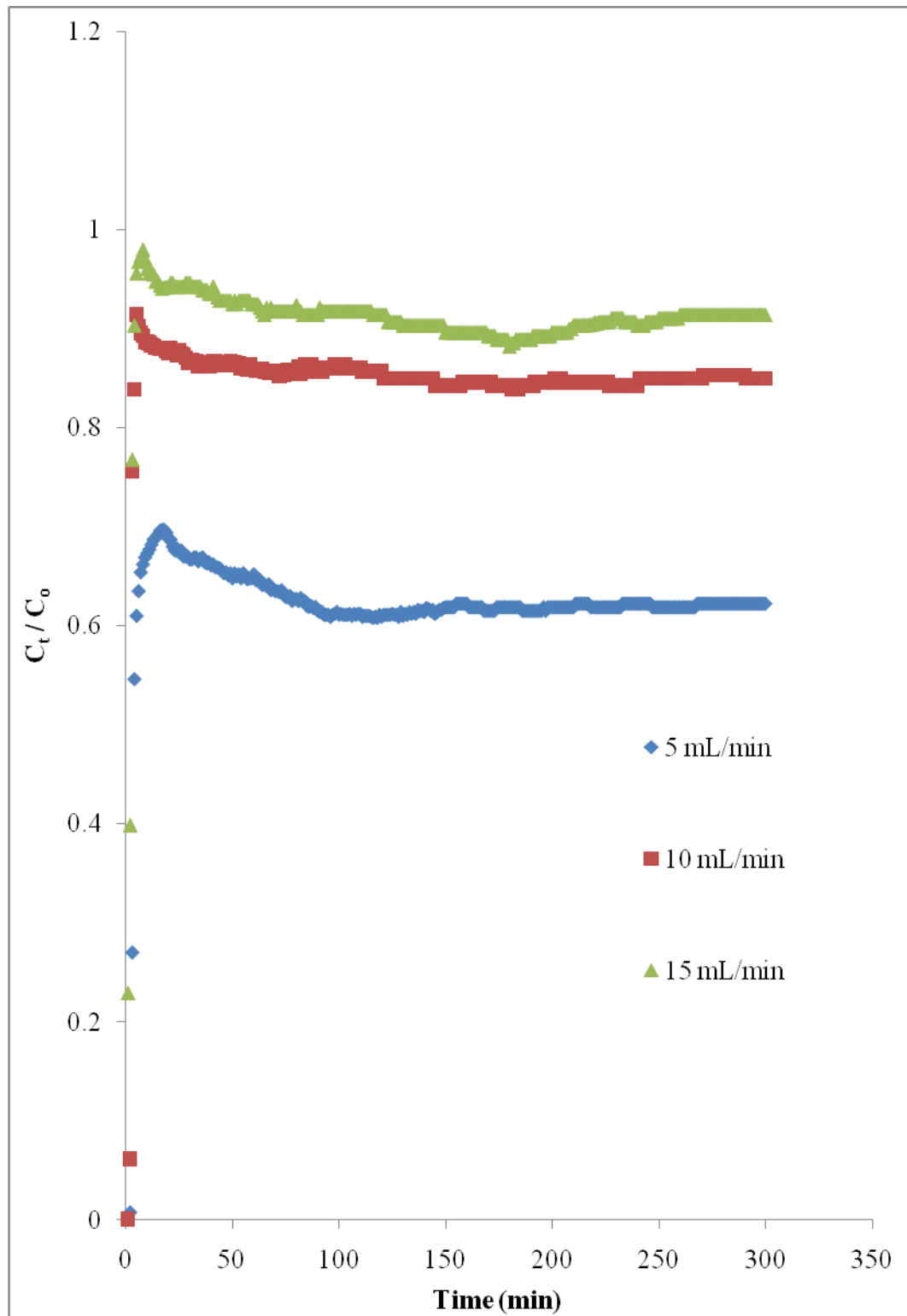
Figure 4.50: Effect of flow rate on the breakthrough curve of RO16 in single dye solutions
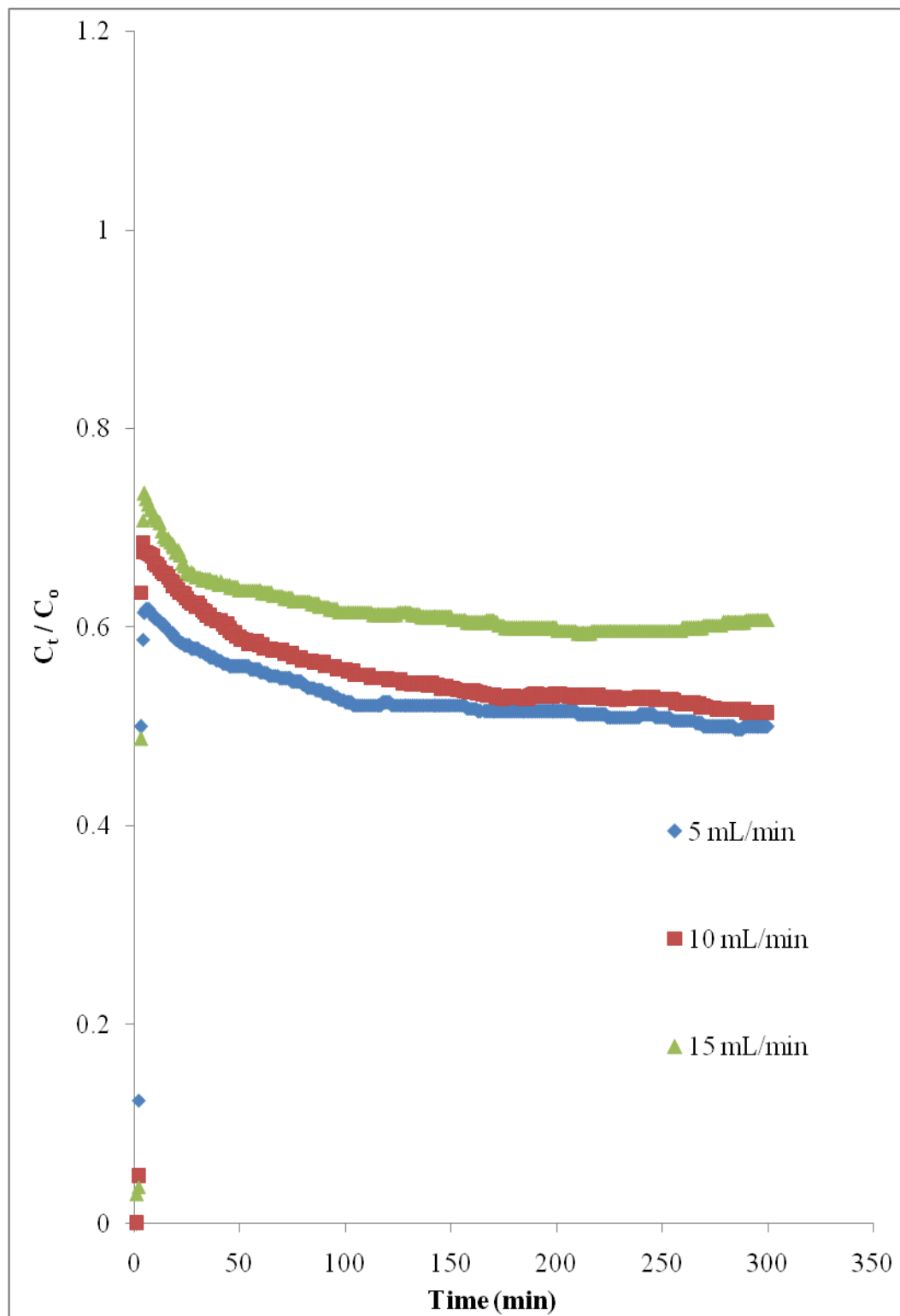
Figure 4.51: Effect of flow rate on the breakthrough curve of RO16 in binary dye solutions

4.6.6 Clark Model

Clark model is a mathematical model that incorporates Freundlich equation (Clark, 1987). As such, this model could be a suitable model for modeling the experimental data as the previous finding showed that the adsorption of MB and RO16 onto ERH in single and binary dye solutions fitted well in Freundlich isotherm. The equation involved is as follows:

$$\frac{C_t}{C_0} = \left(\frac{1}{1+Ae^{-rt}}\right)^{1/n-1}$$

(4.21)

where,

C_t = Eluant concentration at time t (mg/L)

C_0 = Influent concentration (mg/L)

A= Clark equation constant

r= Clark equation constant (1/min)

n= Freundlich constant

The experimental data for the effect of flow rate was modeled using Clark model and the predicted breakthrough curve showed a good agreement with the experimental breakthrough curve for the adsorption of MB in both single and binary dye solutions (Figures 4.52 and 4.53). Since the breakthrough curves of RO16 did not show a typical 'S' shape, hence Clark model was not applied into it.
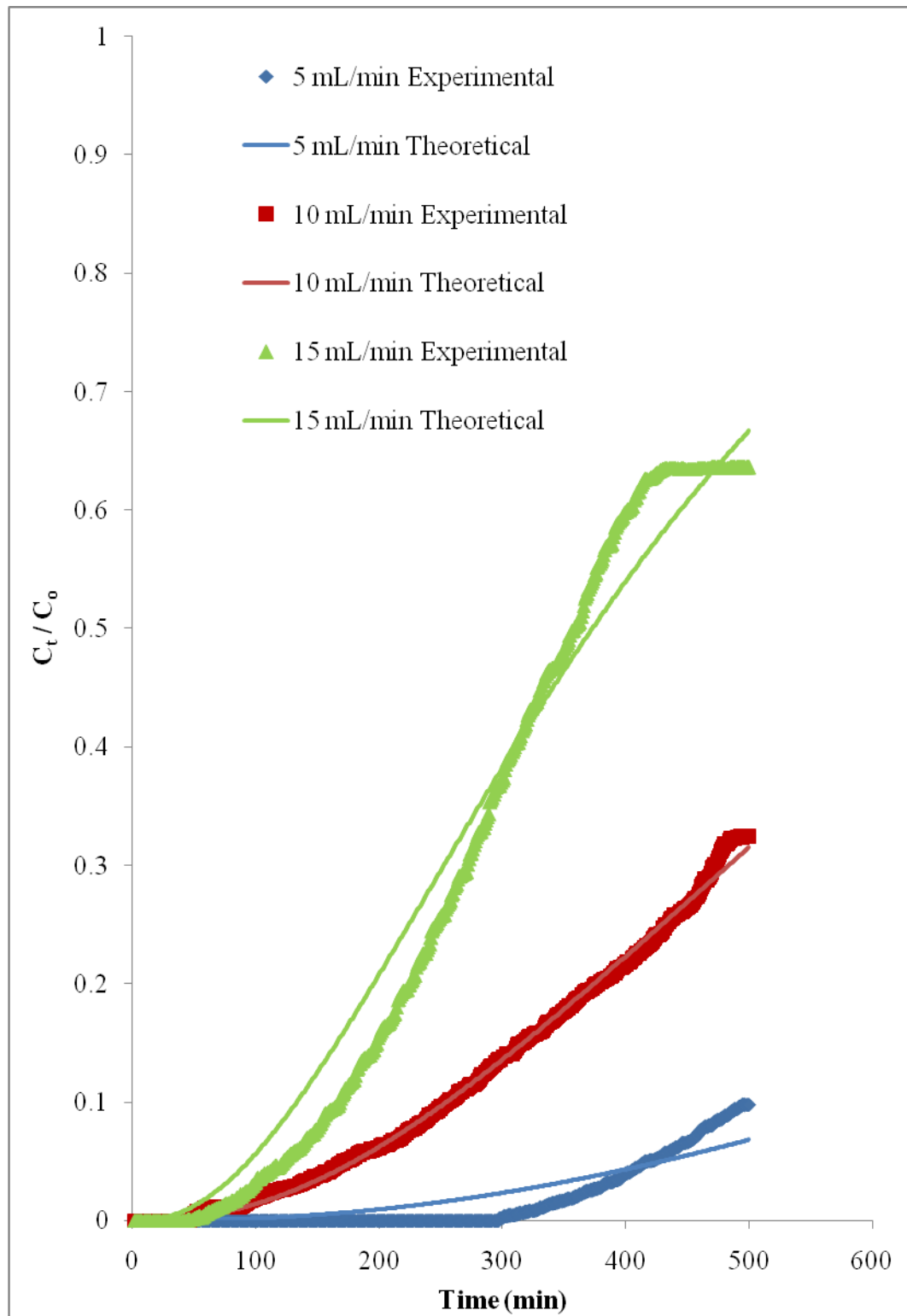
Figure 4.52: Comparison between the experimental breakthrough curves and the Clark model predicted breakthrough curves at different flow rates for single MB
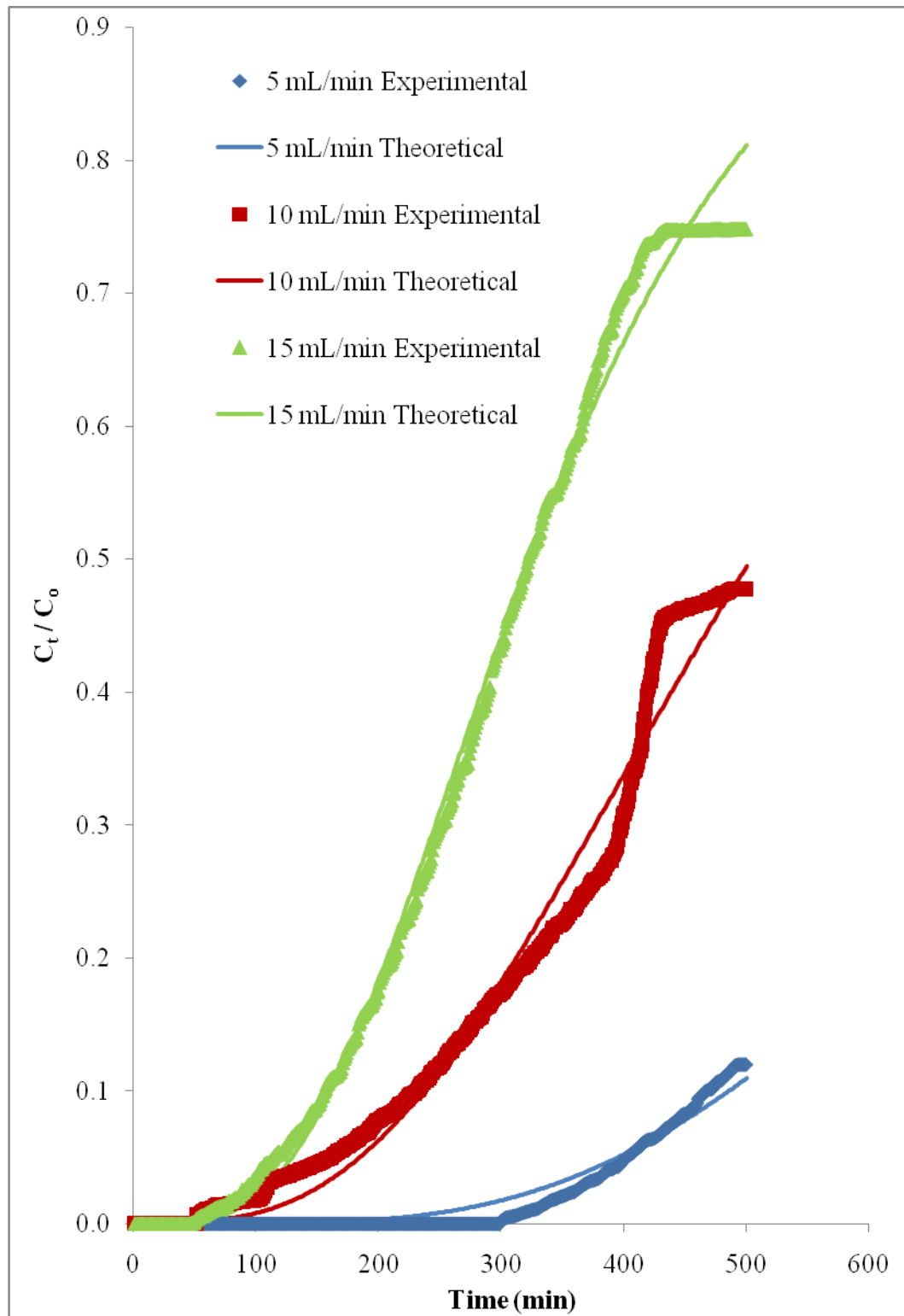
Figure 4.53: Comparison between the experimental breakthrough curves and the Clark model predicted breakthrough curves at different flow rates for binary MB

4.7 Optimisation using Statistical Experimental Methodology

4.7.1 Plackett Burman Design

The operational variables that have a significant effect on the dye uptake were determined using Plackett Burman. Six variables (pH, contact time, adsorbent dosage, initial dye concentration, agitation rate and temperature) were used in this study and screened in 12 experimental designs. The uptake of dyes was taken as the response. These experimental designs were used to screen out unimportant variables. The observed and predicted percentage uptakes of both MB and RO16 were shown in Tables 4.13 to 4.16. The data obtained was evaluated in the Analysis of variance (ANOVA).

4.7.1.1 Evaluation of Variables Affecting Percentage Uptake of Dyes

Analysis of variance (ANOVA) results of the variables studied were presented in Tables 4.17 to 4.18. The model F-value of 15.34 and 7.66 for MB in single and binary dye solutions, respectively implies that the model is significant. From Table 4.17, the Prob>F value for pH and adsorbent dosage was less than 0.05 which indicates that the model terms are significant for single MB uptake whereas for binary MB, the significant terms were found to be pH and contact time (Table 4.18).

Table 4.13: Plackett-Burman design and results for the uptake of single MB

Dye	Experimental Run	Variables						Observed response (%)	Predicted response (%)
		pH	Contact Time (min)	Adsorbent dosage (g)	Initial concentration (mg/L)	Temperature (^{o}C)	Agitation rate (rpm)		
Single MB	1	10	5	0.05	15	30	200	95.79	90.05
	2	10	5	0.20	25	70	50	97.51	100.30
	3	10	240	0.05	15	70	50	97.74	97.51
	4	2	5	0.05	15	30	50	65.00	65.64
	5	2	5	0.05	25	70	50	68.10	67.49
	6	2	5	0.2	15	70	200	80.43	83.54
	7	10	240	0.05	25	70	200	98.27	96.31
	8	2	240	0.2	25	30	50	85.16	77.24
	9	10	5	0.2	25	30	200	97.44	97.24
	10	10	240	0.2	15	30	50	97.52	102.85
	11	2	240	0.05	25	30	200	60.95	68.84
	12	2	240	0.2	15	70	200	91.06	87.95

Table 4.14: Plackett-Burman design and results for the uptake of single RO16

Dye	Experimental Run	Variables						Observed response (%)	Predicted response (%)
		pH	Contact Time (min)	Adsorbent dosage (g)	Initial concentration (mg/L)	Temperature (^{o}C)	Agitation rate (rpm)		
Single RO 16	1	10	5	0.05	15	30	200	5.46	-9.55
	2	10	5	0.2	25	70	50	2.10	5.96
	3	10	240	0.05	15	70	50	2.04	9.64
	4	2	5	0.05	15	30	50	17.87	24.74
	5	2	5	0.05	25	70	50	48.39	36.87
	6	2	5	0.2	15	70	200	33.83	46.66
	7	10	240	0.05	25	70	200	27.31	27.37
	8	2	240	0.2	25	30	50	77.98	70.63
	9	10	5	0.2	25	30	200	8.60	11.56
	10	10	240	0.2	15	30	50	18.08	18.61
	11	2	240	0.05	25	30	200	55.27	67.26
	12	2	240	0.2	15	70	200	84.28	71.45

171

Table 4.15: Plackett-Burman design and results for the uptake of binary MB

Dye	Experimental Run	Variables						Observed response (%)	Predicted response (%)
		pH	Contact Time (min)	Adsorbent dosage (g)	Initial concentration (mg/L)	Temperature (^{o}C)	Agitation rate (rpm)		
Binary MB	1	10	5	0.05	15	30	200	93.11	91.54
	2	10	5	0.2	25	70	50	94.25	96.69
	3	10	240	0.05	15	70	50	98.44	96.43
	4	2	5	0.05	15	30	50	72.56	75.83
	5	2	5	0.05	25	70	50	80.71	78.91
	6	2	5	0.2	15	70	200	83.63	81.83
	7	10	240	0.05	25	70	200	97.68	99.05
	8	2	240	0.2	25	30	50	87.13	84.94
	9	10	5	0.2	25	30	200	96.77	96.23
	10	10	240	0.2	15	30	50	97.74	98.04
	11	2	240	0.05	25	30	200	82.15	82.87
	12	2	240	0.2	15	70	200	84.46	86.26

Table 4.16: Plackett-Burman design and results for the uptake of binary RO16

Dye	Experimental Run	Variables						Observed response (%)	Predicted response (%)
		pH	Contact Time (min)	Adsorbent dosage (g)	Initial concentration (mg/L)	Temperature (^{o}C)	Agitation rate (rpm)		
Binary RO 16	1	10	5	0.05	15	30	200	31.34	36.71
	2	10	5	0.2	25	70	50	35.47	38.17
	3	10	240	0.05	15	70	50	40.74	40.61
	4	2	5	0.05	15	30	50	73.21	69.31
	5	2	5	0.05	25	70	50	68.50	78.91
	6	2	5	0.2	15	70	200	73.97	74.19
	7	10	240	0.05	25	70	200	46.10	43.71
	8	2	240	0.2	25	30	50	80.00	82.85
	9	10	5	0.2	25	30	200	46.47	42.26
	10	10	240	0.2	15	30	50	48.50	47.16
	11	2	240	0.05	25	30	200	79.17	80.39
	12	2	240	0.2	15	70	200	82.39	82.18

Table 4.17: Regression analysis (ANOVA) of Plackett-Burman for the uptake of single MB

Source	Degree of Freedom	Sum of Square	Mean Square	F-value	Prob>F
Model	6	2007.52	334.59	7.66	0.0205
pH	1	1486.75	1486.75	34.06	0.0021
Contact time	1	58.21	58.21	1.33	0.3004
Temperature	1	81.38	81.38	1.86	0.2304
Initial dye concentration	1	33.70	33.70	0.77	0.4198
Agitation rate	1	13.89	13.89	0.32	0.5971
Adsorbent Dosage	1	333.59	333.59	7.64	0.0396
Residual	5	218.28	43.66		
Total	11	2225.80			

Table 4.18: Regression analysis (ANOVA) of Plackett-Burman for the uptake of binary MB

Source	Degree of freedom	Sum of Square	Mean Square	F-value	Prob>F
Model	6	744.09	124.01	15.34	0.0044
pH	1	635.84	635.84	78.66	0.0003
Contact time	1	58.83	58.83	7.28	0.0429
Temperature	1	7.86	7.86	0.97	0.3694
Initial dye concentration	1	6.38	6.38	0.79	0.4150
Agitation rate	1	4.05	4.05	0.50	0.5107
Adsorbent Dosage	1	31.14	31.14	3.85	0.1069
Residual	5	40.41	8.08		
Total	11	784.5			

Two significant variables, pH and contact time showed Prob>F value less than 0.05 for RO16 in both single and binary dye solutions (Tables 4.19 and 4.20). The model for the uptake of single and binary RO16 was convincing with model F-value of 6.66 and 37.73, respectively.

Table 4.19: Regression analysis (ANOVA) of Plackett-Burman for the uptake of single RO16

Source	Degree of freedom	Sum of Square	Mean Square	F-value	Prob>F
Model	6	8105.37	1350.89	6.66	0.0275
pH	1	5377.60	5377.60	26.52	0.0036
Contact time	1	1842.89	1842.89	9.09	0.0296
Temperature	1	17.98	17.98	0.089	0.7778
Initial dye concentration	1	281.20	281.20	1.39	0.2919
Agitation rate	1	194.33	194.33	0.96	0.3725
Adsorbent Dosage	1	391.36	391.36	1.93	0.2234
Residual	5	1013.78	202.76		
Total	11	9119.15			

Table 4.20: Regression analysis (ANOVA) of Plackett-Burman for the uptake of binary RO16

Source	Degree of freedom	Sum of Square	Mean Square	F-value	Prob>F
Model	6	3910.27	651.71	37.73	0.0005
pH	1	3626.86	3626.86	209.95	< 0.0001
Contact time	1	191.52	191.52	11.09	0.0208
Temperature	1	11.06	11.06	0.64	0.4599
Initial dye concentration	1	2.58	2.58	0.15	0.7153
Agitation rate	1	14.13	14.13	0.82	0.4073
Adorbent Dosage	1	64.13	64.13	3.17	0.1120
Residual	5	86.37	17.27		
Total	11	3996.64			

4.7.1.2 Verification of Plackett Burman Design Model

The experimental conditions were chosen based on the highest desirability. All the experimental conditions, predicted and experimental percentage uptake were presented in Tables 4.21 and 4.22. It was clearly showed that the experimental values agreed well with the predicted values with a relatively small percentage error, ranging from 0.19 % to 8.83 % for both MB and RO16 in single and binary dye solutions.

Table 4.21: Plackett-Burman model validation for single MB and RO16

Dye system	Factors						Percentage Uptake (%)	
	pH	Contact time	Adsorbent dosage	Initial concentration	Agitation	Temperature	Predicted	Experimental
Single MB	9.78	45.47	0.17	16.27	165.87	34.83	98.54	99.75
Single RO16	2.00	239.61	0.20	25.00	200.00	34.17	78.74	76.53

Table 4.22: Plackett-Burman model validation for binary MB and RO16

Dye system	Factors						Percentage Uptake (%)	
	pH	Contact time	Adsorbent dosage	Initial concentration	Agitation	Temperature	Predicted	Experimental
Binary MB	9.87	212.61	0.19	21.39	108.99	36.29	98.75	96.87
Binary RO16	2.01	216.54	0.20	16.93	192.83	35.67	82.98	82.29

4.7.2 Response Surface Methodology (RSM)

A factorial central composite design (CCD) model for significant variables with replicates was used in this study. The CCD with three variables, pH, contact time and adsorbent dosage that have significant effect on the uptake of dyes was implemented using Design Expert Version 7.1.3. Each independent variable was coded at five different levels between -1.414 (minimum ranges of variables) to +1.414 (maximum ranges of variables) as shown in Tables 4.23 to 4.26. These coded variables were applied into the 12 experimental run generated by CCD model under RSM.

Table 4.23: Experimental range and levels of independent variables for single MB

Factors	Factor Code	Range and levels (coded)				
		-1.414	-1	0	+1	+1.414
pH	A	2.00	3.17	6.00	8.83	10.00
Dosage (g)	B	0.05	0.07	0.13	0.18	0.20

Table 4.24: Experimental range and levels of independent variables for binary MB

Factors	Factor Code	Range and levels (coded)				
		-1.414	-1	0	+1	+1.414
pH	A	2.00	3.17	6.00	8.83	10.00
Contact time (min)	B	5.00	39.41	122.50	205.59	240.00

Table 4.25: Experimental range and levels of independent variables for single RO16

Factors	Factor Code	Range and levels (coded)				
		-1.414	-1	0	+1	+1.414
pH	A	2.00	3.17	6.00	8.83	10.00
Contact time (min)	B	5.00	39.41	122.50	205.59	240.00

Table 4.26: Experimental range and levels of independent variables for binary RO16

Factors	Factor Code	Range and levels (coded)				
		-1.414	-1	0	+1	+1.414
pH	A	2.00	3.17	6.00	8.83	10.00
Contact time (min)	B	5.00	39.41	122.50	205.59	240.00

4.7.2.1 Data Analysis by RSM

RSM was employed to characterise the individual and interactive effects of the significant variables for the uptake of MB and RO16 in both single and binary dye solutions. pH and adsorbent dosage were significant in affecting the percentage uptake of single MB. Therefore, the effect of pH and adsorbent dosage in the percentage uptake of single MB was applied into the modified cubic model that describe the correspondence of the 2 variables and the uptake for MB as shown below:

$$\% \text{ Uptake} = 98.06 + 5.17A + 3.89B - 1.62AB - 3.52A^2 - 1.69B^2$$

$$- 0.94AB^2 \tag{4.22}$$

where A = pH and B = Adsorbent dosage

The significant variables in affecting the uptake of MB and RO16 in binary system as well as single RO16 were found to be pH and contact time. The mentioned cubic model is as follow:

MB in binary dye solution

$$\% \text{ Uptake} = 93.78 + 5.8A + 6.93B - 0.72AB - 3.11A^2 - 1.86B^2 - 3.30A^2B$$

$$- 1.57AB^2 \tag{4.23}$$

where A = pH and B = Contact time

RO16 in single dye solution

$$\% \text{ Uptake} = 9.94 - 15.67A + 4.02B - 3.28AB + 8.90A^2 - 0.73B^2 + 0.6A^2B$$

$$+ 6.35AB^2 \tag{4.24}$$

RO16 in binary dye solution

% Uptake = 36.24 − 22.87A + 18.92B − 0.92 AB + 3.49A^2 + 0.54B^2 − 8.09 A^{2}B

$\qquad$ + 4.65AB^2 $\hfill$ (4.25)

where pH = A and B = Contact time

$\qquad$ The ANOVA tables for MB in both single and binary dye solutions were shown in Tables 4.27 and 4.28, respectively. Results showed that the value of coefficient of determination (R^2) for single and binary MB were 0.9987 and 0.9976, respectively. The closer the R^2 to unity, the better it predicts the response (Chauhan et al., 2006). Moreover, the R^2 values were in reasonable agreement with the adjusted R^2 which ensured a satisfactory adjustment of a cubic model to the experimental data. The value of Prob>F obtained for the 2 variables, pH and adsorbent dosage, in single MB was < 0.0001 indicated that the mathematical models generated were highly significant. The same Prob>F value was obtained for binary MB (Table 4.28). The adequate precision evidence the ratio of signal to noise was well in control, 77.316 and 51.265 for single and binary MB, respectively. These values were higher than the standard value of 4 (desirable) and can be used to navigate the design space (Singh et al., 2008). Coefficient of variance (C.V.) indicates the precision and reliability of the experiment which favours lower percentage value. For single and binary MB, the C.V. values are 0.32 % and 0.56 %, respectively. The insignificant in lack-of-fit for single and binary MB implies that the tested model is valid.

Table 4.27: Regression analysis (ANOVA) for the uptake of single MB

Source	Degree of freedom	Sum of Square	Mean Square	F-value	P
Model	6	406.47	67.75	749.03	< 0.0001
A	1	106.73	106.73	1180.01	< 0.0001
B	1	121.02	121.02	1338.02	< 0.0001
AB	1	10.56	10.56	116.78	< 0.0001
A^2	1	85.98	85.98	950.63	< 0.0001
B^2	1	19.94	19.94	220.49	< 0.0001
AB^2	1	1.77	1.77	19.56	0.0045
Residual	6	0.54	0.09		
Lack of fit	2	0.41	0.21	6.22	0.0592

R^2: 0.9987, Adjusted R^2: 0.9973, Predicted R^2: 0.9738, Adequate precision: 77.316 and C.V.: 0.32 %

Table 4.28: Regression analysis (ANOVA) for the uptake of binary MB

Source	Degree of freedom	Sum of Square	Mean Square	F-value	P
Model	7	534.80	76.40	294.02	< 0.0001
A	1	134.48	134.48	517.53	< 0.0001
B	1	192.08	192.08	739.20	< 0.0001
AB	1	2.10	2.10	8.09	0.0361
A^2	1	67.23	67.23	258.73	< 0.0001
B^2	1	24.03	24.03	92.49	0.0002
A^2B	1	21.84	21.84	84.05	0.0003
AB^2	1	4.95	4.95	19.05	0.0073
Residual	5	1.30	0.26		
Lack of fit	1	0.55	0.55	2.95	0.1611

R^2: 0.9976, Adjusted R^2: 0.9942, Predicted R^2: 0.9320, Adequate precision: 51.265 and C.V.: 0.56 %

Figure 4.54 showed the 3D plot of the interaction between the two factors: pH and adsorbent dosage for MB in single dye solution. Higher uptake was noticed when the pH and adsorbent dosage were at its higher point. At low pH, the surface of the adsorbent was surrounded by hydrogen ions (H^+) which prevented the MB dye molecules from approaching the binding sites. With increasing pH, the carboxyl groups are predominantly deprotonated and result in adsorption sites that were available for binding with MB. Higher adsorbent dosage led to an increase in active sites for adsorption; hence a higher percentage uptake of MB is anticipated. The optimum conditions of the variables for MB were pH 6.85 and 0.14 g of adsorbent.

As in Figure 4.55, the 3D plot revealed that similar trend whereby the percentage uptake of binary MB increased with increasing pH. The increase in contact time between dye molecules and adsorbent allows complete interaction and attainment of interaction. Hence, the uptake of MB in binary dye solution increases when contact time increased. The optimum conditions of the variables for binary MB were pH 6.77 and 205.58 minutes.

The ANOVA tables for RO16 in both single and binary dye solutions were shown in Tables 4.29 and 4.30, respectively. From Tables 4.29 and 4.30, the model F-value for both single and binary RO16 was 8417.25 and 10082.03, respectively. These values indicate that the models were significant. There is only a 0.01 % of chance that a model F-value could occur due to noise. As for the value of coefficient of determination (R^2), 0.9999 was obtained for both single and binary RO16. Both R^2 values were also in reasonable agreement with adjusted R^2 of 0.9998 for RO16 in single and binary dye solutions. Moreover, the Prob>F values obtained indicate the pH and contact time are significant model terms in the uptake of both single and binary RO16 since it is less than 0.0001 (Tables 4.29 and 4.30). The C.V. values for single and binary RO16 are 1.26 % and 0.72 %, respectively. The insignificant in lack-of-fit for MB and RO16 implies that the tested model is valid. As for single RO16, the adequate precision is 318.104 whereas for RO16 in binary dye solution is 299.284. Both values were found to be higher than the desirable value of 4.
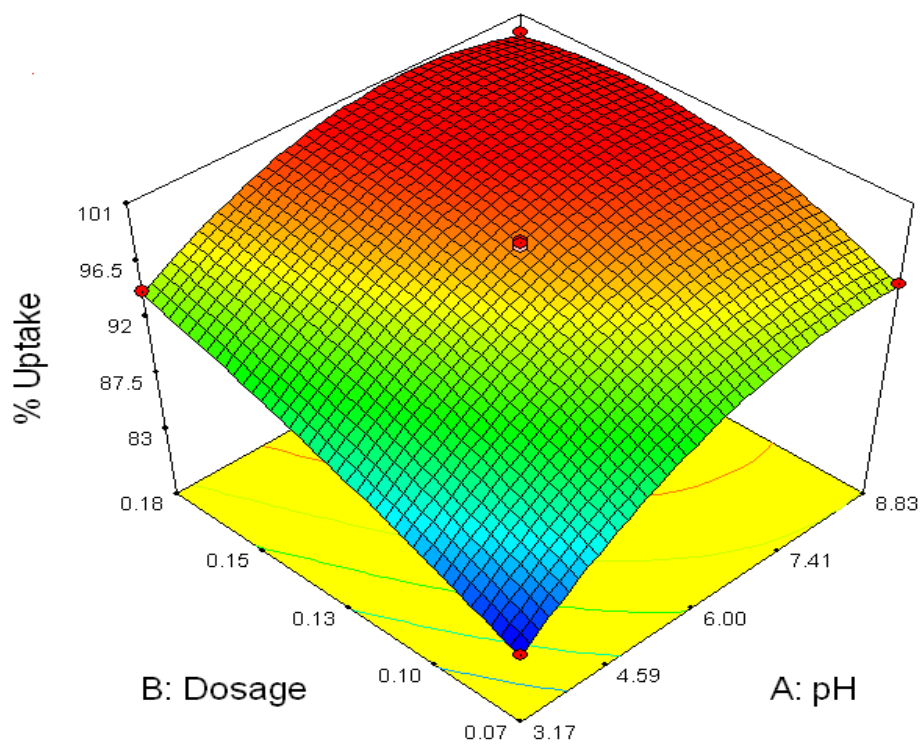
Figure 4.54: 3D surface plot for uptake of single MB solution as a function of pH and adsorbent dosage
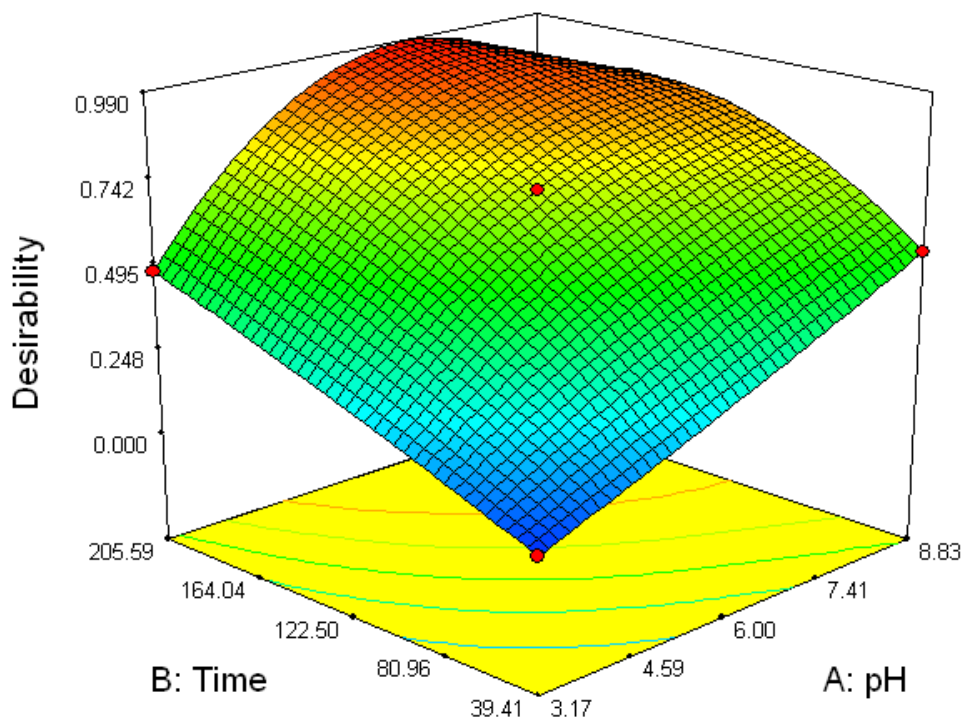
Figure 4.55: 3D surface plot for uptake of binary MB solution as a function of pH and contact time

Table 4.29: Regression analysis (ANOVA) for the uptake of single RO16

Source	Degree of Freedom	Sum of Square	Mean Square	F-value	P
Model	7	2098.17	2098.17	8417.25	< 0.0001
A	1	982.13	982.13	27580.21	< 0.0001
B	1	64.64	64.64	1815.18	< 0.0001
AB	1	43.10	43.10	1210.31	< 0.0001
A^2	1	550.56	550.56	15460.88	< 0.0001
B^2	1	3.67	3.67	103.04	0.0002
A^2B	1	0.71	0.71	20.06	0.0065
AB^2	1	80.70	80.70	2266.09	< 0.0001
Residual	5	0.18	0.036		
Lack of fit	1	6.05×10^{-3}	6.05×10^{-3}	0.14	0.7266

R^2: 0.9999, Adjusted R^2: 0.9998, Predicted R^2: 0.9997, Adequate precision: 318.104 and C.V.: 1.26 %

Table 4.30: Regression analysis (ANOVA) for the uptake of binary RO16

Source	Degree of Freedom	Sum of Square	Mean Square	F-value	P
Model	7	5409.51	772.79	10082.03	< 0.0001
A	1	2093.05	2093.05	27306.52	< 0.0001
B	1	1431.13	1431.13	18670.91	< 0.0001
AB	1	3.42	3.42	44.65	0.0011
A^2	1	83.55	83.55	1103.05	< 0.0001
B^2	1	2.00	2.00	26.10	0.0037
A^2B	1	130.90	130.90	1707.76	< 0.0001
AB^2	1	43.24	43.24	564.16	< 0.0001
Residual	5	0.38	0.077		
Lack of fit	1	0.21	0.21	4.91	0.0910

R^2: 0.9999, Adjusted R^2: 0.9998, Predicted R^2: 0.9975, Adequate precision: 299.284 and C.V.: 0.72 %

The 3D plots for single and binary RO16 were shown in Figures 4.56 and 4.57. From the plots, it showed that the maximum percentage uptake occurred when the pH was at it minimum point and contact time at its maximum point. When pH increased, this lead to the deprotonation of surface groups and the presence of excess OH^-, resulted in the electrostatic repulsion between RO16 and negatively charged sites. The increase in contact time between dye molecules and adsorbent allows complete interaction and attainment of interaction. The optimum pH value for the uptake of single and binary RO16 was 3.17. As for the contact time, 168.83 minutes and 205.59 minutes were found to be the optimum values for both single and binary RO16, respectively.
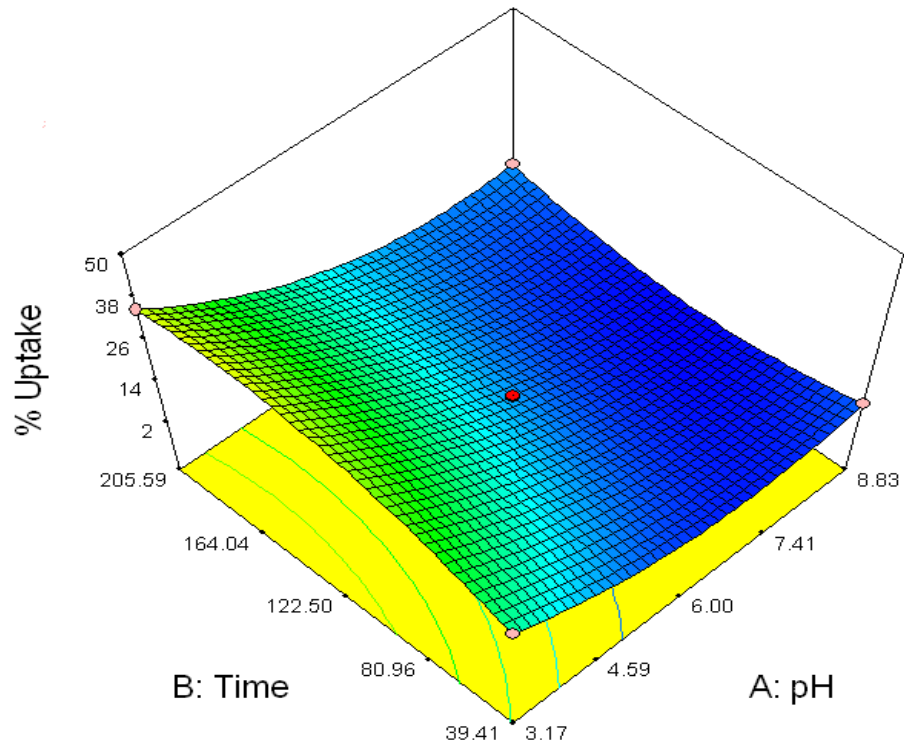
Figure 4.56: 3D surface plot for uptake of single RO16 solution as a function of pH and contact time
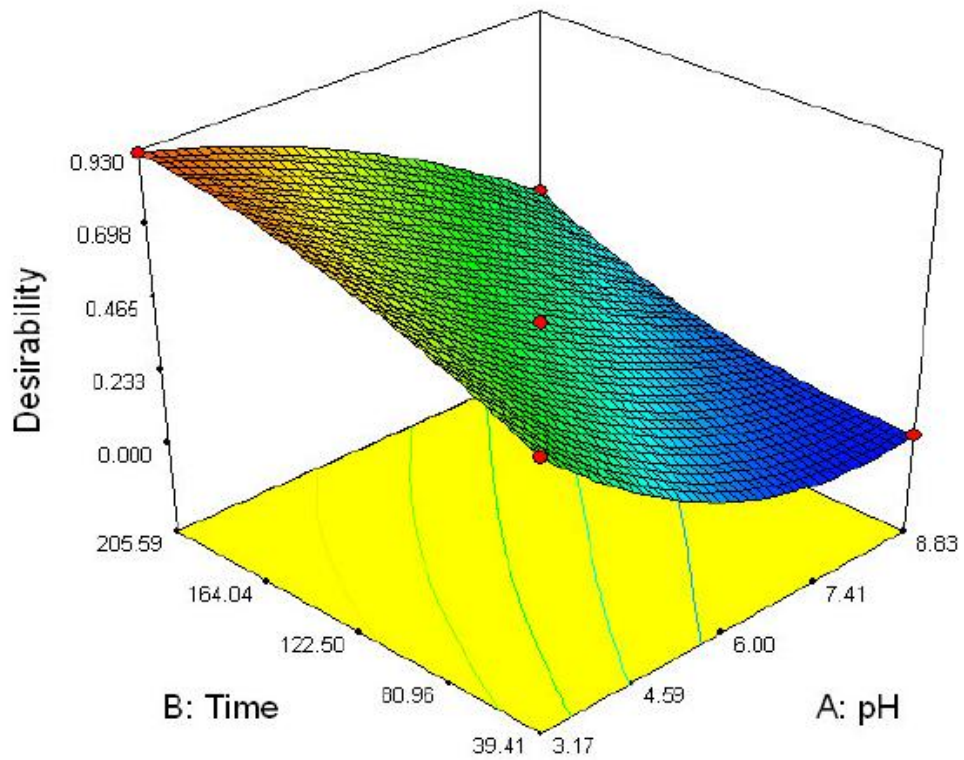
Figure 4.57: 3D surface plot for uptake of binary RO16 solution as a function of pH and contact time

4.7.2.2 Verification of RSM Model

A series of experiments were carried out according to the experimental conditions with highest desirability generated by Design Expert v 7.1.3 to check for the validity of the model equations for MB and RO16 in both single and binary dye solutions. The experimental data obtained agreed well with the predicted value with percentage error of 0.35 % for single MB, 0.199 % for binary MB, 8.83 % and 0.231 % for single and binary RO16, respectively. The model F-value of 749.03 for single MB and 294.02 for binary MB indicated that the models were significant and valid. Similarly, there is only a 0.01 % of chance that a model F-value of 8417.5 (single RO16) and 10082.03 (binary RO16) could occur due to noise.

4.8 Batch Experiments on Heavy Metal Ion

4.8.1   Effect of pH

The effect of pH on the uptake of both Cu(II) and Cd(II) ions using ERH was shown in Figure 4.58. It is clear that the adsorption of both Cu(II) and Cd (II) ions onto ERH increased with increasing pH. This is due to the carboxyl groups of ERH were predominantly protonated and the surface was surrounded by the hydronium ions (H^+) at low pH. This will decrease the metal ions interaction with the binding sites of the ERH due to the greater repulsive forces.
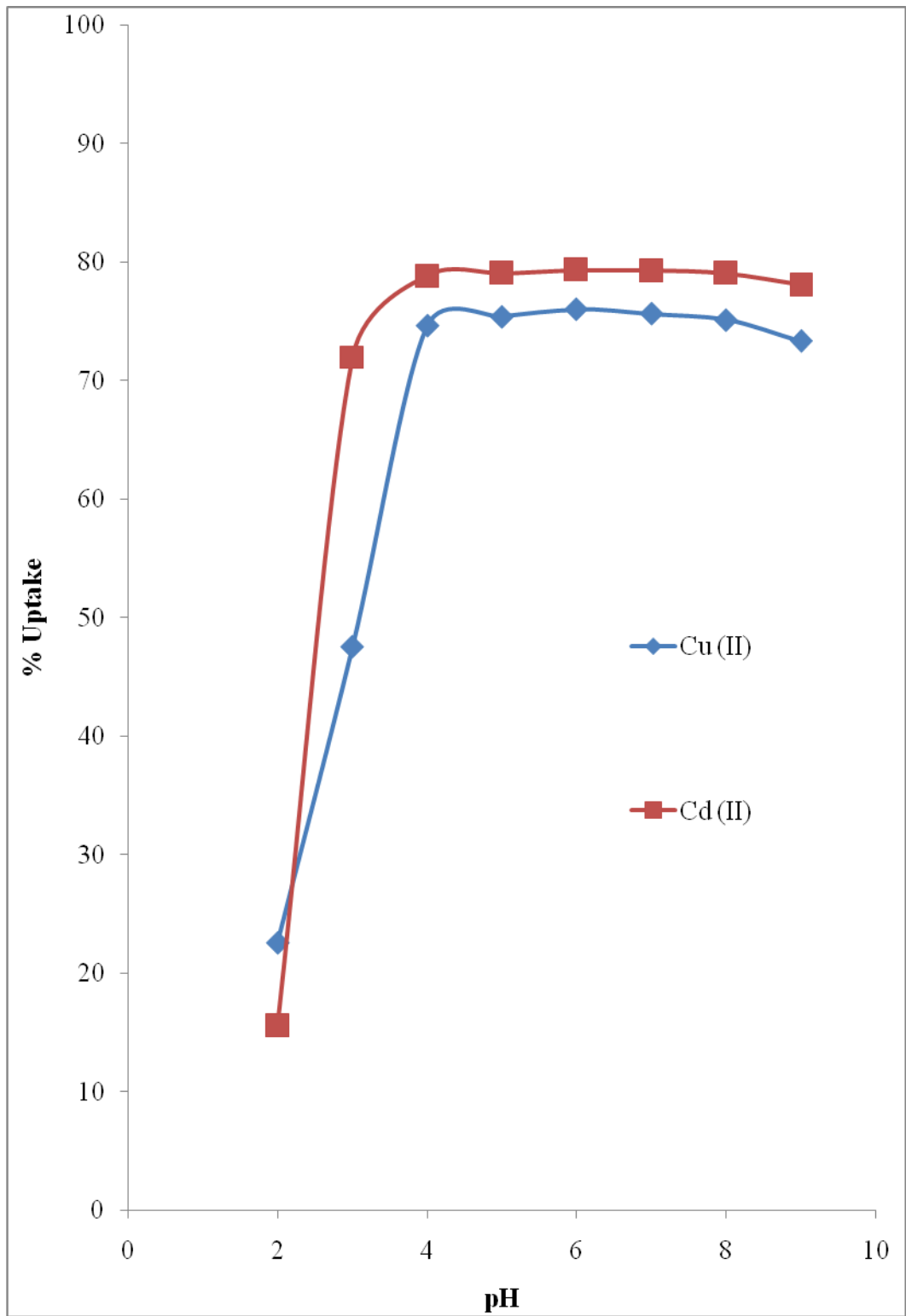
Figure 4.58: Effect of pH on the adsorption of Cu (II) and Cd (II) ions

At higher pH, more effective adsorption was observed due to the deprotonated carboxyl groups and the overall surface of ERH became negatively charged in the presence of hydroxyl ions (OH⁻).

In a study carried out by Arivoli et al., (2007), results showed that both Cu(II) and Fe(II) ions were effectively adsorbed onto acid activated low cost pandanus carbon at alkaline condition due to the presence of ionic COOH groups which deprotonated at higher pH. Similar trend was also reported in a study conducted by Wong et al., (2003). They studied the effect of pH on the uptake of Copper and lead ions by tartaric acid modified rice husk (TARH). At low pH values, the surface of the adsorbent was surrounded by the hydrogen ions (H^+) that hinder the access, by repulsive forces, to the surface functional groups by the metals ion. The uptake of both metal ions by TARH was much higher at high pH values.

4.8.2 Effect of Initial Metal Ion Concentrations and Contact Time

As shown in Figures 4.59 and 4.60, the percentage uptake of both Cd (II) and Cu (II) ions decreased with increasing metal ion concentration. This is because at lower ion concentrations, metal ions are adsorbed onto the specific adsorption sites, but due to the increasing ion concentration, the adsorption sites are being saturated. Therefore, the percentage uptake of both Cd (II) and Cu (II) ions would be affected. As reported by Ozer et al., (2004), the percentage uptake of Cu (II) ion at higher initial concentration levels showed a decreasing trend.
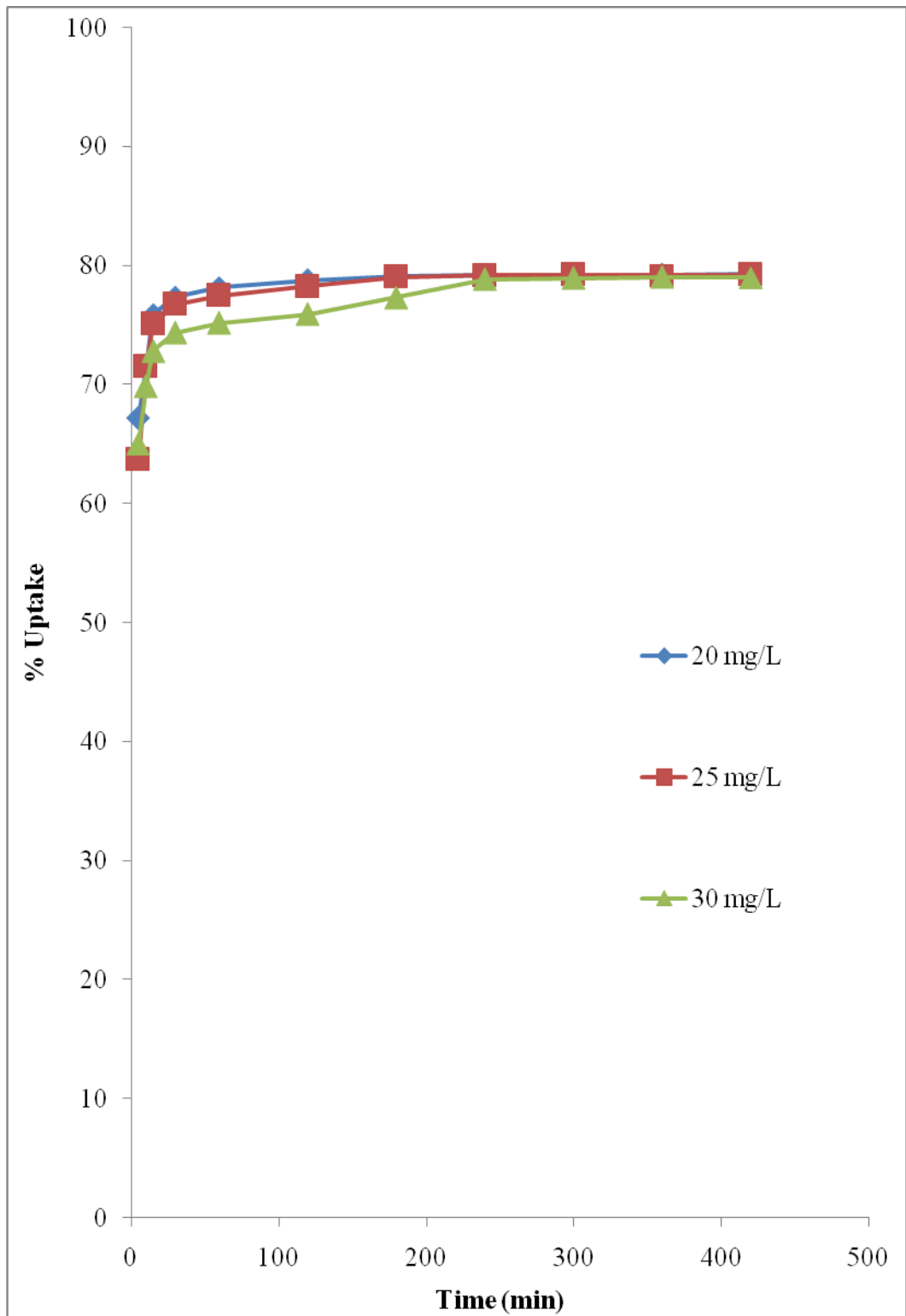
Figure 4.59: Effect of intitial concentration and contact time on the adsorption of Cd (II) ion
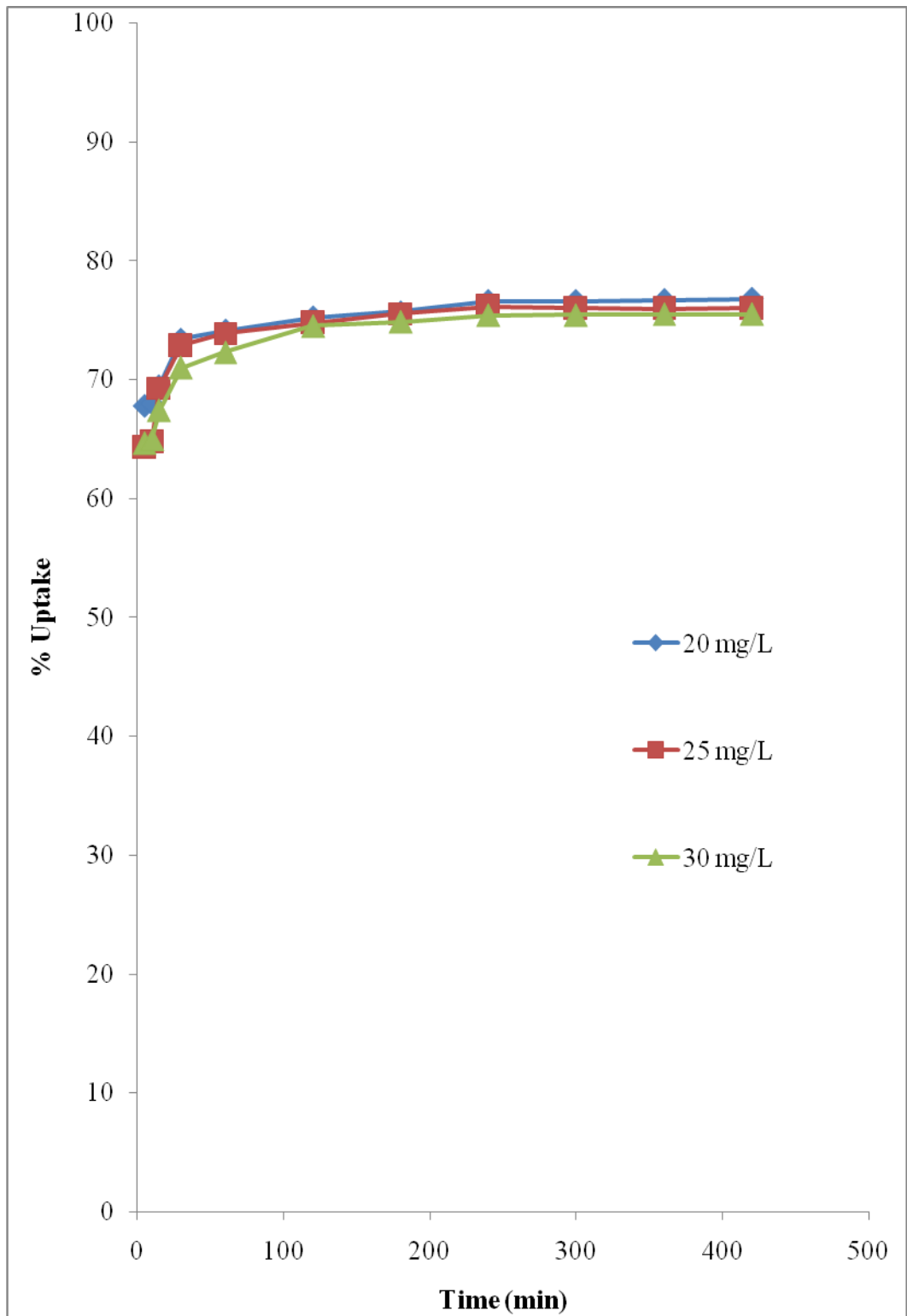
Figure 4.60: Effect of intitial concentration and contact time on the adsorption of Cu (II) ion

This is due to the fact that at lower ion concentrations, all Cu (II) ions present in solution could interact with the adsorption sites and thus the percentage uptake of Cu (II) ion was higher. Whereas at higher ion concentrations, the uptake of Cu (II) ion was lower due to saturation of adsorption sites.

Contact time is another important parameter for the adsorption of both Cd (II) and Cu (II) ions. Results showed that the percentage uptake of Cd (II) ion by ERH was rapid within the first 30 minutes, slowing down between 60 and 180 minutes and reached equilibrium after 240 minutes (Figure 4.59). Similar behaviour was observed for Cu (II) ion as shown in Figure 4.60. The uptake rate for both Cd (II) and Cu (II) ions was high at the beginning due to more adsorption site available for the adsorption and slower rate was observed with increasing contact time due to a quick exhaustion of the adsorption sites.

Comparable trend was noticed for the uptake of chromium ion using acid activated carbon (Arivoli et al., 2007). The results obtained revealed that percentage uptake of chromium ion decreased with increasing metal ion concentration. However, they suggested that the actual amount of chromium ions adsorbed per unit mass of carbon displayed an opposite trend. At lower concentration, the ratio of chromium ions to the available adsorption sites is low consequently the fractional adsorption becomes independent of initial metal ion concentrations. Whereas at higher concentration, the adsorption sites becomes fewer and thus percentage uptake of chromium ion is dependent upon initial metal ion concentrations.

4.8.3 Adsorption Kinetics

The study of the adsorption kinetics using different initial metal ion concentrations presents valuable insight into the reaction mechanism of adsorption. In order to investigate the potential rate-controlling steps involved in the adsorption of Cd (II) and Cu (II) ions by ERH, the experimental data were fitted into both pseudo-first and pseudo-second order kinetic models. The pseudo-first order and pseudo-second order equations were expressed as in equations (4.7) and (4.8), respectively.

The acquiescence between the experimental data and the predicted values was expressed by correlation coefficients (R^2). High R^2 value indicates the kinetics of the adsorption was well described by the model. The adsorption capacities and R^2 values based on both kinetic models were summarised in Table 4.31. As shown in Table 4.31, the pseudo-second order model shows better correlation ($R^2 \approx 1$) of the adsorption data than the pseudo-first order model. Besides, the calculated adsorption capacities based on pseudo-second order model agreed well with the experimental values. Hence, suggesting that the rate-controlling step may be chemisorption rather than diffusion (Wong et al., 2003).

Table 4.31: Adsorption capacities and correlation coefficients based on pseudo-first and pseudo-second order kinetics

Metal ions	Initial Concentration (mg/L)	Pseudo-first order		Pseudo-second order		Experimental adsorption capacities (mg/g)
		Adsorption capacities (mg/g)	R^2	Adsorption capacities (mg/g)	R^2	
Cd (II)	20	7.031	0.416	3.187	0.999	3.171
	25	16.331	0.408	3.984	1.000	3.961
	30	25.704	0.644	4.785	1.000	4.742
Cu (II)	20	7.161	0.655	3.086	1.000	3.071
	25	16.519	0.551	3.817	1.000	3.799
	30	25.882	0.647	4.566	1.000	4.531

As reported by Ho and McKay (2000), the values of q_e, k_2 and h against C_o in the corresponding linear plots of the pseudo-second order equation can be regressed to obtain expressions for these values in terms of initial concentration (C_o) as in equations (4.9), (4.10) and (4.11). Table 4.32 showed the empirical parameters for predicted q_e, k_2 and h from C_o.

Table 4.32: Empirical parameters for predicted q_e, k_2 and h from C_o

Metal ions	A_q (g/mg)	B_q (g/L)	A_k (mg min/g)	B_k (mg^2min/g L)	A_h (gmin/mg)	B_h (gmin/L)
Cd (II)	-0.001	6.3	24.69	-473	0.882	-12.6
Cu (II)	0.009	6.292	14.31	-184.8	0.074	9.576

The theoretical model derived for Cd (II) and Cu (II) ions at concentration 20 – 30 mg/L was applied to the uptake of both ions and the results was compared to the experimental values as shown in Figures 4.61 and 4.62. The theoretical curve agreed well with the experimental values for both Cd (II) and Cu (II) ions.
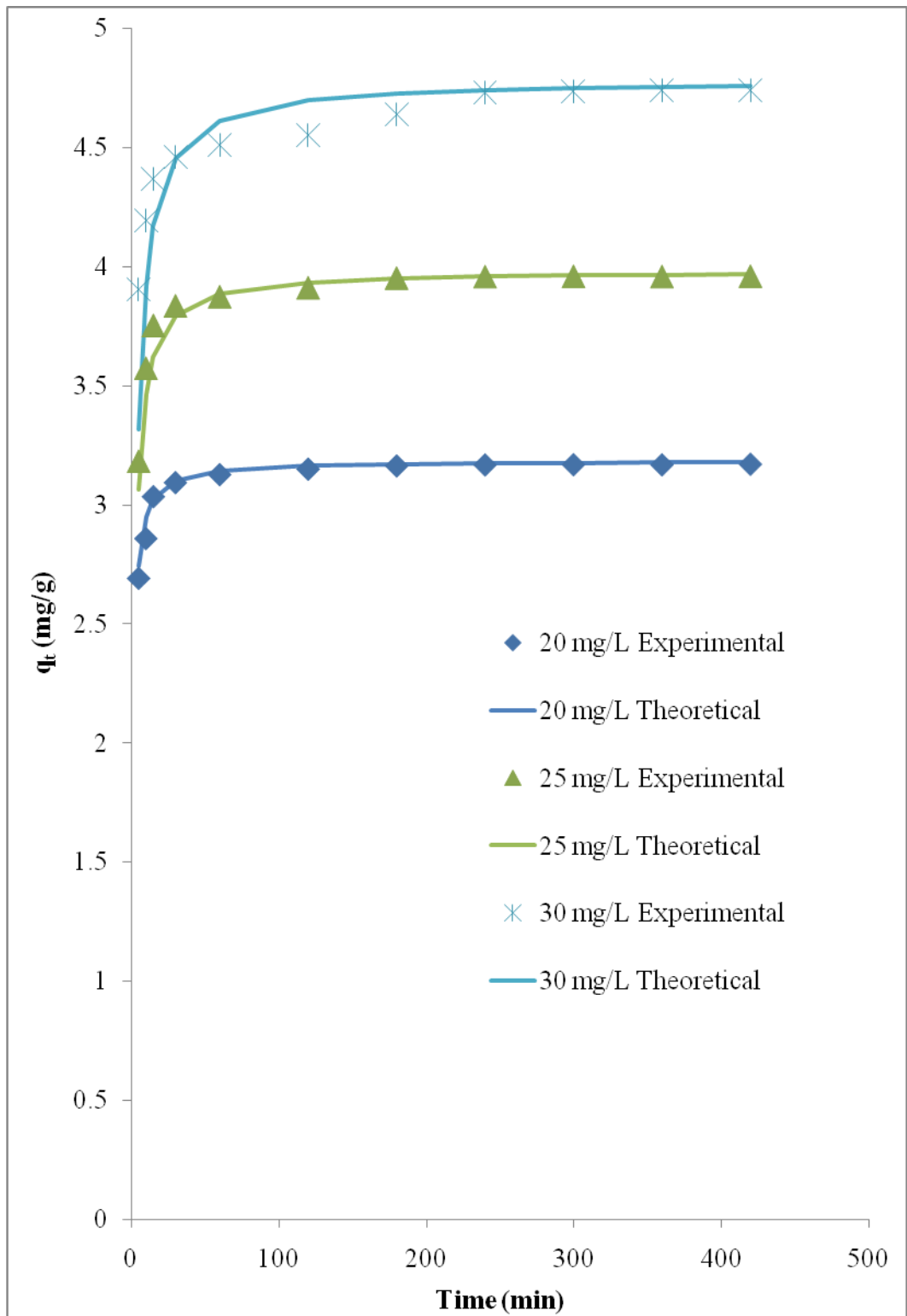
Figure 4.61: Comparison between the measured and pseudo-second order modelled time profiles for Cd (II) ion
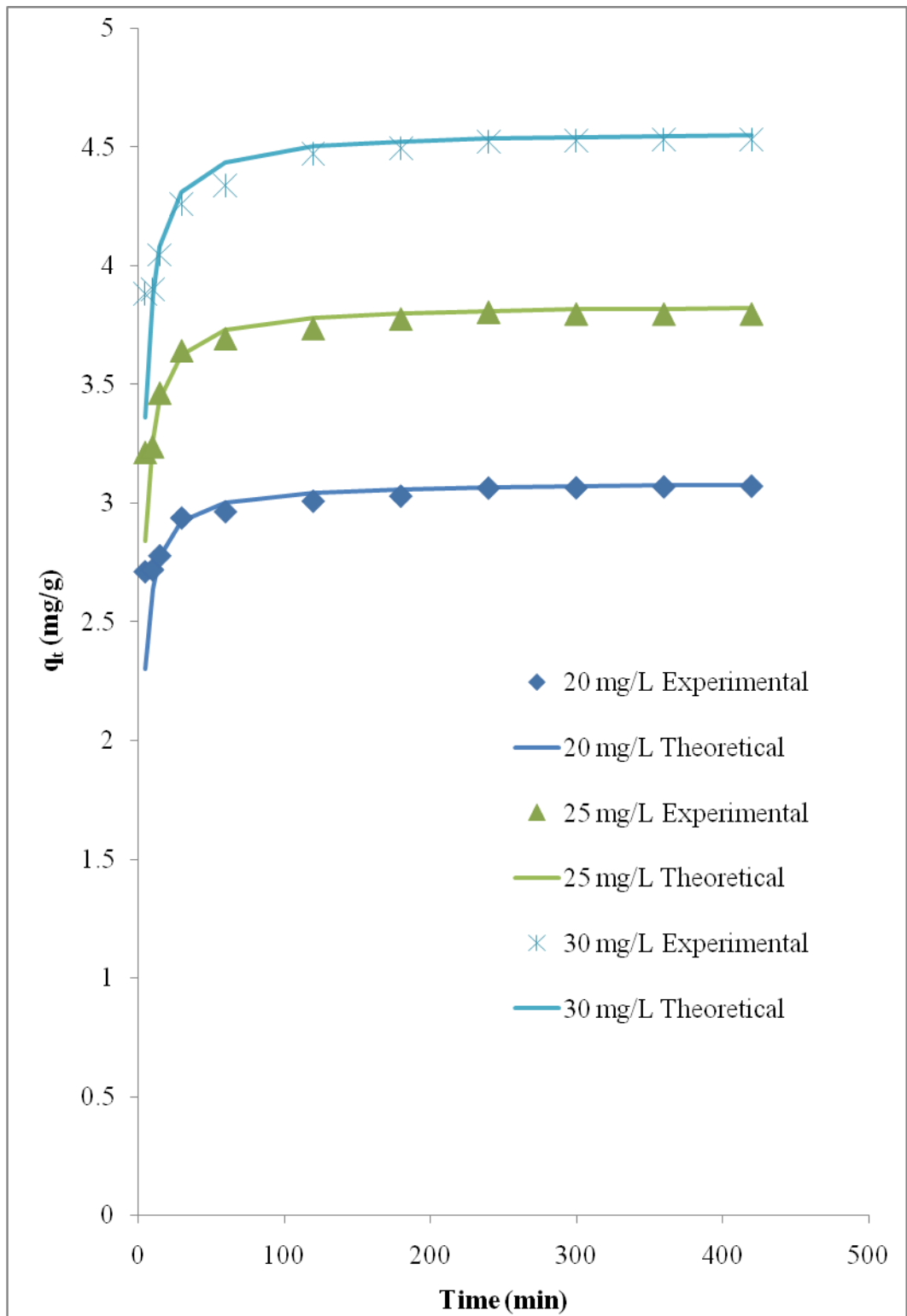
Figure 4.62: Comparison between the measured and pseudo-second order modelled time profiles for Cd (II) ion

4.8.4 Intraparticle Diffusion

The conventional method used in determining the mechanism involved in the adsorption process is by fitting the experimental data into intraparticle diffusion plot. Weber and Moris (1963) reported that the plot of q_t versus $\sqrt{t}$ should yield a straight line passing through the origin if intraparticle diffusion is the only rate-controlling step. The intraparticle diffusion coefficient, K_p can be obtained from the slope of the plot q_t versus $\sqrt{t}$ and its expression was shown in equation (4.12).

The multi linearity of the plot q_t versus $\sqrt{t}$ indicating that there are two or more rate-determining steps involved and are influencing the adsorption process. As shown in Figures 4.63 and 4.64, the initial curve portion is attributed to rapid external diffusion of metal ions while the linear portion is due to the intraparticle diffusion followed by a flat portion where the intraparticle diffusion starts to slow down due to the low concentration of metal ion and lesser available adsorption sites. Deviation of plot from the origin indicates that intraparticle diffusion is not the only rate-determining step for the adsorption of both Cd (II) and Cu (II) ions.
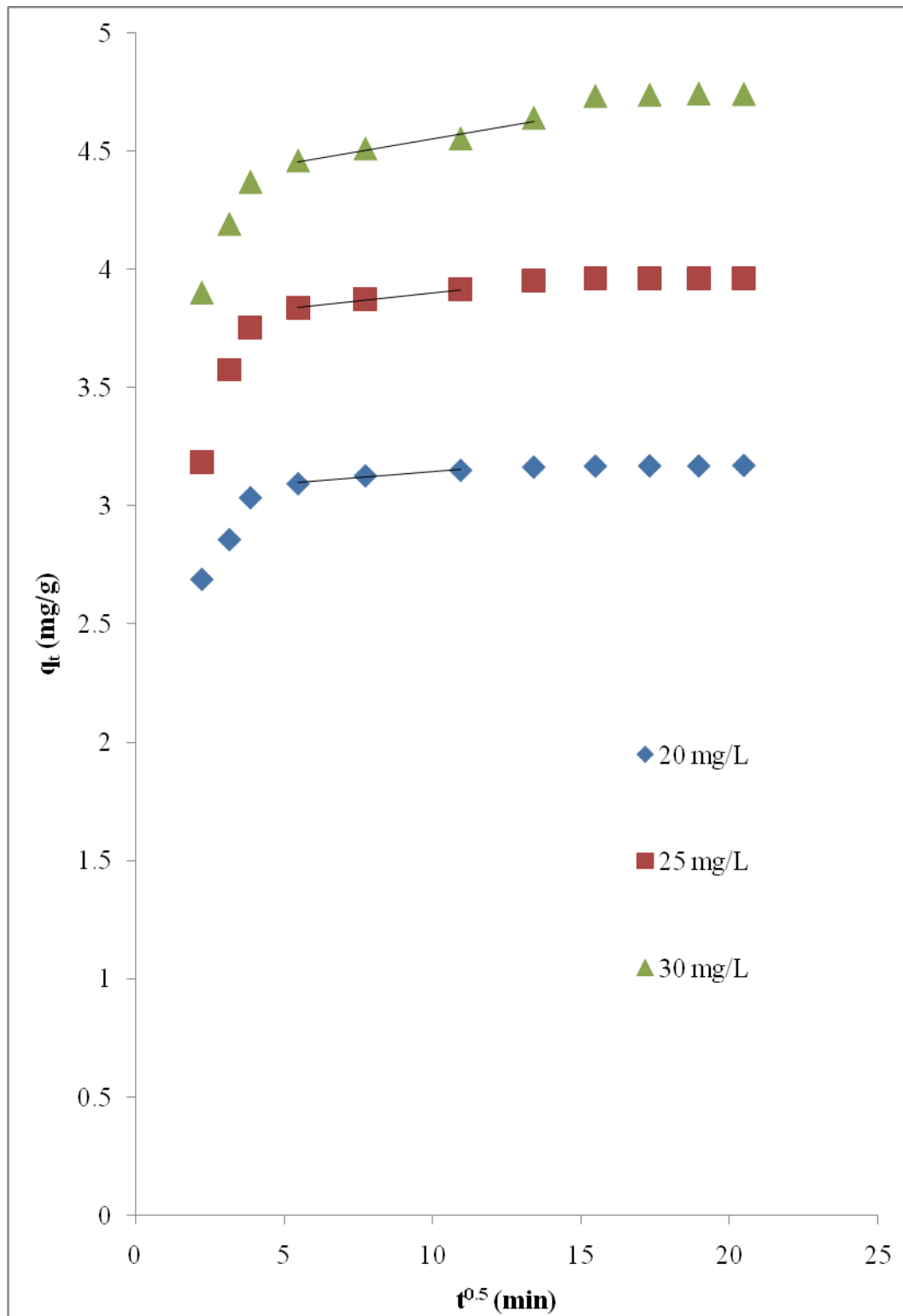
Figure 4.63: Intraparticle diffusion of Cd (II) ion in ERH
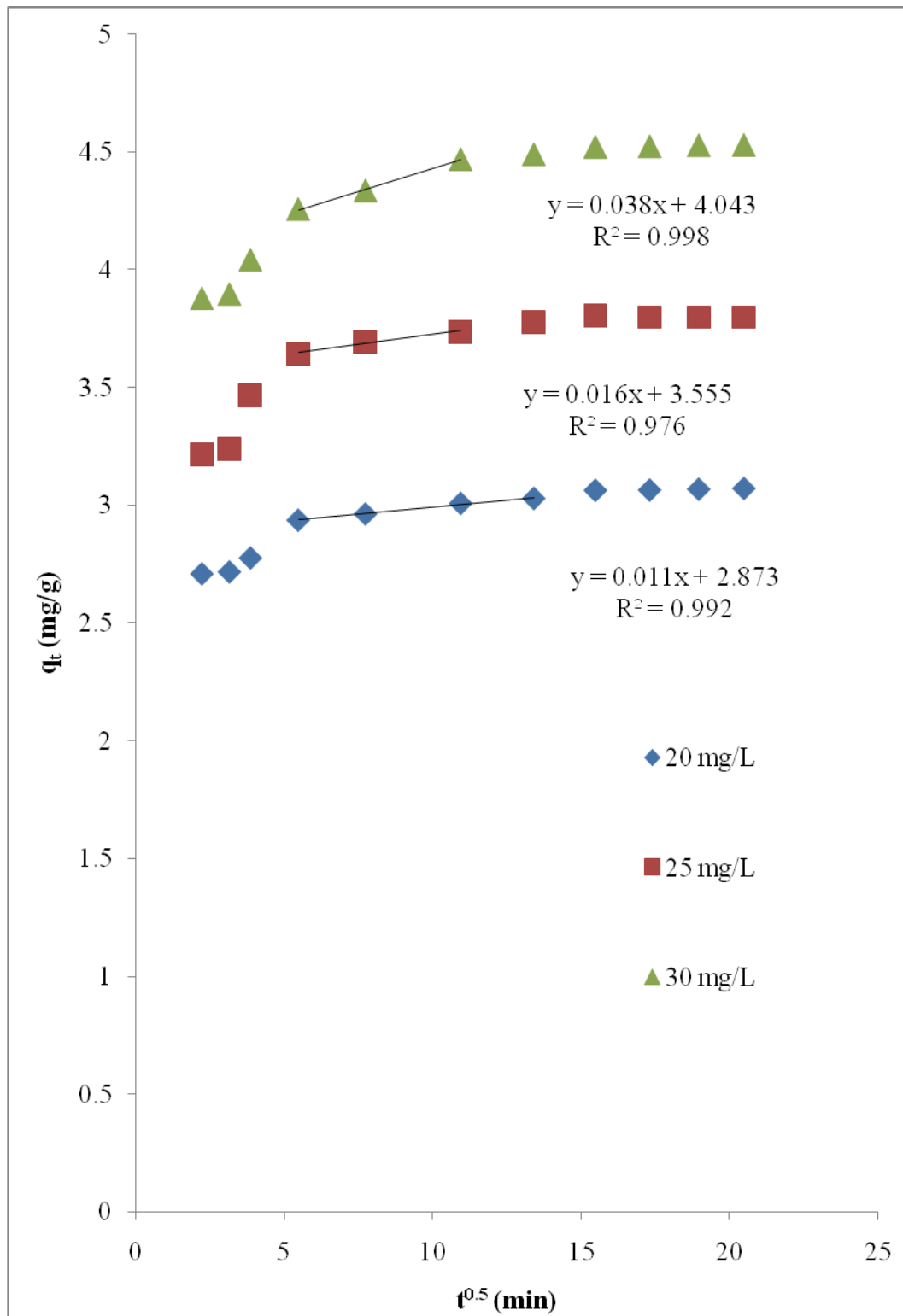
Figure 4.64: Intraparticle diffusion of Cd (II) ion in ERH

Similar case was observed in the adsorption of Cu (II) and Cd (II) ions onto nitric acid modified rice husk (Ong et al., 2007). The plot of q_t versus $\sqrt{t}$ for Cu (II) and Cd (II) ions adsorption was found to be deviated from the origin indicating that intraparticle diffusion is not the only rate-determining step. The first curve portion of the plot is due to the diffusion of metal ions through the solution to the external surface (boundary layer diffusion) of the modified rice husk whereas the second linear portion is attributed to the intraparticle diffusion.

As shown in Table 4.33, the value of K_p is higher when the concentration of metal ion increased. This indicates that the driving force of the metal ions from the bulk solution onto the surface of ERH and diffusion into the particle increased. The intercept of the plots reflect the extent of the boundary layer effect, the larger the intercept, the greater the contribution of surface adsorption in the rate controlling step. Results showed that as the concentration of metal ion increases, the value of intercept increased. This is because at higher concentration, the amount of metal ion per unit mass of ERH increase and thus more boundary layer diffusion occurs.

Table 4.33: Intraparticle diffusion coefficients, regression coefficients and the intercept of plots for the adsorption of Cd (II) and Cu (II) ions

Metal ions	Initial metal ion concentration (mg/L)	K_p (mg/g min$^{0.5}$)	Intercept (mg/g)
Cd (II)	20	0.010	3.041
	25	0.013	3.763
	30	0.021	4.339
Cu (II)	20	0.011	2.873
	25	0.016	3.555
	30	0.038	4.043

4.8.5 Adsorption Isotherm

The adsorption of heavy metals by ERH is a function of the equilibrium metal ion concentration in solution at constant pH and temperature. Two models have been used to describe the adsorption behaviour between the two phases in the adsorption system, namely Langmuir and Freundlich models. Langmuir model is based on the assumption that the adsorption occurs on a homogeneous surface with monolayer coverage whereas Freundlich model assumes multilayer adsorption onto a heterogeneous surface was assumed by Freundlich model.

The linerised Langmuir and Freundlich models were stated in equations 4.14 and 4.15. The plots of C_e / N_e versus C_e for both Cu (II) and Cd (II) were shown in Figures 4.65 and 4.66, respectively. A straight line plot was obtained with regression coefficient (R^2) value of 0.980 and 0.988 for Cu (II) and Cd (II) ions, respectively. As for Freundlich model, the plots of log N_e versus log C_e for both Cu (II) and Cd (II) ions were shown in Figures 4.67 and 4.68. The R^2 value for Cu (II) and Cd (II) was found to be 0.787 and 0.976, respectively.

By comparing both models in terms of R^2 values Langmuir isotherm model exhibit a better fitting for the adsorption of both metal ions. This indicates the adsorption of Cu (II) and Cd (II) ions formed monolayer coverage on a homogeneous surface of adsorbent. The maximum adsorption capacity of both Cu (II) and Cd (II) ions were calculated to be 7.9 mg/g and 12.9 mg/g, respectively.
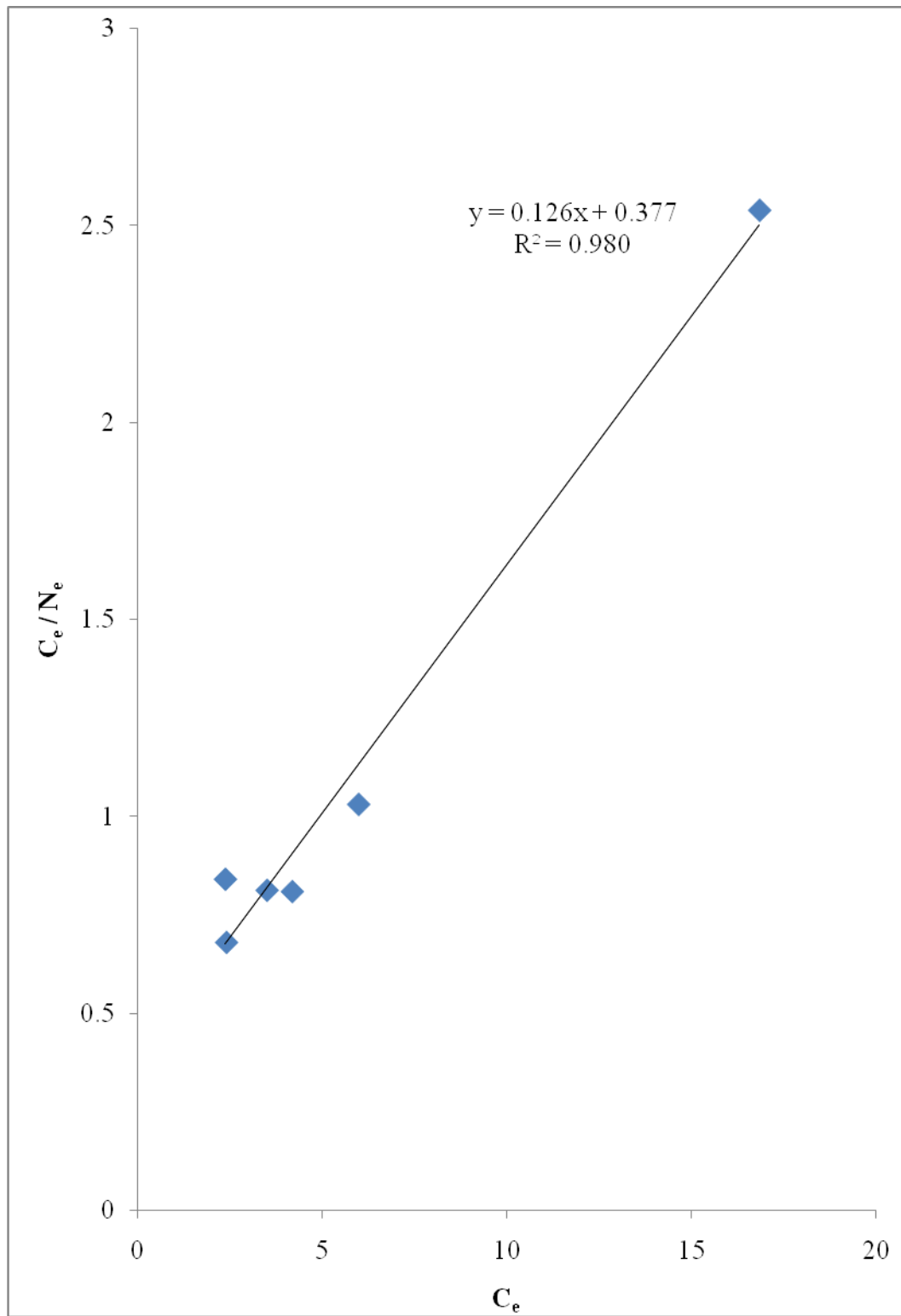
Figure 4.65: Langmuir plot for Cu(II) ion

$$y = 0.077x + 1.033$$
$$R^2 = 0.988$$
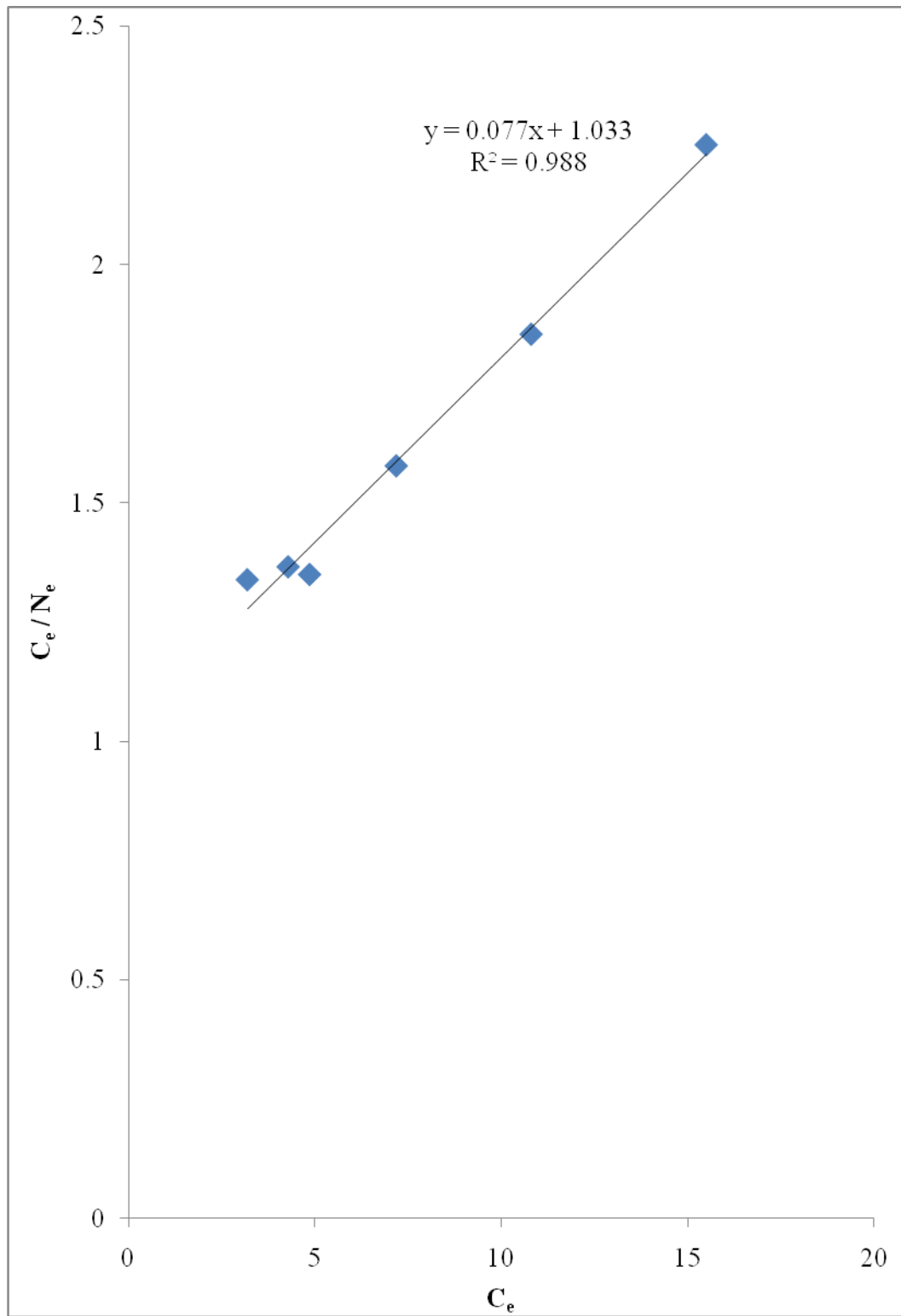
Figure 4.66: Langmuir plot for Cd(II) ion
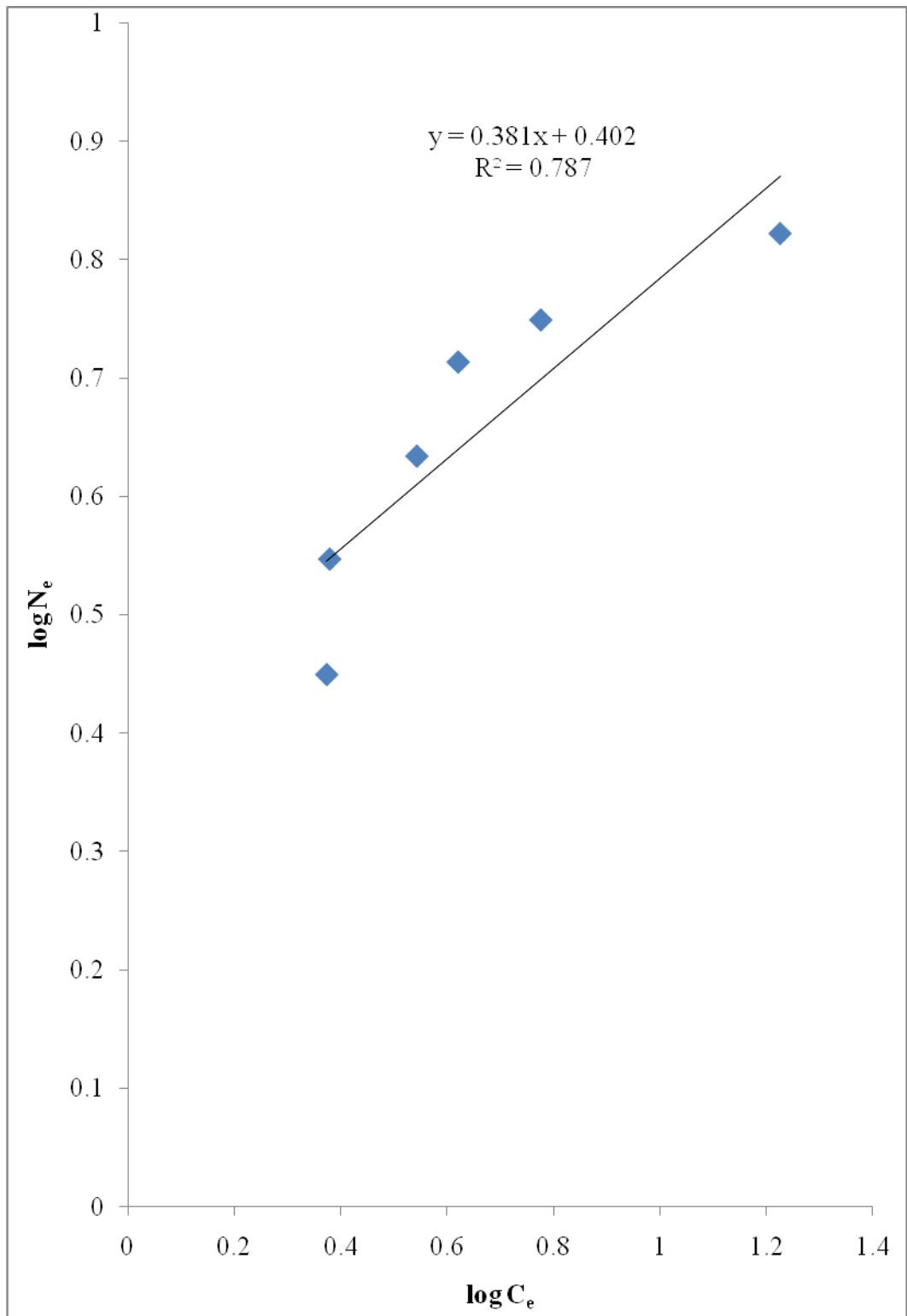
Figure 4.67: Freundlich plot for Cu(II) ion
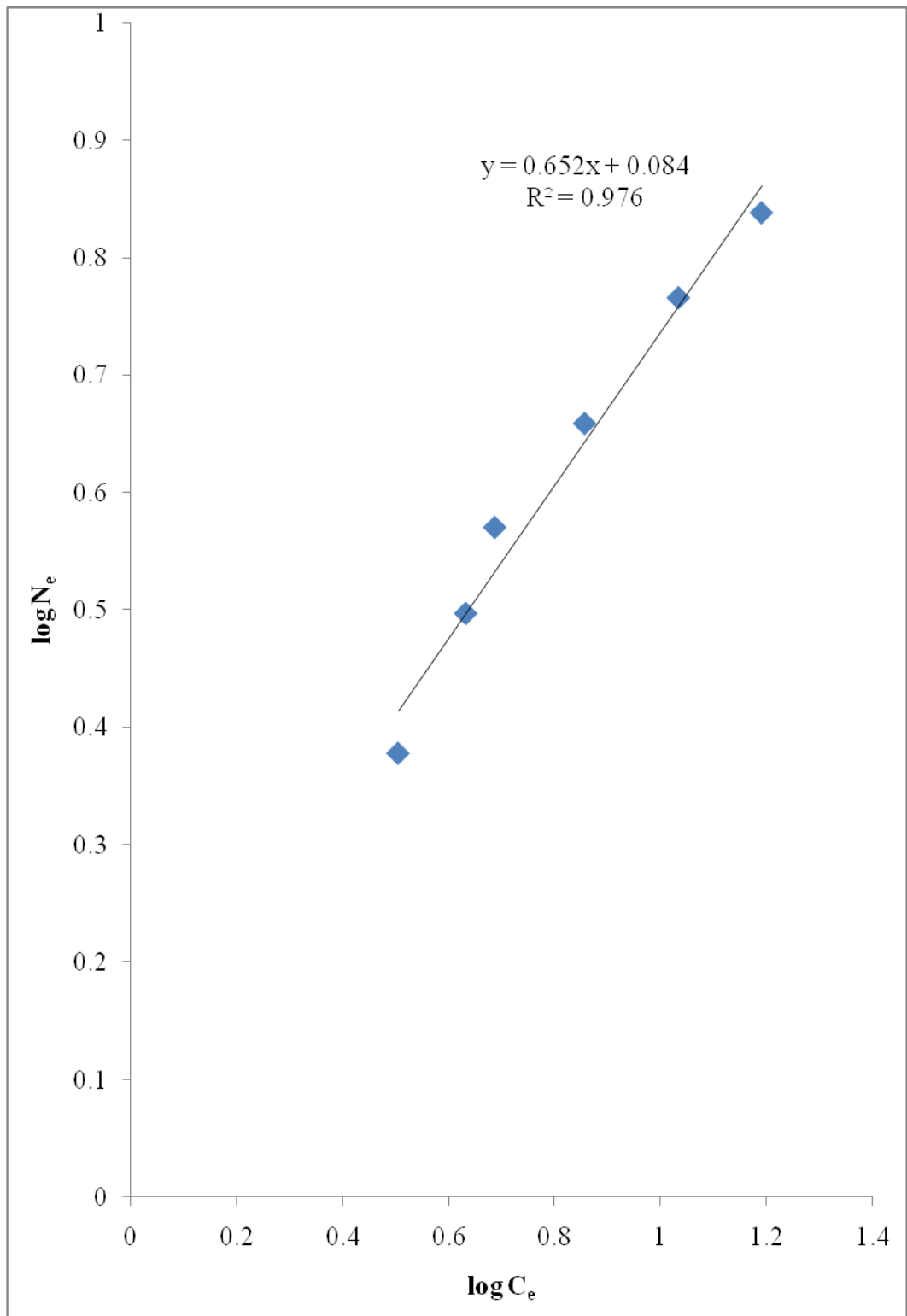
Figure 4.68: Freundlich plot for Cd(II) ion

Table 4.34: Comparison of maximum adsorption capacity of both Cd (II) and Cu (II) ions onto various adsorbents

Metal ion	Adsorbent	Maximum adsorption capacity (mg/g)	Reference
Cd (II)	ERH	12.987	This work
Cd (II)	Nitric acid modified rice husk	11.03	Ong et al. (2007)
Cu (II)	ERH	7.936	This work
Cu (II)	Sawdust	22.5	Lim et al. (2008)

4.8.6 Chelating Effect

In the study of chelating effect on the adsorption of Cu(II) and Cd(II) ions, salicylic acid was used as a chelating agent. A mixture of metal ion and chelator was prepared in different mole ratio as shown in Table 4.35. The percentage uptake of Cu(II) ion was decreased by 61.79% with increasing ratio of metal ion to salicylic acid from 1:0 to 1:5. This phenomenon indicates that the salicylic acid possesses a stronger chelating ability as compared to ERH. Same trend was observed for adsorption of Cd(II) ions in the presence of salicylic acid. The binding of metal ions to the salicylic acid is more efficient because the binding mechanism was occurred under homogeneous condition (both metal ion and chelator are in liquid state) whereas the adsorption of metal ions onto ERH was under heterogeneous condition (occurred between solid and liquid).

Similar case was reported in the study of Wong et al. (2003) where the adsorption of Cu (II) and Pb (II) ions onto tartaric acid modified rice husk (TARH) was being studied. In the presence of various chelators such as nitrolotriacetic acid (NTA), salicylic acid (SA) and EDTA, the adsorption of both Cu (II) and Pb (II) ions was inhibited. Higher molar ratios of chelator restrain the uptake of both

Cu (II) and Pb (II) ions. This is due to the formation of stable complexes between the metal ions and the chelators.

Table 4.35: Mole ratio of metal ion to chelator

1 mole metal ion : Chelator ratios	% Uptake of Cu(II) ion	% Uptake of Cd(II) ion
0.0	66.78	69.13
0.5	8.92	16.89
1.0	8.37	11.99
2.0	5.60	10.29
5.0	4.99	9.16

CHAPTER 5

CONCLUSION

The present study showed that EDTA modified rice husk (ERH) was capable to act as a single adsorbent to remove both MB and RO16. FTIR analysis revealed that both NRH and ERH spectra showed no significant difference in functional groups. From the SEM micrograph, it was noticed that the surface texture of the rice husk has become smoother after the modification with EDTA. Surface topography of both NRH and ERH was analysed by using AFM and the results revealed that ERH is having a more intense topography.

The percentage uptake of MB and RO16 was depended on pH, initial dye concentration and contact time. The optimal pH for the uptake of MB was in the range of 4 to 9 whereas for the uptake of RO16 was at 2. The uptake of dyes was increased with increasing adsorbent dosage and agitation rate. As for the effect of temperature, the uptake of MB reduced with an increase in temperature. However, a reverse trend was observed for RO16. Surface area of ERH was found to have noticeable effect on the adsorption of MB and RO16 in single and binary dye solutions. The experimental data was well fitted to Freundlich isotherm and pseudo-second order model. An enhancement was observed for the removal of binary RO16.

The experimental data indicated that the adsorption process of both dyes onto ERH was more favorable at lower influent concentration, higher bed depth,

and lower flow rate. The adsorption of RO16 showed a rapid breakthrough in the first 5 minutes followed by a gradual adsorption. The predicted breakthrough curves from Clark model agreed well with the experimental breakthrough curves at various flow rates.

By using Plackett-Burman design, pH and contact time were identified as significant variables in affecting the uptake of binary MB as well as single and binary RO16. RSM was used to determine the optimum conditions of the variables for maximum removal of dyes. The optimum conditions were: pH 6.85 and 0.14 g for single MB; pH 6.77 and 205.58 minutes for binary MB; pH 3.17 and 168.83 minutes for single RO16; pH 3.17 and 205.59 minutes for binary RO16.

The percentage uptake of copper and Cadmium ions increases with increasing pH and decreasing initial metal ion concentration. The adsorption behaviour of both metal ions fitted well in Langmuir isotherm. Maximum adsorption capacity for copper and cadmium ions was calculated to be 7.9 mg/g and 12.9 mg/g, respectively. Higher ratios of chelators to metal ions restrain the removal of both metal ions.

RECOMMADATIONS FOR FURTHER STUDIES

From this study, it was found that there several potential areas for further studies. They are listed as follow:

i.   Using ERH for the removal of dyes from a wide range of textile wastewater.

ii. The potential of ERH in the removal of other pollutants such as phenol, phosphorus and arsenic from wastewater.

LIST OF REFERENCES

Abbas, H.S., Thamer, J.M. and Jenan, A.N., 2012. Equilibrium and kinetics studies of adsorption of heavy metals onto activated carbon. *Canadian Journal on Chemical Engineering & Technology*, 3(4).

Adie, D.B., Okuofu, C.A. and Osakwe, C., 2012. Isothermal and batch adsorption studies of the use of *Borassus Aethiopium* and *Cocos Nucifera* for wastewater treatment. *American International Journal of Comtemporary Research*, 2(7).

Attia, A.A., Girgis, B.S. and Fathy, N.A., 2008. Removal of methylene blue by carbons derived from peach stones by H_3PO_4 activation: Batch and column studies. *Dyes and Pigments*, 76, pp. 282 – 289.

Ahmad, A.A., Hameed, B.H. and Ahmad, A.L., 2009. Removal of disperse dye from aqueous solution using waste – derived activated carbon: Optimization study. *Journal of Hazardous Materials*, 170, pp. 612 – 619.

Agiri, G.O. and Akaranta, O., 2009. Adsorption of metal ions by dye treated cassava mesocarp. *Scientific Research and Essay*, 4, pp. 526 – 530.

Al-Degs, Y.S., Khraisheh, M.A.M., Allen, S.J. and Ahmad, M.N., 2009. Adsorption characteristics of reactive dyes in columns of activated carbon. *Journal of Hazardous Materials*, 165, pp. 944 – 949.

Alam, M.Z., Mansor, M.F. and Jalal, K.C.A., 2009. Optimization of decolorization of methylene blue by lignin peroxidase enzyme produced from sewage sludge with phanerocheate chrysosporium. J*ournal of Hazardous Materials*, 162, pp. 708 – 715.

Ansari, R. and Mosayebzadeh, Z., 2010. Removal of basic dye methylene blue from aqueous solutions using sawdust and sawdust coated with polypyrrole. *Journal of the Iranian Chemical Society*, 7, pp. 339 – 350.

Annual Report of Bernas Sdn Bhd., 2008, [Online]. Available at : http://www.bernas.com.my/index.php?option=com_content&view=article&id=105:annual-report-2009&catid=53:annual-reports. [Accessed on 8th June 2009].

Arivoli, S., Martin, P., Prasath, D. and Thenkuzhali, M., 2007. Adsorption of chromium ion by acid activated low cost carbon. *Electronic Journal of Environmental Agricultural Food Chemistry*, 6, pp. 2323 – 2340.

Ai, L.H. and Jiang, J., 2010. Fast removal of organic dyes from aqueous solutions by AC/ferrospinel composite. *Desalination*, 262, pp. 134 – 140.

Amin, N.K., 2008. Removal of reactive dye from aqueous solutions by adsorption onto activated carbons prepared from sugarcane bagasse pith. *Desalination,* 223, pp. 152 – 161.

Amin, N.K., 2009. Removal of direct blue − 106 dye from aqueous solution using new activated carbons developed from pomegranate peel. *Journal of Hazardous Materials*, 165, pp. 52 − 62.

Anirudhan, T.S., Suchithra, P.S. and Radhakrishnan, P.G., 2009. Synthesis and characterization of humic acid immobilized − polymer/bentonite composites and their ability to absorb basic dyes from aqueous solutions. *Applied Clay Science*, 43, pp. 336 − 342.

Atar, N. and Olgun, A., 2009. Removal of basic and acid dyes from aqueous solutions by a waste containing boron impurity. *Desalination*, 249, pp. 109 − 115.

Argun, M.E., Dursun, S., Ozdemir, C. and Karatas, M., 2007. Heavy metal adsorption by modified oak sawdust: thermodynamics and kinetics. *Journal of Hazardous Materials*, 141, pp. 77 − 85.

Asuha, S., Zhou, X.G. and Zhao, S., 2010. Adsorption of Methyl Orange and Cr(VI) on mesoporous TiO_2 prepared by hydrothermal method. *Journal of Hazardous Materials*, 181, pp. 204 − 210.

Barragan, B.E., Costa, C. and Marquez, M.C., 2007. Biodegradation of azo dyes by bacteria inoculated on solid media. *Dyes and Pigments*, 75, pp. 73 − 81.

Bromley − Challenor, K.C.A., Knapp, J.C., Zhang, Z., Gray, N.C.C., Hetheridge, M.J. and Evans, M.R., 2000. Decolorization of an azo dye by unacclimated activated sludge under anaerobic conditions. *Water Research*, 34, pp. 4410 − 4418.

Badmus, M.A.O., Audu, T.O.K. and Anyata, B.U., 2007a. Removal of lead ion from industrial wastewaters by activated carbon prepared from periwinkle shells (*Typanotonus fuscatus*). *Journal of Engineering and Environmental Science*, 81, pp. 251 − 268.

Badmus, M.A.O., Audu, T.O.K. and Anyata, B.U., 2007b. Removal of heavy metal from industrial wastewater using hydrogen peroxide. *African Journal of Biotechnology*, 6, pp. 238 − 242.

Barron − Zambrano, J., Szygula, A., Ruiz, M., Maria Sastre, A. and Guibal, E., 2010. Biosorption of Reactive Black 5 from aqueous solutions by chitosan. *Journal of Environmental Management*, 91, pp. 2669 − 2675.

Bhatnagar, A., Vilar, V.J.P., Botelho, C.M.S. and Boaventura, R.A.R., 2010. Coconut − based biosorbents for water treatment. *Advances in Colloid and Interface Science*, 160, pp. 1 − 15.

Bhatnagar, A. and Jain, A.K., 2006. Column studies of phenols and dyes removal from aqueous solutions utilizing fertilizer industry waste. *International Journal of Agricultural Research*, 1, pp. 161 − 168.

Bohart, G. and Adams, E.N., 1920. Some aspects of the behavior of charcoal with respect to chlorine. *Journal of American Chemistry Society*, 42, p. 523.

Chun, Y.Y., Arouab, M.K. and Daudb, W.M.A.W., 2009. Fixed − bed adsorption of metal ions from aqueous solution on polyethyleneimine − impregnated palm shell activated carbon. *Chemical Engineering Journal*, 148, pp. 8 − 14.

Chandra, T.C., Mirna, M.M., Sudaryanto, Y. and Ismadji, S., 2007. Adsorption of basic dye onto activated carbon prepared from durian shell: Studies of adsorption equilibrium and kinetics. *Chemical Engineering Journal*, 127, pp. 121 − 129.

Chang, Y.N., Huang, J.C., Lee, C.C., Shih, I.L. and Yzeng, Y.M., 2002. Use of response surface methodology to optimize culture medium for production of lovastatin by Monascus ruber. *Enzyme and Microbial Technology*, 30, pp. 889 − 894.

Cheng, B., Le, Y., Cai, W.Q. and Yu, J.G., 2010. Synthesis of hierarchical $Ni(OH)_2$ and NiO nanosheets and their adsorption kinetics and isotherms to Congo Red in water. *Journal of Hazardous Materials*, 185, pp. 889 − 897.

Cheung, W.H., Szeto, Y.S. and Mckay, G., 2009. Enhancing the adsorption capacities of acid dyes by chitosan nano particles. *Bioresource Technology*, 100, pp. 1143 − 1148.

Chuah, T.G., Jumasiah, A., Azni, I., Katayon, S. and Thomas Chong, S.Y., 2005. Rice husk as a potentially low – cost biosorbent for heavy metal and dye removal: An overview. *Desalination*, 175, pp. 305 − 316.

Chauhan, K., Trivedi, U. and Patel, K.C., 2006. Application of response surface methodology for optimization of lactic acid production using date juice. *Journal of Microbial and Biotechnology*, 16, pp. 1410 − 1415.

Clark, R.M., 1987. Evaluating the cost and performance of field − scale granular activated carbon systems. *Environmental Science and Technology*, 21, pp. 573 − 580.

Dabrowski, A., Podkoscielny, P., Hubicki, Z. and Barczak, M., 2005. Adsorption of phenolic compounds by activated carbon – a critical review. *Chemosphere*, 58, pp. 1049 − 1070.

Demirbas, A., 2009. Agricultural based activated carbons for the removal of dyes from aqueous solutions: A review. *Journal of Hazardous Materials*, 167, pp. 1 − 9.

Davis, J.A., Volesky, B. and Vierra, R.H.S.F., 2000. Sargassum seaweed as biosorbent for heavy metals. *Water Research*, 34, pp. 4270 − 4278.

Daifullah, A.A.M., Awwad, N.S. and El – Reefy, S.A., 2004. Purification of wet phosphoric acid from ferric ions using modified rice husk. *Chemical Engineering and Processing*, 43, pp. 193 − 201.

El − Ashtoukhy, E.S.Z., Amin, N.K. and Abdelwahab, O., 2007. Removal of lead (II) and copper (II) from aqueous solution using pomegranate peel as new adsorbent. *Desalination*, 223, pp. 162 − 173.

Environmental Quality (Industrial Effluent) Regulation., 2009, [Online]. Available at: http://www.water-treatment.com.cn/resources/discharge-standards/malaysia_sewage-industrial-effluent-quality-mal2509.pdf [Accessed on 8th June 2009].

Fairus, M.D., Rusdin, L. and Yusof, M.N., 2007. The removal of basic dye (Methylene Blue) from aqueous solutions by adsorption on activated carbon prepared from palm oil fibre. *In Proceedings of the Science and Social Research Conference, CSSR.*

Faria, P.C.C., Orfao, J.J.M. and Pereira, M.F.R., 2004. Adsorption of anionic and cationic dyes on activated carbons with different surface chemistries. *Water Research*, 38, pp. 2043 – 2052.

Forgacs, E., Cserhati, T. and Oros, G., 2004. Removal of synthetic dyes from wastewaters: a review. *Environment International*, 30, pp. 953 – 971.

Fu, Y.Z. and Viraraghavan, T., 2003. Column studies for biosorption of dyes from aqueous solutions on immobilized *Aspergillus niger* fungal biomass. *Water SA*, 29, pp. 465 – 472.

Gad, H.M.H. and El − Sayed, A.A., 2009. Activated carbon from agricultural by − products for the removal of rhodamine − B from aqueous solution. *Journal of Hazardous Materials*, 168, pp. 1070 – 1081.

Gabaldon, C. and Gonzalez, J.A., 2000. Cadmium and Copper removal by a Granular Activated Carbon in laboratory column systems. *Separation Science and Technology*, 35, pp. 1039 − 1053.

Gupta, V.K. and Suhas, 2009. Application of low − cost adsorbents for dye removal − A review. *Journal of Hazardous Materials*, 90, pp. 2313 - 2342.

Guo, Y.P., Yang, S.F., Fu, W.Y., Qi, J.R., Li, R.Z., Wang, Z.C. and Xu, H.D., 2003. Adsorption of malachite green on micro − and mesoporous rice husk based active carbon. *Dyes and Pigments*, 56, pp. 219 – 229.

Gupta, V.K., Ali, I., Saini, V.K., Van, T., Van der Bruggen, B., Vandecasteele, C., 2005. Removal of dyes from wastewater using bottom ash. *Industrial & Engineering Chemistry Research*, 44, pp. 3655 – 3664.

Guan, J.F., Liu, J., Hu, X.F., Liu, Z.W. and Lin, H., 2009. Application on dyeing wastewater treatment by tourmaline. *Proceedings of 3rd International Conference on Bioinformatics and Biomedical Engineering, ICBBE.*

Gusmão, K.A.G., Gurgel, L.V.A., Melo, T.M.S., Gil, L.F., 2013. Adsorption studies of methylene blue and gentian violet on sugarcane bagasse modified with EDTA dianhydride (EDTAD) in aqueous solutions: Kinetic and equilibrium aspects. *Journal of Environmental Management*, 118, pp. 135 – 143.

Guven, G., Perendeci, A. and Tanyolac, A., 2008. Electrochemical treatment of deproteinated whey wastewater and optimisation of treatment conditions with response surface methodology. *Journal of Hazardous Materials*, 157, pp. 69 – 78.

Gong, R.M., Jin, Y.B., Sun, J. and Zhong, K.D., 2008. Preparation and utilization of rice straw bearing carboxyl groups for removal of basic dyes from aqueous solution. *Dyes and Pigments*, 76, pp. 519 – 524.

Hameed, B.H., Din, A.T.M. and Ahmad, A.L., 2007. Adsorption of methylene blue onto bamboo – based activated carbon: Kinetics and equilibrium studies. *Journal of Hazardous Materials*, 141, pp. 819 – 825.

Hameed, B.H., 2008b. Evaluation of papaya seeds as a novel non – conventional low – cost adsorbent for removal of methylene blue. *Journal of Hazardous Materials*, 162, pp. 939 – 944.

Hameed, B.H., Mahmoud, D.K. and Ahmad, A.L., 2008a. Sorption equilibrium and kinetics of basic dye from aqueous solution using banana stalk waste. *Journal of Hazardous Materials*, 158, pp. 499 – 506.

Hameed, B.H., 2008c. Removal of cationic dye from aqueous solution using jackfruit peel as non – conventional low – cost adsorbent. *Journal of Hazardous Materials*, 162, pp. 344 – 350.

Hameed, B.H. and Hakimi, H., 2008. Utilization of durian (Durio zibethinus Murray) peel as low cost adsorbent for the removal of acid dye from aqueous solutions. *Biochemical Engineering Journal*, 39, pp. 338 – 343.

Hamdaoui, O. and Chiha, M., 2007. Removal of methylene blue from aqueous solutions by wheat bran. *Acta Chimica Slovenica*, 54, pp. 407 – 418.

Han, R.P., Ding, D.D., Xu, Y.F., Zou, W.H., Wang, Y.F., Li, Y.F. and Zou, L.N., 2008. Use of rice husk for adsorption of Congo red from aqueous solution in column mode. *Bioresource Technology*, 99, pp. 2938 – 2946.

Han, R.P., Wang, Y.F., Yu, W.H., Zou,W.H., Shi, J. and Liu, H.M., 2007. Biosorption of methylene blue from aqueous solution by rice husk in a fixed – bed column. *Journal of Hazardous Materials*, 141, pp. 713 – 718.

Hashem, M.A., 2007. Adsorption of lead ions from aqueous solution by okra wastes. *International Journal of Physical Sciences*, 2, pp. 178 – 184.

Hao, G.P., Li, W.C., Wang, S., Zhang, S.F. and Lu, A.H., 2010. Tubular structured ordered mesoporous carbon as an efficient sorbent for the removal of dyes from aqueous solutions. *Elsevier*, 48, pp. 3330 – 3339.

Hema, M. and Arivoli, S., 2007. Comparative study on the adsorption kinetics and thermodynamics of dyes onto acid activated low cost carbon. *International Journal of Physical Sciences*, 2, pp. 010 – 017.

Hsu, S.T. and Pan, T.C., 2007. Adsorption of paraquat using methacrylic acid – modified rice husk. *Bioresource Technology*, 98, pp. 3617 – 3621.

Ho, Y.S. and Mckay, G., 1999. Pseudo second order model for sorption process. *Process Biochemistry*, 34, pp. 451 – 465.

Ho, Y.S. and McKay, G., 2000. The kinetics of sorption of divalent metals ions onto sphagnum moss peat. *Water Research*, 34, pp. 735 – 742.

Interim National Water Quality Standard for Malaysia., 2004, [Online]. Available at:
http://www.nahrim.gov.my/download/pkkaas/Table%202_%20INTERIM%20NATIONAL%20WATER%20QUALITY%20STANDARDS%20FOR%20MALAYSIA.pdf [Accessed on 8th June 2009].

Ioannides, C. and Lewis, D.F.V., 2004. Cytochromes P450 in the bioactivation of chemicals. *Current Topics in Medicinal Chemistry*, 4, pp. 1767 – 1788.

Igwe, J.C. and Abia, A.A., 2007. Adsorption kinetics and intraparticulate diffusivities for the bioremediation of Co (II), Fe (II) and Cu (II) ions from waste water using modified and unmodified maize cob. *International Journal of Physical Sciences*, 2, pp. 119 – 127.

Janos, P., Coskun, S., Pilarova, V. and Rejnek, J., 2009. Removal of basic (Methylene Blue) and acid (Egacid Orange) dyes from waters by adsorption on chemically treated wood shavings. *Bioresource Technology*, 100, pp. 1450 – 1453.

Junior, O.K., Gurgel, L.V.A., de Melo, J.C.P., Botaro, V.R., Melo, T.M.S., de Freitas Gil, R.P. and Gil, L.F., 2006. Adsorption of heavy metal ion from aqueous single metal solution by chemically modified sugarcane bagasse. *Bioresource Technology*, 98, pp. 1291 – 1297.

Ju, D.J., Byun, I.G., Park, J.J., Lee, C.H., Ahn, G.H. and Park, T.J., 2008. Biosorption of a reactive dye (Rhodamine – B) from an aqueous solution using dried biomass of activated sludge. *Bioresource Technology*, 99, pp. 7971 – 7975.

Kadirvelu, K., Kavipriya, M., Karthika, C., Radhika, M., Vennilamani, N. and Pattabhi, S., 2003. Utilization of various agricultural waste for activated carbon preparation and application for the removal of dyes and metal ions from aqueous solutions. *Bioresource Technology*, 87, pp. 129 – 132.

Kannan, N. and Murugavel, S., 2007. Column studies on the removal of dyes Rhodamine – B, Congo Red, and Acid Violet by adsorption on various adsorbents. *Electronic Journal of Environmental, Agricultural and Food Chemistry*, 6, pp. 1860.

Kanawade, S.M., Gaikwad, R.W. and Misal, S.A., 2010. Low cost sugarcane bagasse ash as an adsorbent for dye removal from dye effluent. *International Journal of Chemical Engineering and Applications*, 1(4), pp. 309 – 318.

Kaikake, K., Hoaki, K., Sunada, H., Dhakal, R.P. and Baba, Y., 2007. Removal of characteristics of metal ions using degreased coffee beans: Adsorption equilibrium of cadmium(II). *Bioresource Technology*, 98, pp. 2787 – 2791.

Kavitha, D. and Namasivayam, C., 2007. Recycling coir pith, an agricultural solid waste, for the removal of procion orange from wastewater. *Dyes and Pigments*, 74, pp. 237 – 248.

Khaled, A., El Nemr, A., El – Sikaily, A. and Abdelwahab, O., 2009. Treatment of artificial textile dye effluent containing direct yellow 12 by orange peel carbon. *Desalination*, 238, pp. 210 – 232.

Kulbat, E., Olanczuk – Neyman, K., Quant, B., Geneja, M. and Haustein, E., 2003. Heavy metals removal in the mechanical – biological wastewater treatment plant Wschod' in Gdansk. *Polish Journal of Environmental Studies*, 12, pp. 635 – 641.

Kumar, P.S., Ramalingam, S., Senthamarai, C., Niranjanaa, M., Vijayalakshmi, P. and Sivanesan, S., 2010. Adsorption of dye from aqueous solution by cashew nut shell: Studies on equilibrium isotherm, kinetics and thermodynamics of interactions. *Desalination*, 261, pp. 52 – 60.

Kumar, U., 2006. Agricultural products and by – products as low cost adsorbent for heavy metals removal from water and wastewater. *Scientific Research and Essay*, 1, pp. 033 – 037.

Ko, D.C.K., Porter, J.F. and McKay, G., 2000. Optimized correlations for the fixed – bed adsorption of metal ions on bone char. *Chemical Engineering Science*, 55, pp. 5819 – 5829.

Lagergren, S. and Svenska, B.K., 1898. Zur theorie der sogenannten adsorption geloester stoffe. *Veternskapsakad Handlingar*, 24, pp. 1 – 39.

Lakshmi, U.R., Srivastava, V.C., Mall, I.D. and Lataye, D.H., 2009. Rice husk ash as an effective adsorbent: Evaluation of adsorptive characteristics for Indigo Carmine dye. *Journal of Environmental Management*, 90, pp. 710 – 720.

Laszlo, J.A. and Dintzis, F.R., 1994. Crop residues as ion – exchange materials: Treatment of soybean hull and sugar beat fiber (pulp) with epichlorohydrin to improve cation – exchange capacity and physical stability. *Journal of Applied Polymer Science*, 52, pp. 531 – 538.

Lee, C.K., Ong, S.T. and Zainal, Z., 2008. Ethylenediamine modified rice hull as a sorbent for the removal of Basic Blue 3 and Reactive Orange 16. *International Journal of Environmental and Pollution*, 34, pp. 246 – 260.

Low, K.S., Lee, C.K. and Leo, A.C., 1994. Removal of metals from electroplating wastes using banana pith. *Bioresource Technology*, 51, pp. 227 – 231.

Lim, J.H., Kang, H.M., Kim, L.H. and Ko, S.O., 2008. Removal of heavy metals by sawdust adsorption: Equilibrium and kinetic studies. *Environmental Engineering Resource*, 13, pp. 79 – 84.

Liu, F.F., Teng, S.X., Song, R.H. and Wang, S.G., 2010. Adsorption of methylene blue on anaerobic granular sludge: Effect of functional groups. *Desalination*, 263, pp. 11 – 17.

Li, Q., Zhai, J., Zhang, W., Wang, M. and Zhou, J., 2007. Kinetic studies of adsorption of Pb(II), Cr(III) and Cu(II) from aqueous solution by sawdust and modified peanut husk. *Journal of Hazardous Materials*, 141, pp. 163 – 167.

Li, Q., Zhai, J.P., Zhang, W.Y., Wang, M.M. and Zhou, J., 2008. A study on adsorption of Pb(II) and Cu(II) from aqueous solution by peanut husk. *Bulletin of the Chemical Society of Ethiopia*, 22, pp. 19 – 26.

Mane, V.S., Mall, I.D. and Srivastava, V.C., 2007. Kinetic and equilibrium isotherm studies for the adsorptive removal of Brilliant Green dye from aqueous solution by rice husk ash. *Journal of Environmental Management*, 84, pp. 390 – 400.

Martin, M., Davila, J., Maria, P.E.G. and Virginia, H.M., 2009. Performance of mango seed adsorbents in the adsorption of anthraquinone and azo dyes in single and binary aqueous solutions. *Bioresource Technology*, 100, pp. 6199 – 6206.

Marshall, W.E., Champagne, E.T. and Evans, J.W., 1993. Use of rice milling by – product (hulls and bran) to remove metal ions from aqueous solution. *Journal of Environmental Science and Health, Part A*, 28, pp. 1977 – 1992.

Matthews, R., 2003. *The adsorption of dyes using kudzu, peanut hulls and MDF sawdust*. PhD Thesis, Queens University of Belfast.

McKay, G., Geundi, E.I. and Nassar, M.M., 1987. Equilibrium studies during the removal of dyestuffs from aqueous solutions using bagasse pith. *Water Research*, 21, pp. 1513 – 1520.

Memon, S.Q., Memon, N., Shah, S.W., Khuhawar, M.Y. and Bhanger, M.I., 2007. Sawdust – a green and economical sorbent for the removal of cadmium(II) ions. *Journal of Hazardous Materials*, 139, pp. 116 – 121.

Menkiti, M.C. and Onukwuli, O.D., 2011. Studies on dye removal from aqueous media using activated coal and clay: An adsorption approach. *New York Science Journal*, 4, p. 2.

Muthadhi, A., Anitha, R. and Kothandaraman, S., 2007. Rice husk ash – Properties and its uses: A review. *Journal of the Institution of Engineers*, 88, pp. 50 – 56.

Mittal, A., Kurup, L. and Mittal, J., 2007. Freundlich and Langmuir adsorption isotherms and kinetics for the removal of Tartrazine from aqueous solutions using hen feathers. *Journal of Hazardous Materials*, 146, pp. 243 – 248.

Namasivayam, C. and Sureshkumar, M.V., 2006. Anionic dye adsorption characteristics of surfactant – modified coir pith, a 'waste' lignocellulosic polymer. *Journal of Applied Polymer Science*, 100, pp. 1538 – 1546.

Netpradit, S., Thiravetyan, P. and Towprayoon, S., 2003. Application of waste metal hydroxide sludge for adsorption of azo reactive dyes. *Water Research*, 37, pp. 763 – 772.

Noroozi, B., Sorial, G.A., Bahrami, H. and Arami, M., 2008. Adsorption of binary mixtures of cationic dyes. *Dyes and Pigments*, 76, pp. 784 – 791.

Nwabanne, J.T. and Mordi, M.I., 2009. Equilibrium uptake and sorption dynamics for the removal of a basic dye using bamboo. *African Journal of Biotechnology*, 8, pp. 1555 – 1559.

Oei, B.C., Ibrahim, S., Wang, S.B. and Ang. H.M., 2009. Surfactant modified barley straw for the removal of acid and reactive dyes from aqueous solution. *Bioresource Technology*, 100, pp. 4292 – 4295.

Oliveira, L.S., Franca, A.S., Alves, T.M. and Rocha, S.D.F., 2008. Evaluation of untreated coffee husks as potential biosorbents for treatment of dye contaminated waters. *Journal of Hazardous Materials*, 155, pp. 507 – 512.

Oladoja, N.A., Aboluwoye, C.O., Oladimeji, Y.B., Ashogbon, A.O. and Otemuyiwa, I.O., 2008. Studies on castor seed shell as a sorbent in basic dye contaminated wastewater remediation. *Desalination*, 227, pp. 190 – 203.

Ong, S.A., Seng, C.E. and Lim, P.E., 2007. Kinetics of adsorption of Cu(II) and Cd(II) from aqueous solution on rice husk and modified rice husk. *Electronic Journal of Environmental, Agricultural and Food Chemistry*, 6, pp. 1764 – 1774.

Ong, S.T., 2006. *Removal of basic and reactive dyes by sorption using ethylenediamine modified rice hull*. PhD Thesis, Universiti Putra Malaysia, Malaysia.

Ong, S.T., Lee, C.K. and Zainal, Z., 2007. Removal of basic and reactive dyes using ethylenediamine modified rice hull. *Bioresource Technology*, 98, pp. 2792 – 2799.

Ong, S.T., Tay, E.H., Ha, S.T., Lee, W.N. and Keng, P.S., 2009. Equilibrium and continuous flow studies on the sorption of Congo Red using ethylenediamine modified rice hulls. *International Journal of Physical Sciences*, 4, pp. 683 – 690.

Ong, S.T., Lee, W.N., Keng, P.S., Lee, S.L., Hung, Y.T. and Ha, S.T., 2010. Equilibrium studies and kinetics mechanism for the removal of basic and reactive dyes in both single and binary systems using EDTA modified rice husk. *International Journal of Physical Sciences*, 5, pp. 582 – 595.

Ong, S.T., Keng, P.S. and Lee, C.K., 2010. Basic and reactive dyes sorption enhancement of rice hull through chemical modification. *American Journal of Applied Sciences*, 7, pp. 447 – 452.

Oglun, A. and Atar, N., 2009. Equilibrium and kinetic adsorption study of basic yellow 28 and basic red 46 by a boron industry waste. *Journal of Hazardous Materials*, 161, pp. 148 – 156.

Ozer, A., Ozer, D. and Ozer, A., 2004. The adsorption of copper(II) ions onto dehydrated wheat bran (DWB): determination of the equilibrium and thermodynamic parameters. *Process Biochemistry*, 39, pp. 2183 – 2191.

Ozer, A. and Pirincci, H.B., 2006. The adsorption of Cd(II) ions on sulfuric acid – treated wheat bran. *Journal of Hazardous Materials*, 137, pp. 849 – 855.

Pavan, F.A., Lima, E.C., Dias, S.L.P. and Mazzocato, A.C., 2008. Methylene blue biosorption from aqueous solutions by yellow passion fruit waste. *Journal of Hazardous Materials*, 150, pp. 703 – 712.

Ponnusami, V., Vikram, S. and Srivastava, S.N., 2008. Guava (Psidium guajava) leaf powder: Novel adsorbent for removal of methylene blue from aqueous solutions. *Journal of Hazardous Materials*, 152, pp. 276 – 286.

Prasad, C.S., Maiti, K.N. and Venugopal, R., 2000. Effect of rice husk ash in white ware composition. *Ceramics International*, 27, p. 629.

Pinheiro, E.R., Silva, I.M.D.A., Gonzaga, L.V., Amante, E.R., Teofilo, R.F., Ferreira, M.M.C. and Amboni, R.D.M.C., 2008. Optimisation of extraction of high – ester pectin from passion fruit peel (Passiflora edulis flavicarpa) with citric acid by using response surface methodology. *Bioresource Technology*, 99, pp. 5561 – 5566.

Rahmadini, S., Ishak, A. and Ibrahim, A., 2011. Effect of rice husk surface modification by LENR on the mechanical properties of NR/HDPE reinforced rice husk composite. *Sains Malaysiana*, 40, pp. 749 – 756.

Ravikumar, K., Ramalingam, S., Krishnan, S. and Balu, K., 2006. Application of response surface methodology to optimize the process variables for Reactive Red and Acid Brown dye removal using a novel adsorbent. *Dyes and Pigments*, 70, pp. 18 – 26.

Saad, S.A., Isa, K.Md. and Bahari, R., 2010. Chemically modified sugarcane bagasse as a potential low – cost adsorbent for dye removal. *Desalination*, 264, pp. 123 – 128.

Saffaj, N., Loukili, H., Younssi, S.A., Albizane, A., Bouhria, M., Persin, M. and Larbot, A., 2004. Filtration of solution containing heavy metals and dyes by means of ultrafiltration membranes deposited on support made of Moroccan clay. *Desalination*, 168, pp. 301 – 306.

Satish, P., Sameer, R. and Naseema, P., 2010. Removal of methylene blue, a basic dye from aqueous solutions by adsorption using teak tree (*Tectona grandis*) bark powder. *International Journal of Environmental Sciences*, 1(5), pp. 711 – 726.

Senthilkumar, S.R., Dempsey, M., Krishnan, C. and Gunasekaran, P., 2008. Optimisation of biobleaching of paper pulp in an expanded bed bioreactor with immobilised alkali stable xylanase by using response surface methodology. *Bioresource Technology*, 99, pp. 7781 – 7787.

Shiau, C.Y. and Pan, C.C., 2004. Adsorption of basic dyes from aqueous solution by various adsorbent. *Separation Science and Technology*, 39, pp. 1733 – 1750.

Sharma, P., Singh, L. and Dilbaghi, N., 2009. Response surface methodological approach for the decolorisation of simulated dye effluent using Aspergillus fumigates Fresenius. *Journal of Hazardous Materials*, 161, pp. 1081 – 1086.

Shukla, S.R. and Roshan, S.P., 2005. Adsorption of Cu(II), Ni(II) and Zn(II) on modified jute fibres. *Bioresource Technology*, 96: 1430 – 1438.

Slampova, A., Smela, D., Vondrackova, A., Jancarova, I. and Kuban, V., 2001. Determination of synthetic colorants in foodstuffs. *Chemical Listy*, 95, pp. 163–168.

Stolz, A. 2001. Basic and applied aspects in the microbial degradation of azodyes. *Applied Microbiology and Biotechnology*, 56, pp. 69 – 80.

Sulak, M.T., Demirbas, E. and Kobya, M., 2007. Removal of Astrazon Yellow 7GL from aqueous solutions by adsorption onto wheat bran. *Bioresource Technology*, 98, pp. 2590 – 2598.

Suteu, D., Malutan, T. and Bilba, D., 2010. Removal of reactive dye Brilliant Red HE – 3B from aqueous solutions by industrial lignin: Equilibrium and kinetics modeling. *Desalination*, 255, pp. 84 – 90.

Sudha, R., Kalpana, K., Rajachandrasekar, T. and Arivoli, S., 2007. Comparative study on the adsorption kinetics and thermodynamics of metal ions onto acid activated low cost pandanus carbon. *E-Journal of Chemistry*, 4, pp. 238 – 254.

Sureshkumar, M.V. and Namasivayam, C., 2008. Adsorption behavior of Direct Red 12B and Rhodamine B from water onto surfactant-modified coconut coir pith. *Colloids and Surfaces, A: Physicochemical and Engineering Aspects*, 317, pp. 277 – 283.

Singh, G., Ahuja, N., Batish, M., Capalash, N. and Sharma, P., 2008. Biobleaching of wheat straw – rich soda pulp with alkalophilic laccase from γ – proteobacterium JB: Optimization of process parameters using response surface methodology. *Bioresource Technology*, 99, pp. 7472 – 7479.

Sivakumar, P. and Palanisamy, P.N., 2009. Packed bed column studies for the removal of acid blue 92 and basic red 29 using non-conventional adsorbent. *Indian Journal of Chemical Technology*, 16, pp. 301 – 307.

Tan, I.A.W. and Hameed, B.H., 2010. Adsorption isotherms, kinetics, thermodynamics and desorption studies of basic dyes on activated carbon derived from oil palm empty fruit bunch. *Journal of Applied Sciences*, 10, pp. 2565 – 2571.

Tan, I.A.W., Ahmad, A.H. and Hameed, B.H., 2008. Adsorption of basic dye on high – surface – area activated carbon prepared from coconut husk: Equilibrium, kinetic and thermodynamic studies. *Journal of Hazardous Materials*, 154, pp. 337 – 346.

Tavares, A.P.M., Cristovao, R.O., Loureiro, J.M., Boaventura, R.A.R. and Macedo, E.A., 2009. Application of statistical experimental methodology to optimize reactive dye decolourization by commercial laccase. *Journal of Hazardous Materials*, 162, pp. 1255 – 1260.

Taveres, A.P.M., Coelho, M.A.Z., Agapito, M.S.M., Countinho, J.A.P. and Xavier, A.M.R.B., 2005. Selection and optimization of culture medium for exopolysaccharide production by Coriolus (Trametes) versicolor. *Journal of Microbiology and Biotechnology*, 21, pp. 1499 – 1507.

Tsai, W.T., Hsu, H.C., Su, T.Y., Lin, K.Y. and Lin, C.M., 2007. Removal of basic dye (methylene blue) from wastewaters utilizing beer brewery waste. *Journal of Hazardous Materials*, 154, pp. 73 – 78.

Uddin, Md.T., Islam, Md.A., Mahmud, S. and Rukanuzzaman, Md., 2009. Adsorptive removal of methylene blue by tea waste. *Journal of Hazardous Materials*, 164, pp. 53 – 60.

Vadivelan, V. and Kumar, K.V., 2005. Equilibrium, kinetics, mechanism, and process design for the sorption of methylene blue onto rice husk. *Journal of Colloid and Interface Science*, 286, pp. 90–100.

Wan Ngah, W.S. and Hanafiah, M.A.K.M., 2007. Removal of heavy metal ions from wastewater by chemically plant wastes as adsorbent: A review. *Bioresources Technology*, 99, pp. 3935 – 3948.

Weuster-Botz, D., 2000. Experimental design for fermentation media development: statistical design or global random search. *Journal of Bioscience and Bioengineering*, 90, pp. 473 – 483.

Wong, K.K., Lee, C.K., Low, K.S. and Haron, M.J., 2003. Removal of Cu and Pb by tartaric acid modified rice husk from aqueous solutions. *Chemosphere*, 50, pp. 23 – 28.

Yasin, Y., Hussein, M.Z. and Ahmad, F.H., 2007. Adsorption of methylene blue onto treated activated carbon. *The Malaysian Journal of Analytical Sciences*, 11, pp. 400 – 406.

Zee van der, F.P., Lettinga, G. and Field, J.A., 2000. The role of (auto)catalysis in the mechanism of an anaerobic azo reduction. *Water Science and Technology*, 42, pp. 301 – 308.